



LIBRARY  
Michigan State  
University

This is to certify that the  
dissertation entitled

Degradation of polycyclic aromatic hydrocarbons (PAHs)  
in aqueous media using alternating current

presented by

Emmanuel Samman Pepprah

has been accepted towards fulfillment  
of the requirements for the

Ph.D. degree in Environmental Engineering



Major Professor's Signature

12 Dec. 2007

Date

**PLACE IN RETURN BOX** to remove this checkout from your record.  
**TO AVOID FINES** return on or before date due.  
**MAY BE RECALLED** with earlier due date if requested.

DATE DUE	DATE DUE	DATE DUE

**DEGRADATION OF POLYCYCLIC AROMATIC HYDROCARBONS  
(PAHs) IN AQUEOUS MEDIA USING ALTERNATING CURRENT**

**By**

**Emmanuel Samman Pepprah**

**A DISSERTATION**

**Submitted to  
Michigan State University  
in partial fulfillment of the requirements  
for the degree of**

**DOCTOR OF PHILOSOPHY**

**Department of Civil and Environmental Engineering**

**2007**



## ABSTRACT

### DEGRADATION OF POLYCYCLIC AROMATIC HYDROCARBONS (PAHs) IN AQUEOUS MEDIA USING ALTERNATING CURRENT

By

Emmanuel S. Pepprah

Abiotic treatment techniques such as ozonation, hydrogen peroxide oxidation, UV irradiation, chlorination electrochemical oxidation, sonochemical oxidation, etc. have been extensively investigated and applied for the treatment of water and wastewater containing organic compounds such as polycyclic aromatic hydrocarbons (PAHs). In contaminated soils, biodegradation and surfactants are often employed as a treatment technique to degrade or “wash” PAHs *in situ*. Published electrochemical studies have focused on the use of direct current (DC) to degrade organics in solution. However, relatively few studies have explored the potential of using alternating current (AC) to degrade organics in solution. In this dissertation, AC is explored for the degradation of PAHs in aqueous solutions. The effect of AC waveform shape, current density and frequency, and supporting electrolyte on the rate of degradation of PAHs was investigated to determine optimum conditions required for potential pilot-scale implementation of the proposed treatment technique. Degradation rates and byproducts formed were compared when AC, DC and ultrasound delivered at the same output power were separately applied to spiked aqueous solutions containing PAHs. Degradation byproducts and mechanisms were identified. Naphthalene, phenanthrene and pyrene were used as the model PAH compounds.

The key findings of this study are: (1) Similar to DC, AC can degrade PAHs in solution; (2) DC was more efficient in degrading PAHs than AC at an equivalent root mean square (rms) current density. However, potential field-scale application using AC would be cheaper for capital cost because no rectification is required; (3) Degradation rates increased with the increase in current density and decreased with increased AC frequency; (4) For square, sine, and triangular AC waveforms explored, square wave AC signal produced the fastest degradation at an equivalent peak current density; (5) Both DC and ultrasound, at an equivalent output power exhibited comparable degradation rates for naphthalene whereas, AC at 60 Hz showed relatively low degradation rate at the same output power; (6) Similar to electrochemical degradation of PAHs using DC reported in published studies, hydroxyl radicals were identified as the key oxidizing agents in both sonochemical and electrochemical degradation using AC in this study; and (7) Both diffusion and migration processes were responsible for the rate of mass transfer of PAHs to the reaction sites (surface of electrodes or in the vicinity of the electrodes) where the PAHs were degraded or converted by the hydroxyl radicals. However, migration was the dominant mass transfer phenomenon responsible for the degradation of PAHs in the AC and DC electrochemical cells.

**Keywords:** Electrokinetics, ground-water contamination, organic chemicals, PAH, naphthalene, salicylic acid, phenanthrene, pyrene, alternating current (AC), direct current (DC), AC frequency, AC waveform, electrolysis, electrochemical degradation, sonochemical degradation, and hydroxyl radical.

## **DEDICATION**

“In all things, give thanks to the Lord.” I therefore thank the Almighty God for giving me the strength and wisdom to complete this work. I dedicate this dissertation to my wonderful wife, Kesewa Pepprah, son, Michael Pepprah, and daughter, Chelsea Pepprah.

## ACKNOWLEDGEMENT

I am very grateful to my lovely wife, Kesewa Pepprah, my son, Michael Pepprah and daughter, Chelsea Pepprah for their prayers, support and patience.

My sincere gratitude goes to my academic advisor, Dr. Milind V. Khire for his guidance and support during my stay as a Ph.D student at Michigan State University.

I am indebted to my guidance committee members, especially Dr. Dan Jones for his assistance in running mass spectrometry tests and identification of degradation byproducts. I also thank Dr. Hui Li and Dr. Volodymyr Tarabara for their useful comments and suggestions.

I extend my utmost thanks to the Department of Civil and Environmental Engineering, Michigan State University for partially funding my Ph.D program by offering me teaching assistantship.

I am grateful to Mr. Joseph Leykam at the RTSF Macromolecular Core Facility for his technical support during the analysis of samples, and Mr. James C. Brenton for his technical assistance related to the fabrication of the test cells. I am also thankful to Prof. Satish Udpa and Mr. Michael Shiu C. Chan for their help with the selection of the function generator, oscilloscope, and the amplifiers.

This project has been funded by the U.S. National Science Foundation (NSF) Grant No. BES-0402772. However, this dissertation has not been reviewed by NSF.

## TABLE OF CONTENTS

LIST OF TABLES .....	X
LIST OF FIGURES .....	XII
KEY OF ABBREVIATIONS .....	XVI
KEY OF SYMBOLS .....	XVII
INTRODUCTION .....	1
BACKGROUND ON PAHs.....	1
EXISTING REMEDIATION TECHNIQUES .....	3
ELECTROCHEMICAL DEGRADTION OF ORGANICS .....	3
Type of Electrical Current .....	3
Target Organic Compounds.....	5
Electrodes.....	7
Supporting Electrolyte .....	8
Analytical Techniques .....	9
DEGRADTION OF ORGANICS USING ULTRASOUND.....	9
Ultrasound Equipment .....	9
Target Compounds.....	10
OBJECTIVES AND METHODOLOGY .....	12
DISSERTATION ORGANIZATION .....	14
PAPER NO. 1: ELECTROREMEDIATION OF NAPHTHALENE IN AQUEOUS SOLUTION USING ALTERNATING AND DIRECT CURRENTS .....	16
ABSTRACT .....	16
INTRODUCTION.....	17
BACKGROUND.....	18
DC Electrolysis .....	18
AC Electrolysis .....	20
OBJECTIVES .....	21
MATERIALS AND EXPERIMENTAL METHODOLOGY .....	21
Reaction Chamber.....	23
Electrical Equipment.....	24
Spiked Solution Preparation .....	24
Supporting Electrolyte .....	25
Testing Procedure .....	27
Sampling .....	29
Experimental Parameters Monitored .....	30

RESULTS AND DISCUSSION.....	30
Supporting Electrolyte: NaCl.....	31
Supporting Electrolyte: Na <sub>2</sub> SO <sub>4</sub> .....	38
DC Tests.....	38
AC Tests.....	40
Intermediate Byproducts.....	42
Temperature.....	47
pH.....	47
Redox Potential and Dissolved Oxygen.....	49
Electrical Conductivity.....	50
Supporting Electrolyte: Na <sub>2</sub> SO <sub>4</sub> .....	50
SUMMARY AND CONCLUSIONS.....	50

PAPER NO. 2: DEGRADATION OF PHENANTHRENE AND PYRENE IN SOLUTION USING ALTERNATING CURRENT.....	53
ABSTRACT.....	53
INTRODUCTION.....	54
OBJECTIVES.....	55
MATERIALS AND EXPERIMENTAL METHODOLOGY.....	56
Reaction Chamber.....	58
Electrical Equipment.....	59
Spiked Solution Preparation.....	59
Testing Procedure.....	61
Monitored Experimental Parameters.....	63
RESULTS AND DISCUSSION.....	64
Electrochemical Degradation of Phenanthrene in Solution.....	66
Effect of Current Density.....	66
Oxidizing Agents.....	68
Hydroxyl Radical Test.....	69
Degradation Kinetics.....	71
Effect of Type of Supporting Electrode.....	72
Effect of AC Frequency.....	74
Effect of AC Waveform.....	78
Electrode Fouling.....	80
Electrochemical Degradation of Pyrene in Solution.....	80
Effect of Current Density.....	80
Effect of Type of Supporting Electrode.....	83
Effect of AC Frequency.....	84
Effect of AC Waveform.....	84
Modeled versus Measured Concentrations of Phenanthrene and Pyrene.....	85
Electrode Mass Decay.....	93
Intermediate Byproducts.....	93
SUMMARY AND CONCLUSIONS.....	97

PAPER NO. 3: EFFECT OF ALTERNATING CURRENT WAVEFORM AND FREQUENCY ON THE DEGRADATION OF NAPHTHALENE IN AQUEOUS SOLUTION.....	99
ABSTRACT .....	99
INTRODUCTION.....	100
MATERIALS AND EXPERIMENTAL METHODOLOGY .....	104
Reaction Chamber.....	106
Electrical Equipment.....	106
Spiked Solution Preparation .....	107
Testing Procedure .....	108
Experimental Parameters Monitored .....	110
RESULTS AND DISCUSSION.....	110
Effect of AC Waveform.....	112
Effect of AC Frequency.....	115
Hydroxyl Radical Probe Study .....	122
Hydroxyl Radical Scavenger Study.....	125
Modeled versus Measured Concentrations of Naphthalene.....	127
Effect of Convection Mass Flux .....	133
Intermediate Byproducts.....	135
Reaction Mechanism and Pathway .....	136
Divided Cell Setup.....	139
Measured Initial and Final Key Test Parameters.....	142
SUMMARY AND CONCLUSIONS .....	148

PAPER NO. 4: A COMPARATIVE STUDY OF SONOCHEMICAL AND ELECTROCHEMICAL DEGRADATION OF NAPHTHALENE IN AQUEOUS SOLUTION.....	151
ABSTRACT .....	151
INTRODUCTION.....	152
MATERIALS AND EXPERIMENTAL METHODOLOGY .....	155
Reaction Chambers .....	158
Electrical Equipment.....	158
Ultrasound Equipment .....	159
Spiked Solution Preparation .....	159
Testing Procedure .....	160
Experimental Parameters Monitored .....	161
RESULTS AND DISCUSSION.....	162
Effect of Power (AC, DC and Ultrasound).....	163
Similarities between Sonochemical and Electrochemical Degradation.....	165
Oxidizing Agents .....	165
Degradation Kinetics .....	169
Degradation Byproducts .....	169
Heat Generation .....	170
Mechanism for OH Radical Generation .....	171
Reaction Site .....	172

Reaction Mechanism and Pathway .....	173
Modeled versus Measured Concentrations of Naphthalene.....	179
SUMMARY AND CONCLUSIONS .....	190
PAPER NO. 5: DEGRADATION OF NAPHTHALENE IN THE AQUEOUS PHASE OF SPIKED SATURATED OTTAWA SAND .....	192
ABSTRACT .....	192
INTRODUCTION.....	193
MATERIALS AND EXPERIMENTAL METHODOLOGY .....	194
Reaction Chamber.....	196
Electrical Equipment.....	196
Spiked Sand .....	196
Testing Procedure .....	197
RESULTS AND DISCUSSION .....	198
Comparison of Degradation Rates .....	198
Comparison of Degradation Rates in Spiked Sand Using AC and DC .....	202
Effect of Current Density.....	206
Effect of AC Frequency.....	207
Experimental Parameters Monitored .....	208
SUMMARY AND CONCLUSIONS .....	209
SUMMARY AND CONCLUSIONS .....	210
REFERENCES .....	213



## LIST OF TABLES

### **PAPER NO. 1: ELECTROREMEDIATION OF NAPHTHALENE IN AQUEOUS SOLUTION USING ALTERNATING AND DIRECT CURRENTS**

Table 1-1:	Experimental variables.....	25
Table 1-2:	Measured initial and final values of temperature, pH, standard redox potential, dissolved oxygen concentration, and electrical conductivity of test cell and control cell solutions.....	45

### **PAPER NO. 2: DEGRADATION OF PHENANTHRENE AND PYRENE IN SOLUTION USING ALTERNATING CURRENT**

Table 2-1:	Summary of Experimental Parameters.....	64
Table 2-2:	Measured initial and final values of temperature, pH, standard redox potential, and electrical conductivity of test cell and control cell solutions.....	95

### **PAPER NO. 3: EFFECT OF ALTERNATING CURRENT WAVEFORM AND FREQUENCY ON THE DEGRADATION OF NAPHTHALENE IN AQUEOUS SOLUTION**

Table 3-1:	Summary of Experimental Parameters.....	111
Table 3-2:	Summary of Experimental Results.....	118
Table 3-3:	Summary of Measured Initial and Final Key Test Parameters.....	143

### **PAPER NO. 4: A COMPARATIVE STUDY OF SONOCHEMICAL AND ELECTROCHEMICAL DEGRADATION OF NAPHTHALENE IN AQUEOUS SOLUTION**

Table 4-1:	Experimental Variables.....	162
Table 4-2:	Summary of Measured Parameters.....	188

**PAPER NO. 5: DEGRADATION OF NAPHTHALENE IN THE AQUEOUS  
PHASE OF SPIKED SATURATED OTTAWA SAND**

Table 5-1: Summary of Experimental Parameters.....198

Table 5-2: Measured initial and final values of temperature, pH, standard redox potential, and electrical conductivity of test cells.....204

## LIST OF FIGURES

### **PAPER NO. 1: ELECTROREMEDIATION OF NAPHTHALENE IN AQUEOUS SOLUTION USING ALTERNATING AND DIRECT CURRENTS**

Figure 1-1:	Schematic of the experimental setup.....	22
Figure 1-2:	Change in concentration of naphthalene in solution for AC and DC tests with NaCl as supporting electrolyte.....	31
Figure 1-3:	Change in concentration of naphthalene in solution for DC tests with Na <sub>2</sub> SO <sub>4</sub> as supporting electrolyte.....	39
Figure 1-4:	Change in concentration of naphthalene in solution for AC tests with Na <sub>2</sub> SO <sub>4</sub> as supporting electrolyte.....	41

### **PAPER NO. 2: DEGRADATION OF PHENANTHRENE AND PYRENE IN SOLUTION USING ALTERNATING CURRENT**

Figure 2-1:	Schematic of the experimental setup.....	57
Figure 2-2:	Change in concentration of phenanthrene in solution.....	66
Figure 2-3:	Change in concentration of salicylic acid.....	70
Figure 2-4:	Change in concentration of phenanthrene with time using NaCl or Na <sub>2</sub> SO <sub>4</sub> as supporting electrolyte.....	73
Figure 2-5:	Effect of AC frequency on degradation rates of phenanthrene.....	75
Figure 2-6:	Temperature-time profile of test solutions containing only DI water and 30/70 Acetonitrile/DI water.....	76
Figure 2-7:	Effect of AC waveform shape on degradation rates of phenanthrene.....	79
Figure 2-8:	Concentration of pyrene versus time for various current densities.....	81
Figure 2-9:	Change in concentration of pyrene with time using NaCl or Na <sub>2</sub> SO <sub>4</sub> as supporting electrolyte.....	83
Figure 2-10:	Effect of AC frequency on degradation rates of pyrene.....	84
Figure 2-11:	Effect of AC waveform shape on degradation rates of pyrene.....	85

Figure 2-12:	Simulated concentrations <i>versus</i> test data for phenanthrene tests using DC.....	88
Figure 2-13:	Simulated concentrations <i>versus</i> test data for pyrene tests using DC.....	89
<b>PAPER NO. 3: EFFECT OF ALTERNATING CURRENT WAVEFORM AND FREQUENCY ON THE DEGRADATION OF NAPHTHALENE IN AQUEOUS SOLUTION</b>		
Figure 3-1(a):	Plan View of Hypothesized Funnel-and-Gate Electrochemical Reactive Barrier.....	101
Figure 3-1(b):	Cross-section of Hypothesized Funnel-and-Gate Electrochemical Reactive Barrier.....	102
Figure 3-2:	Schematic of the experimental setup.....	105
Figure 3-3:	Effect of AC waveform on the degradation rate of naphthalene.....	113
Figure 3-4:	Square; Sine; and Triangular AC signal having the same peak current..	114
Figure 3-5:	Effect of AC frequency on the degradation rate of naphthalene.....	116
Figure 3-6:	Effect of AC frequency on the pseudo-first-order degradation rate constants.....	121
Figure 3-7:	Effect of AC frequency on the rate of degradation of salicylic acid (hydroxyl radical probe).....	124
Figure 3-8:	Reduced rates of degradation of naphthalene in solutions in the presence of varying concentrations tertiary butanol (hydroxyl radical scavenger).....	126
Figure 3-9:	Simulated concentrations <i>vs</i> test results for naphthalene DC tests.....	129
Figure 3-10:	Effect of stirring on degradation rate of salicylic acid at different AC frequencies.....	134
Figure 3-11:	Simplified electrochemical degradation pathway of naphthalene in aqueous solution.....	137
Figure 3-12:	Change in concentration of naphthalene with time in a divided cell setup using AC and DC.....	140

Figure 3-13: Change in concentration of salicylic acid with time in a divided cell setup using AC and DC..... 142

**PAPER NO. 4: A COMPARATIVE STUDY OF SONOCHEMICAL AND ELECTROCHEMICAL DEGRADATION OF NAPHTHALENE IN AQUEOUS SOLUTION**

Figure 4-1: Schematic of experimental setup for sonochemical degradation of naphthalene in solution..... 156

Figure 4-2: Schematic of experimental setup for electrochemical degradation of naphthalene in solution..... 157

Figure 4-3: Concentration-time profile for both sonochemical and electrical degradation of naphthalene in solution at 30 W and 60 W output power.....163

Figure 4-4: Concentration-time profile for both sonochemical and electrical degradation of salicylic acid (OH radical probe) in solution at 30 W and 60 W output power..... 167

Figure 4-5: *Pseudo*-first-order degradation rate constants with respect to naphthalene and salicylic acid versus power.....168

Figure 4-6: Simplified sonochemical and electrochemical degradation pathway of naphthalene in solution with OH radicals as the primary oxidizing agent..... 175

Figure 4-7: Simplified alternative electrochemical degradation pathway of naphthalene in solution to naphthol with radical cation precursor.....178

Figure 4-8: Simulated concentrations *versus* test data for naphthalene tests using DC.....182

Figure 4-9: Simulated concentrations *versus* test data for salicylic acid tests using DC..... 184

**PAPER NO. 5: AQUEOUS PHASE DEGRADATION OF NAPHTHALENE IN SPIKED SATURATED OTTAWA SAND**

Figure 5-1: Schematic of the experimental setup.....195

Figure 5-2: Comparison of electrochemical degradation of naphthalene in spiked solution and sand using AC..... 199

Figure 5-3:	Comparison of electrochemical degradation of naphthalene in spiked solution and sand using DC.....	201
Figure 5-4:	Comparison of electrochemical degradation of naphthalene in spiked sand using AC and DC.....	202
Figure 5-5:	Effect of current density on electrochemical degradation of naphthalene in spiked sand using AC.....	207
Figure 5-6:	Effect of AC frequency on electrochemical degradation of naphthalene in spiked sand using AC.....	208

## KEY OF ABBREVIATIONS

AC = Alternating Current

API = Atmospheric pressure ionization

APCI = Atmospheric Pressure Chemical Ionization

ATSDR = Agency for Toxic Substance and Disease Registry

DC = Direct Current

DI = de-ionized

DO = Dissolved Oxygen

ESI = Electrospray Ionization

FERB = Funnel-and-gate Electrochemical Redox Barrier

HLB = Hydrophilic Lipophilic Balance

HPLC = High Performance Liquid Chromatography

LC = Liquid Chromatography

LCR = Inductance-Capacitance-Resistance

MCL = Maximum Contaminant Level

MDL = Method Detection Limit

MGP = Manufactured Gas Plant

MS = Mass Spectrometry

OH<sup>·</sup> = Hydroxyl Radical

PAH = Polycyclic Aromatic Hydrocarbon

RMS = Root Mean Square

USEPA = United States Environmental Protection Agency

UV = Ultraviolet

## KEY OF SYMBOLS

$C$  = Concentration at time ( $t$ ).

$C_0$  = Initial Concentration

$D$  = Diffusion coefficient

$E$  = Electrical potential

$f$  = AC frequency

$F$  = Faraday's constant

$j$  = current density

$J$  = Mass flux

$k$  = decay constant

$I_p$  = Peak Current

$I_{rms}$  = Root Mean Square Current

$R$  = Molar gas constant

$T$  = Temperature in Kelvin

$v$  = Linear velocity of solution

$V_p$  = Peak Voltage

$V_{rms}$  = Root Mean Square Voltage

$x$  = Distance in the  $x$  direction

$z$  = charge on a reacting species

$Z$  = Impedance



## **INTRODUCTION**

### **BACKGROUND ON PAHS**

Polycyclic Aromatic Hydrocarbons (PAHs) are a group of aromatic compounds consisting of two or more fused benzene rings. PAHs have been contaminants of concerns (COCs) over the past few decades because their toxicity and tendency to contaminate air, water, and soil. They are formed by incomplete combustion of coal, oil, or gas and organic matter such as grilled meat or tobacco. PAH contamination in the environment originates from sources such as volcanoes, forest fires, burning coal, automobile exhaust, discharges from industrial or wastewater treatment plants, or evaporation into air from contaminated soil or water.

PAHs occur in the atmosphere in both the solid phase (as particulates) and in the vapor phase. Three-ring PAH compounds are found in the atmosphere primarily in the gaseous phase, whereas, five- and six-ring PAHs are found mainly in the solid phase; four-ring PAH compounds are found in both phases (ASTDR 1995). Basu and Saxena (1978a) reported concentrations of selected PAHs in surface waters used as drinking water sources in four U.S. cities (Huntington, West Virginia; Buffalo, New York; and Pittsburgh and Philadelphia, Pennsylvania). Total concentrations of PAHs ranged from 4.7 ng/L in Buffalo to 600 ng/L in Pittsburgh. Data summarized by Sorrel et al. (1980) indicate low levels of PAHs in finished drinking waters of the United States. Reported maximum concentrations for total PAHs (based on measurement of 15 PAHs) in the drinking water of 10 cities ranged from 4 to 24 ng/L; concentrations in untreated water ranged from 6 to 125 ng/L. The relatively low concentrations of PAHs in finished drinking water were attributed to efficient water treatment processes as well low water

1

solubility of  
ranging from  
phenanthrene  
concentration  
range of 3  
concentration  
of the Nation  
the range of  
(Cole et al.  
Zappoli (19  
concentration  
ng L (phen...  
approximate  
Human  
fires or coal  
least 600 of  
Environment  
potential ca  
phenanthrene  
benzene ring

solubility of PAHs. Shiraishi et al. (1985) found PAHs in tap water at concentrations ranging from 0.1 to 1.0 ng/L, primarily as chlorinated derivatives of naphthalene, phenanthrene, fluorene, and fluoranthene. Basu and Saxena (1978b) reported total PAH concentrations in groundwater from three sites in Illinois, Indiana, and Ohio to be in the range of 3 to 20 ng/L. PAHs have been detected in urban runoff generally at concentrations much higher than those reported for surface water. Data collected as part of the Nationwide Urban Runoff Program indicate concentrations of individual PAHs in the range of 300 to 10,000 ng/L, with the concentrations of most PAHs above 1,000 ng/L (Cole et al. 1984). Industrial effluents also have elevated PAH levels. Morselli and Zappoli (1988) reported elevated PAH levels in refinery waste waters, with concentrations for most PAHs in the range of 400 ng/L (benzo[b]fluoranthene) to 16,000 ng/L (phenanthrene). Staples et al. (1985) reported median concentrations in sediment of approximately 500 µg/kg (dry weight) for 15 PAHs.

Human exposure to PAHs usually occurs by breathing air contaminated by wild fires or coal tar, or by eating foods that have been grilled. PAHs have been found in at least 600 of the 1,430 National Priorities List (NPL) sites identified by the United States Environmental Protection Agency (USEPA) (ASTDR 1995). PAHs are classified as potential carcinogens. Examples of PAHs include naphthalene (two benzene rings), phenanthrene (three benzene rings), anthracene (three benzene rings), pyrene (four benzene rings), benzo[a]pyrene (five benzene rings).

**EXISTING**

Several projects  
have been  
pilot-scale

- Granular  
contact  
reactors

- Permeable  
reactors

- Bioreactors  
contact

- Advanced  
UV irradiation  
some  
to degrade

- Membrane  
reactors  
are used  
removal

**ELECTRO**

Type of Electrode  
Electrochemical  
media to generate

## **EXISTING REMEDIATION TECHNIQUES**

Several potential remediation technologies for cleaning contaminated water and soils have been investigated at the laboratory scale and some of them have been applied in pilot-scale or field-scale settings. These technologies are summarized as follows.

- Granular activated carbon (GAC) adsorption techniques involve transferring contaminants from a liquid phase to a solid phase by sorption. In this process, no reactions take place and hence there is no degradation of the COC;
- Permeable reactive barriers (PRBs) with zero valent iron, limestone, compost, etc. have been used to treat contaminated groundwater;
- Bioremediation involves the use of microorganisms to degrade organic contaminants;
- Advanced oxidation treatments such as ozonation, hydrogen peroxide oxidation, UV irradiation, photochemical reactions, and Fenton oxidation or a combination of some of the above involves the generation of highly oxidizing OH radicals (OH<sup>•</sup>) to degrade contaminants in solution; and
- Membrane processes such as microfiltration, nanofiltration, and reverse osmosis are used to remove particles in water that are too small for conventional filters to remove.

## **ELECTROCHEMICAL DEGRADATION OF ORGANICS**

### **Type of Electrical Current**

Electrochemical methods typically involve electric current across electrodes in aqueous media to generate redox reactions. Numerous studies (e.g. Alshwabkeh and Sarahney



2005; Li e  
Cominelli  
degradation  
contaminant  
er al. 2005  
contaminant  
Alshwabke  
correspondi  
applied in e  
al 1991; H.  
Major  
although s  
Alshwabke  
review by W  
actual sites.  
1989; Lager  
substances.  
Before field  
objects and  
characteristic  
For m  
under an elec  
will result in

2005; Li *et al.* 2005; Goel *et al.* 2003; Stock and Bunce 2002; Saracco *et al.* 2000; Comminellis 1994) and applications (Kreysa G., Heitz E. 1986) on electrochemical degradation methods have focused on the use of direct current (DC) to degrade organic contaminants in solution. However, only a few studies (Chin and Cheng 1985; Nakamura *et al.* 2005) have explored the use of alternating current (AC) to degrade organic contaminants in solution. Reported applied currents have ranged between as low as 1 mA (Alshawabkeh and Sarahney 2005) and as high as 10,000 mA (Saracco *et al.* 2003) corresponding to current densities of  $0.075 \text{ mA/cm}^2$  and  $50 \text{ mA/cm}^2$ . Current densities applied in electroremediation of soils are commonly in the range  $0.025 - 5 \text{ A/m}^2$  (Acar *et al.* 1991; Hamed *et al.* 1991).

Majority of work on electroremediation has been conducted on laboratory scale, although some pilot-scale tests have been conducted (Gibbs 1966; Acar and Alshawabkeh 1996; Ho *et al.* 1997). Other examples of field trials are outlined in a review by Will (1995). A number of problems not encountered in the laboratory arise at actual sites, e.g. the presence of large objects ( $> 10 \text{ cm}$ ) buried in the soil (Lageman *et al.* 1989; Lageman 1993). Both conducting materials, such as metal objects, and resistive substances, such as concrete, will disrupt the normal current path (Page and Page 2002). Before field trials can be performed, site investigations are necessary to locate such objects and to provide information on the nature and distribution of contaminants and characteristics of the soil (Lindgren *et al.* 1998).

For molecular substances, electro-osmosis is the predominant form of transport under an electric field, although partial dissociation into ions of some organic molecules will result in electromigration as well (Page and Page 2002). Lageman *et al.* (1990) has

demonstrates  
feasible. R  
contaminan  
application

**Current Eff**

Stock and B

dechlorinat

to  $\geq 93\%$  of

applied cur

also report

electrocatal

to the fact th

reaction of

of atrazine

hydrogen be

surface and

**Target Org.**

Rajeshwar et

degradation

organic com

electrochem



demonstrated that the removal of a range of aromatic organic compounds from soils was feasible. Reddy and Saichek (2004) conducted laboratory investigation to determine contaminant mass removal from low permeability clay, by using periodic voltage application and surfactants.

### **Current Efficiency**

Stock and Bunce (2002) applied 5, 10, 20, 50, 100 and 200 mA currents to study the dechlorination efficiency of atrazine and reported that when applied currents  $\geq 20$  mA led to  $\geq 93\%$  loss of initial atrazine within 30 minutes. The current efficiency decreased as applied current increased and was greatest (16%) at 10 mA. Yusem and Pitauro (1992) also reported a decrease in current efficiency with increased applied current in electrocatalytic hydrogenation of soybean. Stock and Bunce (2002) attributed this trend to the fact that a greater proportion of adsorbed hydrogen ( $H_{ads}$ ) was lost to unproductive reaction of hydrogen gas evolution instead of participating in the dechlorination reaction of atrazine. At high current densities, the rate of electrochemical generation of adsorbed hydrogen becomes faster than the rate at which the substrate can migrate to the electrode surface and become adsorbed.

### **Target Organic Compounds**

Rajeshwar *et al.* (1994) and Rodgers *et al.* (1999) have demonstrated that electrochemical degradation can be used to treat waste water containing toxic and non-biodegradable organic compounds. Among others, organic compounds that have been used in published electrochemical degradation studies include:

(A)

• Ph

2f

• Co

(S)

• Atr

Bur

• 2,4-

332

• 2,4-

(Yas

• Sal

• 5,5-d

(Mar

• Trich

Degradation

Sonochemic

degradation

Thompson

aqueous sol

stem transfe

the indirect

- Naphthalene, with concentrations ranging between 8.3 mg/L to 35 mg/L (Alshwabkeh and Sarahney 2005; Goel *et al.* 2003);
- Phenol, with concentrations ranging between 100 mg/L to 9,400 mg/L (Li *et al.* 2005; Chin and Cheng 1985);
- Coumaric acid, with concentrations ranging between 10 mg/L to 400 mg/L (Saracco *et al.* 2003);
- Atrazine, with concentrations ranging between 4 mg/L to 83 mg/L (Stock and Bunce 2002);
- 2,4-dichlorophenoxyacetic acid, with concentrations ranging between 55 mg/L to 332 mg/L (Yasman *et al.* 2004);
- 2,4-dichlorophenol, with concentrations ranging between 57 mg/L to 244 mg/L (Yasman *et al.* 2004);
- Salicylic acid at a concentration of 1,000 mg/L (Marselli *et al.* 2003);
- 5,5-dimethyl-1-pyrroline-*N*-oxide (DMPO) at a concentration of 1,130 mg/L (Marselli *et al.* 2003); and
- Trichlorobenzene, at a concentration of 119 µg/L (Nakamura *et al.* 2005).

### **Degradation By-products**

Sonochemical degradation of organics in solution generally occurs through two distinct degradation pathways: oxidation by hydroxyl radicals and pyrolytic decomposition (Thompson and Doraiswamy 1999). In electrochemical oxidation, organic compounds in aqueous solutions can be oxidized on an anode (anodic oxidation) by indirect oxygen atom transfer and direct electron transfer (Rodgers *et al.* 1999; Kirk *et al.* 1985). During the indirect oxygen atom transfer, oxygen radicals, especially the hydroxyl radicals

generated

in 2001. S

readily rea

cause the r

The

aromatic c

2000. Otta

the presen

concluded

oxidation

sufficient

formation

the oxidat

One of the

surface, wh

attacked by

position, the

organic mol

## Electrodes

Various typ

including:

- Titani

0.12

generated from water electrolysis, help in the oxidation of organic substances (Iniesta *et al.* 2001; Simond *et al.* 1997; Comninellis 1994; Lee *et al.* 1981). The hydroxyl radicals readily react with the organic molecules adsorbed on or in the vicinity of the anode to cause the reaction presented below in Eq. 3 (Simond *et al.* 1997).

The formation of quinones has been reported by researchers who also observed aromatic quinones during electrolytic oxidation of aromatic hydrocarbons (Brillas *et al.* 2000; Oturan 2000; Panizza *et al.* 2000). GC/MS analysis by Goel *et al.* (2003) indicated the presence of 1,4-naphthoquinone when naphthalene solutions were electrolyzed and concluded that naphthalene degradation could be due to direct anodic oxidation, oxidation by an intermediate (e.g. hydroxyl radicals), or a combination of both. With sufficient OH<sup>•</sup> radicals in the reaction medium, ring cleavage may occur leading to the formation of carboxylic acids. Li *et al.* (2005) reported that benzoquinone formed from the oxidation of phenol could be degraded with ring breakage to various carboxylic acids. One of the proposed mechanisms involves the adsorption of benzoquinone onto the anode surface, which gives up an electron, and the carbon that is double-bonded with oxygen is attacked by a neighboring hydroxyl radical. When this process is repeated at the *para* position, the ring could be opened and benzoquinone would be broken down into small organic molecules such as carboxylic acids (Houk *et al.* 1998; Lund and Baizer 1991).

### **Electrodes**

Various types of electrodes that have been used in electrochemical degradation studies including:

- Titanium core with mixed metal coating with dimensions 10.2 cm by 1.3 cm by 0.12 cm (Alshawabkeh and Sarahney 2005);

r  
c  
• T  
a  
s  
• E  
e  
• F  
s  
• T  
• R  
• T  
P

Support  
Salts are  
electrical  
value. So  
studies in

• S  
2

- Stainless steel cathode (6.35 cm by 3.18 cm by 0.07 cm) and titanium anode with mixed metal oxide anode (6.35 cm by 3.18 cm by 0.07 cm) separated by a distance of 1.4 cm (Goel *et al.* 2003);
- Ti/SnO<sub>2</sub>-Sb, Ti/RuO<sub>2</sub>, and Pt anodes with dimensions 3 cm by 2 cm by 0.15 cm and stainless steel plates of the same dimensions were used as cathodes. The separation between the electrodes was 0.8 cm (Li *et al.* 2005);
- Boron-doped diamond and lead oxide anodes, 20 cm<sup>2</sup> area was exposed to the electrolyte (Panniza and Cerisola 2003);
- Platinized titanium anode and stainless steel plate as cathode, the electrode surface area was 200 cm<sup>2</sup> (Saracco *et al.* 2000);
- Ti-Ru-Sn-SbO<sub>2</sub>, Ti/Pt and carbon electrodes (Panizza *et al.* 2000);
- Reticulated vitreous carbon (RVC) (Stock and Bunce 2002); and
- Ti/SnO<sub>2</sub>-Sb and Ti/IrO<sub>2</sub> anodes with 4 cm<sup>2</sup> surface area and the cathode was a platinum spiral enclosed in a 10 ml porous porcelain pot (Comninellis 1994).

### **Supporting Electrolyte**

Salts are normally added to reacting media as supporting electrolyte to increase the electrical conductivity in order to reduce the voltage required to produce a given current value. Some supporting electrolytes that have been used in published electrochemical studies include:

- Sodium chloride, 50 ml of 0.2 M NaCl was used (Alshawabkeh and Sarahney 2005); 0 up to 10 g/L (Panizza *et al.* 2000);

2.

- S
- L
- S
- I

Analytical

Analytical

identify de

degradati

(HPLC),

(LCMS),

Carbon

Spectroph

Chromato

DEGRAD

Ultrasoun

Various ty

organics. T



- Sodium sulfate ( $\text{Na}_2\text{SO}_4$ ), 1.42 g/L (Goel *et al.* 2003); 35.5 g/L (Li *et al.* 2005); 2.84 g/L (Saracco *et al.* 2000); 21.3 g/L (Stock and Bunce 2002);
- Sodium nitrate ( $\text{NaNO}_3$ ) (Alshawabkeh and Sarahney 2005);
- Lithium chloride ( $\text{LiCl}$ ), 6.36 g/L (Stock and Bunce 2002);
- Sodium hydroxide ( $\text{NaOH}$ ), 0.8 g/L (Nakamura *et al.* 2005); and
- 1 M sulfuric acid ( $\text{H}_2\text{SO}_4$ ) (Stock and Bunce 2002; Chin and Cheng 1985).

### **Analytical Techniques**

Analytical techniques that have been used to quantify concentrations and to qualitatively identify degradation by products of organic contaminants in sonochemical and electrical degradation studies include among others: High Performance Liquid Chromatography (HPLC), Gas Chromatography (GC), Liquid Chromatography / Mass Spectrometry (LC/MS), Gas Chromatography / Mass Spectrometry (MS), LC/MS/MS, Total Organic Carbon (TOC) Analyzer, Chemical Oxygen Demand (COD) Analyzer, Spectrophotometer, Electron Spin Resonance (ESR), Micellar Electrokinetic Capillary Chromatography (MECC), and Solid-Phase Micro-Extraction (SPME).

## **DEGRADTION OF ORGANICS USING ULTRASOUND**

### **Ultrasound Equipment**

Various types of ultrasound equipment have been used in sonochemical degradation of organics. These include:

•

•

•

•

Target

Organic

among

•

•

•

•

r

- An Ultrason 250 (LabPlant Ltd., UK) operating at a frequency of 80 Hz, and UP 400S (Dr Hielscher GmbH, Germany) operating at a frequency of 24 Hz. Ultrasound energy was delivered through horn-type probes (Psillakis *et al* 2004).
- An IKA Labortechnik IKASONIC U50 control unit operating at a frequency of 30 Hz. Ultrasound energy was delivered *via* titanium probes (Little *et al.* 2002).
- An ultrasonic transducer UES 1.5 – 660 pulsar (Ultrasonic Energy Systems Inc.) operating at 640 – 690 Hz frequency (Kim *et al.* 2002).
- Three ultrasound systems, a vibrating plate reactor (VPR, 358 Hz), a near field acoustical processor (NAP, 16 & 20 Hz), and radial tube resonator (RTR, 20 Hz). Ultrasound energy was delivered through transducers with areas 25 cm<sup>2</sup>, 1262 cm<sup>2</sup>, and 376 cm<sup>2</sup>, for VPR, NAP, and RTR respectively (Hung *et al.* 2002).
- A Misonics sonicator operating at a frequency of 20 kHz. The ultrasound energy was delivered through a horn-type titanium probe (Goskonda *et al.* 2002).

### **Target Compounds**

Organic compounds that have been used in sonochemical degradation studies include, among others:

- Methyl *tert*-Butyl Ether (MTBE) at a concentration of 37 mg/L (Hung *et al.* 2002);
- 2,4-dinitrophenol at a concentration of 20 mg/L (Guo *et al.* 2005);
- Phenanthrene, at a concentration of 1.25 mg/L (Wheat and Tumeo 1997);
- Biphenyl at concentrations ranging between 0.6 mg/L (Little *et al.* 2002) and 1.25 mg/L (Wheat and Tumeo 1997);

- All 16 PAHs listed by USEPA at total initial concentration of 480  $\mu\text{g/L}$  (Psillakis *et al.* 2003); and
- Organic pollutants in landfill leachate, with initial COD of 4770  $\text{mg/L}$  (Wang *et al.* 2005).

1

## OBJECTIVE

The key

of PAHs

phenanth

electroch

investigat

degradati

on degrad

electrode

oxidation

rate of deg

energy (A

Labo

above. The

Tests were

1-liter sol

eliminate

the cap. U

MHz Swe

consisted

AC DC an

current me

## OBJECTIVES AND METHODOLOGY

The key objectives of this dissertation were to: (1) evaluate electrochemical degradation of PAHs in spiked aqueous solutions using an alternating current (AC). Naphthalene, phenanthrene and pyrene were used as model PAH compounds; (2) evaluate electrochemical degradation of PAHs in saturated spiked Ottawa sand using AC; (3) investigate the effect of current density, AC waveform shape and frequency on the degradation rates of naphthalene; (4) compare the efficiency of DC and an equivalent AC on degradation rates of PAHs; (5) prove that anodic oxidation of PAHs occurred on both electrodes when AC electrolysis was used unlike DC electrolysis in which anodic oxidation of naphthalene occurred on only one electrode (the anode); and (6) compare the rate of degradation of PAHs in aqueous solution using ultrasound energy and electrical energy (AC and DC) delivered at the same output power.

Laboratory scale tests were conducted in order to achieve the objectives listed above. The test cell setup consisted of a 1 liter Pyrex glass beaker with a Teflon cap. Tests were conducted in batch modes in undivided cell as well as divided cell setup with 1-liter solution in each compartment. These materials of the cell were selected to eliminate or reduce sorption of the contaminants onto the walls of the reaction vessel and the cap. Untreated Titanium plates were used as electrodes for this study. A 0.1 Hz to 2 MHz Sweep Function Generator was used to generate the AC signals. The power supply consisted of a bipolar operational power supply/amplifier capable of producing 200 V AC/DC and 1 A AC/DC output or a maximum electrical power of 200 W. Voltage and current measurements were obtained with the aid of an oscilloscope. The ultrasound

equipment

frequency

At

(98% pur

mixture :

the collec

solutions

naphthal

identificat

and pyrene

pyrene in

compound

solutions

concentrat

just enoug

binary sol

increase th

(Na<sub>2</sub>SO<sub>4</sub>)

of sodium

solution to

Prior

performanc

equipment used was a Sonics VCX 750 that operated in a continuous mode at a fixed frequency of 20 kHz.

Aqueous solutions, spiked with naphthalene were prepared by adding naphthalene (98% purity) crystals to deionized (DI) water in a capped Pyrex bottle and allowing the mixture to stand. The excess suspended naphthalene crystals were then filtered off and the collected filtrate was used for the tests. The average concentration of naphthalene solutions used in this study was 20 mg/L (~0.15 mM) so that adequate amounts of naphthalene would be available in solution for quantification of concentrations and identification of degradation byproducts. Due to relatively low solubility of phenanthrene and pyrene in water, a cosolvent (acetonitrile) was used to dissolve phenanthrene and pyrene into solution at concentrations greater than the aqueous solubility of the compounds. 10 mg or 5 mg/L of phenanthrene or pyrene crystals were added to one liter solutions of acetonitrile (30%) and deionized (DI) water (70%) (v/v) to achieve target concentrations of 10 mg/L or 5 mg/L, respectively. The proportion of acetonitrile was just enough to ensure that the PAH with the lower solubility, pyrene, remained in the binary solution without precipitating out to form crystals in the solution. In order to increase the electrical conductivity of the electrolyte, NaCl and anhydrous sodium sulfate ( $\text{Na}_2\text{SO}_4$ ) were added as the supporting electrolytes in separate sets of experiments. 0.5 g of sodium chloride (NaCl) or sodium sulfate ( $\text{Na}_2\text{SO}_4$ ) crystals were added to 1 liter test solution to produce 500 mg/L NaCl or  $\text{Na}_2\text{SO}_4$  solution.

Prior to passing AC through the cells, initial samples were taken for high performance liquid chromatography (HPLC) analyses. During the tests, samples were



taken for  
samples  
Samples  
analyses  
cells exce  
at the sam

DISSER

This disse  
the degrad  
the effect  
naphthalen  
phenanthro

addresses  
naphthalen  
used to de  
electrochem  
to prove t

unlike DC  
anode). Et  
experiment  
and migrat  
of naphtha

taken for HPLC analyses at elapsed time intervals of 1, 2, 4, 8, 24, and 48 hours. The samples were analyzed directly without extracting the PAH from the aqueous solution. Samples were also collected for Liquid Chromatography / Mass Spectrometry (LC/MS) analyses to determine the degradation products formed. Control cells, similar to the test cells except without any current passed through them were set up, sampled, and analyzed at the same time intervals as the test cells.

## **DISSERTATION ORGANIZATION**

This dissertation has been organized into five sections. The first paper compares the degradation of naphthalene in spiked aqueous solution using AC and DC, as well as the effect of current density and the supporting electrolyte on the rates of degradation for naphthalene. The second paper investigates the electrochemical degradation of phenanthrene and pyrene in 30% acetonitrile and 70% de-ionized (DI). The third paper addresses the effect of AC waveform and frequency on the degradation rates of naphthalene in spiked aqueous solution. Hydroxyl radical probes and scavengers were used to demonstrate that hydroxyl radicals were the primary oxidizing agents in both electrochemical and sonochemical degradation of organics. A divided cell setup was used to prove that anodic oxidation of PAHs occurs on both electrodes in AC electrolysis, unlike DC electrolysis in which anodic oxidation occurs on only one electrode (the anode). Effect of current density and AC frequency is evaluated in this paper using experimental data as well as modeling the degradation of the PAHs using 1-D diffusion and migration equation. The fourth paper presents a comparative study of the degradation of naphthalene in spiked aqueous solution using electrical (AC and DC) energy and

ultras

satura

1

ultrasound energy. The fifth paper presents the degradation of naphthalene in spiked saturated Ottawa sand using AC and DC.

PAPE  
AQU

ABSTR

The key

the degr

of curren

used to c

sulfate c

byproduct

naphthalen

Naphthalen

subjected

using NaCl

naphthalen

effect of

aqueous s

m.A cm<sup>2</sup> c

AC peak c

87% and

DC applic

# **PAPER NO. 1: ELECTROREMEDIATION OF NAPHTHALENE IN AQUEOUS SOLUTION USING ALTERNATING AND DIRECT CURRENTS**

## **ABSTRACT**

The key objectives of this study were to evaluate the use of alternating current (AC) for the degradation of naphthalene in spiked aqueous solutions and to investigate the effect of current density on the degradation rates of naphthalene. Direct current (DC) was also used to compare the rates of degradation. Sodium chloride (NaCl) and anhydrous sodium sulfate ( $\text{Na}_2\text{SO}_4$ ) were used as the supporting electrolytes. Degradation rates and byproducts formed were investigated when DC and AC were separately passed through naphthalene solutions. A square wave AC, having a frequency of 0.1 was used. Naphthalene solutions having an initial concentration of about 20 mg/L (~0.15 mM) were subjected to an AC peak current density of  $6 \text{ mA/cm}^2$  and DC density of  $6 \text{ mA/cm}^2$ , using NaCl as the supporting electrolyte. About 70% reduction in concentration of the naphthalene in solution was observed after a period of 48 hrs when DC was applied. The effect of current density on the electrochemical degradation rate of naphthalene in aqueous solution was also investigated at current densities of  $1 \text{ mA/cm}^2$  (AC; DC),  $3 \text{ mA/cm}^2$  (AC; DC), and  $6 \text{ mA/cm}^2$  (AC; DC) using  $\text{Na}_2\text{SO}_4$  as the supporting electrolyte. AC peak current densities of 1, 3, and  $6 \text{ mA/cm}^2$  resulted in overall conversions of 77%, 87% and 95%, respectively, of naphthalene in solution and the corresponding values for DC application were 95% for all current densities except the initial degradation rates

were hi

hydroxy

## INTRO

Polycycli

chemical

carcinoge

consist o

arranged

to Lee et

Harvey (

animals. I

PAH (Cen

estimates

across the

quantities

benzo(a)P

water sup

range from

Re

concern a

techniques

approache

were higher for higher DC densities. Based on the degradation products formed, hydroxylation is believed to be the key mechanism for the degradation of naphthalene.

## **INTRODUCTION**

Polycyclic aromatic hydrocarbons (PAHs) are a group of ubiquitous and nonionic organic chemicals that are of great environmental concern due to their toxicity and suspected carcinogenicity (Fernández et al. 2000). PAHs are a class of organic compounds that consist of two or more fused benzene rings and/or pentacyclic molecules that are arranged in various chemical configurations (Bamforth and Singleton 2005). According to Lee et al. (1981), PAHs are the largest class of chemical carcinogens. Clar (1964) and Harvey (1991) have reported in detail about the evidence of PAH carcinogenicity in animals. In general, the greater the number of benzene rings, the higher the toxicity of the PAH (Cerniglia 1992). The United States Environmental Protection Agency (USEPA) estimates that 3,000 to 5,000 former manufactured gas plant (MGP) sites are located across the United States and many of these contaminated sites contain substantial quantities of PAHs (USEPA 2000). The USEPA maximum contaminant level (MCL) for benzo[a]pyrene (PAHs) is 0.2 µg/L (epa.gov). PAHs have been found in some drinking water supplies in the United States and background levels of PAHs in drinking water range from 4 ng/L to 24 ng/L (ATSDR 1995).

Remediation of contaminated soil and groundwater is an important issue that is of concern among environmentalists and hydrogeologists. *In-situ* and *ex-situ* treatment techniques may be used to remediate contaminated soil and groundwater. Several approaches including biodegradation and advanced oxidation processes have been used to



1

degre

aque

meth

medi

BAC. G

The d

variou

condu

solutio

DC El

Alshav

electro

setup.

with a

electro

with m

0.12-cm

increas

m.A.L.

concent

transfor

naphthal

degrade PAHs in solution. Electrochemical degradation of organic contaminants in aqueous solution is an emerging remediation technique. Existing electrochemical redox methods depend on passing a direct current (DC) through electrodes in an aqueous medium.

## **BACKGROUND**

The degradation of organics such as PAHs, phenol, benzene etc. has been investigated by various researchers using DC electrolysis. However, relatively few studies have been conducted where AC electrolysis was explored for the degradation of organics in solutions.

### **DC Electrolysis**

Alshawabkeh and Sarahney (2005) investigated the effect of DC density on electrochemically enhanced transformation of naphthalene in solution. A divided cell setup, connected by a glass tube was used. Each compartment was a 550 ml glass bottle with a Nafion membrane in the connecting glass tube physically separated the electrolytes in the two compartments. The electrodes were made up of titanium mesh with mixed metal oxide coating. The electrodes were 10.2-cm-long by 5.0-cm-wide by 0.12-cm-thick. 50 ml NaCl solution (0.2 M) was used as supporting electrolyte to increase the electrical conductivity of the electrolyte. Three DC densities: 1 mA/L, 9 mA/L, and 18 mA/L were used to explore naphthalene transformation at two initial concentrations (13 mg/L and 25 mg/L). Both concentration levels depicted increase in transformation rates with increase in the current density. The transformation rate of naphthalene was enhanced by electro-generation of  $\text{Cl}_{2(g)}$  from  $\text{Cl}^-$  in solution. The pH of

the anolyte

potential

mA L cur

four by pr

Go

initial con

study we

stainless

mesh an

was used

at curren

degradat

1,4-naph

Li

electroch

mg L us

density c

beakers

$\text{Na}_2\text{SO}_4$

$\text{F. SnO}_2$

the anolyte dropped from its initial value of about 5.5 to 1.9 and the corresponding redox potential increased from about 500 mV to 1380 mV at the end of the test period when 9 mA/L current density was used. Transformation of naphthalene at the anolyte produced four byproducts as indicated by relatively small peaks on the chromatogram.

Goel *et al.* (2003) explored the degradation of naphthalene in solution (having an initial concentration of about  $9.8 \pm 1.5$  mg/L using DC. The reactor vessels used for this study were 500 ml amber-colored bottles undivided cells. The electrodes consisted of a stainless steel cathode and a 6.35-cm-long by 3.18-cm-wide by 0.15-cm-thick titanium mesh anode with mixed metal oxide coating. 1.42 g/L sodium sulfate ( $\text{Na}_2\text{SO}_4$ ) (0.01 M) was used to increase the conductivity of the electrolyte. The solutions were electrolyzed at current densities ranging from  $1.2 \text{ mA/cm}^2$  to  $9.9 \text{ mA/cm}^2$ . In this study, naphthalene degradation rates were insensitive to current density and independent of the system pH. 1,4-naphthoquinone was identified as a byproduct of the electrolysis.

Li *et al.* (2005) conducted laboratory experiments on the kinetics and pathway of electrochemical degradation of phenol having initial concentrations equal to 100 and 490 mg/L using three materials for the anode: Ti/SnO<sub>2</sub>-Sb, Ti/RuO<sub>2</sub>, and Pt at a current density of  $20 \text{ mA/cm}^2$ . The tests were conducted in batch electrolysis using 100 ml glass beakers and the electrodes were 3-cm-long by 2-cm-wide by 0.15-cm-thick. 0.25 M Na<sub>2</sub>SO<sub>4</sub> was used as the supporting electrolyte. The fastest degradation occurred on Ti/SnO<sub>2</sub>-Sb followed by Pt followed by the Ti/RuO<sub>2</sub> anode. Nevertheless, complete

3

phenol r

electroch

AC Elect

Chin and

and the

reference

acid. A

electrolys

used as a

magnitud

frequency

hydroqu

Na

an initial

15V AC

electrode

long by 3

long and

NaCl (20

2-ethyl-1-

trichloro

phenol removal was achieved by all the anodes. Intermediate byproducts of the electrochemical degradation of naphthalene included benzoquinone and organic acids.

### **AC Electrolysis**

Chin and Cheng (1985) superimposed a constant alternating voltage onto a DC potential and the resulting composite potential wave was applied between the working and reference electrodes. The electrolyte consisted of 0.01 to 0.1 M phenol in 1 M sulfuric acid. A platinum foil having 12.5 cm<sup>2</sup> area was used as the anode for batch cell electrolysis of phenol. A 1 liter glass jar immersed in a constant temperature bath was used as an undivided cell. The rate of conversion of phenol increased with increasing magnitude of the alternating voltage and decreased with increasing alternating voltage frequency. Phenol was oxidized to benzoquinone and eventually reduced to hydroquinone.

Nakamura *et al.* (2005) investigated the decomposition of trichlorobenzene having an initial concentration of 0.66  $\mu$ M by AC electrolysis in aqueous solution. A 30-kHz, 15V AC potential was applied to the working electrode, counter electrode, and ground electrode. Each electrode was a titanium plate coated with platinum and was 17.5-cm-long by 3.5-cm-wide by 0.1-cm-thick. The reactor was an undivided cell, about 19 cm long and 9.5 cm in diameter with a cap. The supporting electrolytes were NaOH and NaCl (20 mM). Trichlorobenzene was degraded to intermediate products which included 2-ethyl-1-hexanol when NaOH was used as the supporting electrolyte and to trichloromethane when NaCl was used as the supporting electrolyte.

1

OBJE

The key

can be

and (2)

Naphth

compo

2003) r

similar

naphth

PAHs.

MATE

The ex

detailed

## **OBJECTIVES**

The key objectives of this study were to: (1) demonstrate that alternating current (AC) can be used for electrochemical degradation of naphthalene in a spiked aqueous solution; and (2) investigate the effect of current density on the degradation rates of naphthalene. Naphthalene, which contains two fused benzene rings, was selected as a model PAH compound because in published studies (Alshawabkeh and Sarahney 2005); Goel *et al.* 2003) naphthalene has been used. Also, naphthalene has chemical and physical properties similar to other PAHs, except that it is more soluble in water, a property that makes naphthalene more available in aqueous solution and more exposed to reactivity than other PAHs.

## **MATERIALS AND EXPERIMENTAL METHODOLOGY**

The experimental setup is illustrated in Figure 1-1 and the various components are detailed as follows:





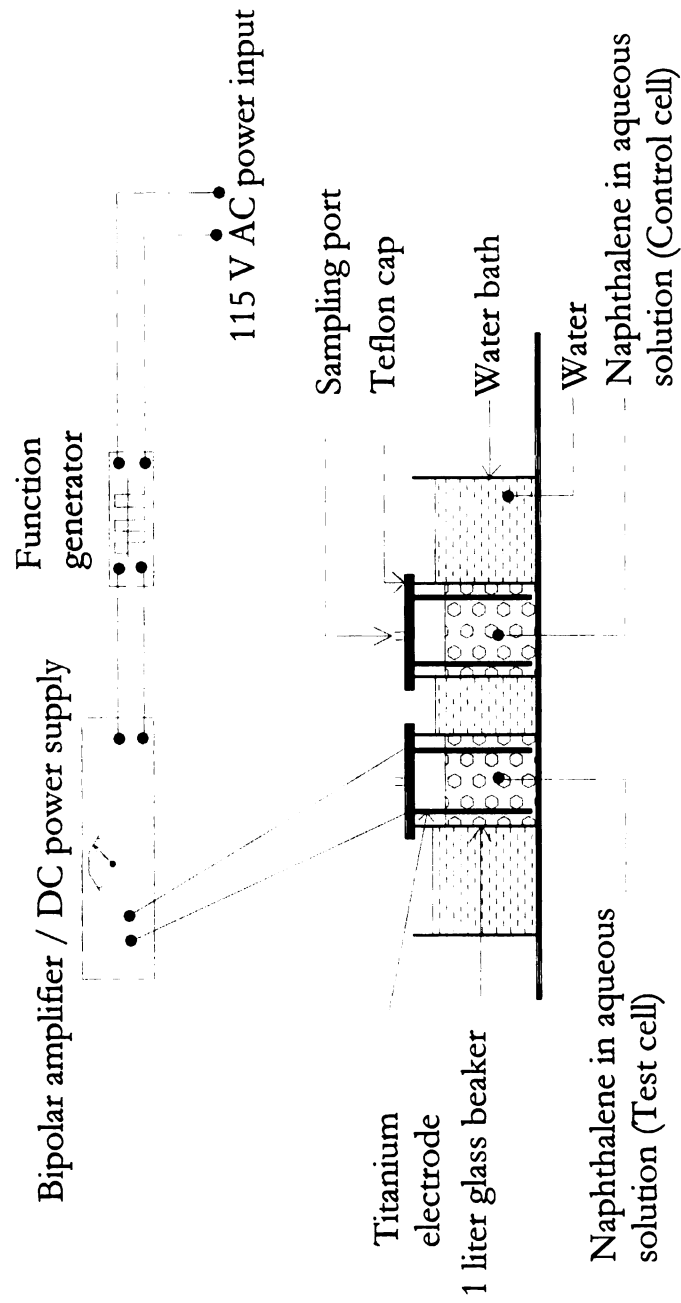


Figure 1-1: Schematic of the experimental setup

1

**Reaction**

The test

consisted

were se

walls of

applicati

Grade 2

Alshawa

(1994) a

and SnO

cheaper

project.

condition

used as

between

electrode

as sample

and DC

carried o

were used

was obser

spiked w

## Reaction Chamber

The test cells (reaction chambers), which were undivided cells operating in batch modes, consisted of one liter Pyrex glass beakers with a snugly fit Teflon cap. These materials were selected to eliminate or reduce sorption of naphthalene and byproducts onto the walls of the reaction vessel and cap. The test solution was not mixed during the application of the current. Ultra corrosion-resistant pure high strength titanium sheets, Grade 2 (98.9%, purity) and Grade 5 (95%, purity) were used as electrodes for this study. Alshawabkeh and Sarahney (2005), Goel et al. (2003), Li et al. (2005), and Comninellis (1994) used titanium as a base metal and coated it with mixed metal oxides ( $\text{RuO}_2$ ,  $\text{IrO}_2$ , and  $\text{SnO}_2$ ). The titanium plates used in this study were not coated. Uncoated titanium is cheaper than gold, platinum, or titanium coated electrodes and hence was selected for this project. Titanium offers more resistance to corrosion in a wide range of aggressive conditions and can therefore be used for potential field application. The titanium sheets used as electrodes in this project were 12.0-cm-long by 5.0-cm-wide and the distance between them was maintained equal to 8.0 cm. The contact area of the solution with each electrode was  $55 \text{ cm}^2$  at the beginning of the test and decreased to approximately  $53 \text{ cm}^2$  as samples were collected for analyses. The thickness of the electrodes used for the AC and DC application was 1.7 mm for Grade 2 electrodes. However, few DC tests were carried out with thicker ( $\sim 3.2 \text{ mm}$ ) Grade 5 electrodes (Table 1-1). Thicker electrodes were used for the DC application because substantial loss of electrode mass of the anode was observed when thinner electrodes were tested. The volume of the aqueous solutions spiked with naphthalene in the test and control cells was one liter.



Electric

An AC

generate

AC when

to the p

from ne

stays the

current i

the other

peak vol

equivalen

The pow

producing

**Spiked S**

Aqueous

purity) cr

to stand.

dissolves

2003). is

solution.

collected

## **Electrical Equipment**

An AC function generator/counter capable of delivering 20  $V_{p-p}$  (AC) was used to generate a square wave AC. An AC square wave was selected because unlike a sinusoidal AC where during a single cycle, the voltage gradually increases from negative maximum to the positive maximum and back again, an AC square wave function shifts suddenly from negative to positive, stays there for half a cycle, and then jumps to full negative and stays there for half a cycle. Therefore, in one half cycle of the AC wave, the alternating current instantaneously flows in one direction and then flows in the opposite direction in the other half cycle. The root mean square voltage ( $V_{rms}$ ) of a square wave is equal to its peak voltage ( $V_p$ ) unlike a sine wave whose  $V_{rms}$  is equal to  $0.707V_p$ . Hence, an equivalent square wave current delivers more electrical power for the same peak voltage. The power supply consisted of a bipolar operational power supply/amplifier capable of producing 200 V AC and 1 A AC output or a maximum electrical power of 200 W.

## **Spiked Solution Preparation**

Aqueous solutions, spiked with naphthalene were prepared by adding naphthalene (98% purity) crystals to deionized (DI) water in a capped Pyrex bottle and allowing the mixture to stand. The greater the retention time, the greater the amount of naphthalene that dissolves into solution, until its aqueous solubility of 32.2 mg/L (Schwarzenbach et al. 2003), is reached when there is no more increase in the concentration of naphthalene in solution. The excess suspended naphthalene crystals were then filtered off and the collected filtrate was used for the tests. The average concentration of naphthalene

solution

naphthal

identific

Support

In order

sodium

experim

---

Support

Electro

---

NaCl

---

NaCl

---

NaCl

---

Na<sub>2</sub>SO<sub>4</sub>

---

Na<sub>2</sub>SO<sub>4</sub>

---

Na<sub>2</sub>SO<sub>4</sub>

---

Na<sub>2</sub>SO<sub>4</sub>

---

solutions used in this study was 20 mg/L (~0.15 mM) so that adequate amounts of naphthalene would be available in solution for quantification of concentrations and identification of degradation byproducts.

### Supporting Electrolyte

In order to increase the electrical conductivity of the electrolyte, NaCl and anhydrous sodium sulfate ( $\text{Na}_2\text{SO}_4$ ) were used as supporting electrolytes in separate sets of experiments (Table 1-1).

Table 1-1: Experimental variables.

Supporting Electrolyte	Applied Current (mA)	Electrode Grade, (%Purity); and Thickness (mm)	Current Density			Total Tests
			mA	mA/cm <sup>2</sup>	mA/cm <sup>3</sup>	
NaCl	330 (AC)	Grade 2 (98.9%); 1.7 mm	330	6	0.33	2
NaCl	330 (DC)	Grade 5 (95%); 3.2 mm	330	6	0.33	2
NaCl	0 (Control)	Grade 2 (98.9%); 1.7 mm	0	0	0	2
$\text{Na}_2\text{SO}_4$	55 (AC)	Grade 2 (98.9%); 1.7 mm	55	1	0.055	2
$\text{Na}_2\text{SO}_4$	55 (DC)	Grade 2 (98.9%); 1.7 mm	55	1	0.055	2
$\text{Na}_2\text{SO}_4$	165 (AC)	Grade 2 (98.9%); 1.7 mm	165	3	0.165	2
$\text{Na}_2\text{SO}_4$	165 (DC)	Grade 2 (98.9%); 1.7 mm	165	3	0.165	2





Table

Na<sub>2</sub>S

Na<sub>2</sub>S

Na<sub>2</sub>S

Note

1. 7

2. 7

naphtha

the degr

electroly

resultant

concentr

densities

Saracco

Na<sub>2</sub>SO<sub>4</sub>

reduce th

operating

Table 1-1 Cont'd

Na <sub>2</sub> SO <sub>4</sub>	330 (AC)	Grade 2 (98.9%); 1.7 mm	330	6	0.33	2
Na <sub>2</sub> SO <sub>4</sub>	330 (DC)	Grade 2 (98.9%); 1.7 mm	330	6	0.33	2
Na <sub>2</sub> SO <sub>4</sub>	0 (Control)	Grade 2 (98.9%); 1.7 mm	0	0	0	2
				<b>Total Number of Tests:</b>		<b>20</b>

## Notes:

1. The frequency of the AC for all the tests was 0.1 Hz.
2. The volume of the test solution was 1 liter.

Alshawabkeh and Sarahney (2005) used NaCl in electrochemical degradation of naphthalene in aqueous solution and showed that electro generation of Cl<sub>2(g)</sub> enhances the degradation of naphthalene in solution. For experiments with NaCl as supporting electrolyte, 0.5 g of sodium chloride crystals were dissolved in a one-liter solution. The resultant concentration of NaCl was approximately 500 mg/L (~8.5 mM). This concentration which is relatively low was selected in order to achieve the target current densities that could be delivered by the power supply available for the tests in this study. Saracco *et al.* (2000) performed tests where electrolyte salt concentrations (e.g. NaCl, Na<sub>2</sub>SO<sub>4</sub>, H<sub>2</sub>SO<sub>4</sub>) ranged from 0.2 – 2 M and reported that higher salt concentrations reduce the electrical resistance between the electrodes and hence will reduce the operating costs. However, greater salt concentration would result in greater post-



treatme

represent

500 mg

degrad...

selected

at 500 m

potentia

support...

test sol...

material

formed a

than the

### Testing I

Prior to

for ana

Chromat

analyses

square w

frequency

electroly

with incre

treatment costs and hence would be less favorable. The only exception might be represented by discharging the treated effluent into the sea (Saracco *et al.* 2000).

For experiments with Na<sub>2</sub>SO<sub>4</sub> as the supporting electrolyte, a concentration of 500 mg/L (~3.5 mM) was used. Goel *et al.* (2003) used sodium sulfate in electrochemical degradation of naphthalene in aqueous solution using DC. This concentration was selected because the USEPA has proposed a maximum contaminant level goal of sulfate at 500 mg/L (~3.5 mM) and hence the proposed electrochemical degradation technique is potentially environmentally friendly. Unlike when NaCl was used, using Na<sub>2</sub>SO<sub>4</sub> as the supporting electrolyte did not result in any significant mass loss of the electrodes, and the test solutions did not form any precipitates as a result of corrosion of the electrode material, particularly the anode in the DC tests. Also no chlorinated by products were formed as was the case when NaCl was used. Chlorinated by products may be more toxic than the parent compound.

### **Testing Procedure**

Prior to passing current through the solution in the cells, initial samples were collected for analyzing naphthalene concentration using High Performance Liquid Chromatography (HPLC). Liquid Chromatography/Mass Spectrometry (LC/MS) analyses were also conducted on test cell samples as well as control cell samples. An AC square wave, having a frequency of 0.1 Hz was applied to the AC cell test cells. This AC frequency was selected because Chin and Cheng (1985) conducted a study on AC electrolysis using phenol and reported that the rate of conversion of phenol decreased with increasing alternating voltage frequency. Hence, we used the lowest AC frequency

1

product  
density  
also inv  
at these  
current  
electroly  
was carr  
T  
average  
in contac  
analyses  
current de  
A  
using NaCl  
mass (~ 6  
the soluti  
electrodes  
negligible  
various cur  
summarize

produced by the function generator that was available for this study. The effect of AC density on the rate of electrochemical degradation of naphthalene in aqueous solution was also investigated by maintaining the frequency constant at 0.1 Hz. Tests were performed at these three AC densities: 1 mA/cm<sup>2</sup> (55 mA peak current), 3 mA/cm<sup>2</sup> (165 mA peak current), and 6 mA/cm<sup>2</sup> (330 mA peak current) using Na<sub>2</sub>SO<sub>4</sub> as the supporting electrolyte. An additional test for AC density equal to 6 mA/cm<sup>2</sup> (165 mA peak current) was carried out using NaCl as the supporting electrolyte.

The AC peak current density was obtained by dividing the peak current by the average area of each electrode in contact with the solution. The level of the test solutions in contact with the electrode decreased as samples were collected for measurements and analyses. Therefore the reported current density is average value of the initial and final current densities.

A test at DC density equal to 6 mA/cm<sup>2</sup> (165 mA, peak current) was carried out using NaCl as the supporting electrolyte. However, the anode lost a significant amount of mass (~ 6%) within 24 hours of the application of the DC and formation of precipitates in the solution was observed. However, during an equivalent AC test, the mass loss of both electrodes was negligible (< 1%) and the mass loss for DC as well as AC tests was negligible when Na<sub>2</sub>SO<sub>4</sub> was used as the supporting electrolyte. Hence, more tests at various current densities were carried out with Na<sub>2</sub>SO<sub>4</sub> as the supporting electrolyte as summarized in Table 1-1.

Sampli

Replica

solution

samplin

error ba

normali

total fe

24. and

electrica

samples

with U

extractin

interfere

(Alshawa

detector

column.

The flow

(v) ace

minutes

prepared

with an a

naphthal

## Sampling

Replicate tests were performed to evaluate the change in concentration of naphthalene in solution with time. A summary of tests carried out is presented in Table 1-1. For each sampling round, two samples were analyzed with HPLC to quantify concentrations. The error bars in Figures 1-2, 1-3, and 1-4 represent the maximum and minimum values of the normalized concentration ( $C/C_0$ ) for the initial test and the replicate test recorded for the total four samples.

Samples were collected for HPLC analysis at time intervals equal to 0, 1, 2, 4, 8, 24, and 48 hrs. The reaction chamber was not mixed. Samples were collected while the electrical current was applied and the test was not paused during sampling. The analysis of the samples to determine the concentration of naphthalene in aqueous solution was consistent with U.S EPA Methods 550, 610 and 8310. Samples were analyzed directly without extracting the PAH from the aqueous solution. This procedure minimizes potential interferences from reagents, solvents and glassware required for the extraction method (Alshawabkeh and Sarahney, 2005). HPLC analyses were performed using a tunable UV detector (detection at 254 nm), a Supelco Supelcosil LC-PAH, 250 mm x 4.6 mm x 5  $\mu$ m column, an automated gradient controller, and deionized water/acetonitrile mobile phase. The flow rate of the mobile phase was 1.5 mL/min and the column was flushed with 1:99 (v/v) acetonitrile/water for 5 minutes followed by 60:40 (v/v) acetonitrile/water for 30 minutes and by 100:0 (v/v) acetonitrile/water for 15 minutes. Standard solutions were prepared to bracket the expected concentration level of the analytes. Calibration curves with an average obtained  $R^2$  value of 0.998 were used to determine the concentration of naphthalene in the aqueous solution as the test progressed.





was set

cells an

heat gen

cell to a

were pla

at 1 °C h

### Experi

Apart fro

other ex

conducti

meter eq

probe, w

the spike

electrica

spiked s

### RESUL T

Table 1-

A control cell, similar to the test cells except with no current flowing through it was set up, sampled and analyzed at the same time intervals as the test cells. The test cells and the control cells were placed in the same water bath in order to distribute the heat generated as a result of Joule heating in the test cell. This also allowed the control cell to attain approximately the same temperature as the test cells. Replicate control cells were placed in the temperature chamber where the temperature of the chamber was fixed at 1 °C higher than the maximum temperature measured in the test cell.

### **Experimental Parameters Monitored**

Apart from monitoring the concentration of naphthalene in aqueous solution over time, other experimental parameters monitored included pH, temperature, redox potential, conductivity, and dissolved oxygen of the solution. A portable dissolved oxygen/pH meter equipped with a pH electrode, an oxidation-reduction probe and dissolved oxygen probe, was used to measure pH, redox potential and dissolved oxygen, respectively, of the spiked solutions over time. An electrical conductivity meter was used to measure the electrical conductivity and a thermometer was used to measure the temperature of the spiked solutions in the control and test cells

## **RESULTS AND DISCUSSION**

Table 1-1 outlines the experimental program.

Suppo

Figure

AC and

electro

1.

Normalized Naphthalene Concentration, C/Co

0.8

0.6

0.4

0.2

0

Figure 1-  
NaCl as

### Supporting Electrolyte: NaCl

Figure 1-2 shows the average concentration of naphthalene in solution over time in the AC and DC test cells as well as in the control cell when NaCl was used as the supporting electrolyte for AC peak density and DC density was equal to  $6 \text{ mA/cm}^2$ .

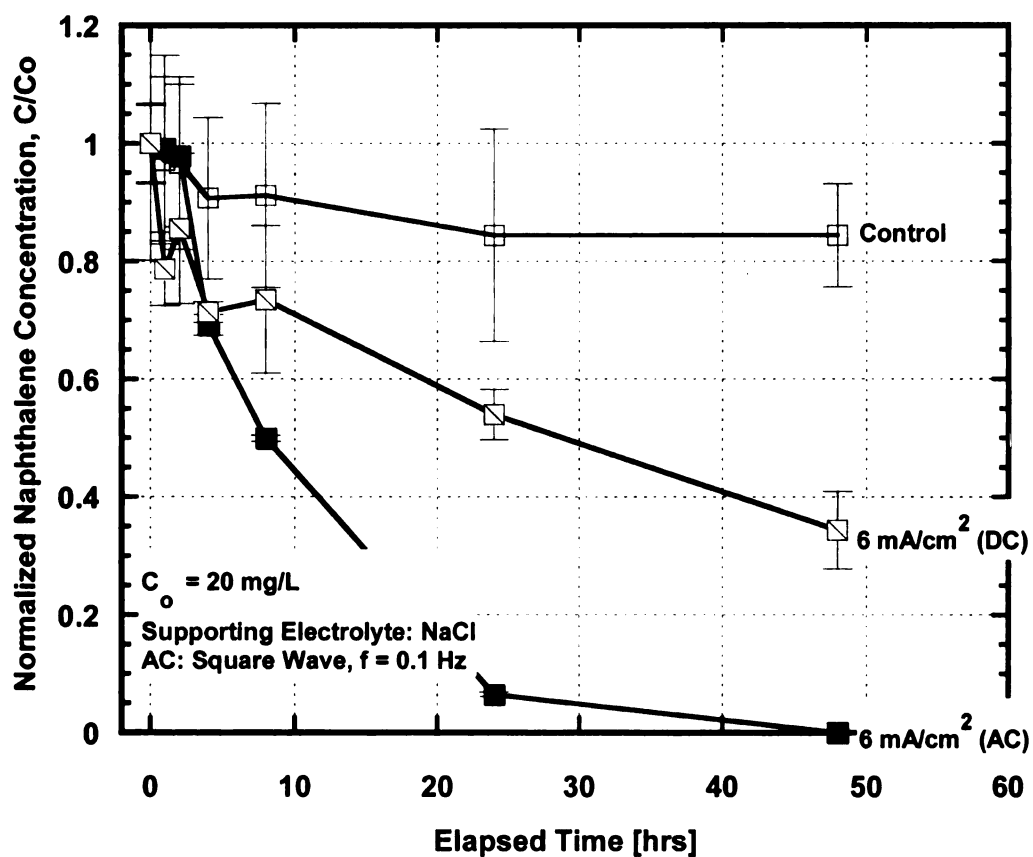


Figure 1-2: Change in concentration of naphthalene in solution for AC and DC tests with NaCl as supporting electrolyte.

1

The e

(C C)

of AC

mg L

detecte

chroma

degrada

method

is the c

concentr

degradat

order rat

hrs.

F

time in

concentr

about 70

period of

correspon

Unlike th

The error bars represent the maximum and minimum values of the concentration ratio ( $C/C_0$ ) for the initial test ( $t = 0$ ), and for samples collected during the 48-hour application of AC or DC.

By electrolyzing naphthalene solution having an initial concentration of about 20 mg/L (~0.15 mM) with an AC peak current density of  $6 \text{ mA/cm}^2$ , no naphthalene was detected in the spiked aqueous solution in the test cell after a period of 48 hrs. The chromatograms produced by the HPLC indicated several peaks corresponding to the degradation products, most of which had lower molecular weight than naphthalene. The method detection limit (MDL) for naphthalene was  $59 \text{ }\mu\text{g/L}$ . A plot of  $\ln[C/C_0]$  where  $C$  is the concentration of naphthalene in solution at time,  $t$  and  $C_0$  is the initial ( $t = 0$ ) concentration of naphthalene in solution, versus time depicted a *pseudo* first-order degradation kinetics ( $R^2 = 0.995$ ) of naphthalene in solution. The observed *pseudo* first-order rate constant ( $k_{\text{obs}}$ ) was  $1.21 \times 10^{-1} \text{ hr}^{-1}$ , and the corresponding half-life was 5.7 hrs.

Figure 1-2 also shows the average concentration of naphthalene in solution over time in the DC test cell. By electrolyzing naphthalene solution having an initial concentration of about 20 mg/L (~0.15 mM) with a direct current density of  $6 \text{ mA/cm}^2$ , about 70% reduction in concentration of the naphthalene in solution was observed after a period of 48 hrs. The chromatograms produced by the HPLC indicated several peaks corresponding to the degradation products similar to those observed for the AC tests. Unlike the AC test, a plot of  $\ln[C/C_0]$  versus time of the DC test did not indicate a good

correla

experim

DC tes

system

electro

dimens

was ob

100 g.

could n

the ma

Perhaps

observ

Electro

as show

is signi

et al. (2

their cos

sorption

control

products

correlation for a *pseudo* first-order degradation kinetics ( $R^2 = 0.865$ ) under our experimental conditions.

Figure 1-2 shows that faster degradation rate was observed in the AC test than the DC test. This shows that using AC for electrochemical degradation of naphthalene in our system seemed to be more efficient than using DC. Furthermore, because the surface of electrodes was not prepared by the deposition of a layer of metal oxide to produce dimensionally stable electrodes, about 6% loss in the mass of the anode in the DC test was observed at the end of the test period. Initial mass of the electrode was approximately 100 g. However, during the AC test, loss of mass of the electrodes was insignificant and could not be measured with a weighing scale having an accuracy of 0.01 g. The loss in the mass of the anode in the DC test was visible from the pitting of the electrode. Perhaps, the pitting of the anode resulted in fouling the electrode surface and hence the observed reduction in degradation rate of naphthalene as compared to the DC test cell. Electrode pitting did not occur for the AC tests.

Decrease in naphthalene concentration in the control cell over time was observed as shown in Figure 1-2. However, the loss of naphthalene from solution in the control cell is significantly less compared to the decrease observed for the AC and DC test cells. Goel et al. (2003) and Alshwabkeh and Sarahney (2005) also reported naphthalene loss in their control cells over time and attributed it to factors such as volatilization, potential sorption to cell components etc. The chromatograms produced by the HPLC for the control cell did not show any peaks except the naphthalene peak. Thus, no degradation products were formed indicating that no reactions occurred in the control cell.



1

that e

oxidat

electro

Pinson

electro

oxidizin

al. (2)

radicals

same re

products

involved

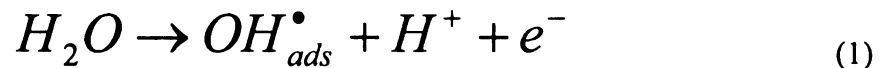
atoms (3)

electrode

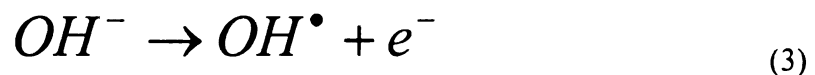
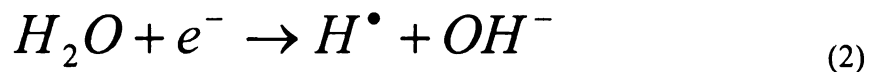
Formation

reactive s

Comninellis (1994), Brillas *et al.* (2000), and Panizza *et al.* (2000) have reported that electrochemical systems generate hydroxyl radicals ( $\text{OH}^\cdot$ ) at the anode due to the oxidation of water:



Among oxygen radicals such as  $\text{O}_2^{\cdot-}$ ,  $\text{OH}^\cdot$ ,  $\text{HO}_2^\cdot$ , and ROO that may be generated electrochemically in solution, the hydroxyl radical ( $\text{OH}^\cdot$ ) is the most reactive (Oturán and Pinson 1995). Brillas *et al.* (2000) also reported that the primary oxidizing agent in an electrochemical degradation study was the hydroxyl radical, although secondary oxidizing agents such as  $\text{H}_2\text{O}_2$  and  $\text{HO}_2^\cdot$  radicals could have been formed. Nakamura *et al.* (2005) proposed a mechanism based on selective redox reactions with various radicals generated by AC electrolysis that allows both oxidation and reduction at the same reaction site between adjacent electrodes. Based on the analyses of intermediate products of the degradation process, Nakamura *et al.* (2005) reported that the mechanism involved selective redox reactions with short-lived and highly reactive radicals: hydrogen atoms ( $\text{H}^\cdot$ ) and hydroxyl radicals ( $\text{OH}^\cdot$ ) that are electrochemically generated on the electrodes as presented in Equations 2 and 3.



Formation of hydroxylated degradation products in this study indicated that the primary reactive species in the test cells might have been hydroxyl radicals ( $\text{OH}^\cdot$ ).



classified  
as the  
and an  
AC vol  
reversal  
naphth  
electro  
oxidati  
"passiv  
polarit  
depend  
of the e  
while th  
subsequ  
potenti  
the peri  
It  
indirect  
products  
formati  
2005). T  
has been

Chen *et al.* (2003) reported that under AC voltages, the electrodes cannot be classified as fixed anode or cathode. One electrode acts as the cathode in a half cycle and as the anode in the other half cycle and therefore both cathodic electrochemical reactions and anodic electrochemical reactions under DC voltages occur on each electrode under AC voltages. Thus, in this study, by applying an AC, which resulted in constant polarity reversal of the electrodes at a rate dependent upon the AC frequency, anodic oxidation of naphthalene in solution occurred on both electrodes. A majority of published work on electrochemical degradation has focused on the use of DC. This relies mainly on anodic oxidation to degrade non-polar organic compounds and hence the cathode acts as a “passive” electrode in the oxidation process. However, when an AC is used, the constant polarity reversal ensures that both electrodes participate in the oxidation process, depending on their polarity in a given AC cycle. During the one half of a cycle when one of the electrodes has a positive electrical potential, it instantaneously acts as the anode while the other electrode, at a negative electrical potential, acts as the cathode. In the subsequent half cycle, polarities are reversed and the electrodes acquire electrical potentials opposite to what they had in the previous cycle and this continues throughout the period of application of the AC.

Besides direct anodic oxidation, organic pollutants can also be degraded by indirect electrolyses, generating in-situ chemical reactants to convert them to less harmful products (Panizza and Cericola 2003). The presence of chloride ions may result in the formation of chlorine gas instead of oxygen gas at the anode (Alshawabkeh and Sarahney 2005). The mechanism of electro generation of chlorine from chloride ions in solution has been presented by Panizza *et al.* (2000) as shown in Equations 4 to 6.

The hy

enhanc

treatme

1996).

reducti

have be

enhanc

support

solutio

the sol

with a

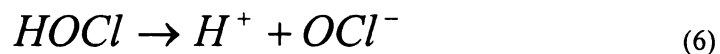
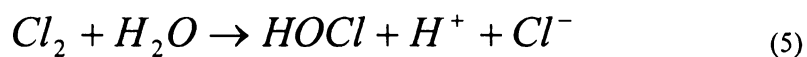
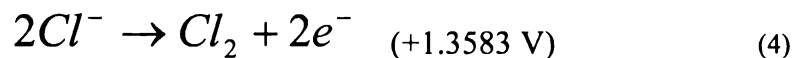
electro

both hy

AC ve

(instan

produc



The hypochlorous acid (HOCl) formed (Equation 5) acts as an oxidizing agent, thus enhancing the overall degradation. Electro-generated  $Cl_{2(g)}$  has been used in the treatment of landfill leachate and textile effluent (Chiang *et al.* 1995; Naumczyk *et al.* 1996), and in both cases, complete removal of ammonia and accompanying COD reduction was achieved. Therefore, we believe that the degradation of naphthalene could have been due to anodic oxidation (on the instantaneous anodes for AC tests) which was enhanced by the electro generation of chlorine gas in solution when NaCl was used as the supporting electrolyte.

The evolution of gases at both electrodes was observed as the electrolysis of the solution using AC progressed. Nakamura *et al.* (2005) also reported evolution of gases in the solution during the test when AC electrolysis was carried out at room temperature with a square wave having a frequency equal to 30 kHz and 15 V amplitude using electrodes made up of titanium coated with platinum. Chen *et al.* (2003) reported that both hydrogen and oxygen were deposited on the silver electrodes of the capacitors under AC voltages. In the half cycle, when one electrode is at a positive electrical potential (instantaneous anode), oxygen gas is produced at that electrode and hydrogen gas is produced at the other electrode (instantaneous cathode) according to Equation 7:

2A

4A

gas at

support

visible

corrod.

as the

format

at the

might b

the test

that ins

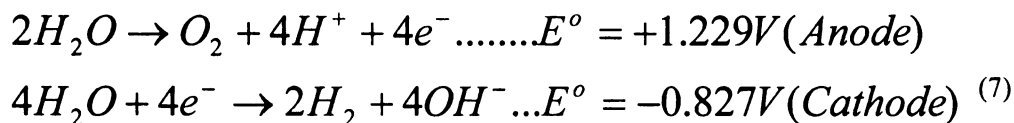
acted as

8 or Eq

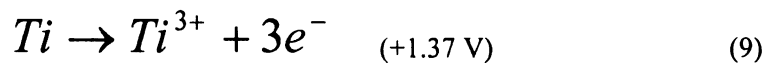
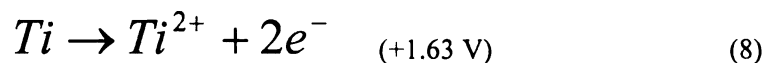
This als

These s

naphtha



The presence of chloride ions in the solutions might also have generated chlorine gas at the instantaneous anode according to Equation 4. In the DC test with NaCl as the supporting electrolyte, evolution of gas was observed on the cathode (probably H<sub>2</sub>). No visible gas bubbles were observed at the anode. Instead, the electrode material started corroding as soon as the DC was applied to the test cell. The test solution turned cloudy as the test progressed, accompanied by pitting and flaking of the anode material, and formation of precipitates in the solution. It is possible that Cl<sub>2(g)</sub> instead of O<sub>2(g)</sub> evolved at the anode because Cl<sup>-</sup> were preferentially oxidized at the anode (Equation 4). This might have resulted in the formation of titanium chloride complexes that precipitated in the test solution, which made the solution cloudy as the test progressed. It is also likely that instead of the oxidation of either water or Cl<sup>-</sup> ions at the anode, the titanium anode acted as a reactive anode and hence dissolved into the test solution according to Equation 8 or Equation 9,



This also, could have formed titanium complexes that precipitated out of the test solution. These competing reactions at the anode decreased the rate of anodic oxidation of naphthalene. However, in the tests involving the application of AC to the test cells,



1

contin.

cycle

anode

other

reduct.

acquir

oxidat

cathod

evolut

radical

decomp

subsequ

the deg

more ef

support

cheaper

High wa

expensiv

**Support**

*DC Test*

Figure 1

current d

continuous evolution of gases was observed on both electrodes. Thus, during the half cycle of the AC, when one electrode acquires a positive electrical potential (instantaneous anode), water molecules are oxidized and  $O_{2(g)}$  is evolved, and  $H_{2(g)}$  is evolved at the other electrode, with a negative electrical potential (instantaneous cathode) by the reduction of water molecules. In the subsequent half cycle of the AC, the electrodes acquire electrical potentials opposite to what they had in the previous cycle and the oxidation and reduction of water molecules continued at the instantaneous anode and cathode, respectively. These cycles continue throughout the application of the AC. The evolution of  $O_{2(g)}$  on both electrodes might have resulted in the formation organic radicals and subsequently organic hydroperoxides which were relatively unstable. The decomposition of such intermediates led to molecular breakdown and formation of subsequent intermediates with lower carbon numbers (Comminellis 1994). This enhanced the degradation rate of naphthalene in the AC test cells and hence AC appeared to be more effective in degrading naphthalene as compared to DC when NaCl was used as the supporting electrolyte. An advantage of AC over DC is that AC is readily available and cheaper in terms of capital cost because no rectification is required to convert it to DC. High wattage DC power supplies are relatively expensive and hence would be relatively expensive for full-scale remediation.

#### **Supporting Electrolyte: $Na_2SO_4$**

##### *DC Tests*

Figure 1-3 shows the average concentration of naphthalene in aqueous solution when the current densities of the applied DC were  $1 \text{ mA/cm}^2$ ,  $3 \text{ mA/cm}^2$ , and  $6 \text{ mA/cm}^2$ .

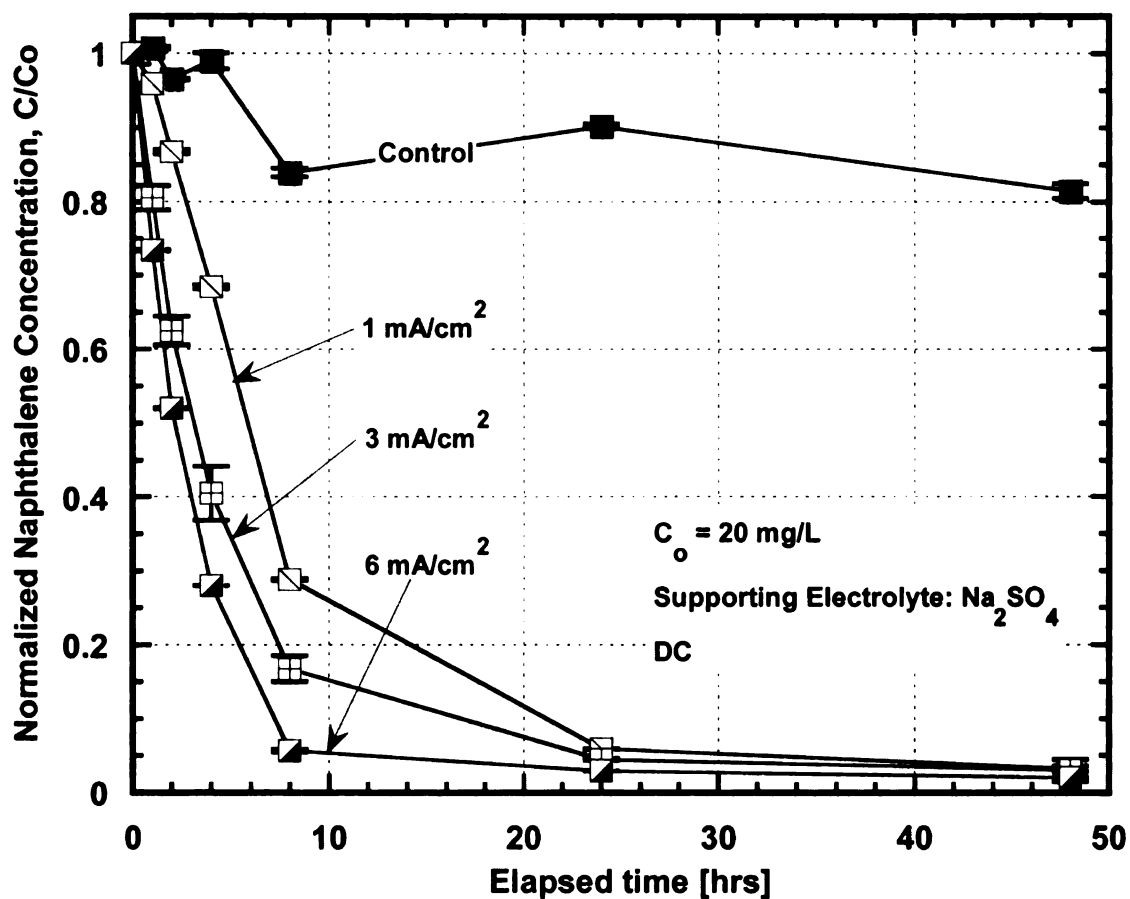


Figure 1-3: Change in concentration of naphthalene in solution for DC tests with  $\text{Na}_2\text{SO}_4$  as supporting electrolyte.

For each sampling round, two samples were analyzed with HPLC to quantify naphthalene concentration. Figure 1-3 presents the average concentration reported from these duplicate samples and two additional duplicate samples analyzed for a replicate test cell. The error bars represent the maximum and minimum values of the concentration ratio ( $C/C_0$ ) for the initial test ( $t = 0$ ), and for samples collected during the 48-hour application of DC. When 55 mA current (current density  $\sim 1 \text{ mA/cm}^2$ ) was passed through the naphthalene test solution, about 95% reduction in the concentration of naphthalene was observed within 24 hrs. Similarly, by passing 165 mA and 330 mA currents (current

densit

in the

Howe

Thus,

naphth

in crea

depict

experim

1.39 · 10

0.9953)

correspo

period,

observe

potentia

test cells

AC Test

Figure 1

peak cur

densities  $\sim 3$  and  $6 \text{ mA/cm}^2$ ) through the naphthalene test solution, about 95% reduction in the concentration of naphthalene in the aqueous solution was observed within 24 hrs. However, the initial rate of degradation was greatest for the highest current density. Thus, the higher the applied DC current density, the faster was the degradation rate of naphthalene in solution. Alshwabkeh and Sarahney (2005) have reported similar increase in naphthalene degradation rates with increasing applied current density.

A plot of  $\ln[C/C_0]$  versus time for the initial degradation rate (up to 8 hrs) depicted a *pseudo*-first-order degradation kinetics for naphthalene in solution under our experimental conditions. The observed *pseudo*-first-order degradation rate constants were  $1.39 \times 10^{-1} \text{ hr}^{-1}$  ( $R^2 = 0.9274$ ),  $2.24 \times 10^{-1} \text{ hr}^{-1}$  ( $R^2 = 0.9997$ ), and  $3.49 \times 10^{-1} \text{ hr}^{-1}$  ( $R^2 = 0.9953$ ) for DC densities of  $1 \text{ mA/cm}^2$ ,  $3 \text{ mA/cm}^2$ , and  $6 \text{ mA/cm}^2$ , respectively. The corresponding half-lives were 5 hrs, 3 hrs, and 2 hrs, respectively. During the 48-hr test period, about 20% reduction in the concentration of naphthalene in the control cell was observed. This reduction in the concentration may have been due to volatilization, and potential sorption to cell components. However, unlike the HPLC chromatogram for the test cells, the control cell did not show any peaks corresponding to potential byproducts.

#### *AC Tests*

Figure 1-4 shows the average concentration of naphthalene in aqueous solution when the peak current densities of the applied DC were  $1 \text{ mA/cm}^2$ ,  $3 \text{ mA/cm}^2$ , and  $6 \text{ mA/cm}^2$ .

Normalized Naphthalene Concentration, C/C<sub>0</sub>

Figure  
as supp

The ov

three c

greater

degrad

they ev

at (195

the effi

depleted

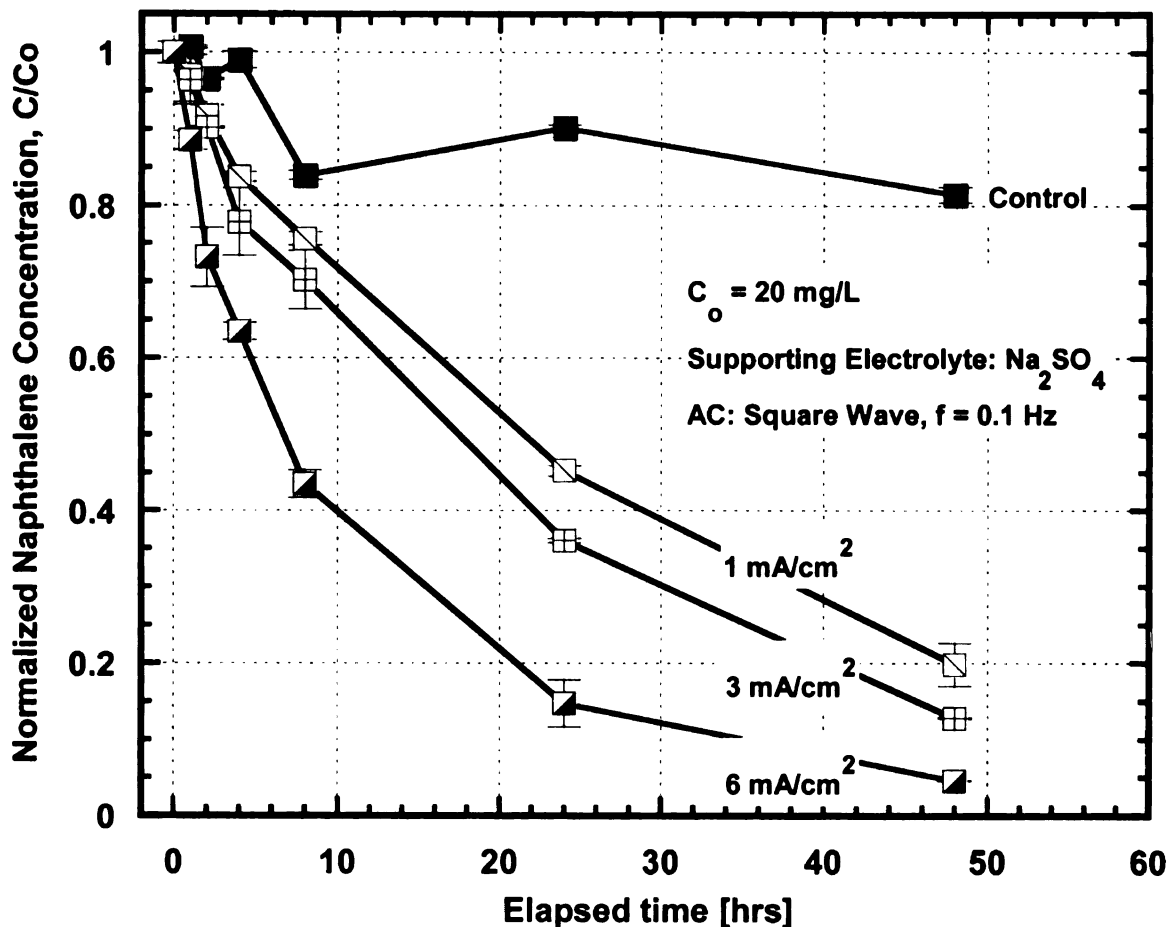


Figure 1-4: Change in concentration of naphthalene in solution for AC tests with  $\text{Na}_2\text{SO}_4$  as supporting electrolyte.

The overall rates of degradation of naphthalene during the 48-hr test duration for these three current densities were approximately 77%, 87%, and 95%, respectively. Thus, the greater the magnitude of applied AC (or alternating voltage), the faster was the rate of degradation of naphthalene. Chin and Cheng (1985) have reported a similar trend when they evaluated degradation of phenol at various applied alternating voltages. Kappana *et al.* (1952) used AC electrolysis for the oxidation of glucose to gluconate and showed that the efficiency increased with increasing AC density. A plot of  $\ln[C/C_0]$  versus time depicted a *pseudo* first-order degradation kinetics ( $R^2 = 0.995$ ) of naphthalene in solution

1

under

const.

densit

half-l

density

when

**Interm**

Liquid

product

electro

chemic

Hydro

degrada

used to

the ana

from th

control

mass sp

um co

mobile

column



under our experimental conditions. The observed *pseudo* first-order degradation rate constants ( $k_{\text{obs}}$ ) were  $3.37 \times 10^{-2} \text{ hr}^{-1}$ ,  $4.29 \times 10^{-2} \text{ hr}^{-1}$ ,  $6.84 \times 10^{-2} \text{ hr}^{-1}$  for applied AC densities of  $1 \text{ mA/cm}^2$ ,  $3 \text{ mA/cm}^2$ , and  $6 \text{ mA/cm}^2$ , respectively, and the corresponding half-lives were 21 hrs, 16 hrs, and 10 hrs.

Thus, DC degraded naphthalene at a faster rate than AC for a given current density as depicted by the pseudo-first-order degradation rate constants and half-lives, when  $\text{Na}_2\text{SO}_4$  was used as the supporting electrolyte.

### **Intermediate Byproducts**

Liquid Chromatography with mass spectrometry (LC/MS) analysis of degradation products was conducted for the AC and DC test cells containing NaCl as the supporting electrolyte. LC/MS was carried out in these ionization modes: +/- atmospheric pressure chemical ionization mode (APCI), and +/- electro-spray ionization mode (ESI). Oasis Hydrophilic Lipophilic Balance (HLB) extraction cartridges were used to extract degradation byproducts from the sample solutions and acetonitrile and DI water were used to elute them from the cartridges. Acetonitrile and DI water were used as blanks in the analysis to eliminate observed peaks of chemicals identified by MS that originated from these solvents and the LC column. LC/MS analysis was also conducted on the control samples. LC/MS analyses were performed using a Waters Quattro Micro API mass spectrometer, a Thermo Hypersil – Keystone BetaBasic - 18, 150 mm x 1.0 mm x 5  $\mu\text{m}$  column, an automated gradient controller, and deionized water (DI)/acetonitrile mobile phase. The flow rate of the mobile phase was maintained at 0.15 mL/min and the column was flushed with 10:90 (v/v) acetonitrile/DI water for 10 minutes followed by

60-40

water

AC

benzene

degrade

acid

progre

the for

reported

of nap

(2000)

quinone

byprod

degrad

radical

experim

chlorin

indicate

with sn

beyond

from th

60:40 (v/v) acetonitrile/ DI water for 30 minutes, and by 100:0 (v/v) acetonitrile/ DI water for 10 minutes.

LC/MS analyses indicated that the key degradation products formed during the AC tests were dihydroxynaphthalene, naphthoquinone, chloronaphthol, benzenedicarboxylic acid, and malic acid. For the DC tests, the electrochemical degradation products were dihydroxynaphthalene, naphthoquinone, benzenedicarboxylic acid, and malic acid. The exact isomers formed were not determined. As the tests progressed, the color change of the test solutions to light yellow might have been due to the formation of naphthoquinone in the solutions. Formation of quinones has been reported due the hydroxylation process in oxidizing media (Oturán 2000). The formation of naphthoquinone is consistent with the findings by Brillas *et al.* (2000), Panizza *et al.* (2000), and Saracco *et al.* (2000) who also have reported the formation of aromatic quinones during electrolytic oxidation of aromatic hydrocarbons.

GC/MS analysis by Goel *et al.* (2003) reported 1,4-naphthoquinone as the reaction byproduct when naphthalene solutions were electrolyzed and concluded that naphthalene degradation is due to direct anodic oxidation, oxidation by an intermediate (e.g. hydroxyl radicals), or a combination of both. Goel *et al.* (2003) also reported that chlorination experiments at pH 4 formed monochlorinated (1-chloro and 2-chloronaphthalene) and chlorinated naphthoquinones. HPLC analysis by Alshawabkeh and Sarahney (2005) indicated that transformation of naphthalene at the anolyte produced four compounds with small peaks that had retention time of 12.0 – 12.5 min. Gas phase sampling was beyond the scope of this study. Hence, any volatile byproducts which may have escaped from the solution were not detected or analyzed.

Table 1-2 summarizes the measured initial and final values of temperature, pH, standard redox potential, dissolved oxygen concentration, and electrical conductivity of the test solutions. These parameters are discussed as follows.

1

Table 1-2: Measured initial and final values of temperature, pH, standard redox potential, dissolved oxygen concentration, and electrical conductivity of test cell and control cell solutions

Supporting Electrolyte	Current density		Temperature (°C)		pH		Standard redox potential (mV)		Dissolved oxygen concentration (mg/L)		Electrical conductivity ( $\mu\text{S}/\text{cm}$ )	
	(mA/cm <sup>2</sup> )	(mA/L)	Initial	Final	Initial	Final	Initial	Final	Initial	Final	Initial	Final
NaCl	6 (AC)	330	19.5	25.2	6.4	10.7	330	614	7.0	8.6	1150	1550
NaCl	6 (DC)	330	19.1	24.0	6.3	11.5	378	40	7.5	3.5	1150	1800
NaCl	0	0	19.5	19.1	6.3	6.5	360	370	7.5	7.9	1150	1157
Na <sub>2</sub> SO <sub>4</sub>	1 (AC)	55	19.0	16.3	6.8	4.2	412	446	3.6	4.4	804	828
Na <sub>2</sub> SO <sub>4</sub>	1 (DC)	55	19.2	17.7	6.5	11.2	446	193	3.6	6.4	838	1135
Na <sub>2</sub> SO <sub>4</sub>	3 (AC)	165	19.2	18.0	6.5	4.5	394	415	4.6	6.5	811	818
Na <sub>2</sub> SO <sub>4</sub>	3 (DC)	165	19.2	22.7	6.5	11.5	447	177	3.9	7.1	838	1172



Table 1-2 Cont'd

Na <sub>2</sub> SO <sub>4</sub>	6 (AC)	330	19.1	24.0	6.6	5.16	412	480	3.8	6.4	804	827
Na <sub>2</sub> SO <sub>4</sub>	6 (DC)	330	19.2	22.4	6.4	11.6	418	147	4.2	6.2	881	1256
Na <sub>2</sub> SO <sub>4</sub>	0	0	19.2	19.0	6.5	6.5	394	422	4.6	7.4	811	810

Note: The frequency of the applied AC was 0.1 Hz



Temp

The to

the te

water

tempe

centro

within

Hence

pH

The in

measur

the DO

electro

produ

produ

having

the tin

molec

ions d

## **Temperature**

The test cells and control cells (first set) were placed in a water bath. Heat generated in the test cells due to Joule heating by the electrical current was distributed through the water bath to the control cell and hence both cells attained approximately constant temperature. However, the temperature of the test cells was up to 6 °C higher than the control cell temperature at the highest current density (Table 1-2). The temperature within all test cells ranged between 19 °C and 25 °C throughout the testing period. Hence, a duplicate control cell was placed in the temperature chamber at 26 °C.

## **pH**

The initial pH of all test cell solutions ranged from 6.3 to 6.8. The final pH which was measured 48 hours after the application of AC ranged from 4.2 to 5.2 and 11.2 to 11.5 for the DC cells. The only exception was the AC test cell with NaCl as the supporting electrolyte which had a final pH of 10.7. The oxidation of water molecules at the anode produced  $H^+$  ions in solution while the reduction of water molecules at the cathode produced  $OH^-$  ions in solution according to Equation 7. Also, formation of byproducts having acidic properties is another possible source of  $H^+$  ions in solution. Therefore at the time of measurement of the final pH values in the AC tests, the oxidation of water molecules was more prominent than its reduction and hence the generation of more  $H^+$  ions decreased the pH of the solutions.

cell >

the s.

meas.

11.2

of ga

electro

of the

acted q

Cl<sub>2</sub> g.

contin

test. T

molec

in inc

cathod

throug

electro

(Pt) a:

approa

Continuous bubbling of gases was observed on both electrodes in all the AC test cell solutions throughout the testing period. During the  $6 \text{ mA/cm}^2$  AC test with NaCl as the supporting electrolyte, it is likely that water reduction was dominant at the time of measurement. In all the DC tests, the final measured pH of the solutions ranged between 11.2 and 11.5, indicating that water reduction was more prominent. No visible bubbling of gas was observed at the anode during the DC test with NaCl as the supporting electrolyte. Instead, the anode corroded throughout the test, which resulted in a mass loss of the anode at the end of the test. Therefore instead of water oxidation, the anode also acted as a reactive electrode and lost mass according to Equations 8 and 9.

The presence of chloride ions in solution could have resulted in the generation of  $\text{Cl}_2(\text{g})$  (Equation 4) at the anode, which was not visible to the unaided eye. However, continuous bubbling of gas was observed at the cathode throughout the duration of the test. The gas evolved at the cathode was probably  $\text{H}_2(\text{g})$  from the reduction of water molecules (Equation 7), accompanied by the generation of  $\text{OH}^-$  ions in solution, resulting in increased pH of the test solution. No measurable loss of mass was recorded for the cathode. The pH of the control cell solutions remained approximately constant at 6.5 throughout the testing period.

Li *et al.* (2005) reported a drop in pH from 5.3 to below 4.0 when DC was used to electrolyze phenol solution in a cell with 0.25 M  $\text{Na}_2\text{SO}_4$  as electrolyte using platinum (Pt) and Ti/RuO<sub>2</sub> anodes. A drop in pH from 5.3 to about 3.5 after 5 hrs, which approached 7.0 after 18 hrs using Ti/SnO<sub>2</sub>-Sb anode was also reported by the authors. Li

1

et al.  
acid  
report  
elect  
titan  
Redo  
The n  
gener  
oxidiz  
molec  
bubb  
Cl<sub>2</sub>g  
meas  
values  
observ  
observ  
in red  
gener  
support

*et al.* (2005) concluded that the drop in pH was apparently caused by the formation of acidic substances from the phenol degradation. Alshawabkeh and Sarahney (2005) reported a drop in pH from about 5.8 to 1.9 in the anolyte when DC was used to electrolyze naphthalene in aqueous solution containing 50 ml of 0.2 M NaCl using titanium electrodes with mixed metal oxide coating.

### **Redox Potential and Dissolved Oxygen**

The measured final standard redox potential values for all the AC test cell solutions were generally higher than the initial values indicating that the solutions became more oxidizing as the tests progressed. Therefore it is likely that the oxidation of water molecules was dominant in all AC test cell solutions and hence most of the observed gas bubbles could have been due to the evolution of  $O_{2(g)}$ , and to some degree  $H_{2(g)}$  and /or  $Cl_{2(g)}$  (for NaCl as the supporting electrolyte). In the DC test cell solutions, the measured final standard redox potential values were significantly lower than the initial values and hence reduction of water molecules was more prominent. Therefore the observed gas bubbles on the cathode likely contained  $H_{2(g)}$ . No visible gas bubbles were observed at the anode. The control cell, however, did not register any significant change in redox potential.

The measured final dissolved oxygen concentration in all test cell solutions were generally higher than the initial values except in the  $6 \text{ mA/cm}^2$  AC cell with NaCl as the supporting electrolyte, which recorded a drop from 7.5 mg/L to 3.5 mg/L (Table 1-2).



Elect

Supp

For th

condu

mass

could

electr

electr

likely

loss of

Supp

The

$\text{Na}_2\text{SO}_4$

No les

corros

byprod

increas

SUMM

The ke

naphth

on the

the rate

## **Electrical Conductivity**

### *Supporting Electrolyte: NaCl*

For the AC test cells solutions containing NaCl as the supporting electrolyte, the final conductivity of the solutions was greater than the initial value. Slight loss in the electrode mass was also observed for the AC tests. Due to the mass loss, the metallic electrode could have leached ions (probably titanium ions) into the solution, which increased the electrical conductivity of the solution. In the DC tests, significant increase in the electrical conductivity of the solutions was recorded at the end of the tests. This was likely due to the continuous leaching of titanium ions into solution from the significant loss of mass (~ 6%) and pitting of the electrode material that was observed.

### *Supporting Electrolyte: Na<sub>2</sub>SO<sub>4</sub>*

The final measured electrical conductivity of all AC test cell solutions containing Na<sub>2</sub>SO<sub>4</sub> as the supporting electrolyte was approximately the same as the initial values. No loss of mass of electrode was recorded in these tests and hence potential electrode corrosion followed by leaching into the solution did not occur. Also, it is likely that the byproducts formed did not have ion dissociation properties that would have significantly increased the conductivity of the solution.

## **SUMMARY AND CONCLUSIONS**

The key objectives of this study were to evaluate the use of AC for the degradation of naphthalene in a spiked aqueous solution and to investigate the effect of current density on the degradation rates of naphthalene. Direct current (DC) was also used to compare the rates of degradation. A square wave AC, having a frequency of 0.1 Hz and current



denst:

as the

•

•

•

•

•

densities equal to 1, 3, and 6 mA/cm<sup>2</sup> were used. NaCl and anhydrous Na<sub>2</sub>SO<sub>4</sub> were used as the supporting electrolytes. The key conclusions of this study are as follows.

- Both AC and DC are capable of degrading naphthalene in aqueous solution into hydroxylated byproducts;
- DC, at a given current density, degraded naphthalene at a rate faster than AC having a frequency equal to 0.1 Hz, with an equivalent current density as the DC density. However, for NaCl as the supporting electrolyte, the presence of chloride ions in solution resulted in the corrosion of the anode, which fouled the anode surface and hence resulted in a degradation rate for DC test cell that was less than that for the AC test cell at the same current density.
- The higher the DC or AC peak density, the higher the degradation rate of naphthalene in solution.
- The AC test cell solutions generally became acidic (oxidizing environment) at the end of the 48-hr testing period whereas the DC test cells solutions became alkaline (reducing environment).
- An advantage of using an AC instead DC for electrochemical degradation is that an AC is readily available from the power grid and no rectification is required. Also, in AC electrolysis, the corrosion of reactive electrode material in this study was significantly less compared to the loss of mass of anode observed for DC electrolysis, resulting in pitting of the electrode. However, the efficiency of DC in degrading naphthalene in solution was higher than an AC, especially when the electrodes were stable did not significantly dissolve into solution. Hence, the treatment time for an AC having 0.1 Hz frequency would be longer than an

equivalent DC. The treatment time may be further impacted if a greater frequency, such as 60 Hz, which is available from the power grid is used for the AC. Additional lab-scale as well pilot-scale experiments are needed to evaluate the effect of frequency and the shape of the AC signal.

ABS

The

degr.

bypr

cont.

AC d

90°

the a

concl

m.A

degr.

decre

AC p

squat

phen

high

dihy

acid

indi

equa

## PAPER NO. 2: DEGRADATION OF PHENANTHRENE AND PYRENE IN SOLUTION USING ALTERNATING CURRENT

### ABSTRACT

The objective of this study was to use an alternating current (AC) to investigate the degradation of phenanthrene and pyrene in spiked aqueous solutions. Degradation rates and byproducts formed were investigated when a square wave AC was applied to solutions containing pyrene and phenanthrene. Phenanthrene and pyrene solutions were subjected to AC densities equal to  $3.0 \text{ mA/cm}^2$ ,  $10.2 \text{ mA/cm}^2$  and  $18.5 \text{ mA/cm}^2$ . About 65%, 75% and 90% reductions in the initial concentrations of phenanthrene were observed within 48 hrs of the application of the current densities, respectively. Similarly, about 90% reduction in the concentrations of pyrene solutions was observed within 48 hrs of application for  $3.0 \text{ mA/cm}^2$ ,  $10.2 \text{ mA/cm}^2$  and  $18.5 \text{ mA/cm}^2$  AC densities. However, the rate of initial degradation was faster for higher AC densities. Increase in the AC frequency resulted in a decrease in the degradation rate of both phenanthrene and pyrene in solution. A square-wave AC produced a higher degradation rate than a sine wave supplied at an *rms* (root mean square) current density of  $10.2 \text{ mA/cm}^2$  and frequency of 60 Hz in the degradation of phenanthrene. Using sodium chloride (NaCl) as the supporting electrolyte resulted in higher degradation rates than using sodium sulfate ( $\text{Na}_2\text{SO}_4$ ). Formation of 2,3-dihydroxybenzoic acid and 2,5-dihydroxybenzoic acid from the degradation of salicylic acid (a hydroxyl radical probe) was consistent with the findings in literature which indicated that hydroxyl radicals were the primary oxidizing agent. The *Nernst-Planck* equation was used to model the rate of mass transfer to the electrodes, where reactions



were

agreed

other

INTF

Poly

of tw

vari

con

(seve

persi

1992

struc

orig

anti

prin

burn

more

wide

em

of in

the l

cont

were expected to occur. The simulated concentration-time profiles were in reasonable agreement with the observed concentrations. The primary degradation products, among others, included phenanthrenequinone and pyrenequinone.

## INTRODUCTION

Polycyclic aromatic hydrocarbons (PAHs) are a class of organic compounds that consist of two or more fused benzene rings and/or pentacyclic molecules that are arranged in various chemical configurations (Bamforth and Singleton 2005). Of environmental concern are primarily the PAHs ranging in size from naphthalene (two rings) to coronene (seven rings) (Johnson *et al.* 2005). They are highly recalcitrant molecules that can persist in the environment due to their hydrophobicity and low water solubility (Cerniglia 1992) as well as the presence of dense cloud of  $\pi$ -electrons on both sides of the ring structures, making them resistant to nucleophilic attack (Johnson *et al.* 2005). They originate from two main sources: these are natural (biogenic and geochemical) and anthropogenic (Mueller *et al.* 1996). The PAHs present in the atmosphere are derived principally from the combustion of fossil fuels in heat and power generation, refuse burning and coke ovens (Bjorseth and Ramdahl 1985). These sources together contribute more than 50% of the nationwide (US) emission of benzo[a]pyrene, a hydrocarbon that is widely employed as a standard for PAH emissions (Bjorseth and Ramdahl 1985). Vehicle emissions are another major source of PAH contamination, particularly in the urban areas of industrialized countries, contributing as much as 35% to the total PAH emissions in the USA (Grimmer 1983). Natural sources, such as forest fire and volcanic activity, also contribute to the overall burden, but anthropogenic sources are generally acknowledged

to

Un

for

m.

ha

sh

m

m

m

th

el

P

b

C

T

d

d

s

N

d

s



to be the most important source of PAHs in atmospheric pollution (Grimmer 1983). The United States Environmental Protection Agency (USEPA) estimates that 3,000 to 5,000 former manufactured gas plant (MGP) sites are located across the United States and many of these contaminated sites contain substantial quantities of PAHs (USEPA 2000).

Several approaches including biodegradation and advanced oxidation processes have been used to degrade PAHs in solution. Electrochemistry, a link between physical chemistry and electronic science, has a potential for the development of new advanced methods for water purification (Grimm *et al.* 1998). Existing electrochemical redox methods depend on passing a direct current (DC) across electrodes in an aqueous medium. Direct electrochemical oxidation at the anode (anodic oxidation) may result in the breakdown of organic contaminants, depending on the electrode type and the electrochemical redox potential of the contaminant (Alshawabkeh and Sarahney 2005). Pepprah and Khire (2008) have reported degradation of naphthalene in aqueous solution by subjecting it to an AC and comparing it to the use of DC.

## **OBJECTIVES**

The key objective of this study was to use an alternating current (AC) to investigate the degradation of phenanthrene and pyrene in spiked aqueous solutions. Effect of current density, frequency, and waveform of the AC was also evaluated. AC was used for this study because other researchers (Chin and Cheng 1985; Fedkiw and Chao 1985; Nakamura *et al.* 2005; Pepprah and Khire 2008) have demonstrated that AC is capable of degrading other organic compounds in solution. Phenanthrene was selected due to its structural similarities to many of the higher order PAHs currently recognized as being



hazan

PAH

Laor

study

func

the p

supp

acce

app

Pepp

sol:

elec

NaC

negl

imp

rela

MA

The

des.

hazardous to health (Little *et al.* 2002). In addition, phenanthrene is the most common PAH found at most contaminated Manufactured Gas Plants (MGP) sites (Ko *et al.* 1998; Laor *et al.* 1998). Pyrene was selected due to its similarities to the higher order PAHs.

Square wave AC having frequencies of 0.1 Hz, 1 Hz, and 60 Hz were used in this study. 0.1 Hz frequency is the lowest frequency available on most commonly used function generators including the one used in this study and AC is supplied at 60 Hz from the power grid. The effect of current density, AC frequency and waveform, and type of supporting electrolyte on the degradation rates of the phenanthrene and pyrene in acetonitrile/DI water binary solution were investigated in this study. Comparison of the application of DC and AC signals has been reported by Pepprah and Khire (2008). Pepprah and Khire (2008) reported a faster rate of degradation of naphthalene in aqueous solution for DC when an equivalent density AC was used. However, the significant electrode mass loss (~7.5%) was observed during a 48-hour test when DC was used with NaCl as the electrolyte, whereas, the mass loss during an equivalent AC test was negligible. In addition, AC is readily available from the power grid for potentially implementing the technology at the field-scale where the power demand may be relatively high.

## **MATERIALS AND EXPERIMENTAL METHODOLOGY**

The experimental setup is illustrated in Figure 2-1 and the setup components are described below.

1

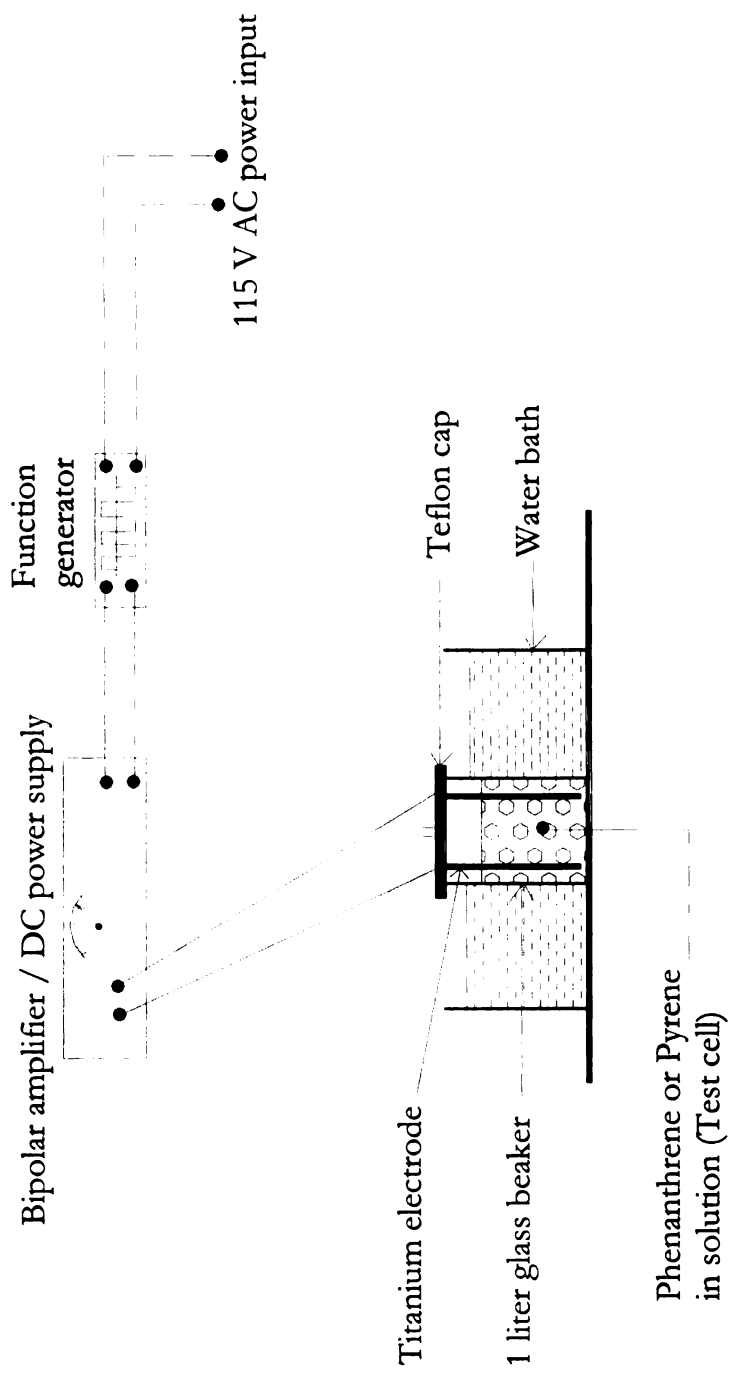


Figure 2-1: Schematic of the experimental setup

1

Reac

The

a l h

elimi

the c

(Ais

base

titan

com

Unco

Titan

henc

of tr

terre

proc

grap

1990

trans

than

titan

1.7

con

sam

## Reaction Chamber

The test setup used for the electrochemical degradation of PAHs in solution consisted of a 1 liter Pyrex glass beaker with a Teflon cap. These materials of the cell were selected to eliminate or reduce sorption of the contaminants onto the walls of the reaction vessel and the cap. Titanium plates were used as electrodes for this study. Other researchers (Alshawabkeh and Sarahney 2005; Li *et al.* 2005; Goel *et al.* 2003) used titanium as a base metal and coated it with mixed metal oxides such as RuO<sub>2</sub>, IrO<sub>2</sub>, and SnO<sub>2</sub>. The titanium plates used in this study were not coated. Uncoated titanium is cheaper than commonly used electrodes such as gold, platinum, or titanium coated with mixed metals. Uncoated titanium electrodes were selected for this project due to budget constraints. Titanium offers resistance to corrosion in a wide range of aggressive conditions and hence has the potential for field scale application. In addition, the total biocompatibility of titanium assures, safer use in humane bone and tissue replacement, harmlessness to terrestrial and marine flora and fauna and non-interference with microbiological processes (Data sheet No. 19, Titanium Information Group). Electrodes made up of graphite and nickel show poor current efficiency in organic degradation (Rodgers *et al.* 1999). In addition, graphite has relatively high impedance to AC and hence power transfer to the sample is not as efficient. Furthermore, titanium anodes are more stable than nickel, lead, zinc or mercury (Data sheet No. 19, Titanium Information Group). The titanium sheets used as electrodes in this project were 12.0-cm-long by 5.0-cm-wide by 1.72-mm-thick and the distance between them was maintained equal to 8.0 cm. The contact area of the solution with the electrode was 55 cm<sup>2</sup> but reduced to 53 cm<sup>2</sup> as samples were collected for analyses during the experiment.



Elect

A (0

AC

neg

there

when

squ

0.7

AC

cons

and

Spik

Due

use

com

ava

byp

mg

Ore

stuc

Pyre

wa



## **Electrical Equipment**

A 0.1 Hz to 2 MHz Sweep Function Generator was used to generate a square wave form AC. A square waveform AC was selected because the voltage shifts suddenly from negative to positive, stays there for half a cycle, and then jumps to full negative and stays there for the rest of the half cycle. This sequence is repeated during the entire period when the square wave AC is applied. Therefore, the root mean square voltage ( $V_{rms}$ ) of a square wave is equal to its peak voltage ( $V_p$ ), unlike a sine wave where  $V_{rms}$  is equal to  $0.707V_p$ . Thus, during a cycle for given voltage and current amplitudes, a square wave AC delivers greater power compared to sinusoidal or other AC signals. The power supply consisted of a bipolar operational power supply/amplifier capable of producing 200 V AC and 1 A AC output or a maximum electrical power of 200 W.

## **Spiked Solution Preparation**

Due to relatively low solubility of phenanthrene and pyrene in water, a cosolvent was used to get appreciable amounts (i.e., greater than the aqueous solubility of the compounds) of phenanthrene and pyrene into solution so that adequate amounts would be available in solution for quantification of concentrations and identification of degradation byproducts. The aqueous solubility of phenanthrene is 1.1 mg/L and for pyrene it is 0.14 mg/L (Schwarzenbach *et al.* 2003). Acetonitrile was selected as the cosolvent because Ottinger *et al.* (1999) used acetonitrile as a cosolvent in electrochemical degradation studies of a model PAH compound, benzo[a]pyrene. 10 mg or 5 mg of phenanthrene or pyrene crystals were added to one liter solutions of acetonitrile (30%) and deionized (DI) water (70%) (v/v) to achieve target concentrations of 10 mg/L or 5 mg/L, respectively.

1

The  
sol  
cry  
(Na  
con  
sele  
solu  
dem  
in th  
com  
beca  
titan  
unlik  
sulfur  
NaCl  
conc  
reduc  
post-  
repre  
we a  
whic

The proportion of acetonitrile was just enough to ensure that the PAH with the lower solubility, pyrene, remained in the binary solution without precipitating out to form crystals in the solution. This was followed by the addition of 0.5 g of sodium chloride (NaCl) or sodium sulfate (Na<sub>2</sub>SO<sub>4</sub>) crystals to the solutions to increase the electrical conductivity of the electrolyte during the electrochemical tests. Sodium chloride was selected as a supporting electrolyte because apart from increasing the conductivity of the solution, Alshawabkeh and Sarahney (2005) and Panizza and Cerisola (2003) have demonstrated that electrogeneration of chlorine gas from chloride ions in solution results in the formation of hypochlorous acid (HOCl), which enhances the oxidation of organic compounds in solution. Also sodium sulfate was selected as a supporting electrolyte because previous studies (Pepprah and Khire 2007) demonstrated that the loss of mass of titanium electrodes during DC or AC electrolysis when Na<sub>2</sub>SO<sub>4</sub> was used was negligible unlike NaCl, which resulted in significant mass loss. Goel *et al.* (2003) also used sodium sulfate in electrochemical degradation of naphthalene in aqueous solution using DC.

Saracco *et al.* (2000) performed tests where electrolyte salt concentrations (e.g. NaCl, Na<sub>2</sub>SO<sub>4</sub>, H<sub>2</sub>SO<sub>4</sub>) ranged from 0.2 to 2 M and reported that higher salt concentrations reduce the electrical resistance between the electrodes and hence will reduce the operating costs. However, greater salt concentration would result in greater post-treatment costs and hence would be less favorable. The only exception might be represented by discharging the treated effluent into the sea (Saracco *et al.* 2000). Hence, we added NaCl or Na<sub>2</sub>SO<sub>4</sub> that yielded a relatively low concentration equal to 0.5 g/L, which was just adequate to achieve the target highest AC density that could be delivered

1

t  
c  
a  
r  
F  
s  
F  
e  
t  
H  
t  
t  
a  
v  
s  
a  
s  
i  
s  
s  
m  
e  
a

by the power supply available for the tests in this study. After NaCl or Na<sub>2</sub>SO<sub>4</sub> was dissolved completely, the solution was filtered and the collected filtrate was used for all analyses and tests.

### **Testing Procedure**

Prior to the commencement of the passage of an AC or DC through the cells, initial samples were collected for high performance liquid chromatography (HPLC) analyses. Replicate tests were conducted for a majority of the tests. The electrical impedance ( $Z$ ) of each test cell was measured using an LCR Meter. The average initial impedance of the test solutions was 100  $\Omega$  and its impedance at the end of the test period was 120  $\Omega$ . However, the final impedance varied depending on the test conditions. For a majority of the tests, 0.1 Hz AC frequency was selected because Chin and Cheng (1985) reported that the rate of conversion of phenol increased with increasing magnitude of the applied alternating voltage superimposed on a DC and decreased with increasing alternating voltage frequency. Hence, we used the lowest AC frequency produced by the function generator that we had available for the study. Additional tests were carried out at 1 Hz and 60 Hz AC frequency to explore the effect of AC frequency on degradation rates. A sine wave AC delivered at 60 Hz was used to compare the effect of AC waveforms (square and sine) on degradation rates. 60 Hz was selected because AC is supplied as a sine wave at 60 Hz from the power grid in the United States. Also, although our power supply device could supply a maximum voltage of 200 V, we were limited by its maximum output current of 1 A. In addition to the current density and frequency, the effect of the initial concentration of phenanthrene and pyrene on degradation rates was also explored.

3

10.2

both

HPL

were

anal

18 f

det

mL

fol

acet

pher

proc

bra

aver

pher

coll

the

tes

tem

heat

The tests were performed at three AC densities of about  $3 \text{ mA/cm}^2$  (165 mA),  $10.2 \text{ mA/cm}^2$  (550 mA peak current), and  $18.5 \text{ mA/cm}^2$  (1,000 mA peak current) for both phenanthrene and pyrene solutions. During the test, samples were collected for HPLC analysis at elapsed time intervals of 0, 1, 2, 4, 8, 24, and 48 hours. The samples were analyzed directly without extracting the PAH from the aqueous solution. HPLC analyses were performed using a tunable UV detector (detection at 254 nm), a Waters C-18 PAH, 250 mm x 4.6 mm x 5  $\mu\text{m}$  column, an automated gradient controller, and deionized water (DI)/acetonitrile mobile phase. The flow rate of the mobile phase was 1.2 mL/min and the column was flushed with 10:90 (v/v) acetonitrile/DI water for 5 minutes followed by 60:40 (v/v) acetonitrile/ DI water for 10 minutes, and by 100:0 (v/v) acetonitrile/ DI water for 5 minutes. This gradient was used for the analysis of phenanthrene and pyrene in order to obtain an appropriate separation of the degradation product peaks on the chromatogram during the tests. Standard solutions were prepared to bracket the expected concentration level of the analytes. Calibration curves with an average obtained  $R^2$  value of 0.998 were used to determine the concentration of phenanthrene and pyrene in the solutions as the test progressed. Samples were also collected for LC/MS scans to determine the degradation products formed.

Control cells, similar to the test cells except without any current passed through them were set up, sampled, and analyzed at the same time intervals as the test cells. The test cells were placed in a relatively large volume water bath maintained at the room temperature to reduce the rate of temperature rise of the test solutions as a result of Joule heating due to the current flowing in the test cell. The control cells were placed in a heat

3

cha

ord

ate

med

ion:

were

and

water

ident

LC

usin

Bea

deic

man

water

by

Mo

Ap

time

tem

Plat



chamber. The maximum temperature of the solution in the test cells reached 46 °C. In order to mimic or exceed the temperatures in the test cells, all control cells were placed in a temperature chamber at a constant temperature equal to 50 °C.

LC/MS analysis of degradation products was conducted in these ionization modes: +/- atmospheric pressure chemical ionization mode (APCI), and +/- electrospray ionization mode (ESI). Oasis Hydrophilic Lipophilic Balance (HLB) extraction cartridges were used to extract degradation byproducts from the sample solutions and acetonitrile and DI water were used to elute them from the cartridges. Hence, both acetonitrile and DI water were used as blanks in the analysis to eliminate observed peaks of chemicals identified by the MS that originated from these solvents and the LC column. Also, LC/MS analysis was conducted on the control samples. LC/MS analyses were performed using Waters Quattro Micro API mass spectrometer, a Thermo Hypersil – Keystone BetaBasic - 18, 150 mm x 1.0 mm x 5 µm column, an automated gradient controller, and deionized water (DI)/acetonitrile mobile phase. The flow rate of the mobile phase was maintained at 0.15 mL/min and the column was flushed with 10:90 (v/v) acetonitrile/DI water for 10 minutes followed by 60:40 (v/v) acetonitrile/ DI water for 30 minutes, and by 100:0 (v/v) acetonitrile/ DI water for 10 minutes.

### **Monitored Experimental Parameters**

Apart from measuring the concentration of phenanthrene and pyrene in solution over time, other experimental parameters monitored included initial and final values of pH, temperature, and electrical conductivity. A dissolved oxygen/pH meter, equipped with a Platinum Series pH Electrode, was used to measure pH of the spiked solution. A portable

conductivity meter was used to measure the electrical conductivity and a microprocessor thermometer was used to measure the temperature of the test cell and control cell solutions.

## RESULTS AND DISCUSSION

Table 2-1 outlines the list of parameters explored in the experimental program.

Table 2-1: Summary of Experimental Parameters

Compound	Initial Concentration $C_0$ [mg/L]	Supporting Electrolyte	AC Frequency [Hz]	AC Waveform	RMS AC Density [mA/cm <sup>2</sup> ]	No. of tests
Phenanthrene	10	NaCl	0.1	Square	3.0	2
Phenanthrene	10	NaCl	0.1	Square	10.2	2
Phenanthrene	10	NaCl	0.1	Square	18.5	1
Phenanthrene	10	Na <sub>2</sub> SO <sub>4</sub>	0.1	Square	10.2	1
Phenanthrene	10	Na <sub>2</sub> SO <sub>4</sub>	1	Square	10.2	2
Phenanthrene	10	Na <sub>2</sub> SO <sub>4</sub>	60	Square	10.2	1
Phenanthrene	10	Na <sub>2</sub> SO <sub>4</sub>	60	Sine	10.2	1
Phenanthrene	10	Na <sub>2</sub> SO <sub>4</sub>	0	DC	3.0	1

1

Ts

P

P

P

Sc

Table 2-1 Cont'd

Phenanthrene	10	Na <sub>2</sub> SO <sub>4</sub>	0	DC	6.0	1
Phenanthrene	10	Na <sub>2</sub> SO <sub>4</sub>	0	DC	10.2	1
Phenanthrene	10	NaCl	Control	-	-	-
Pyrene	5	NaCl	0.1	Square	3.0	2
Pyrene	5	NaCl	0.1	Square	10.2	2
Pyrene	5	NaCl	0.1	Square	18.5	2
Pyrene	5	Na <sub>2</sub> SO <sub>4</sub>	0.1	Square	10.2	1
Pyrene	5	Na <sub>2</sub> SO <sub>4</sub>	1	Square	10.2	1
Pyrene	5	Na <sub>2</sub> SO <sub>4</sub>	60	Square	10.2	2
Pyrene	5	Na <sub>2</sub> SO <sub>4</sub>	60	Sine	10.2	1
Pyrene	5	Na <sub>2</sub> SO <sub>4</sub>	0	DC	3.0	1
Pyrene	5	Na <sub>2</sub> SO <sub>4</sub>	0	DC	6.0	1
Pyrene	5	Na <sub>2</sub> SO <sub>4</sub>	0	DC	10.2	1
Pyrene	5	NaCl	Control	-	-	1
Salicylic Acid	100	NaCl	0.1	Square	10.2	1
					<b>Total no. of tests</b>	<b>29</b>

## Electrochemical Degradation of Phenanthrene in Solution

### Effect of Current Density

Figure 2-2 presents the average concentration of phenanthrene ( $C_0 = 10$  mg/L) collected from the test cells subjected to AC densities equal to  $3.0$  mA/cm<sup>2</sup>,  $10.2$  mA/cm<sup>2</sup> and  $18.5$  mA/cm<sup>2</sup>.

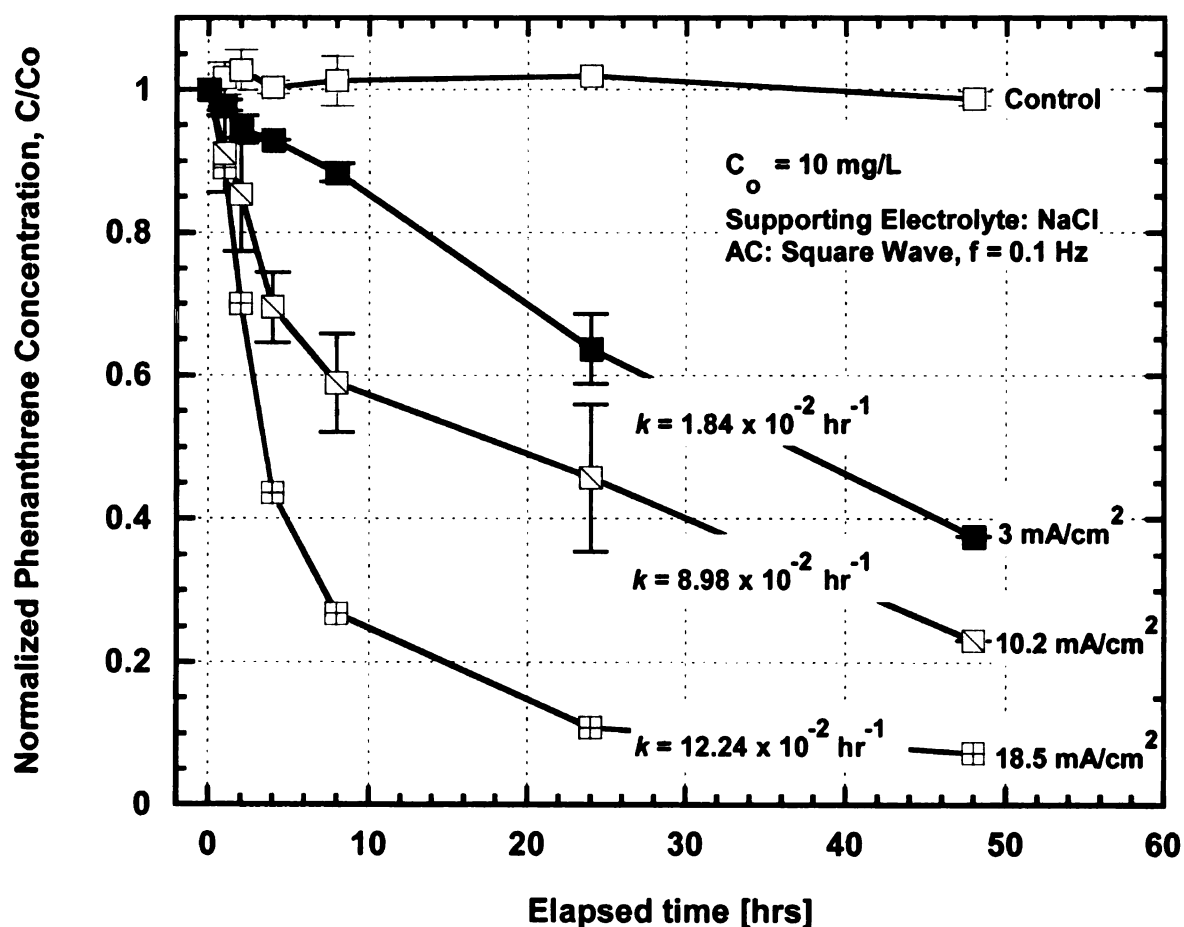


Figure 2-2: Change in concentration of phenanthrene with time

By passing AC having a peak current of 1 A, equivalent to an average AC density of  $18.5$  mA/cm<sup>2</sup> through the phenanthrene solution, about 90% reduction in the concentration of

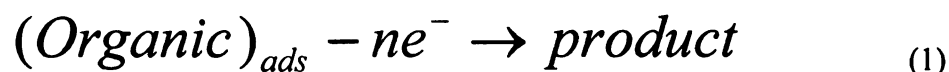
phenanthrene in the solution was observed within 48 hrs. The AC density was obtained by dividing the peak current by the average cross sectional area of the test solution in contact with the electrodes. The level of the test solution in contact with the electrode decreased as samples were collected for measurements and analysis. Therefore an initial current density of  $18.2 \text{ mA/cm}^2$  was applied to the solution and after the 48 hr-testing period; the current density reached about  $18.9 \text{ mA/cm}^2$  resulting in an average value of about  $18.5 \text{ mA/cm}^2$ . By passing AC having a peak current of 0.165 A and 0.550 A, equivalent to an average AC density of  $3.0 \text{ mA/cm}^2$  and  $10.2 \text{ mA/cm}^2$  through the phenanthrene solution, about 65% and 75%, respectively, reduction in the concentration of phenanthrene in the solution was observed within 48 hrs. Thus, increase in current density resulted in an increase in the degradation rate of phenanthrene in solution. This is consistent with the trend observed by Alshawabkeh and Sarahney (2005), who reported an increase in degradation rate of naphthalene as current densities were increased.

A majority of published work on electrochemical degradation has focused on the use of DC. This relies mainly on anodic oxidation to degrade non-polar organic compounds and hence the cathode acts as a “passive” electrode in the oxidation process. Pepprah and Khire (2008) have reported that when an AC is used, the constant polarity reversal ensures that both electrodes participate in the oxidation process, depending on their polarity in a given AC cycle. During the one half of a cycle when one of the electrodes has a positive electrical potential, it instantaneously acts as the anode while the other electrode, at a negative electrical potential, acts as the cathode. In the subsequent half cycle, polarities are reversed and the electrodes acquire electrical potentials opposite

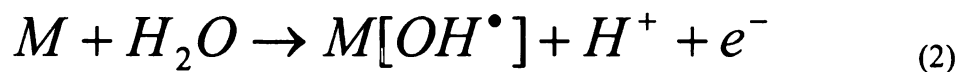
to what they had in the previous cycle and this continues throughout the period of application of the AC.

### *Oxidizing Agents*

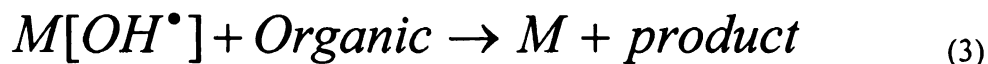
Organic compounds in aqueous solutions can be oxidized on an anode (anodic oxidation) by direct electron transfer and indirect oxygen atom transfer (Polcaro *et al.* 1999; Iniesta *et al.* 2001; Rodgers *et al.* 1999; Chiang *et al.* 1995; Kirk *et al.* 1985). In the direct electron transfer process, organics are adsorbed on the anode surface and give up electrons to the anode (Li *et al.* 2005) as presented in Equation 1



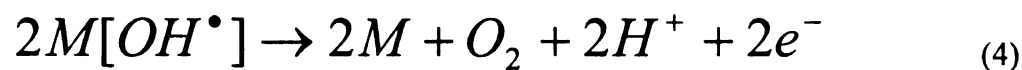
During the indirect oxygen atom transfer, oxygen radicals, especially the hydroxyl radicals generated from water electrolysis, help in the oxidation of organic substances (Iniesta *et al.* 2001; Simond *et al.* 1997; Comninellis 1994; Lee *et al.* 1981). The formation of hydroxyl radicals on the anode surface can be expressed by Equation 2, where M stands for the anode (Simond *et al.* 1997; Comninellis 1994)



The hydroxyl radicals readily react with the organic molecules adsorbed on or in the vicinity of the anode to cause the reaction presented below in Equation 3 (Li *et al.* 2005)



Meanwhile, the hydroxyl radicals react with each other to form molecular oxygen to complete the electrolysis of water molecules (Simond *et al.* 1997; Comninellis 1994) as shown in Equation 4



Nakamura *et al.* (2005) proposed a mechanism based on selective redox reactions with various radicals generated by AC electrolysis that allowed both oxidation and reduction at the same reaction site between adjacent electrodes. Based on the analysis of intermediate products of the degradation process, it was revealed that the mechanism involved selective redox reactions with short-lived and highly reactive radicals: hydrogen atoms ( $H^\bullet$ ) and hydroxyl radicals ( $OH^\bullet$ ) that are electrochemically generated on the electrodes. Based on the hydroxylated degradation products formed, it is likely that  $OH^\bullet$  radicals produced in our test solutions were mainly responsible for the degradation of phenanthrene and pyrene.

#### *Hydroxyl Radical Test*

$OH^\bullet$  attack the benzene rings of aromatic compounds to produce hydroxylated compounds. Various  $OH^\bullet$  radical probes and techniques have been used in previous studies to detect the generation of  $OH^\bullet$  in the reaction media. These include salicylic acid (Li *et al.* 2003; Marselli *et al.* 2003; Oturan 2000; Jen *et al.* 1998; Scheck and Frimmel 1995), 4-hydroxybenzoic acid (Anderson *et al.* 1987), benzoic acid (Oturan and Pinson 1995), *para*-chlorobenzoic acid (*p*CBA) (Elovitz and von Guten 1999; Haag and Yao 1992), 2,2-diphenyl-1-picrylhydrazyl (DPPH) (Sehgal *et al.* 1982), 5,5-dimethyl-1-pyrroline-N-oxide (DMPO) and electron spin resonance (ESR) (Marselli *et al.* 2003), *p*-nitrosodimethylaniline (RNO) and spectrophotometer measurements (Tanaka *et al.* 2004), and RNO / ESR (Comninellis 1994). Since ESR methods require expensive and



1

sec  
T  
m  
D  
d  
d

Normalized Salicylic Acid Concentration, C/C<sub>0</sub>

sophisticated equipments; they were not used in this study due to budget constraints. Trapping of  $\text{OH}^\cdot$  using salicylic acid, and HPLC measurements were selected as hydroxyl radical probe technique for this study. Since salicylic acid had a greater solubility in the binary solution, 100 mg/L was used for the electrochemical cell so that enough degradation products would be produced for identification purposes. Figure 2-3 shows a decrease in concentration of salicylic with time.

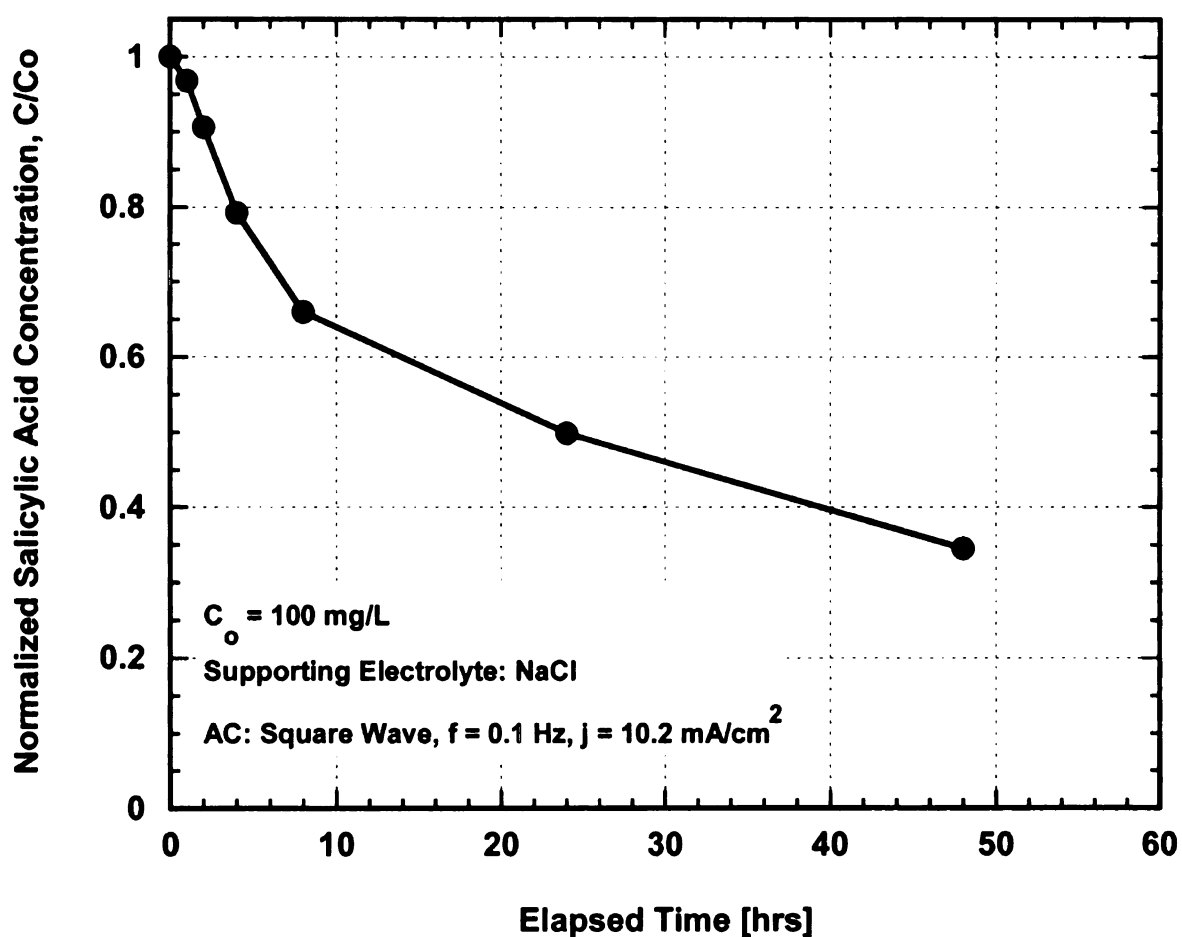


Figure 2-3: Change in concentration of salicylic acid

About 70% reduction in concentration of salicylic acid was achieved in 48 hrs accompanied by the formation of degradation products such as 2,3-dihydroxybenzoic acid and 2,5-dihydroxybenzoic acid. The formation of these degradation products is consistent with numerous studies (e.g., Marselli *et al.* 2003) that hydroxyl radicals were involved in the electrochemical degradation process.

### *Degradation Kinetics*

The initial degradation rate of phenanthrene in solution could be described as *pseudo* first-order decay as shown in Equation 5:

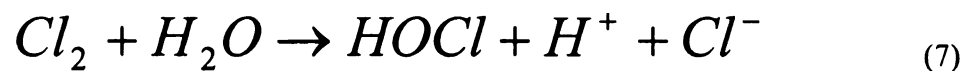
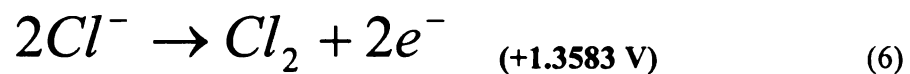
$$\frac{d[C]}{dt} = -k[C] \quad (5)$$

where  $C$  is the concentration of phenanthrene and  $k$  is the *pseudo* first-order degradation rate constant. A plot of  $\ln[C/C_0]$  versus time was used to estimate  $k$ . The  $k$  obtained from Figure 2, for the initial 8 hrs of application of AC density of  $18.5 \text{ mA/cm}^2$  was  $1.22 \times 10^{-1} \text{ hr}^{-1}$  ( $R^2 = 0.99$ ) and the corresponding half-life was 5.7 hrs. Similarly, the degradation rate at an AC density of  $10.2 \text{ mA/cm}^2$  exhibited initial rapid degradation until after 8 hrs when the degradation rate decreased substantially. About 75% reduction in the concentration of phenanthrene in solution was observed during the 48-hour AC application. The initial degradation rate for this AC density was characterized by an observed *pseudo* first-order degradation rate constant ( $k$ ) of  $8.98 \times 10^{-2} \text{ hr}^{-1}$  ( $R^2 = 0.92$ ) and the corresponding half-life was 7.7 hrs. The degradation rate at an AC density of  $3 \text{ mA/cm}^2$  was  $1.84 \times 10^{-2} \text{ hr}^{-1}$  ( $R^2 = 0.99$ ) and the corresponding half-life was 34.7 hrs.

The phenanthrene degradation rate was faster when a higher AC density (or alternating voltage) was used. This finding is consistent with the previous findings (Chin and Cheng 1985) whereby, the rate of conversion of phenol increased with increasing magnitude of alternating voltage superimposed on a DC. During the testing period of 48 hours, as shown in Figure 2-2, no significant reduction in phenanthrene concentration was observed in the control cell.

#### *Effect of Type of Supporting Electrode*

Besides direct anodic oxidation, organic pollutants can also be degraded by indirect electrolyses, generating in situ chemical reactants to convert them to less harmful products (Panizza and Cerisola 2003). The presence of chloride ions may result in the formation of chlorine gas instead of oxygen gas at the anode (Alshawabkeh and Sarahney 2005). The mechanism of electrogeneration of chlorine from chloride ions in solution has been presented by Panizza *et al.* (2000) as shown in Equations 6 to 8.



The hypochlorous acid (HOCl) that is formed (Equation 7) acts as an oxidizing agent, thus enhancing the overall degradation. It has been used in the treatment of landfill leachate and textile effluent (Chiang *et al.* 1995; Naumczyk *et al.* 1996), and in both cases, complete removal of ammonia and accompanying COD reduction was achieved.

On the other hand, it was expected that using Na<sub>2</sub>SO<sub>4</sub> as supporting electrolyte would not



er  
ra  
st  
m  
te

F  
de  
T  
de  
ex

generate additional oxidizing agents in solution that would enhance overall degradation rates. Figure 2-4 shows a plot the concentration time profile of two tests conducted under similar experimental conditions of 10 mg/L phenanthrene initial concentration and 10.2 mA/cm<sup>2</sup> current density, except that NaCl was used as the supporting electrolyte in one test and Na<sub>2</sub>SO<sub>4</sub> in the other test.

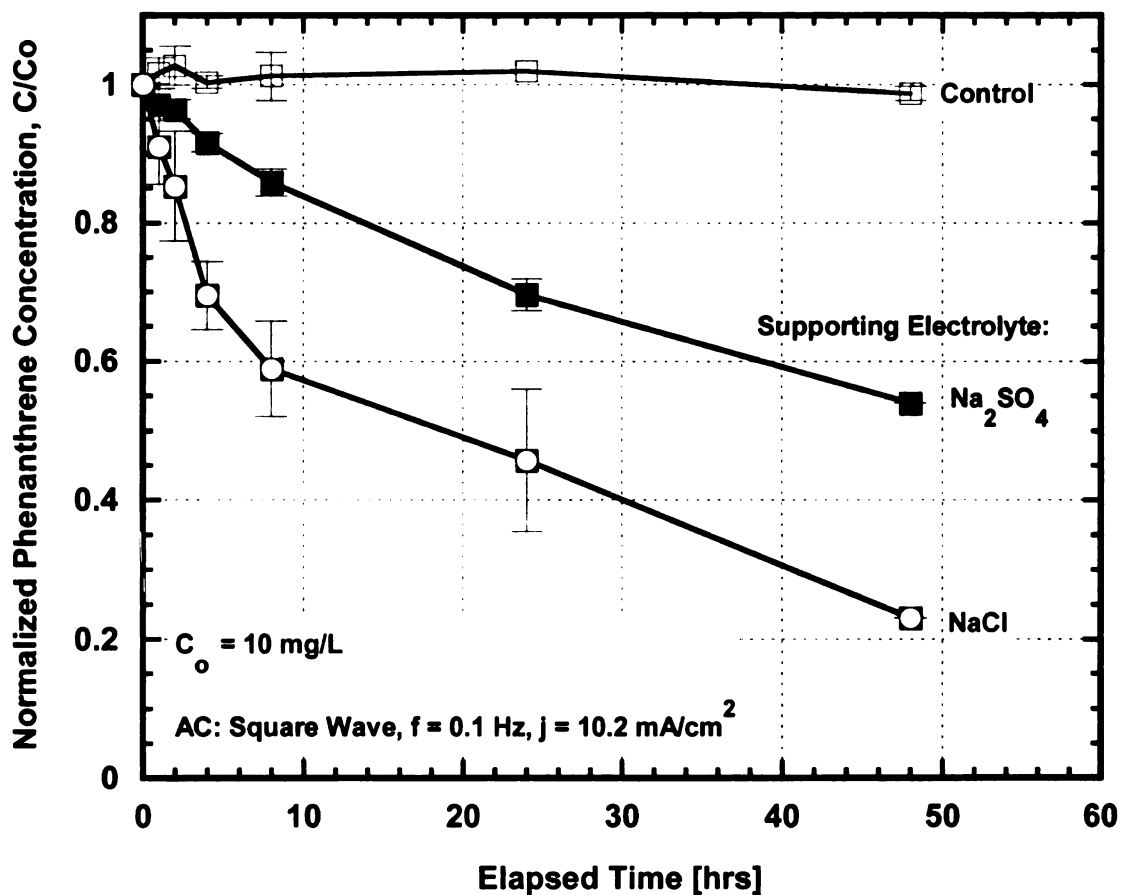


Figure 2-4: Concentration of phenanthrene using NaCl or Na<sub>2</sub>SO<sub>4</sub> as supporting electrolyte

The faster degradation rate exhibited by the test cell containing NaCl confirms that degradation rates were most likely enhanced by the formation of HOCl from the anodic oxidation of Cl<sup>-</sup> to produce chlorine gas in solution. Therefore we believe that the

1

de  
ov  
Et  
S.  
ca  
S.  
l.  
0.  
k.

degradation of phenanthrene in our system could have been due to direct anodic oxidation which was enhanced by the electrogeneration of chlorine gas in solution.

### **Effect of AC Frequency**

Square wave AC having a peak AC density of  $10.2 \text{ mA/cm}^2$  was used to investigate the effect of AC frequency ( $f$ ) on degradation rates of phenanthrene in the test cells. Figure 2-5 shows that applying a square wave peak AC density of  $10.2 \text{ mA/cm}^2$  at frequencies 0.1, 1, and 60 Hz resulted in  $k$  equal to  $1.3 \times 10^{-2} \text{ hr}^{-1}$  ( $R^2 = 0.95$ ),  $0.5 \times 10^{-2} \text{ hr}^{-1}$  ( $R^2 = 0.99$ ),  $0.6 \times 10^{-2} \text{ hr}^{-1}$  ( $R^2 = 0.99$ ), respectively. A DC ( $f = 0$ ) density of  $10.2 \text{ mA/cm}^2$  resulted in  $k$  equal to  $12.4 \times 10^{-2} \text{ hr}^{-1}$  ( $R^2 = 0.96$ ).



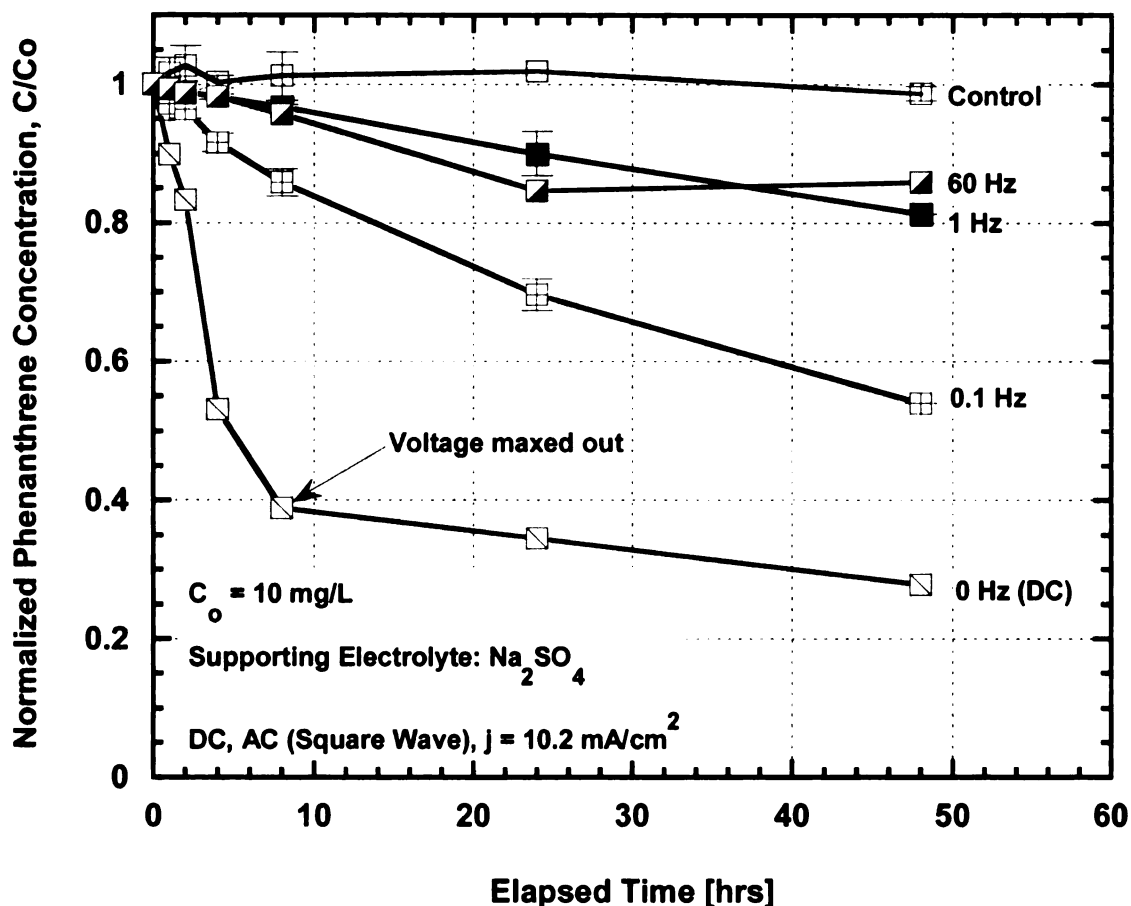


Figure 2-5: Effect of AC frequency on degradation rates of phenanthrene

These results indicate that the rate of degradation of phenanthrene in aqueous solution generally decreased with increasing AC frequency. This finding is consistent with the trend observed by Chin and Cheng (1985) that the rate of conversion of phenol decreased with increasing alternating voltage frequency superimposed on a DC. The voltage supplied by our electrical test equipment maxed out after 8 hrs of application of the DC, thus resulting in decreasing amount of current supplied. This slowed down the degradation rate after 8 hrs. Figure 2-6 shows the temperature-time profile of a typical test solution containing 30% Acetonitrile/70% DI water as solvent with sodium sulfate as

the  
the



F.  
St  
Th  
so  
the  
for  
at  
so  
Ve

the supporting electrolyte and another typical test solution containing 100% DI water as the solvent with sodium sulfate as the supporting electrolyte.

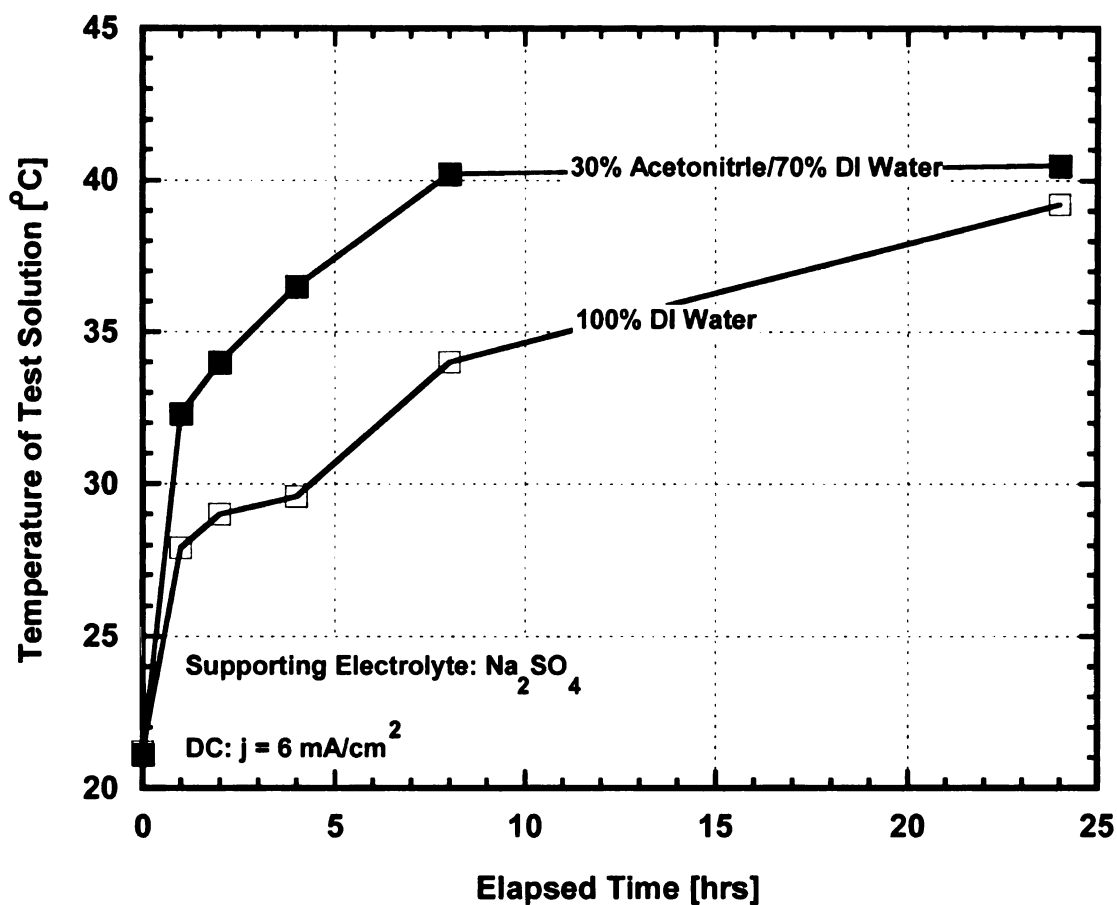
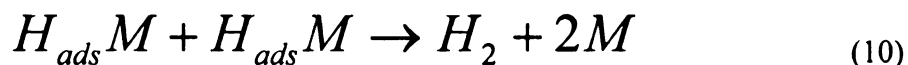
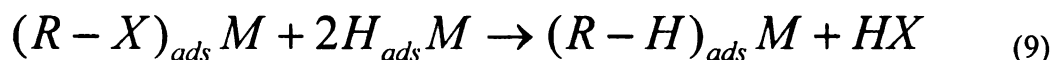


Figure 2-6: Temperature-time profile of test solutions containing only DI water and 30/70 Acetonitrile/DI water

The presence of acetonitrile in the test solution increases the resistance of the test solution. Greater resistance results in greater voltage applied by the amplifier to maintain the given current which results in greater temperature of the solution. Greater temperature further increases the resistance of the solution. In constant current mode, the amplifier automatically adjusted the voltage to compensate for the increase in resistance of the test solution in order to maintain the set current through the test solutions. Therefore after the voltage maxed out at 200 V, the supplied current decreased over time leading the applied

current decreased for the DC tests (Figure 2-5). However, still DC resulted in greater rate of degradation than any AC at an equivalent *rms* current.

Continuous bubbling of gases (probably O<sub>2</sub> and H<sub>2</sub>) in the test solution was observed as the tests progressed, however, the rate of bubbling of the gas decreased as the frequency of the applied AC was increased until no gas bubbles were visible at the electrodes at an AC frequency of 60 Hz. Stock and Bunce (2002) reported that electrocatalytic hydrogenation of hydrogenolysis of atrazine (Equation 9) was in competition with hydrogen evolution, (Equation 10):



According to Equations 4 & 10, if the formation of OH radicals and hydrogen radicals are precursors for the generation of oxygen gas and hydrogen gas at the anode and cathode, respectively, then it is likely that the rate of gas bubbling at the electrode gives an indication of the rate of formation of these radicals at the electrodes. The higher the rate of the observed bubbling of the gas(es), the greater the rate of hydroxyl or hydrogen radical formation at the electrodes. Hence, based on the visual observation of gas bubbles, it is likely that increase in the AC frequency resulted in decrease in the rate of formation of hydroxyl radicals at the electrodes. This impacted the rate of oxidization of phenanthrene at the instantaneous anodes.

Therefore it is probable that either reduced rate of generation of hydroxyl radicals with increased AC frequency, or back-and-forth movement of the reacting molecules that slowed down the rate of movement of reacting molecules to the reaction site (the



ele  
inc  
at  
ap  
E  
Si  
w  
w  
th  
to

electrode), or a combination of both factors resulted in decreased degradation rate with increased AC frequency. It is also possible that competing anodic and cathodic reactions at the same reactions sites (both electrodes) as a result of the polarity reversal of the applied AC slowed down the oxidation of the phenanthrene molecules.

#### *Effect of AC Waveform*

Since AC is supplied as a sign wave at 60 Hz in the United States, the effect of the AC waveform on degradation rates was explored using a 60 Hz square wave and a 60 Hz sine wave. Figure 2-7 shows that a square-wave AC resulted in a greater degradation rate than the sine wave AC supplied at an equivalent *rms* (root mean square) current density equal to  $10.2 \text{ mA/cm}^2$  and frequency of 60 Hz.

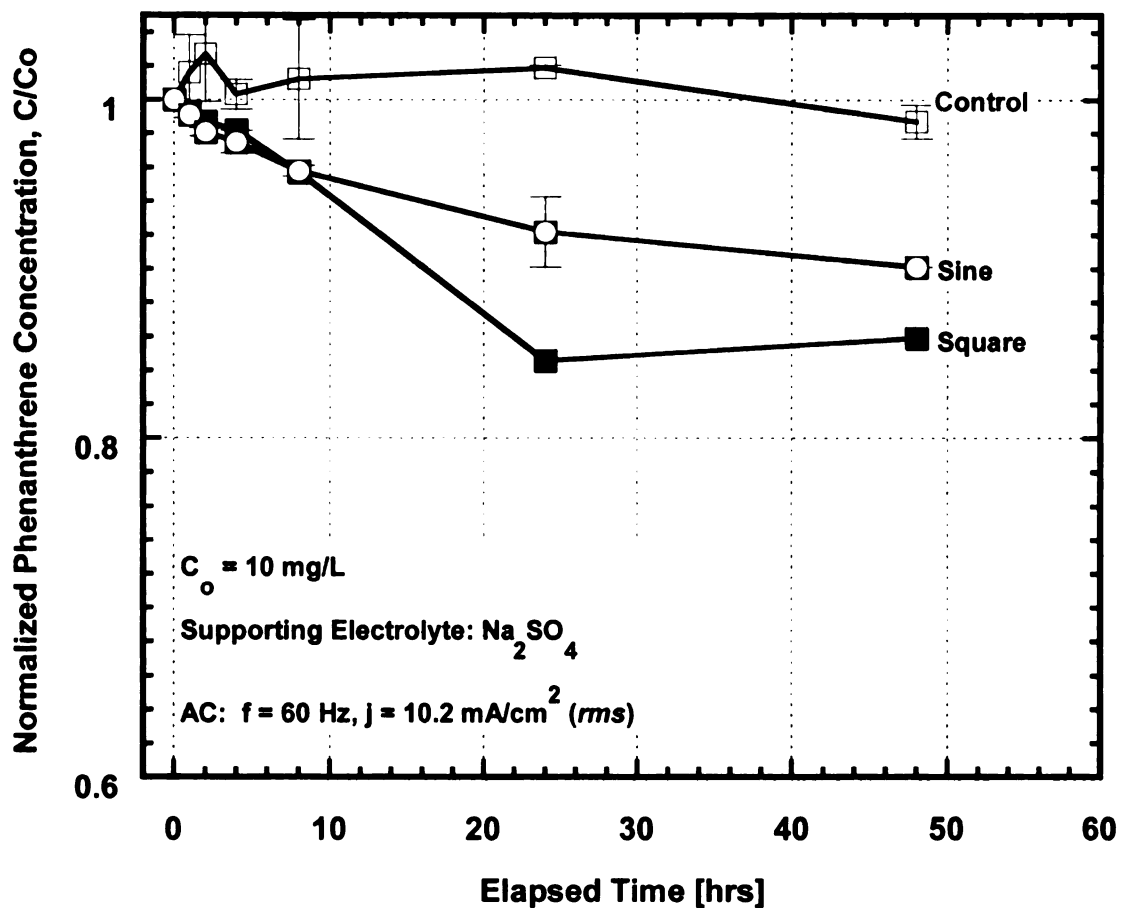


Figure 2-7: Effect of AC waveform shape on degradation rates of phenanthrene

During a single cycle in a sinusoidal AC wave, the voltage or current gradually increases from negative maximum to the positive maximum and back again. For an AC square wave function, the voltage or current shifts suddenly from negative to positive, stays there for half a cycle, and then jumps to full negative and stays there for half a cycle. Therefore, in a cycle of the AC wave, the alternating current instantaneously flows in one direction and then flows in the opposite direction in the other half cycle. Therefore the full peak current for a square wave is felt at any given period in the cycle, unlike the sine wave that sweeps from zero through lower current values until the peak current value is

attained and then sweeps back to zero. Therefore, the square wave was more efficient in degrading phenanthrene than an equivalent sine wave.

### *Electrode Fouling*

The degradation of phenanthrene in solution was characterized by an initial relatively rapid degradation within 0 to 8 hrs of the application of AC and a slower rate from 8 to 48 hrs. The decrease in degradation rate may be due to, among other factors, such as reduced mass of reacting molecules available for reaction, and electrode fouling over time as the new titanium sheet lost its initial metallic sheen (light gray color) to a dark gray color as the test progressed. The electrode fouling was confirmed by utilizing electrodes, which had been used in a previous test to electrolyze replicate phenanthrene test solution. It resulted in decreased degradation rate as compared to the new electrodes. By polishing the electrodes that had been used in previous test with abrasives such that their metallic sheen was restored, degradation rates using the polished electrodes were approximately the same as using new electrodes for the tests.

## **Electrochemical Degradation of Pyrene in Solution**

### *Effect of Current Density*

Figure 2-8 presents the average concentration of pyrene in the test cells at AC densities equal to  $3.0 \text{ mA/cm}^2$ ,  $10.2 \text{ mA/cm}^2$ ,  $18.5 \text{ mA/cm}^2$ , and for the control cell.



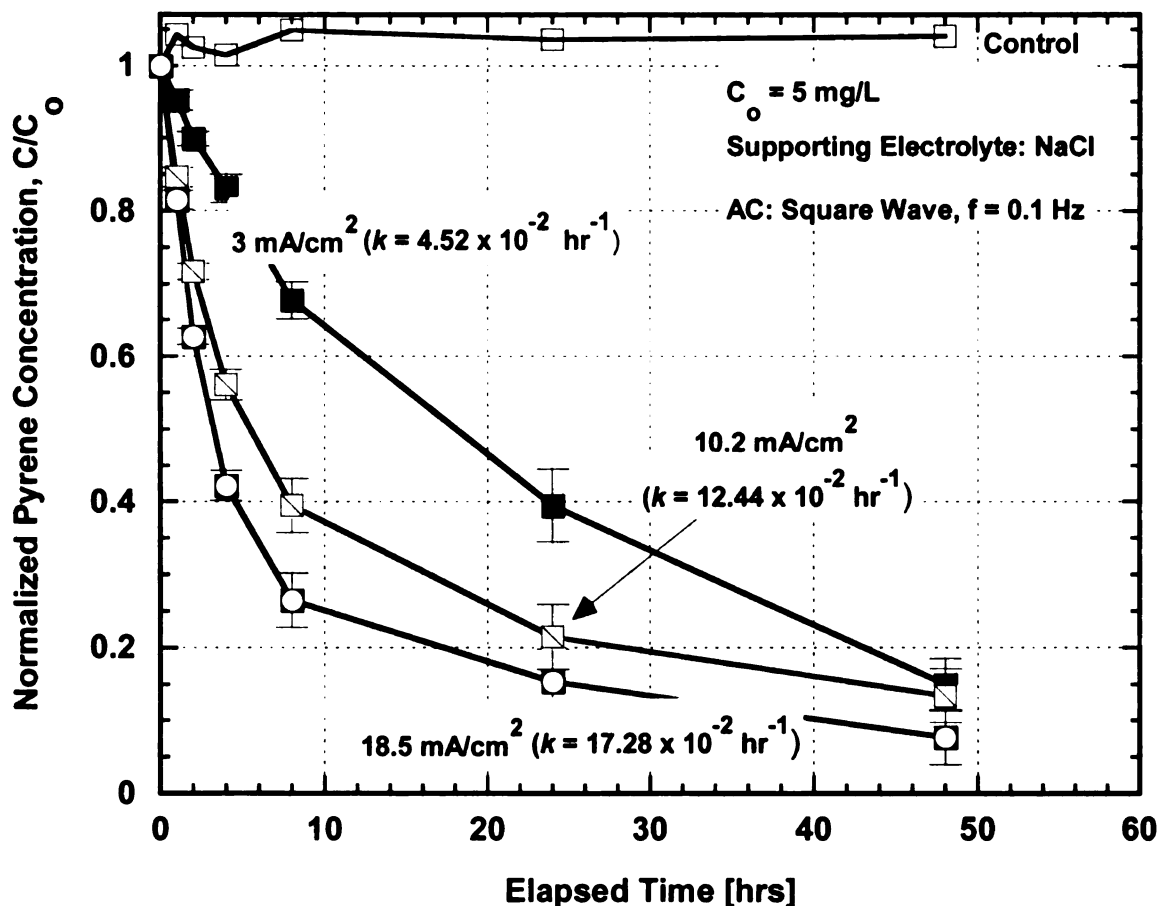


Figure 2-8: Concentration of pyrene versus time for various current densities

For each sampling round, two samples were analyzed using HPLC to quantify concentrations. Figure 2-8 presents the average concentration reported from these two samples and two additional samples from a replicate test cell. The error bars represent the maximum and minimum values recorded for the total four samples. For all three current densities, 90 % reduction in concentration of pyrene in the solution (initial target concentration = 5 mg/L) was observed within 48 hrs. Similar to the phenanthrene solution, the initial degradation rate of phenanthrene in solution could also be described as *pseudo* first-order decay similar to that for phenanthrene presented in Equation 1.

Although initial degradation rates were faster for higher current densities, the lowest current density applied, ultimately resulted in the same percentage degradation after 48 hrs of testing. Hence in terms of savings in electrical energy, it would be more economical in running tests at low current densities.

By comparing the time-concentration profiles of the  $18.5 \text{ mA/cm}^2$  and  $10.2 \text{ mA/cm}^2$  current densities, it can be observed that although these current densities differ by almost a factor of two, their corresponding degradation rates constants differ significantly by less than a factor of two. However, by comparing the time-concentration profiles of the  $10.2 \text{ mA/cm}^2$  and  $3 \text{ mA/cm}^2$  current densities, these current densities differ by about a factor of three and their corresponding degradation rate constants differ approximately by a factor of three. Therefore it can be inferred that beyond a certain current density, the rate of movements of the reactants to the reaction sites (the electrodes) becomes the rate limiting step because excess oxidizing agents are produced at the electrodes to potentially oxidize the reactants. This is consistent with previous studies by Stock and Bunce (2002) who applied currents 5, 10, 20, 50, 100 and 200 mA on the dechlorination efficiency of atrazine and reported that applied currents  $\geq 20 \text{ mA}$  led to  $\geq 93\%$  loss of initial atrazine within 30 minutes. The current efficiency decreased as applied current increased and was greatest (16%) at 10 mA. Yusem and Pitauro (1992) also reported a decrease in current efficiency with increased applied current in electrocatalytic hydrogenation of soyabean. Stock and Bunce attributed this trend to the fact that a greater proportion of  $H_{\text{ads}}$  was lost to unproductive reaction of hydrogen gas evolution instead of participating in the dechlorination reaction of atrazine. Apart from

this explanation, we believe that a greater proportion of the applied current in our system was dissipated as heat as a result of Joule heating, which was evident by increased rate of temperature rise of our test solutions with increased current density. As shown in Figure 2-8, the control cell solution did not indicate any significant reduction in concentration over the entire testing period.

*Effect of Type of Supporting Electrode*

Using NaCl as the supporting electrolyte resulted in a higher degradation rate of pyrene than using Na<sub>2</sub>SO<sub>4</sub> as the supporting electrolyte as shown in Figure 2-9. This is consistent with the results obtained for the tests involving phenanthrene.

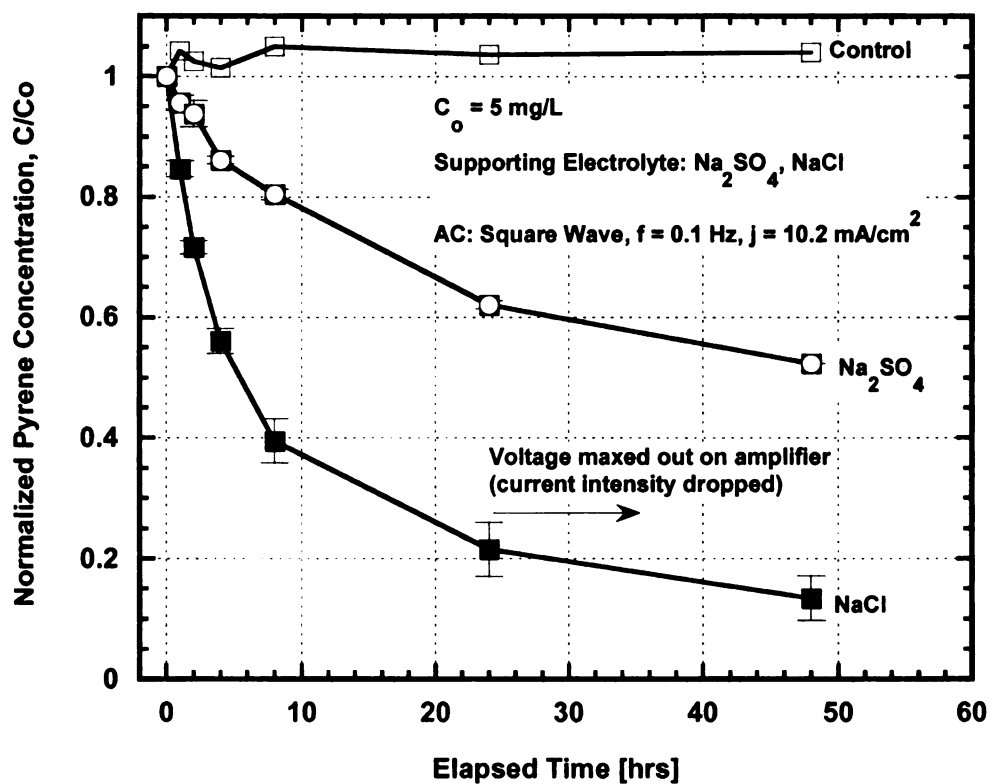


Figure 2-9: Change in concentration of pyrene with time using NaCl or Na<sub>2</sub>SO<sub>4</sub> as supporting electrolyte

### Effect of AC Frequency

Similar to the phenanthrene test cells, increasing AC frequency resulted in decreased rate of degradation of pyrene in solution as shown in Figure 2-10.

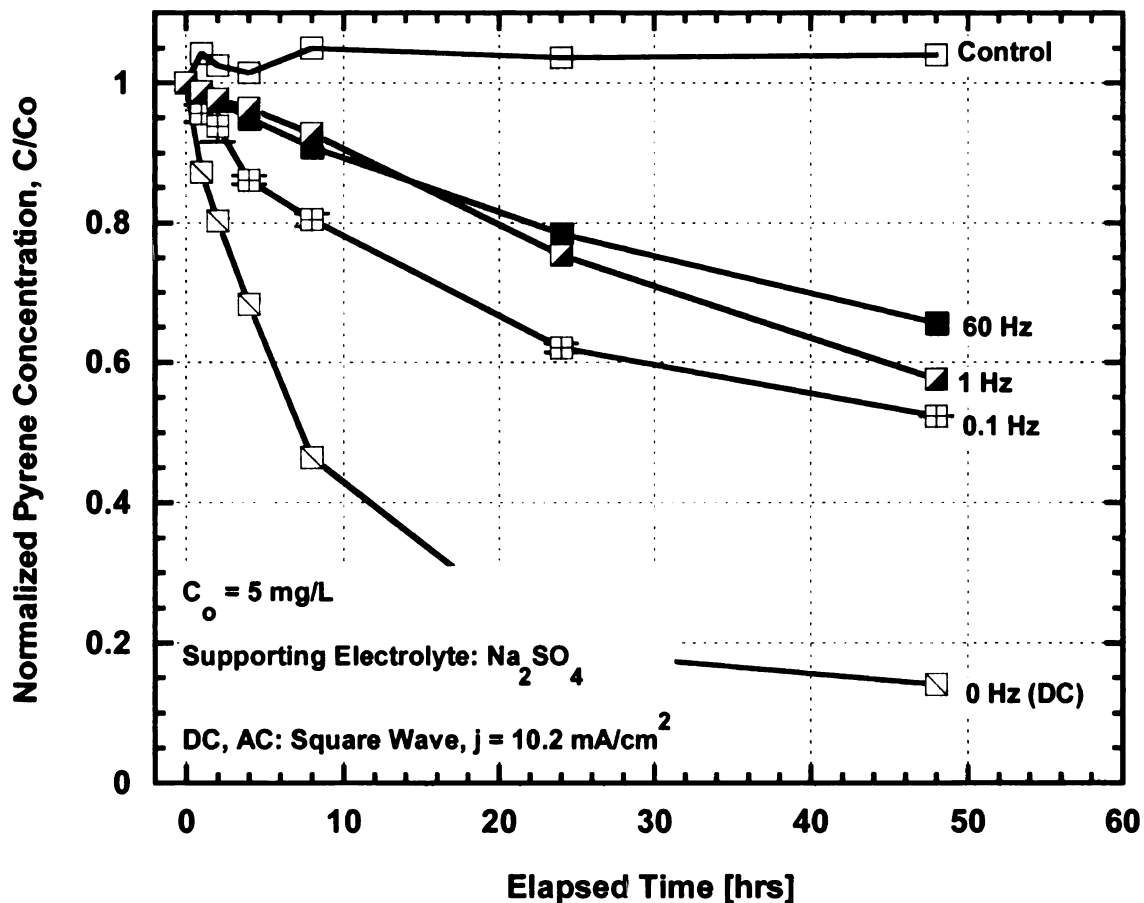


Figure 2-10: Effect of AC frequency on degradation rates of pyrene

### Effect of AC Waveform

AC square wave produced a faster degradation rate than an equivalent AC sine wave as shown in Figure 2-11. This is also consistent with trends observed for phenanthrene.

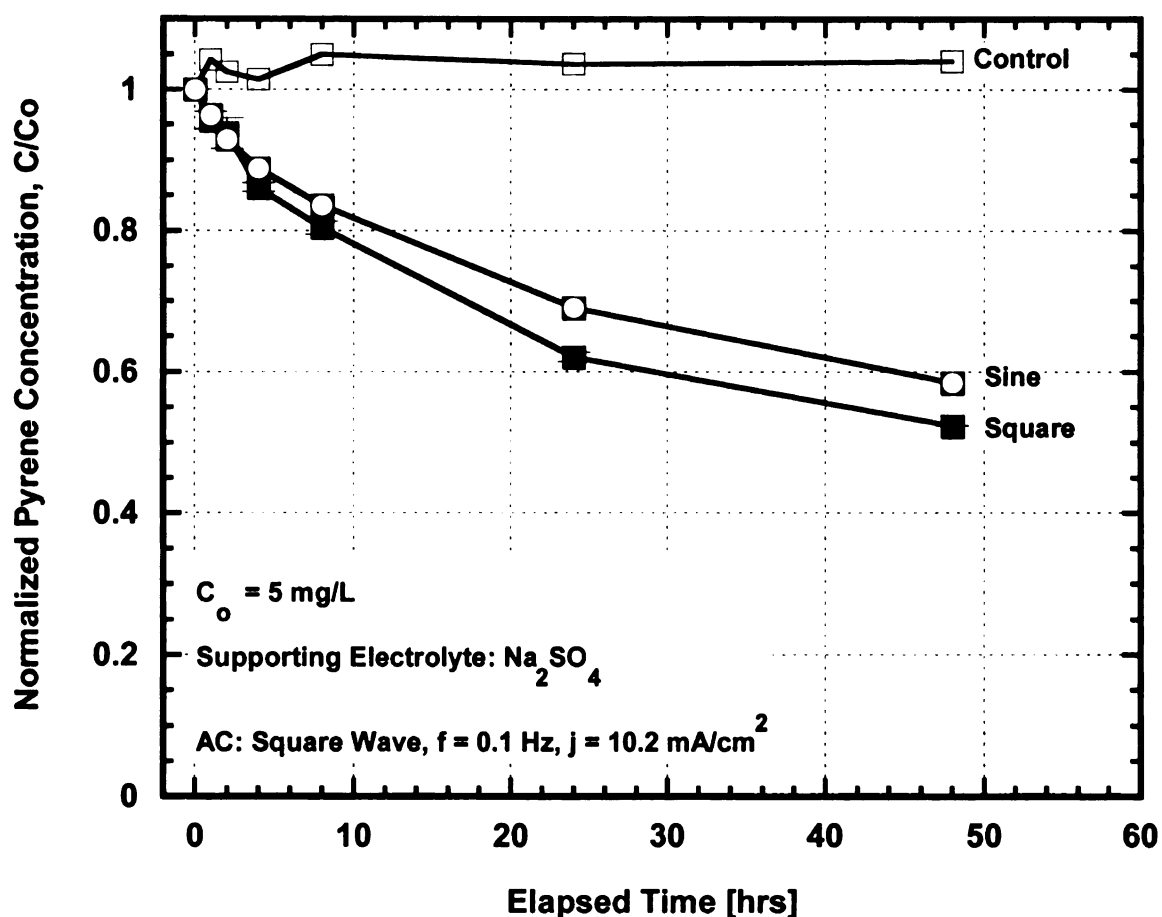


Figure 2-11: Effect of AC waveform shape on degradation rates of pyrene

### Modeled *versus* Measured Concentrations of Phenanthrene and Pyrene

It is generally believed that electrochemical reactions occur mainly on the surface or in the vicinity of the electrodes. Therefore, the rate of reaction of the organic reactants in the test cell depends on the rate of generation of OH radicals at the electrodes as the oxidizing agents, as well as the rate at which the reacting molecules move to the electrodes for subsequent oxidation by the OH radicals. Mass transfer in solution occurs by diffusion, migration and convection. Diffusion and migration result from a gradient in electrochemical potential and convection results from imbalance of forces on the solution when the solution is mixed or stirred (Bard and Faulkner 2001). Assuming a linear mass

transfer, and linear electric field, the mass flux to the electrode can be expressed by the *Nernst-Planck Equation* (Equation 11):

$$J(x) = -D \frac{\partial C(x)}{\partial x} - \frac{zF}{RT} DC \frac{\Delta E}{l} + Cv(x) \quad (11)$$

where  $J$  is the mass flux,  $D$  is the diffusion coefficient of the reacting specie in solution,  $C$  is the instantaneous concentration of the reactants in solution at time  $t$ ,  $x$  is the distance in the  $x$  direction or along the direction of the electrical current,  $z$  is the net charge on the reacting species,  $F$  is Faraday's constant,  $R$  is molar gas constant,  $T$  is temperature (K),  $\Delta E/l$  is the gradient arising from the change in potential  $\Delta E$  over a distance  $l$ , and  $v$  is the linear velocity of the solution. Because the test cell solutions were not stirred, the third term in Eq. 6 can be neglected and hence Equation 11 becomes:

$$J(x) = -D \frac{\partial C(x)}{\partial x} - \frac{zF}{RT} DC \frac{\Delta E}{l} \quad (12)$$

For uncharged reactant, the second term in Equation 12 can be neglected to yield *Fick's* first law of diffusion as follows:

$$J(x) = -D \frac{\partial C(x)}{\partial x} \quad (13)$$

Equation 13 was applied to model the rate of mass transfer of Phenanthrene or pyrene to the electrodes in the DC setup. The following assumptions were made when applying Equation 12 (or Equation 13) to simulate the Phenanthrene or pyrene concentrations:

1. Reactants (Phenanthrene or pyrene) are instantaneously converted to products when they come into contact with the electrode. Hence,  $C(t)$  at the surface of electrode is equal to zero for  $t \geq 0$ . This establishes a concentration gradient that

drives reactants by diffusion to the surface of the electrodes and this condition is considered as the maximum concentration gradient that may be established in a given time step;

2. Steady-state diffusion conditions exist in a given time step which was assumed equal to 1 hr;
3. Linear mass transfer exists in the given time step of 1 hr; and
4. Linear electric field exists in the given time step of 1 hr; and

Equation 13 was applied with  $C$  of phenanthrene equal to  $C_0$  ( $\sim 10$  mg/L); or with  $C$  of pyrene equal to  $C_0$  ( $\sim 5$  mg/L) for  $t = 0$  at the cathode and  $C = 0$  for  $t \geq 0$  at the anode.

Assuming a time step equal to 1 hr, the  $C$  of phenanthrene or pyrene at cathode was estimated by subtracting the mass of phenanthrene or pyrene that moved to the anode for degradation during the previous time step. This computation was carried out for the test duration of 24 hours and the modeled normalized concentrations were compared (Figure 2-11 & 2-12) to the test results for DC tests carried out at  $j = 3$  and  $6$  mA/cm<sup>2</sup>.

Schwarzenbach *et al.* (2003) reported diffusion coefficients of organic solutes equal to about  $3.0 \times 10^{-5}$  cm<sup>2</sup> s<sup>-1</sup> for small molecules to  $5.0 \times 10^{-6}$  cm<sup>2</sup> s<sup>-1</sup> for those of molar mass near 300 g/mol. Based on this data, the diffusion coefficient of phenanthrene was estimated as  $8.0 \times 10^{-6}$  cm<sup>2</sup> s<sup>-1</sup> and that of pyrene as  $7.0 \times 10^{-6}$  cm<sup>2</sup> s<sup>-1</sup> from the diffusion coefficients vs. molar mass chart presented by Schwarzenbach *et al.* (2003). Equation 13 was applied to simulate only diffusion driven mass flux of phenanthrene or pyrene to the anode for oxidation. The simulated normalized concentrations are presented in Figures 2-12 & 2-13.

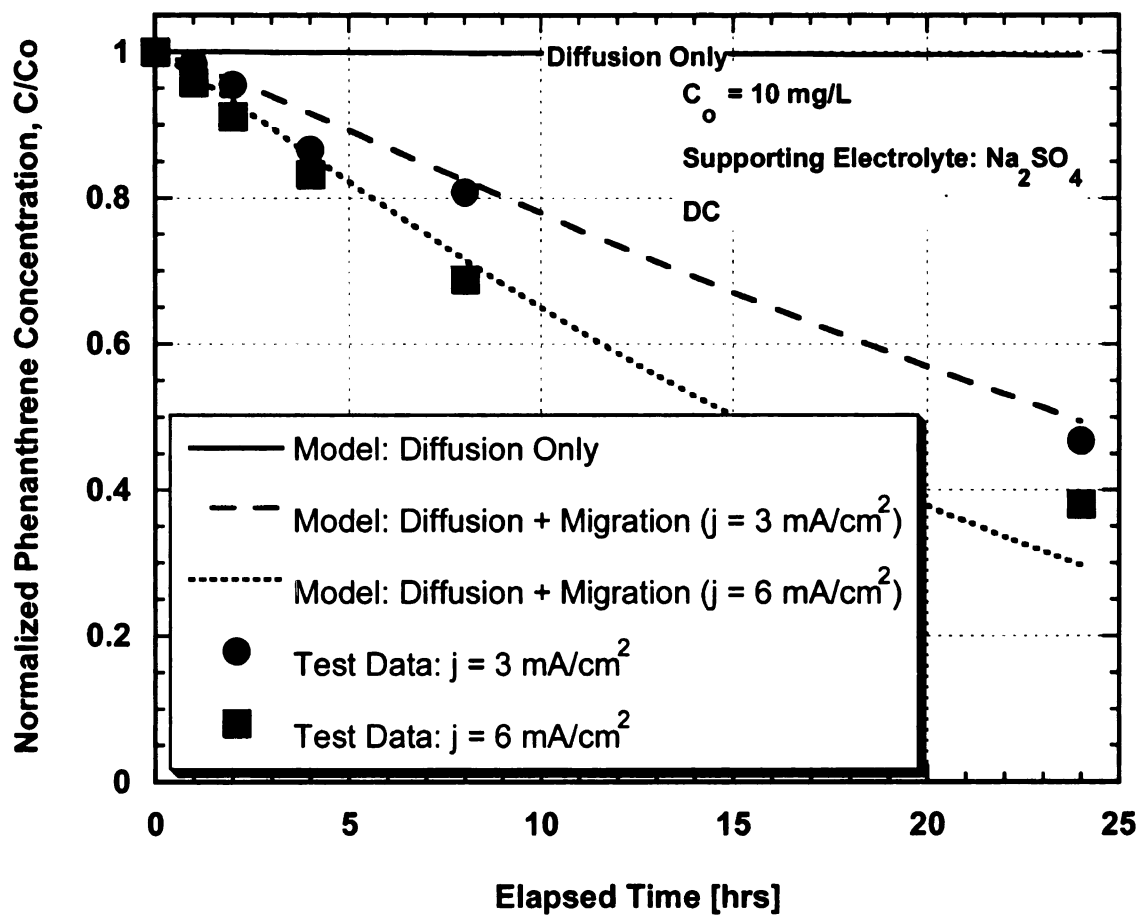


Figure 2-12: Simulated concentrations *versus* test data for phenanthrene tests using DC



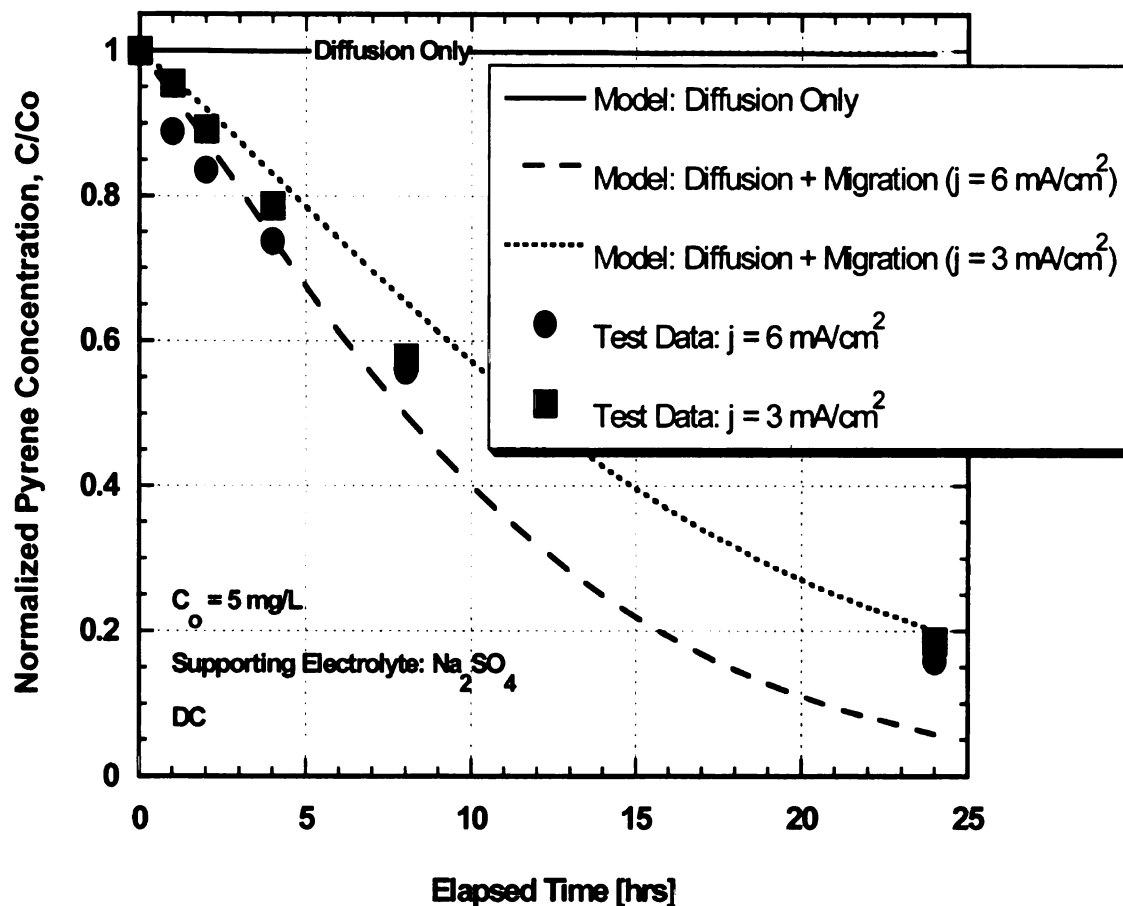


Figure 2-13: Simulated concentrations *versus* test data for pyrene tests using DC

The simulated degradation rate as a result of phenanthrene or pyrene migration to anode only due to diffusion is orders of magnitude less than that observed during the experiments run at DC densities equal to  $3 \text{ mA/cm}^2$  or  $6 \text{ mA/cm}^2$  with  $\text{Na}_2\text{SO}_4$  as the supporting electrolyte. When both diffusion and migration are used for simulating the mass flux of phenanthrene or pyrene to the anode by using Eq. 12, the simulated normalized concentrations are presented in Figures 2-11 & 2-12 when the net charge,  $z$ , was assumed equal to -0.04 and 0.11 for phenanthrene and pyrene respectively.

For neutral molecules such as phenanthrene or pyrene,  $z$  should be equal to zero. However, it is hypothesized that the presence of anions in the test solution (from the supporting electrolyte) imparted an effective negative charge on the phenanthrene or pyrene molecules and rendered them partially negatively charged molecules. These anions dragged the phenanthrene or pyrene molecules along as they migrated to the positively charged electrode (anode), where anodic oxidation resulted in the degradation of the phenanthrene or pyrene molecules. Therefore, the phenanthrene or pyrene molecules moved in the solution as a result of migration simulated by the second term in Equation 12 as well as diffusion. Hence, the rate of migration of naphthalene molecules towards the anode is enhanced by assigning a negative value to  $z$  for phenanthrene or pyrene.

By assigning the phenanthrene and pyrene molecule an effective partial negative charge of -0.04 and -0.11 respectively, the simulated normalized concentrations versus time data fits well with that for the experimental data when  $\text{Na}_2\text{SO}_4$  was used as the supporting electrolyte for DC densities equal to  $3 \text{ mA/cm}^2$  and  $6 \text{ mA/cm}^2$ . The rate of anodic oxidation of phenanthrene or pyrene depends not only on the rate of migration of reacting molecules to the reaction site (the anode or instantaneous anode) but also on the rate of production of OH radicals at the anode (or instantaneous anode). Hence, as the current density is decreased, it may decrease the rate of production of OH radicals at the anode and may become the rate limiting step. When Equation 12 is applied, the rate limiting step assumed is the rate of mass transfer to the anode (by diffusion and migration). Hence, Equation 12 would overestimate the decrease in the concentration (or underestimate the concentration at a given time,  $t$ ) of the reactant when current density is

low enough not to degrade all phenanthrene or pyrene mass diffusing and migrating to the anode (or instantaneous anode). At higher current densities, the predictions from Equation 12 would be more accurate. It is beyond the scope of this study to estimate the rate of hydroxyl radical production as a function of current density and other variables. Hence, it is not possible to calculate analytically at what current densities the assumptions are valid when Equation 12 is applied.

While Equation 12 is for DC and cannot be applied for an AC, it can be used to explain the reduced rate of degradation when AC was applied and as the frequency of the AC was increased from 0.1 to 60 Hz (Figures 2-5 & 2-9). Proposed reasons for the decrease in degradation rates with increased AC frequency are as follows:

1. By assuming that the phenanthrene molecules had an effective partial negative charge of say  $z = -0.04$  under our experimental conditions based on the acceptable fit for DC data, increasing the frequency of the AC resulted in back-and-forth movement of the reacting molecules, and hence the net mass flux of the molecules toward the electrodes was reduced. If the net distance traveled by the phenanthrene molecules to get to an instantaneous anode,  $L$ , in Equation 12, is varied, until the modeled values of concentrations fit with the experimental data for  $f$  equal to 0.1 Hz, 1 Hz, and 60 Hz the values of  $L$  obtained are 30 cm, 100 cm, and 10 cm, respectively, compared to the electrode spacing of 8 cm. For pyrene, AC frequencies of 0.1 Hz, 1 Hz and 60 Hz respectively resulted in  $L$  values of 110 cm, 100 cm, and 110 cm, respectively. Assuming degradation rate at the electrodes are the same for each frequency, it can be hypothesized that increase in the AC frequency results in taking longer duration for a phenanthrene

or pyrene molecule(s) to reach the instantaneous anode. This may be due to the back and forth movement of the molecule as a result of the reversal in the direction of the current proportional to the frequency of the AC.

2. Continuous bubbling of gases at both electrodes (probably O<sub>2</sub> and H<sub>2</sub>) in the test solution was observed as the tests progressed. However, the rate of bubbling of the gas decreased as the frequency of the applied AC was increased until no gas bubbles were visible at an AC frequency of 60 Hz. Simond *et al.* (1997) and Comninellis (1994) reported that the hydroxyl radicals, formed on an anode react with each other to form oxygen gas at the anode to complete the electrolysis of water molecules. Stock and Bunce (2002) reported that hydrogen radicals formed on a cathode react with each other to produce hydrogen gas at the cathode. If the formation of OH radicals and hydrogen radicals are precursors for the generation of oxygen gas and hydrogen gas at the anode and cathode, respectively, then it is likely that the rate of gas bubbling at the electrode gives an indication of the rate of formation of these radicals at the electrodes. The higher the rate of the observed bubbling of the gas(es), the greater the rate of hydroxyl or hydrogen radical formation at the electrodes. Hence, based on the visual observation of gas bubbles, it is likely that increase in the AC frequency resulted in decrease in the rate of formation of hydroxyl radicals at the electrodes. This impacted the rate of oxidization of phenanthrene and pyrene at the instantaneous anodes.
3. Competing anodic reactions (oxidation) and cathodic reactions (reduction) at the same reaction sites (on the surface of the electrodes) may have been responsible for the decrease in the oxidation rate of both phenanthrene (Figure 2-5) and

pyrene (Figure 2-9) as the AC frequency was increased. However, in DC electrolysis, oxidation reactions occurred at the anode only and reduction reactions occurred at the cathode only and hence there was no competing anodic oxidation and cathodic reduction at the same reaction site. Therefore DC was more effective in degrading phenanthrene or pyrene in the test cells.

### **Electrode Mass Decay**

The mass of the electrodes used in the test cells were measured before and after the end of the tests. Less than 1% loss in the mass of the electrodes was observed during the 48-hr test period for all tests. The formation of light brown flaky particles that sunk to the bottom of the solution in the test cells was observed at the end of the testing period when NaCl was used as the supporting electrolyte. After the tests, the solutions were decanted and the residue was soaked in acetonitrile for 24 hrs and then sonicated for 30 minutes. HPLC analysis of the extract showed about 3  $\mu\text{g}$  of phenanthrene in the residue from the phenanthrene tests and about 23  $\mu\text{g}$  of pyrene in the residue from the pyrene tests. These results indicate that the residue formed did not significantly sorb either phenanthrene or pyrene from of the solutions. The dry mass of the residue was about 4 g.

### **Intermediate Byproducts**

LC/MS analyses indicated molecular masses that suggest the formation of degradation products of phenanthrene as three isomers of phenanthrol, dihydroxyphenanthrene, phenanthrenequinone, and naphthalenedicarboxylic acid. The primary degradation products formed during the pyrene tests were pyrenequinone, pyrenol, dihydropyrenol, pyrenedihydrodiol, and chloro-pyrenol. The exact isomers formed were not determined.

These degradation byproducts formed are relatively more soluble than their parent compound (phenanthrene or pyrene), hence it is expected that they would be more bioavailable in solution for subsequent degradation by microorganisms. Chlorinated byproduct such as chloro-pyrenol may be more toxic than the parent compound pyrene. The formation of the quinones is consistent with those found by other researchers who also observed aromatic quinones during electrolytic oxidation of aromatic hydrocarbons (Brillas *et al.* 2000; Oturan 2000; Panizza *et al.* 2000). GC/MS analysis by Goel *et al.* (2003) indicated the presence of 1,4-naphthoquinone when naphthalene solutions were electrolyzed and concluded that naphthalene degradation could be due to direct anodic oxidation, oxidation by an intermediate (e.g. hydroxyl radicals), or a combination of both. LC/MS analysis by Pepprah and Khire (2008) of naphthalene in aqueous solution electrolyzed with a square-wave AC indicated the formation of dihydroxynaphthalene, naphthoquinone, chloronaphthol, benzenedicarboxylic acid, and malic acid as the degradation products. The color of the solution during the tests changed to light yellow after about 4 hrs of electrolyzing the solution with AC. This yellow color may be due to the formation of quinones in solution. Gas phase sampling was beyond the scope of this study. Hence, any volatile byproducts which may have formed and escaped from the solution were not detected or analyzed.

Table 2-2 summarizes the measured initial and final values of temperature, pH, standard redox potential, dissolved oxygen concentration, and electrical conductivity of the test solutions.

Table 2-2: Measured initial and final values of temperature, pH, and electrical conductivity of test cell and control cell solutions

Compound	Supporting Electrolyte	C <sub>0</sub> [mg/L]	AC Wave Form	AC Frequency [Hz]	Current Density [mA/cm <sup>2</sup> ]	Temperature [°C]		pH		Electrical Conductivity [μS]	
						Initial	Final	Initial	Final	Initial	Final
Phenanthrene	10	NaCl	Square	0.1	3.0	20.0	21.6	6.3	6.9	887	855
Phenanthrene	10	NaCl	Square	0.1	10.2	18.3	30.9	6.6	7.8	823	973
Phenanthrene	10	NaCl	Square	0.1	18.5	19.7	44.9	6.5	8.1	828	1023
Phenanthrene	10	Na <sub>2</sub> SO <sub>4</sub>	Square	0.1	10.2	19.8	32.0	7.0	4.3	645	935
Phenanthrene	10	Na <sub>2</sub> SO <sub>4</sub>	Square	1	10.2	19.2	49.0	6.3	6.7	857	875
Phenanthrene	10	Na <sub>2</sub> SO <sub>4</sub>	Square	60	10.2	19.9	32.7	6.5	4.0	675	724
Phenanthrene	10	Na <sub>2</sub> SO <sub>4</sub>	Sine	60	10.2	21.5	36.2	6.5	4.1	675	659
Phenanthrene	10	Na <sub>2</sub> SO <sub>4</sub>	DC	0	3.0	19.2	25.7	5.7	4.3	677	777
Phenanthrene	10	Na <sub>2</sub> SO <sub>4</sub>	DC	0	6.0	21.1	29.9	6.5	4.3	657	1148
Phenanthrene	10	Na <sub>2</sub> SO <sub>4</sub>	DC	0	10.2	21.5	37.3	7.2	4.3	675	1062

Table 2-2 Cont'd

Phenanthrene	10	NaCl	Control	0	0	19.2	49.0	6.3	6.7	857	875
Pyrene	5	NaCl	Square	0.1	3.0	20.0	21.6	6.3	6.9	887	855
Pyrene	5	NaCl	Square	0.1	10.2	18.3	31.2	6.8	7.0	811	902
Pyrene	5	NaCl	Square	0.1	18.5	19.2	46.8	6.4	7.4	817	999
Pyrene	5	Na <sub>2</sub> SO <sub>4</sub>	Square	0.1	10.2	19.5	33.3	5.9	4.2	689	980
Pyrene	5	Na <sub>2</sub> SO <sub>4</sub>	Square	1	10.2	21.4	32.7	5.6	3.5	637	691
Pyrene	5	Na <sub>2</sub> SO <sub>4</sub>	Square	60	10.2	21.1	34.9	5.8	3.9	698	658
Pyrene	5	Na <sub>2</sub> SO <sub>4</sub>	Sine	60	10.2	19.5	32.7	5.9	4.2	680	992
Pyrene	5	Na <sub>2</sub> SO <sub>4</sub>	DC	0	3.0	19.6	25.9	5.9	4.1	682	783
Pyrene	5	Na <sub>2</sub> SO <sub>4</sub>	DC	0	6.0	19.8	30.6	6.0	4.0	668	1170
Pyrene	5	Na <sub>2</sub> SO <sub>4</sub>	DC	0	10.2	21.0	23.9	6.0	3.8	693	849
Pyrene	5	NaCl	Control	0	0	19.2	47.0	6.4	6.5	817	824



## SUMMARY AND CONCLUSIONS

The objective of this study was to use an alternating current (AC) to investigate the degradation of phenanthrene and pyrene in spiked aqueous solutions. Phenanthrene and pyrene solutions having an initial spiked concentration of 10 mg/L or 5 mg/L, respectively, were electrolyzed at three AC densities equal to  $3.0 \text{ mA/cm}^2$ ,  $10.2 \text{ mA/cm}^2$  and  $18.5 \text{ mA/cm}^2$ . A square wave AC having a frequency equal to 0.1 Hz was used in a majority of the experiments. Other frequencies explored were 1 Hz and 60Hz, and degradation rates using 60 Hz sine wave was compared to 60 Hz square wave. The key conclusions are as follows.

1. AC is able to degrade phenanthrene and pyrene in aqueous solutions;
2. Greater the current density, faster the initial rate of degradation;
3. Migration contributed significantly to the movement of reacting molecules to the reaction sites (the electrodes) as compared to diffusion;
4. Increasing the AC frequency resulted in decreased degradation rates;
5. A square wave AC produced a higher degradation rate than a sine wave AC supplied at equal *rms* current density of  $10.2 \text{ mA/cm}^2$  and frequency of 60 Hz in the degradation of phenanthrene;
6. Electrode fouling was one of the reasons for the reduction in the rate of degradation as the test progressed;
7. The degradation rate of both phenanthrene and pyrene in solution could be described as *pseudo* first-order decay; and

8. Formation of 2,3-Dihydroxybenzoic acid and 2,5-Dihydroxybenzoic from the oxidation of salicylic acid is consistent with reported findings that OH radicals were the primary oxidizing agents in electrochemical degradation;
9. The rate of anodic oxidation of phenanthrene and pyrene depends on the rate of production of OH radicals at the anode (or instantaneous anode) as oxidizing agents as well as the rate of migration of reacting molecules to the reaction site (the anode or instantaneous anode). At higher current densities, not only more OH radicals are produced at the anode but also the rate of migration of the reacting molecules to the anode (or instantaneous anode) increases during a DC application. However, when AC is used, the change in the direction of the current decreases the rate of migration of the reactant to the instantaneous anode. Hence, as the frequency of the applied AC increases, the rate of degradation decreases; and
10. Both phenanthrene and pyrene molecules in solution exhibited an “effective” partial negative charge due to the presence of the supporting electrolyte.

### **PAPER NO. 3: EFFECT OF ALTERNATING CURRENT WAVEFORM AND FREQUENCY ON THE DEGRADATION OF NAPHTHALENE IN AQUEOUS SOLUTION**

#### **ABSTRACT**

The key objectives of this study were to: (1) use alternating current (AC) to investigate the effect of AC waveform and frequency on the rate of degradation of naphthalene in aqueous solution; (2) explore the mechanism of degradation of naphthalene when subjected to AC and DC; and (3) prove that anodic oxidation of naphthalene occurred on both electrodes during AC electrolysis, unlike direct current (DC) electrolysis in which anodic oxidation of naphthalene occurred on only one electrode (the anode). The results indicated that at  $3 \text{ mA/cm}^2$  peak AC density, the rate of degradation of naphthalene in aqueous solution having  $\sim 20 \text{ mg/L}$  ( $0.15 \text{ mM}$ ) initial concentration, decreased with increasing AC frequency. For square, sine, and triangular AC signals explored, square wave AC signal resulted in the fastest degradation rate of naphthalene. Hydroxyl radicals were identified as the primary oxidizing agent in the solution. Hydroxylated naphthalene byproducts were detected in both compartments of a divided cell setup indicating that anodic oxidation occurred within both compartments in AC electrolysis, unlike DC electrolysis in which hydroxylated byproducts were detected in only the anolyte but not in the catholyte. The *Nernst-Planck* equation was used to model the rate of mass transfer to the electrodes where reactions were expected to occur. A comparison of the simulated concentration-time profiles with the test results indicate that both diffusion and migration processes were responsible for the rate of mass transfer of naphthalene to the reaction sites (surface of electrodes or in the vicinity of the electrodes) where naphthalene was

degraded or converted by the hydroxyl radicals. However, migration was the dominant phenomenon for mass transfer to the electrodes in the AC and DC electrochemical cells.

## INTRODUCTION

The United States Environmental Protection Agency (USEPA) estimates that 3,000 to 5,000 former manufactured gas plant (MGP) sites are located across the United States and many of these contaminated sites contain substantial quantities of PAHs (USEPA 2000). Remediation of contaminated soil and groundwater is an important issue that is of concern among environmentalists and hydrogeologists. *In-situ* and *ex-situ* treatment techniques may be used to remediate contaminated soil and groundwater. Conventional remediation techniques include pump-and-treat, incineration, long term storage, and soil washing. Other approaches include biodegradation, and advanced oxidation processes. Alshwabkeh and Sarahney (2005) proposed the concept of Electrochemical Redox Barrier (ERB), where contaminants could be potentially degraded by placing electrodes in the soil to intercept the contaminant plume and applying DC to generate the redox conditions required to degrade the contaminants as the groundwater flows through this reactive zone. Pepprah and Khire (2008) reported that AC is capable of degrading PAHs such as naphthalene, phenanthrene, and pyrene in solution resulting in the production of intermediate byproducts such as quinones and diols. A funnel-and-gate (Birke *et al.* 2003; Gupta *et al.* 1998)) electrochemical redox barrier (FERB) (Figures 3-1 a & 1b) may be used for *in-situ* treatment of contaminated plumes.

**PLAN VIEW**

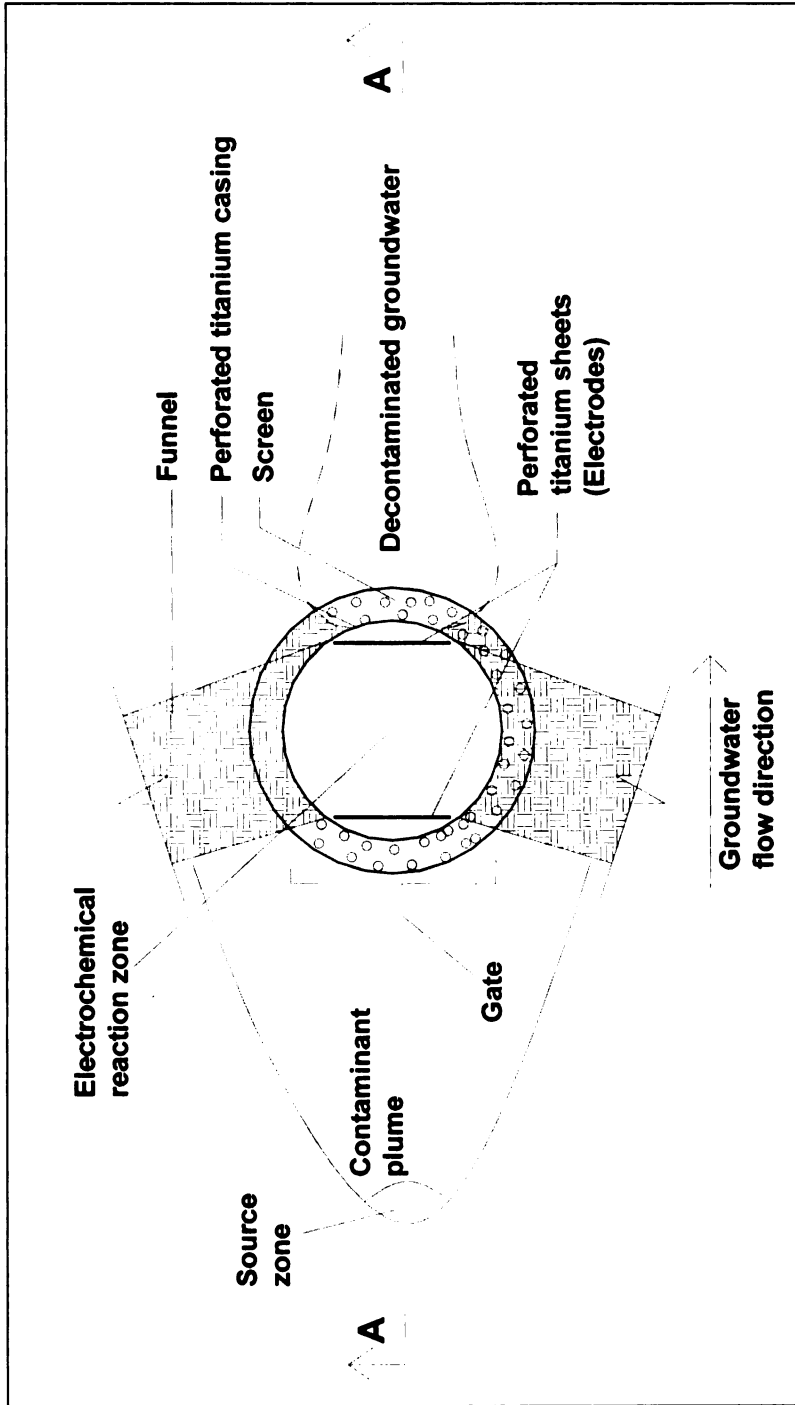


Figure 3-1(a): Plan View of Hypothesized Funnel-and-Gate Electrochemical Reactive Barrier

# CROSS SECTION A - A

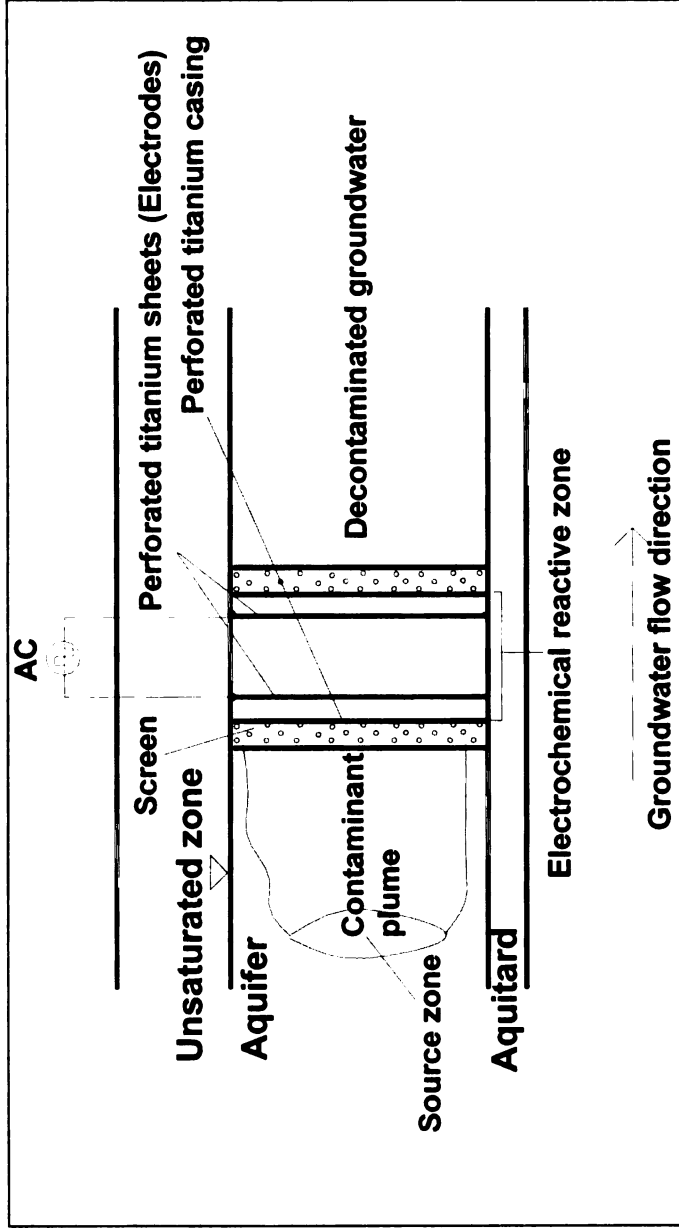


Figure 3-1(b): Cross-section of Hypothesized Funnel-and-Gate Electrochemical Reactive Barrier

The FERB is made up of low hydraulic conductivity cutoff walls, e.g. slurry walls or sheet piles for the funnel with a gate(s) that contain(s) *in-situ* reaction zones. Ground water primarily flows through high conductivity gates. In this approach, the electrodes can be placed in a casing in the gate region containing the groundwater contaminated with PAHs in the subsurface. Furthermore, AC and/or DC are applied to degrade PAHs present in the groundwater. To ensure complete removal of PAHs, several reactive barriers may be constructed in series, down gradient of the contaminant plume to intercept the plume as it travels through these reactive zones. AC electrolysis may also be used as an *ex-situ* treatment technique whereby contaminated groundwater is pumped out of an aquifer for subsequent above surface treatment in an electrochemical reactor.

Pepprah and Khire (2008) have shown that naphthalene in aqueous solution can be degraded by AC electrolysis. They have also presented the effect of current density for a fixed frequency, and type of supporting electrolyte on the rate of degradation of naphthalene. The key objectives of this study were to:

1. investigate the effect of AC waveform and frequency on the rate of degradation of naphthalene in solution, which is a model PAH compound;
2. prove that electrochemically generated hydroxyl radicals (OH<sup>•</sup>) were responsible for the degradation of naphthalene; and
3. demonstrate that anodic oxidation of naphthalene occurred on both electrodes when AC electrolysis was used, while for DC electrolysis, anodic oxidation of naphthalene occurred on only one electrode (the anode).

Pepprah and Khire (2008) have reported that the rate of degradation of naphthalene in aqueous solution in a laboratory scale experiment, increased with

increasing peak AC density. In addition, they also reported that the rate of degradation when NaCl was used as the supporting electrolyte was greater than when Na<sub>2</sub>SO<sub>4</sub> was used as the supporting electrolyte.

Naphthalene, which contains two fused benzene rings, was selected as a model PAH compound because Alshawabkeh and Sarahney (2005), Goel *et al.* (2003), and others have also used naphthalene to investigate electrochemical degradation in aqueous solution. Also, naphthalene has chemical and physical properties similar to other PAHs, except that it is more soluble in water, a property that makes naphthalene more available in aqueous solution and more exposed to reactivity than others PAHs (Alshawabkeh and Sarahney 2005).

## **MATERIALS AND EXPERIMENTAL METHODOLOGY**

The experimental setup is illustrated in Figure 3-2 and the setup components are described below.



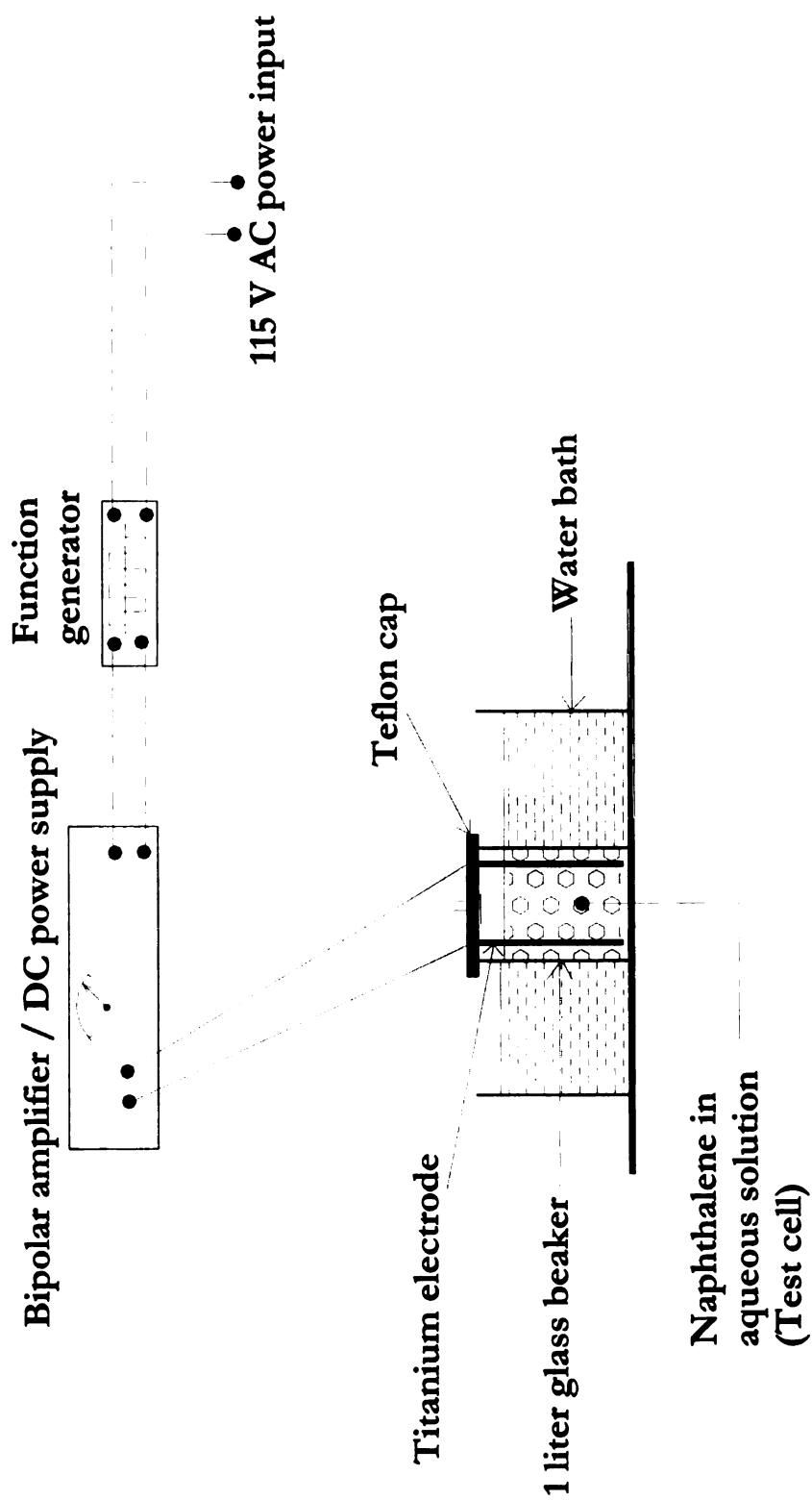


Figure 3-2: Schematic of the experimental setup

### **Reaction Chamber**

The test cell setup consisted of a 1 liter Pyrex glass beaker with a Teflon cap. These materials of the cell were selected to eliminate or reduce sorption of the contaminants onto the walls of the reaction vessel and the cap. Titanium plates (99% purity) were used as electrodes for this study. Other researchers (Alshawabkeh and Sarahney 2005; Li *et al.* 2005; Goel *et al.* 2003) used titanium as a base metal and coated it with mixed metal oxides such as RuO<sub>2</sub>, IrO<sub>2</sub>, and SnO<sub>2</sub>. The titanium plates used in this study were not coated. Uncoated titanium is cheaper than commonly used electrodes such as platinum, or titanium coated electrodes. Hence it was selected for this project. Also, titanium offers resistance to corrosion in a wide range of aggressive conditions (Titanium and the Environment 2002) and thus, could be used for potential field scale application. The titanium sheets used as electrodes in this study were 12.0-cm-long by 5.0-cm-wide by 1.72-mm-thick and the distance between them was maintained equal to 8.0 cm. The active contact area of the solution with the electrode ranged from 53 cm<sup>2</sup> to 55 cm<sup>2</sup> as samples were collected for analyses.

### **Electrical Equipment**

A 2 MHz Sweep Function Generator capable of generating AC signals having frequency ranging from 0.1 Hz to 2 MHz was used. The power supply consisted of a bipolar operational power supply/amplifier capable of producing 200 V AC/DC and 1 A AC/DC output or a maximum electrical power of 200 W. Voltage and current measurements were obtained with the aid of an oscilloscope.

### **Spiked Solution Preparation**

Aqueous solutions, spiked with naphthalene were prepared by adding naphthalene (98%, purity) crystals to one liter of deionized (DI) water in capped Pyrex bottles and allowing the suspensions to stand for more than three days. This was followed by the addition of 0.5 g of anhydrous sodium sulfate ( $\text{Na}_2\text{SO}_4$ ) to each suspension, to increase its electrical conductivity. The excess suspended naphthalene crystals were then filtered off and the collected filtrate was used for the tests. Sodium sulfate was selected as the supporting electrolyte because previous studies (Goel *et al.* 2003) used sodium sulfate in electrochemical degradation of naphthalene in aqueous solution. Also Pepprah and Khire (2008) showed less degeneration of the electrode surface when  $\text{Na}_2\text{SO}_4$  was used compared to when NaCl was used as the supporting electrolyte. The resultant concentration of  $\text{Na}_2\text{SO}_4$  was approximately 500 mg/L (~3.5 mM). This concentration was selected to meet the USEPA has proposed a maximum contaminant level goal of sulfate as 500 mg/L (~3.5 mM). Saracco *et al.* (2000) performed tests where electrolyte salt (e.g. NaCl,  $\text{Na}_2\text{SO}_4$ ) concentrations ranged from 0.2 – 2 M and concluded that higher salt concentrations reduce the electrical resistance between the electrodes and hence will reduce the operating costs. However, greater salt concentration would result in greater post-treatment costs and hence would be less favorable. The only exception might be represented by discharging the treated effluent into the sea (Saracco *et al.* 2000).

## Testing Procedure

Tests were conducted in a batch mode in 1-liter undivided cells as well as in a divided cell setup with 1-liter solution in each (anode and cathode) compartment. Prior to passing current through the cells, initial samples were taken for high performance liquid chromatography (HPLC) analyses. Replicate tests were conducted for majority of the tests. The effect of AC waveform (square, sine and triangular) on the degradation rate of naphthalene in solution was explored at a frequency of 60 Hz. This frequency was selected because AC from the power grid is supplied at 60 Hz frequency in the United States. The effect of AC frequency on the degradation rate of naphthalene was investigated at frequencies 0.1 Hz, 1 Hz, 10 Hz, 100 Hz, and 1,000 Hz using a square wave signal. A square wave signal was selected because our test results indicated that for a given peak current, the square wave was the most efficient among the three wave signals for the electrochemical degradation of naphthalene in the test solutions. Pepprah and Khire (2008) reported that although the initial degradation rate of naphthalene at 6 mA/cm<sup>2</sup> peak AC density was faster, both 3 mA/cm<sup>2</sup> (165 mA, peak current) and 6 mA/cm<sup>2</sup> (330 mA, peak current) AC densities ultimately resulted in approximately the same ultimate degradation after 48 hours of AC electrolysis. Therefore running these tests at a lower AC density resulted in savings in electrical energy expended for the same ultimate conversion of naphthalene. An additional reason for the selection of 3 mA/cm<sup>2</sup> was because the temperature of the test solutions electrolyzed at 3 mA/cm<sup>2</sup> remained approximately constant at the room temperature (~19 °C) throughout the test whereas for the 6 mA/cm<sup>2</sup> current density, the temperature increased to about 25 °C, so that loss of

naphthalene from the test solutions by volatilization as a result of increased temperature is minimized by running the tests at a lower current density. The peak AC density was obtained by dividing the peak current by the average active cross sectional area of the electrodes in contact with the solution. Tests were conducted using  $3 \text{ mA/cm}^2$  square wave at 0.1 Hz with salicylic acid as a hydroxyl radical ( $\text{OH}^\cdot$ ) probe, as well as tertiary butanol as  $\text{OH}^\cdot$  scavenger to explore the degradation mechanism of naphthalene.

During the tests, samples were collected for HPLC analyses at time intervals of 0, 1, 2, 4, 8, 24, and 48 hours. Samples were analyzed directly without extracting the naphthalene from the aqueous solution. This procedure minimized potential interferences from reagents, solvents, and glassware required for the extraction method (Alshwabkeh and Sarahney 2005). HPLC analyses were performed using a diode array detector (detection at 255 nm), a Waters C-18 PAH, 250 mm x 4.6 mm x 5  $\mu\text{m}$  column, an automated gradient controller, and deionized water (DI) / acetonitrile mobile phase. The flow rate of the mobile phase was 1.2 mL/min and the column was flushed with 10:90 (v/v) acetonitrile / DI water for 5 minutes followed by 60:40 (v/v) acetonitrile / DI water for 10 minutes, and by 100:0 (v/v) acetonitrile / DI water for 5 minutes. This gradient was used for the analysis in order to obtain appropriate separation of the degradation product peaks on the chromatograms during the tests. Standard solutions were prepared to bracket the expected concentration level of the analytes. Calibration curves with an average  $R^2$  value of 0.998 were used to determine the concentration of naphthalene in the solutions as the tests progressed. Samples were also collected for Liquid Chromatography/Mass Spectrometry (LC/MS) analyses to determine the degradation

products formed. Control cells, similar to the test cells, except without any current passed through them were set up, sampled, and analyzed at the same time intervals as the test cells. The test cells were placed in a relatively large volume water bath maintained at the room temperature to reduce the rate of temperature rise of the test solutions as a result of Joule heating.

### **Experimental Parameters Monitored**

Apart from monitoring the concentration of naphthalene in aqueous solution over time, other experimental parameters monitored included the initial and final values of pH, temperature, redox potential, electrical conductivity, and dissolved oxygen concentration of the solutions. A portable dissolved oxygen/pH meter, equipped with a pH electrode, an oxidation-reduction probe and dissolved oxygen probe, was used to measure pH, redox potential and dissolved oxygen, respectively, of the test solutions. An electrical conductivity meter was used to measure the electrical conductivity and a thermometer was used to measure the temperature of the spiked solution in the control and test cells throughout the testing period.

## **RESULTS AND DISCUSSION**

Table 3-1 outlines the list of parameters explored and varied in the experimental program.

Table 3-1: Summary of Experimental Parameters

Compound	Cell	AC Frequency [Hz]	AC Waveform	Peak AC Density		No. of tests
				mA/cm <sup>2</sup>	mA/L	
Naphthalene	Undivided	60	Square	3	165	2
Naphthalene	Undivided	60	Sine	3	165	2
Naphthalene	Undivided	60	Triangular	3	165	2
Naphthalene	Undivided	0	DC	3	165	2
Naphthalene	Undivided	0.1	Square	3	165	2
Naphthalene	Undivided	1	Square	3	165	2
Naphthalene	Undivided	10	Square	3	165	2
Naphthalene	Undivided	100	Square	3	165	2
Naphthalene	Undivided	1000	Square	3	165	2
Naphthalene	Undivided	-	-	0 (Control)	0 (Control)	2
Naphthalene	Divided	0.1	Square	3	82.5	1
Naphthalene	Divided	0	DC	3	165	1
Naphthalene	Divided	-	-	0 (Control)	0 (Control)	1
Naphthalene /tert-butanol	Undivided	0.1	Square	3	165	3
Salicylic acid	Undivided	0.1	Square	3	165	1
Salicylic acid	Undivided	10	Square	3	165	1
Salicylic acid	Undivided	1000	Square	3	165	1
Salicylic acid	Undivided	0	DC	3	165	1
Salicylic acid	Divided	0.1	AC	3	165	1

Table 3-1 Cont'd

Salicylic acid	Divided	0	DC	3	165	1
Salicylic acid	Undivided	-	-	0 (Control)	0 (Control)	1
Salicylic acid	Divided	-	-	0 (Control)	0 (Control)	1
					<b>Total Number of Tests</b>	<b>38</b>

Notes:

1. The volume of the test solution in an undivided cell was 1 liter and it was 1 liter for each compartment of the divided cell having total volume equal to 2 liter.
2. All tests were performed by passing 165 mA current (peak AC or DC).
3. Current density  $[\text{mA}/\text{cm}^2] = \text{current} [\text{mA}] / \text{cross sectional area of electrodes} [\text{cm}^2]$
4. Current density  $[\text{mA}/\text{L}] = \text{current} [\text{mA}] / \text{volume of solution} [\text{L}]$

**Effect of AC Waveform**

Figure 3-3 illustrates the effect of the shape of AC wave form on the degradation rate of naphthalene in the test cell solution.



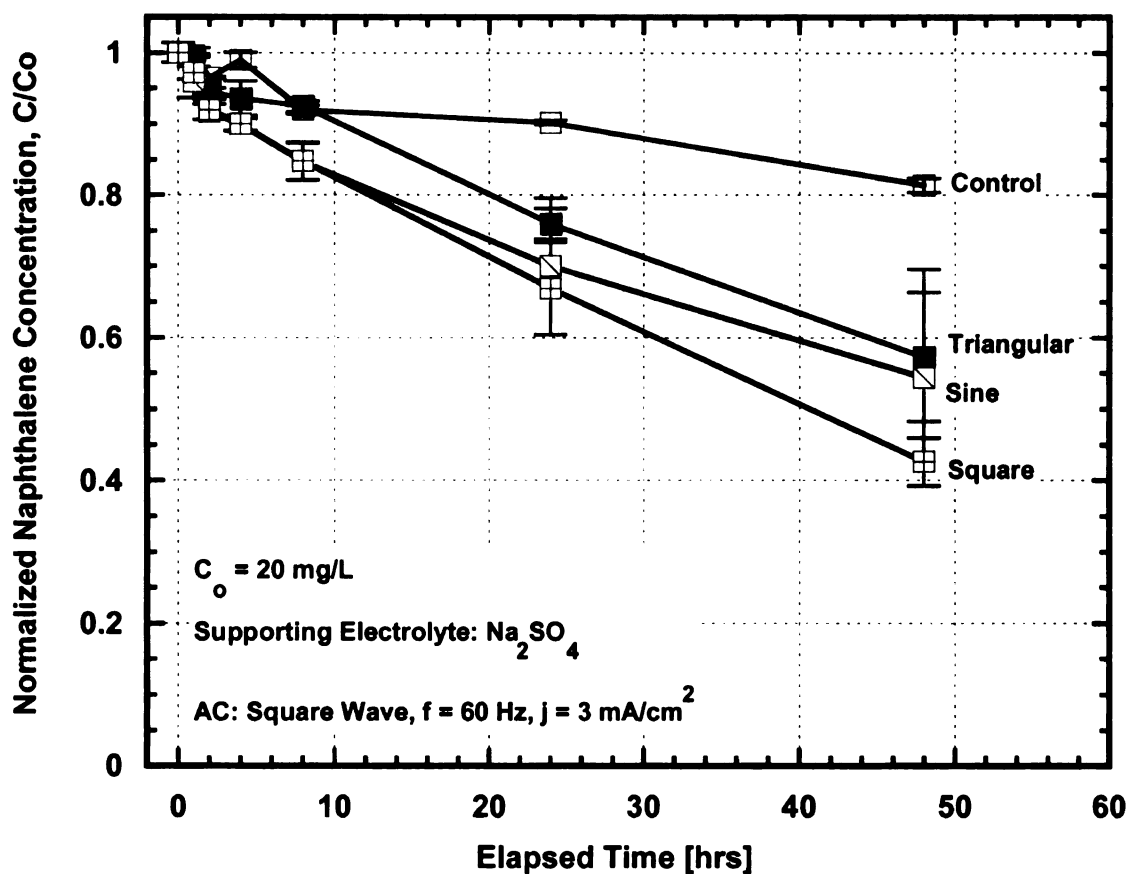


Figure 3-3: Effect of AC waveform on the degradation rate of naphthalene

The error bars in Figure 3-3 represent the maximum and minimum values of the normalized concentration ( $C/C_0$ ) for the initial test and the replicate test recorded for the total four samples. By passing square, sine and triangular wave currents through naphthalene test solutions ( $\sim 20 \text{ mg/L}$  ( $0.15 \text{ mM}$ ) initial concentration) in separate tests, the square wave produced the highest degradation rate ( $k \sim 1.77 \times 10^{-2} \text{ hr}^{-1}$ ), followed by the sine wave ( $k \sim 1.34 \times 10^{-2} \text{ hr}^{-1}$ ), and then the triangular wave ( $k \sim 1.16 \times 10^{-2} \text{ hr}^{-1}$ ). Thus, for a given peak current, the square wave was the most efficient among the three waveforms. The primary reason for this finding is that the rate of degradation is a

function of the root mean square (*rms*) current. The *rms* current,  $I_{rms}$  is the DC equivalent for the AC signal. For a DC signal, the *rms* current is the same as the peak current. Figure 3-4 illustrates a schematic of these three wave forms and the resulting *rms* values are:

$$I_{rms}(\text{Sine}) = 0.707I_p \quad (1)$$

$$I_{rms}(\text{Square}) = I_p \quad (2)$$

$$I_{rms}(\text{Triangular}) = 0.577I_p \quad (3)$$

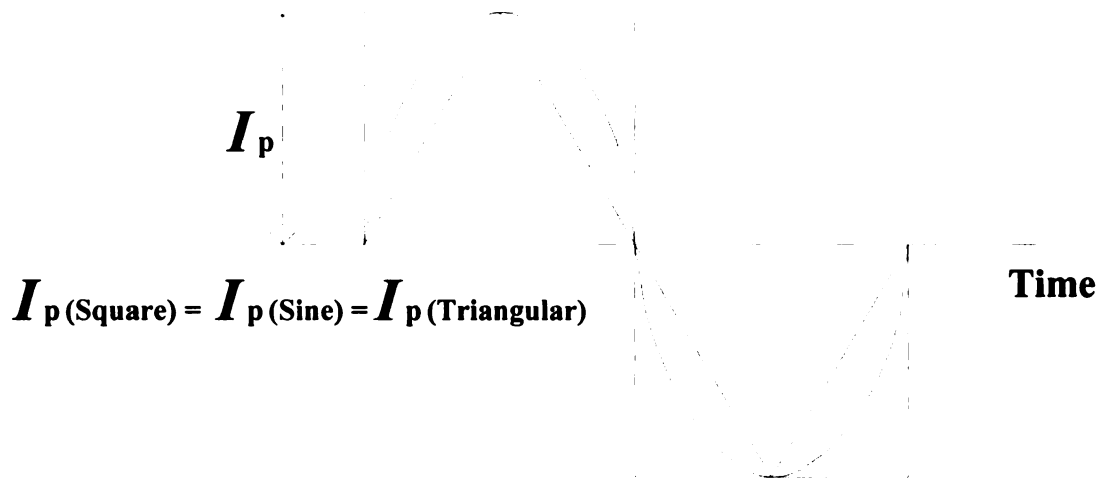


Figure 3-4: Square; Sine; and Triangular AC signal having the same peak current

The greater the magnitude of current passed through the solution for a given period, the greater the degradation rate and hence the observed trend as shown in Figure 3-4.

By applying an AC, which resulted in constant polarity reversal of the electrodes at a rate dependent upon the AC frequency, anodic oxidation of naphthalene in solution

occurred on both electrodes. Previous studies on electrochemical degradation have focused on the use of DC where the cathode acts as a “passive” electrode in the oxidation process. However, when an AC is used, the constant polarity reversal creates anodic oxidation reactions on both electrodes alternately, depending on their polarity in a given AC cycle. During one half of a cycle when one of the electrodes has a positive electrical potential (instantaneous anode), it instantaneously acts as the anode while the other electrode, at a negative electrical potential (instantaneous cathode), instantaneously acts as the cathode. In the subsequent half cycle, polarities are reversed and the electrodes acquire electrical potentials opposite to what they had in the previous cycle and this continues throughout the period of application of the AC.

#### **Effect of AC Frequency**

Square wave AC having a peak AC density of  $3 \text{ mA/cm}^2$  and frequency varying from 0.1 Hz to 1,000 Hz were used to investigate the effect of AC frequency ( $f$ ) on degradation rates of naphthalene in the test cells. Figure 3-5 presents the effect of AC frequency on the degradation of naphthalene.

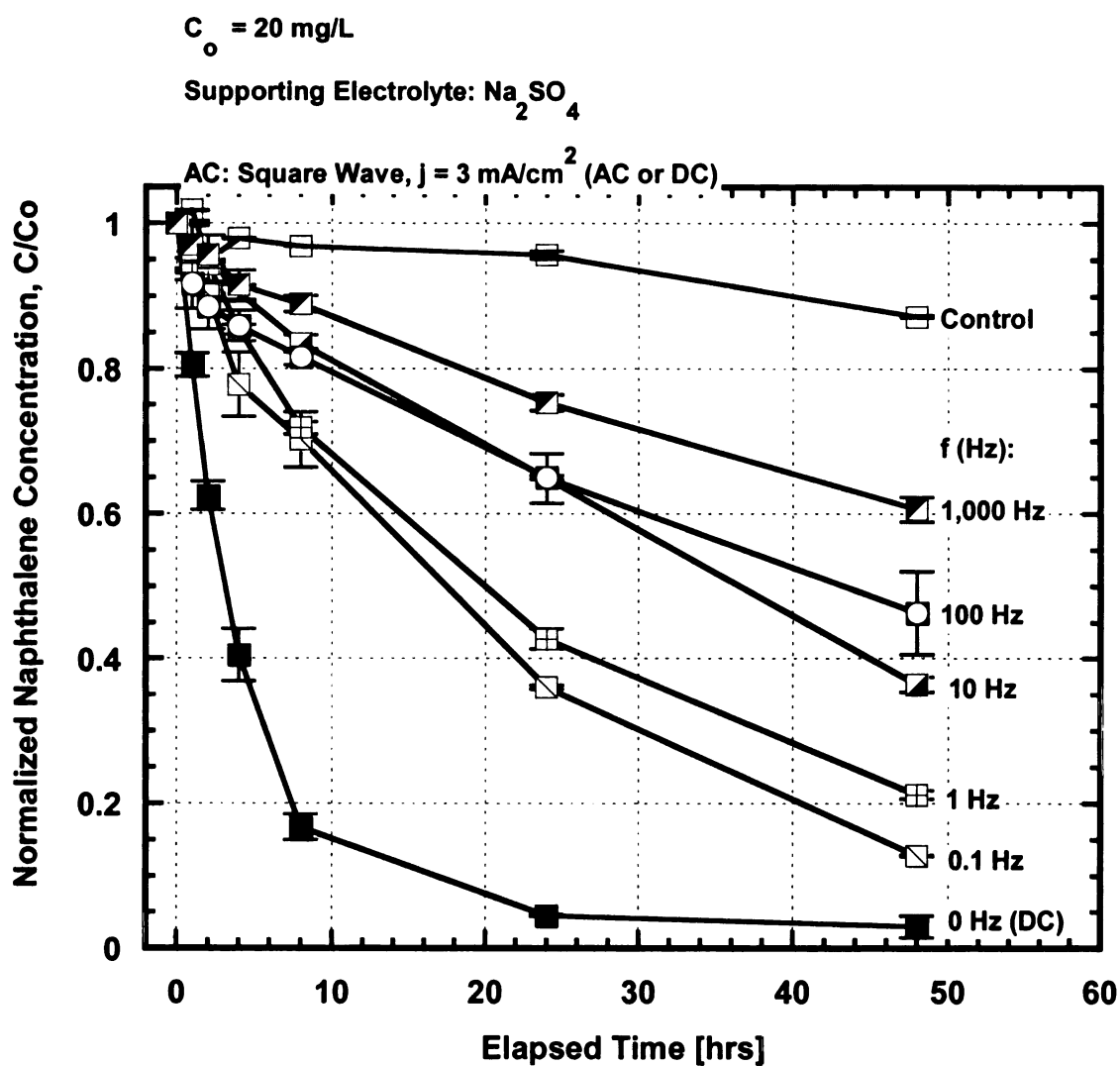


Figure 3-5: Effect of AC frequency on the degradation rate of naphthalene

The overall degradation of naphthalene during the 48-hr period ranged from 41% for the highest frequency ( $f = 1,000 \text{ Hz}$ ) to 87% for the lowest frequency ( $f = 0.1 \text{ Hz}$ ) for a fixed  $I_p$  equal to  $3 \text{ mA/cm}^2$ . A DC ( $f = 0$ ) density of  $3 \text{ mA/cm}^2$  resulted in 96% degradation after 48 hrs of electrolysis. These results indicate that the rate of degradation of naphthalene in aqueous solution decreased with increasing AC frequency. This finding is

consistent with the trend observed by Chin and Cheng (1985) that the rate of conversion of phenol decreased with increasing alternating voltage frequency superimposed on a DC. For the  $3 \text{ mA/cm}^2$  current density used in the tests, at frequencies less than 60 Hz, continuous bubbling of gases at the electrodes may have also contributed to the reduction in concentration of naphthalene in the test solution as a result of sparging. Determining the component of mass loss due to sparging was beyond the scope of this study. However, at frequencies of 60 Hz or more, no gas bubbles were observed with unaided eye.

The degradation of naphthalene in all the test solutions depicted *pseudo*-first-order degradation kinetics. A plot of  $\ln[C/C_0]$  versus time yielded the observed *pseudo*-first-order degradation rate constants ( $k$ ) and corresponding computed half-lives ( $t_{1/2}$ ) which are reported in Table 3-2.

Table 3-2: Summary of Experimental Results

Compound	Cell	AC Frequency [Hz]	AC Waveform	Peak AC Density		$k$ ( $\times 10^{-2}$ ) [ $\text{hr}^{-1}$ ]	$t_{1/2}$ [Hours]	$R^2$	% Degradation after 48 Hrs
				[ $\text{mA}/\text{cm}^2$ ]	[ $\text{mA}/\text{L}$ ]				
Naphthalene	Undivided	60	Square	3	165	1.77	39.16	0.9916	58
Naphthalene	Undivided	60	Sine	3	165	1.34	51.73	0.9528	51
Naphthalene	Undivided	60	Triangular	3	165	1.16	59.75	0.9929	52
Naphthalene	Undivided	0	DC	3	165	14.18	4.88	0.9073	96
Naphthalene	Undivided	0.1	Square	3	165	4.29	16.16	0.9980	87
Naphthalene	Undivided	1	Square	3	165	3.32	20.88	0.9942	78
Naphthalene	Undivided	10	Square	3	165	2.05	20.88	0.9934	65
Naphthalene	Undivided	100	Square	3	165	1.68	41.26	0.9366	60
Naphthalene	Undivided	1000	Square	3	165	1.09	63.59	0.9751	38

Table 3-2 Cont'd

Naphthalene	Undivided	-	-	-	0 (Control)	-	-	-	-
	Divided (Cell 1)	0.1	Square	3	82.5	3.51	19.74	0.9648	80
Naphthalene	Divided (Cell 2)	0.1	Square	3	82.5	3.58	19.36	0.9425	80
	Divided (Anolyte)	0	DC	3	82.5	30.83	2.25	0.9982	99
Naphthalene	Divided (Catholyte)	0	DC		82.5	2.15	32.24	0.9687	62
Naphthalene/tert- butanol (0.15 mM)	Undivided	0.1	Square	3	165	3.53	19.64	0.9966	81
Naphthalene/tert- butanol (1.5 mM)	Undivided	0.1	Square	3	165	3.68	18.84	0.9728	81
Naphthalene/tert- butanol (15 mM)	Undivided	0.1	Square	3	165	2.44	28.41	0.9905	68
Salicylic acid	Undivided	0.1	Square	3	165	3.80	18.24	0.993	88
Salicylic acid	Undivided	10	Square	3	165)	0.80	86.4	0.975	33

Table 3-2 Cont'd

Salicylic acid	Undivided	1000	Square	3	165	-	-	-	2
Salicylic acid	Undivided	0	DC	3	165	18.8	3.67	0.997	99
Salicylic acid	Divided (Cell 1)	0.1	AC	3	165	3.30	21.00	0.9970	72
	Divided (Cell 2)	0.1	AC	3	165	1.80	38.51	0.8990	61
Salicylic acid	Divided (Anolyte)	0	DC	3	165	11.3	6.13	0.9470	92
	Divided (Catholyte)	0	DC	3	165	-	-	-	8

Notes:

1. All tests were performed by passing 165 mA current (peak AC or DC).
2. Current density  $[\text{mA}/\text{cm}^2] = \text{current} [\text{mA}] / \text{cross sectional area of electrodes in contact with the test solution} [\text{cm}^2]$ .
3.  $k$  is observed *pseudo* first-order degradation rate constant of naphthalene in the test cell solutions.
4.  $t_{1/2}$  is the corresponding half-life of  $k$ .
5.  $R^2$  is the coefficient of regression.



For a square wave with peak AC density of  $3 \text{ mA/cm}^2$ , an empirical relationship between the applied AC frequency ( $f$ ) and the observed *pseudo* first-order degradation rate constant ( $k$ ) of naphthalene in aqueous solution at five AC frequencies (0.1 Hz, 1 Hz, 10 Hz, 100 Hz, and 1,000 Hz), was derived from Figure 3-6 as shown in Equation 4

$$k = -0.008 \log f + 0.033 \dots \dots \dots R^2 = 0.9593 \quad (4)$$

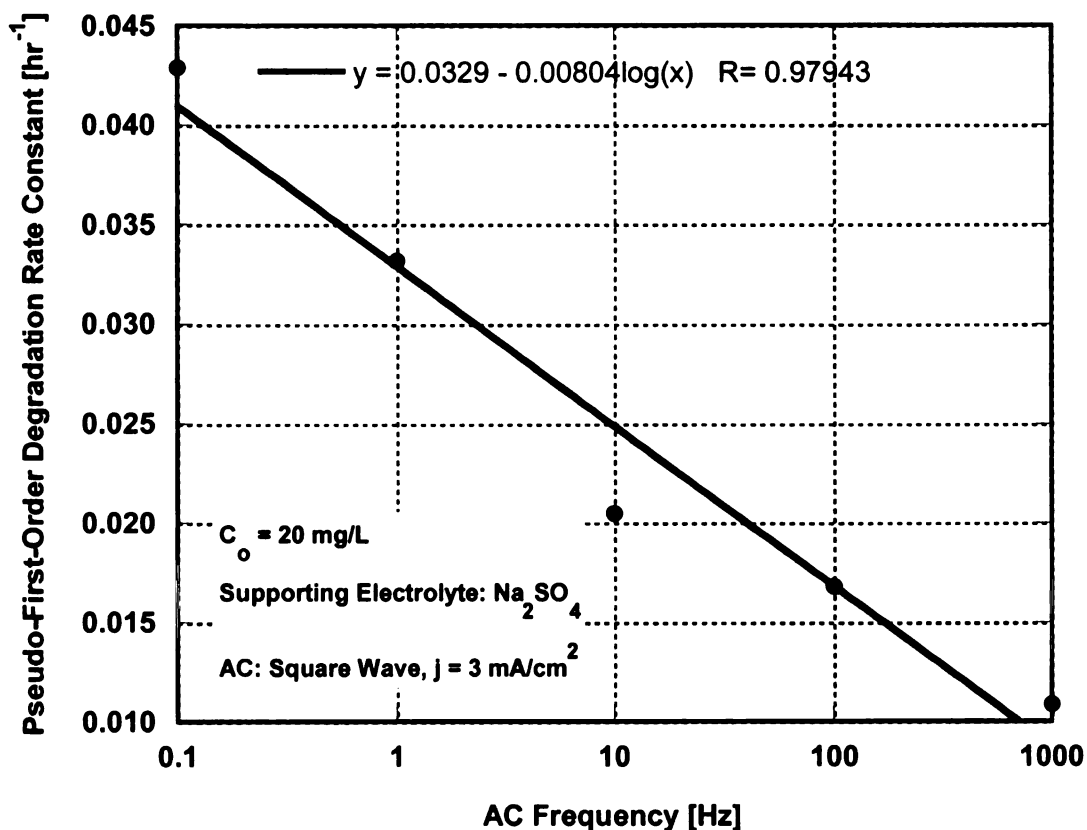


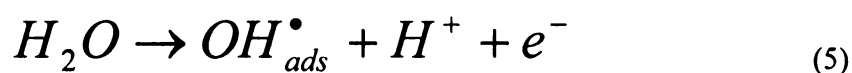
Figure 3-6: Effect of AC frequency on the pseudo-first-order degradation rate constants

Decrease in naphthalene concentration in the control cell over time was observed as shown in Figure 3-5. However, the loss of naphthalene from solution in the control cell is

significantly less compared to the decrease observed for the AC and DC test cells. Goel *et al.* (2003) and Alshwabkeh and Sarahney (2005) also reported naphthalene loss in their control cells over time and attributed it to factors such as volatilization, potential sorption to cell components etc.

### Hydroxyl Radical Probe Study

Brillas *et al.* (2000) reported that electrochemical systems generate hydroxyl radicals at the anode due to the oxidation of water:



Nakamura *et al.* (2005) proposed a mechanism based on selective redox reactions with various radicals generated by AC electrolysis that allowed both oxidation and reduction at the same reaction site between adjacent electrodes. Based on the analysis of intermediate products of the degradation process, it was revealed that the mechanism involved selective redox reactions with short-lived and highly reactive radicals: hydrogen atoms ( $H^{\bullet}$ ) and  $OH^{\bullet}$  that are electrochemically generated at the electrodes (Nakamura *et al.* 2005).

$OH^{\bullet}$  radicals attack the benzene rings of aromatic compounds to produce hydroxylated compounds. Various  $OH^{\bullet}$  radical probes and techniques have been used in published studies to detect the generation of  $OH^{\bullet}$  in reaction media. The probes and methods include salicylic acid (Li *et al.* 2003; Marselli *et al.* 2003; Oturan 2000; Jen *et al.* 1998; Scheck and Frimmel 1995), 4-hydroxybenzoic acid (Anderson *et al.* 1987), benzoic acid (Oturan and Pinson 1995), *para*-chlorobenzoic acid (*p*CBA) (Elovitz and von Guten 1999; Haag and Yao 1992), 2,2-diphenyl-1-picrylhydrazyl (DPPH) (Sehgal *et*

*al.* 1982), 5,5-dimethyl-1-pyrroline-N-oxide (DMPO) and electron spin resonance (ESR) (Marselli *et al.* 2003), p-nitrosodimethylaniline (RNO) and spectrophotometer measurements (Tanaka *et al.* 2004), and RNO / ESR (Comninellis 1994). Because ESR methods require expensive and sophisticated equipment, they were not used in this study due to budget constraints. Trapping of OH<sup>•</sup> using salicylic acid, and HPLC measurements were selected as hydroxyl radical probe technique for this study. Jen *et al.* (1998) reported that the oxidation efficiency of OH<sup>•</sup> is usually limited by the rates of OH<sup>•</sup> generation and hence, increasing the OH<sup>•</sup> generation and keeping it at a high level are the main factors that control the degradation efficiency of aqueous organic substances. Haag and Yao (1992) also reported that in contrast to most other oxidants, reactions of OH<sup>•</sup> with organics containing C-H or C-C multiple bonds generally proceed with rate constants approaching diffusion-controlled limit ( $10^{10} \text{ M}^{-1} \text{ s}^{-1}$ ) and therefore oxidation rates are usually limited by the rate of OH<sup>•</sup> generation and competition by other OH<sup>•</sup> scavengers in solution rather than by inherent reactivity with the oxidant. Figure 3-7 shows the change in concentration of salicylic acid solutions [ $\sim 20 \text{ mg/L}$  (0.14 mM) initial concentration] subjected to square wave signals having  $3 \text{ mA/cm}^2$  peak current density at frequencies equal to 0.1 Hz, 1 Hz, 10 Hz, 100 Hz and 1,000 Hz respectively, and DC ( $f=0$ ) at  $3 \text{ mA/cm}^2$  current density.

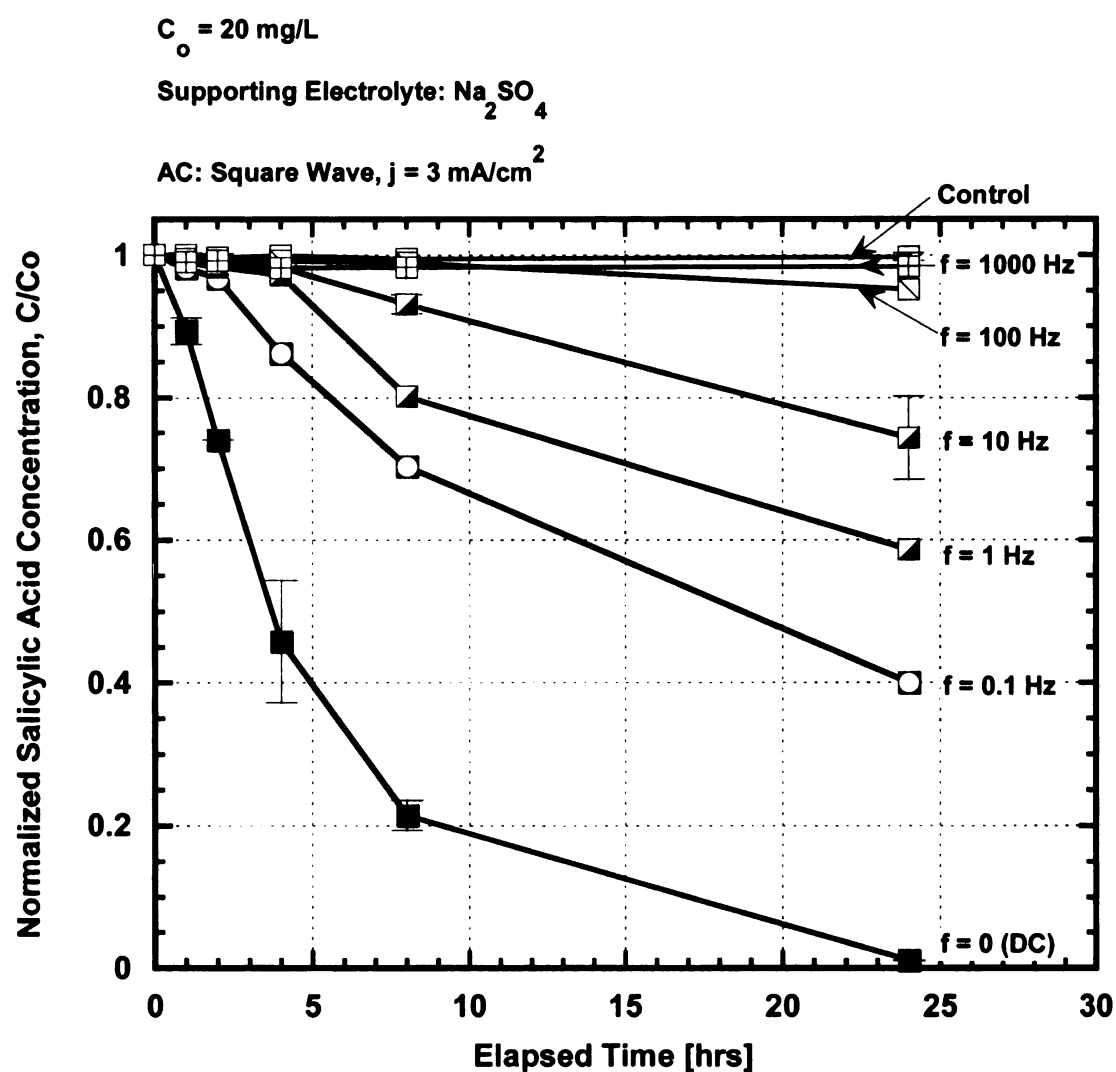


Figure 3-7: Effect of AC frequency on the rate of degradation of salicylic acid (hydroxyl radical probe)

The salicylic acid in solution was hydroxylated to two derivatives, 2,3-dihydroxybenzoic acid and 2,5-dihydroxybenzoic acid which were detected by retention time and UV absorption spectral matching with authentic samples. The lowest AC frequency (0.1 Hz) produced the fastest degradation rate for AC electrolysis, and the 1,000 Hz produced the slowest degradation rate as depicted in Figure 3-7. The DC density,  $3 \text{ mA/cm}^2$  ( $f = 0$ )

showed the fastest degradation rate than all the AC tests. The control cell did not show any measurable reduction in concentration.

### **Hydroxyl Radical Scavenger Study**

Tertiary butanol was used as OH<sup>•</sup> scavengers to further indicate that OH<sup>•</sup> were responsible for the oxidation of naphthalene in the electrochemical cells. Tertiary butanol is widely used as an OH<sup>•</sup> scavenger in radiation chemistry and biochemistry (Wand 1995). Li *et al.* (2003) used tertiary butanol as an OH<sup>•</sup> scavenger and reported that since tertiary butanol reacts preferentially with OH<sup>•</sup>, the amount of OH<sup>•</sup> in the reactor decreased and hence the rate of aniline degradation decreased. Figure 3-8 shows the rate of degradation of naphthalene in the presence of the varying concentrations of the OH<sup>•</sup> scavengers.

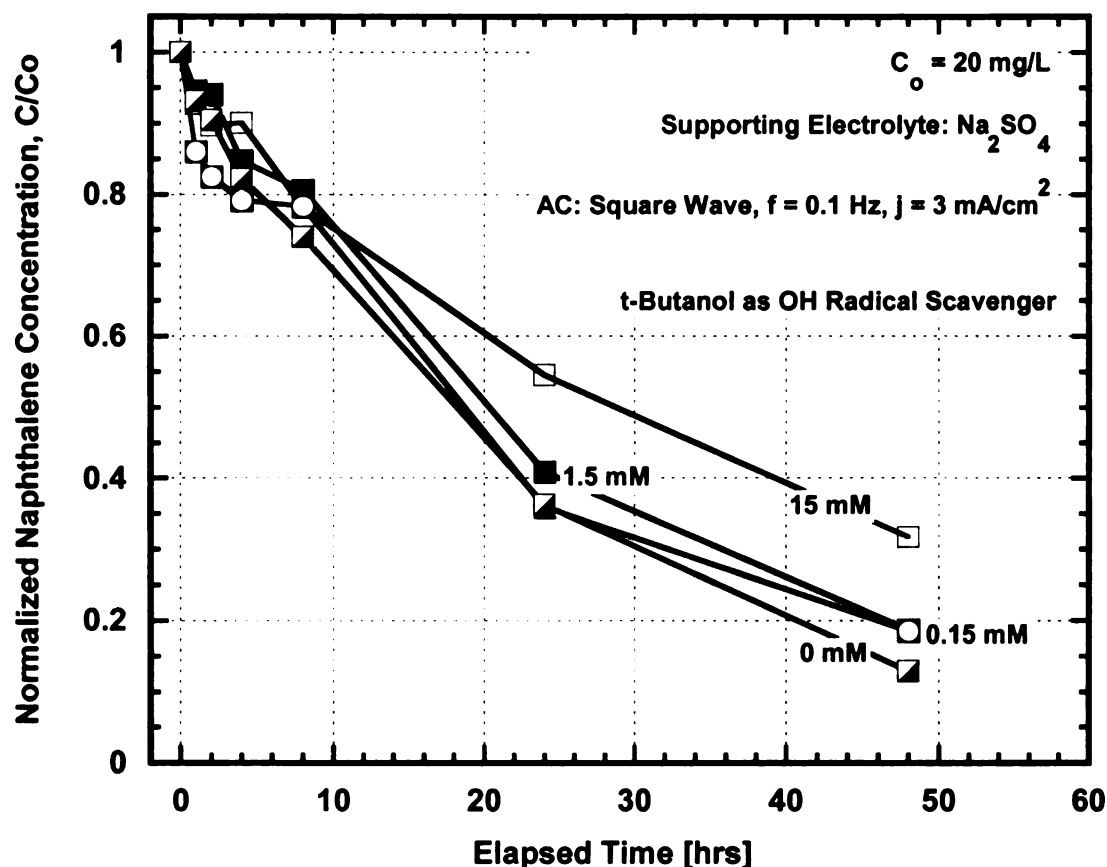


Figure 3-8: Concentration of naphthalene in solution versus time in the presence of varying concentrations tertiary butanol (hydroxyl radical scavenger)

The scavenger reduced the degradation rate of naphthalene as its concentration was sequentially increased in the test cells.

The hydroxylation of the  $\text{OH}^\bullet$  probe (salicylic acid), and the suppression of the degradation of naphthalene in the test cells in the presence of the  $\text{OH}^\bullet$  scavenger, is consistent with numerous studies that OH radicals were the primary oxidizing agent in the electrochemical cells for AC as well as DC tests.

### Modeled *versus* Measured Concentrations of Naphthalene

It is generally believed that electrochemical reactions occur on the surface or in the vicinity of the electrodes. Therefore, the rate of reaction of the organic reactants in the test cell depends on the rate of generation of OH radicals at the electrodes as the oxidizing agents, as well as the rate at which the reacting molecules move to the electrodes for subsequent oxidation by the OH radicals. Mass transfer in solution occurs by diffusion, migration and convection. Diffusion and migration result from a gradient in electrochemical potential and convection results from imbalance of forces on the solution when the solution is mixed or stirred (Bard and Faulkner 2001). Assuming a linear mass transfer, and linear electric field, the mass flux to the electrode can be expressed by the *Nernst-Planck Equation* (Equation 6):

$$J(x) = -D \frac{\partial C(x)}{\partial x} - \frac{zF}{RT} DC \frac{\Delta E}{l} + Cv(x) \quad (6)$$

where  $J$  is the mass flux,  $D$  is the diffusion coefficient of the reacting specie in solution,  $C$  is the instantaneous concentration of the reactants in solution at time  $t$ ,  $x$  is the distance in the  $x$  direction or along the direction of the electrical current,  $z$  is the net charge on the reacting species,  $F$  is Faraday's constant,  $R$  is molar gas constant,  $T$  is temperature (K),  $\Delta E/l$  is the gradient arising from the change in potential  $\Delta E$  over a distance  $l$ , and  $v$  is the linear velocity of the solution. Because the test cell solutions were not stirred, the third term in Equation 6 can be neglected. Hence, Equation 6 becomes:

$$J(x) = -D \frac{\partial C(x)}{\partial x} - \frac{zF}{RT} DC \frac{\Delta E}{l} \quad (7)$$

For uncharged reactant, the second term in Equation 7 can be neglected to yield *Fick's* first law as follows:

$$J(x) = -D \frac{\partial C(x)}{\partial x} \quad (8)$$

Equation 7 was applied to model the rate of mass transfer of naphthalene to the electrodes in the DC setup. The following assumptions were made when applying Equation 7 (or Equation 8) to simulate the naphthalene concentrations:

1. Reactants (naphthalene) are instantaneously converted to products when they come into contact with the electrode. Hence,  $C(t)$  at the surface of electrode is equal to zero for  $t \geq 0$ . This establishes a concentration gradient that drives reactants by diffusion to the surface of the electrodes and this condition is considered as the maximum concentration gradient that may be established in a given time step;
2. Steady-state diffusion conditions exist in a given time step which was assumed equal to 1 hr;
3. Linear mass transfer exists in the given time step of 1 hr; and
4. Linear electric field exists in the given time step of 1 hr.

Equation 7 was applied with  $C$  of naphthalene equal to  $C_0$  ( $\sim 20$  mg/L) for  $t = 0$  at the cathode and  $C = 0$  for  $t \geq 0$  at the anode. Assuming a time step equal to 1 hr, the  $C$  of naphthalene at cathode was estimated by subtracting the mass of naphthalene that moved to the anode for degradation during the previous time step. This computation was carried out for the test duration of 48 hours and the modeled normalized concentrations were compared (Figure 3-9) to the test results for DC tests carried out at  $j = 3$  and  $6$  mA/cm<sup>2</sup>.



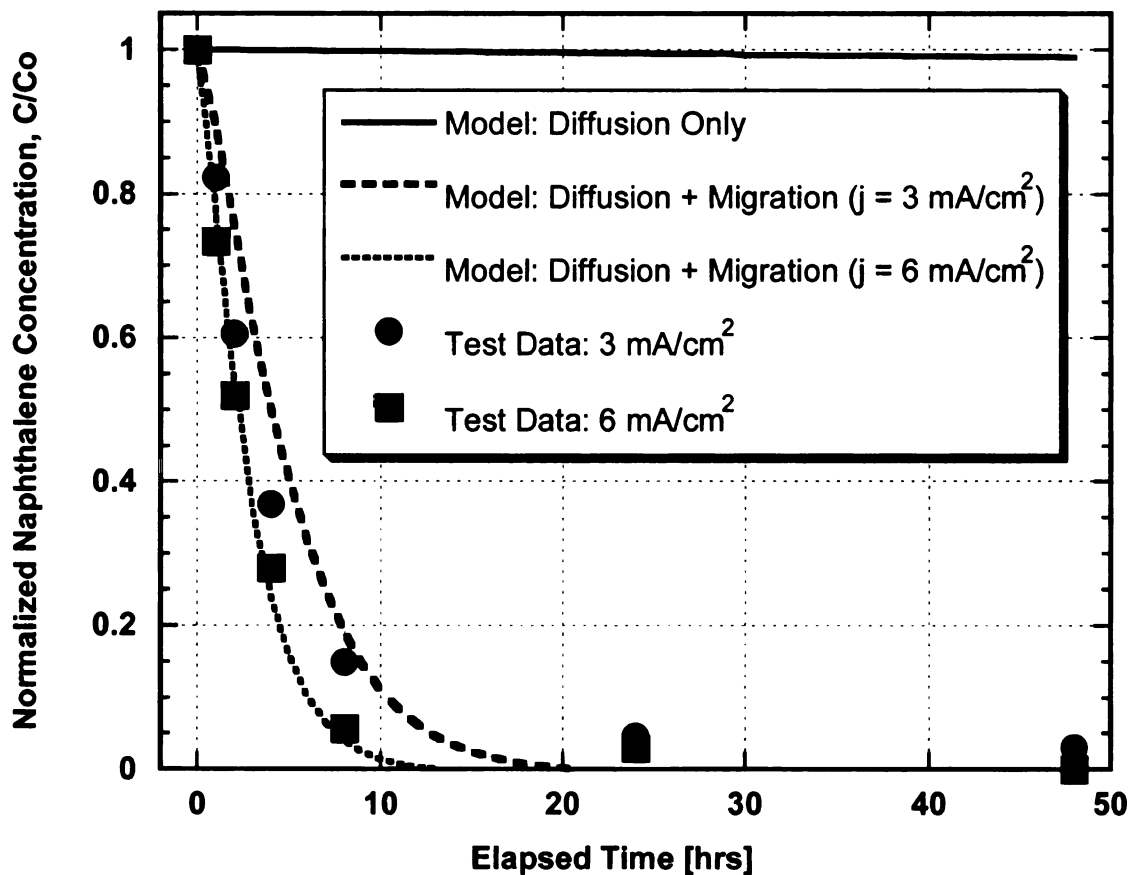


Figure 3-9: Simulated concentrations *versus* test data for naphthalene tests using DC

Schwarzenbach *et al.* (2003) reported diffusion coefficients of organic solutes equal to about  $3.0 \times 10^{-5} \text{ cm}^2 \text{ s}^{-1}$  for small molecules to  $5.0 \times 10^{-6} \text{ cm}^2 \text{ s}^{-1}$  for those of molar mass near 300 g/mol. Based on this data, the diffusion coefficient of naphthalene was estimated as  $9.0 \times 10^{-6} \text{ cm}^2 \text{ s}^{-1}$  from the diffusion coefficients vs. molar mass chart presented by Schwarzenbach *et al.* (2003). Equation 8 was applied to simulate only diffusion driven mass flux of naphthalene to the anode for oxidation. The simulated normalized concentration is presented in Figure 3-9. The simulated degradation rate as a

result of naphthalene migration to anode only due to diffusion is orders of magnitude less than that observed during the experiments run at DC densities equal to  $3 \text{ mA/cm}^2$  or  $6 \text{ mA/cm}^2$  with  $\text{Na}_2\text{SO}_4$  as the supporting electrolyte. When both diffusion and migration are used for simulating the mass flux of naphthalene to the anode by using Equation 7, the simulated normalized concentrations are presented in Figure 3-9 when the net charge,  $z$ , was assumed equal to  $-0.35$  for naphthalene.

For neutral molecules such as naphthalene,  $z$  should be equal to zero. However, it is hypothesized that the presence of anions in the test solution (from the supporting electrolyte) imparts an effective negative charge on the naphthalene molecules. These anions dragged the naphthalene molecules along as they migrated to the positively charged electrode (anode), where anodic oxidation resulted in the degradation of the naphthalene molecules. Therefore, the naphthalene molecules moved in the solution as a result of migration simulated by the second term in Equation 7. Hence, the rate of migration of naphthalene molecules towards the anode is enhanced by assigning a negative value to  $z$  for naphthalene.

By assigning the naphthalene molecule an effective partial negative charge of  $-0.35$ , the simulated normalized concentrations versus time data fits well with that for the experimental data when  $\text{Na}_2\text{SO}_4$  was used as the supporting electrolyte for DC densities equal to  $3 \text{ mA/cm}^2$  and  $6 \text{ mA/cm}^2$ . The rate of anodic oxidation of naphthalene (or salicylic acid) depends not only on the rate of migration of reacting molecules to the reaction site (the anode or instantaneous anode) but also on the rate of production of OH radicals at the anode (or instantaneous anode). Hence, as the current density is decreased,

it may decrease the rate of production of OH radicals at the anode and may become the rate limiting step. When Equation 7 is applied (Figure 3-9), the rate limiting step assumed is the rate of mass transfer to the anode (by diffusion and migration). Hence, Equation 7 would overestimate the decrease in the concentration (or underestimate the concentration at a given time,  $t$ ) of the reactant when current density is low enough to not degrade all naphthalene mass diffusing and migrating to the anode (or instantaneous anode). At higher current densities, the predictions from Equation 7 would be more accurate. It is beyond the scope of this study to estimate the rate of hydroxyl radical production as a function of current density and other variables. Hence, it is not possible to calculate analytically at what current densities the assumptions are valid when Equation 7 is applied.

While Equation 7 is for DC and cannot be applied for an AC, it can be used to explain the reduced rate of degradation when AC was applied and as the frequency of the AC was increased from 0.1 to 1,000 Hz (Figure 3-7). Proposed reasons for the decrease in degradation rates with increased AC frequency are as follows:

1. By assuming that the naphthalene molecules had an effective partial negative charge of say  $z = -0.35$  under our experimental conditions based on the acceptable fit for DC data, increasing the frequency of the AC resulted in back-and-forth movement of the reacting molecules, and hence the net mass flux of the molecules toward the electrodes was reduced. If the net distance traveled by the naphthalene molecules to get to an instantaneous anode,  $L$ , in Equation 7, is varied, until the modeled values of concentrations fit with the experimental data for  $f$  equal to 0.1 Hz, 1 Hz, 10 Hz, 100 Hz, and 1,000 Hz the values of  $L$  obtained are 14 cm, 17

cm, 25 cm, 27 cm, and 45 cm, respectively, compared to the electrode spacing of 8 cm. Assuming degradation rate at the electrodes are the same for each frequency, it can be hypothesized that increase in the AC frequency results in taking longer duration for a naphthalene molecule(s) to reach the instantaneous anode. This may be due to the back and forth movement of the molecule due to the reversal in the direction of the current proportional to the frequency of the AC.

2. Continuous bubbling of gases at both electrodes (probably O<sub>2</sub> and H) in the test solution was observed as the tests progressed. However, the rate of bubbling of the gas decreased as the frequency of the applied AC was increased until no gas bubbles were visible at an AC frequency of 100 Hz or more. Simond *et al.* (1997) and Comninellis (1994) reported that the hydroxyl radicals, formed on an anode react with each other to form oxygen gas at the anode to complete the electrolysis of water molecules. Stock and Bunce (2002) reported that hydrogen radicals formed on a cathode react with each other to produce hydrogen gas at the cathode. If the formation of OH radicals and hydrogen radicals are for the generation of oxygen gas and hydrogen gas at the anode and cathode, respectively, then it is likely that the rate of gas bubbling at the electrode gives an indication of the rate of formation of these radicals at the electrodes. The higher the rate of the observed bubbling of the gas(es), the greater the rate of hydroxyl or hydrogen radical formation at the electrodes. Hence, based on the visual observation of gas bubbles, it is likely that increase in the AC frequency resulted in decrease in the rate of formation of hydroxyl radicals at the electrodes. This impacted the rate of oxidization of naphthalene at the instantaneous anodes.

3. Competing anodic reactions (oxidation) and cathodic reactions (reduction) at the same reaction sites (on the surface of the electrodes) may have been responsible for the decrease in the oxidation rate of both naphthalene (Figure 3-5) and salicylic acid (Figure 3-7) as the AC frequency was increased. However, in DC electrolysis, oxidation reactions occurred at the anode only and reduction reactions occurred at the cathode only and hence there was no competing anodic oxidation and cathodic reduction at the same reaction site. Therefore DC was more effective in degrading naphthalene or salicylic acid in the test cells.

#### **Effect of Convection Mass Flux**

According to Equation 6, stirring the test solutions increases the mass flux towards the electrodes by introducing a convection mass flux component. Additional DC test and AC tests at frequencies of 1 Hz, 10 Hz and 100 Hz were conducted as shown in Figure 3-10.

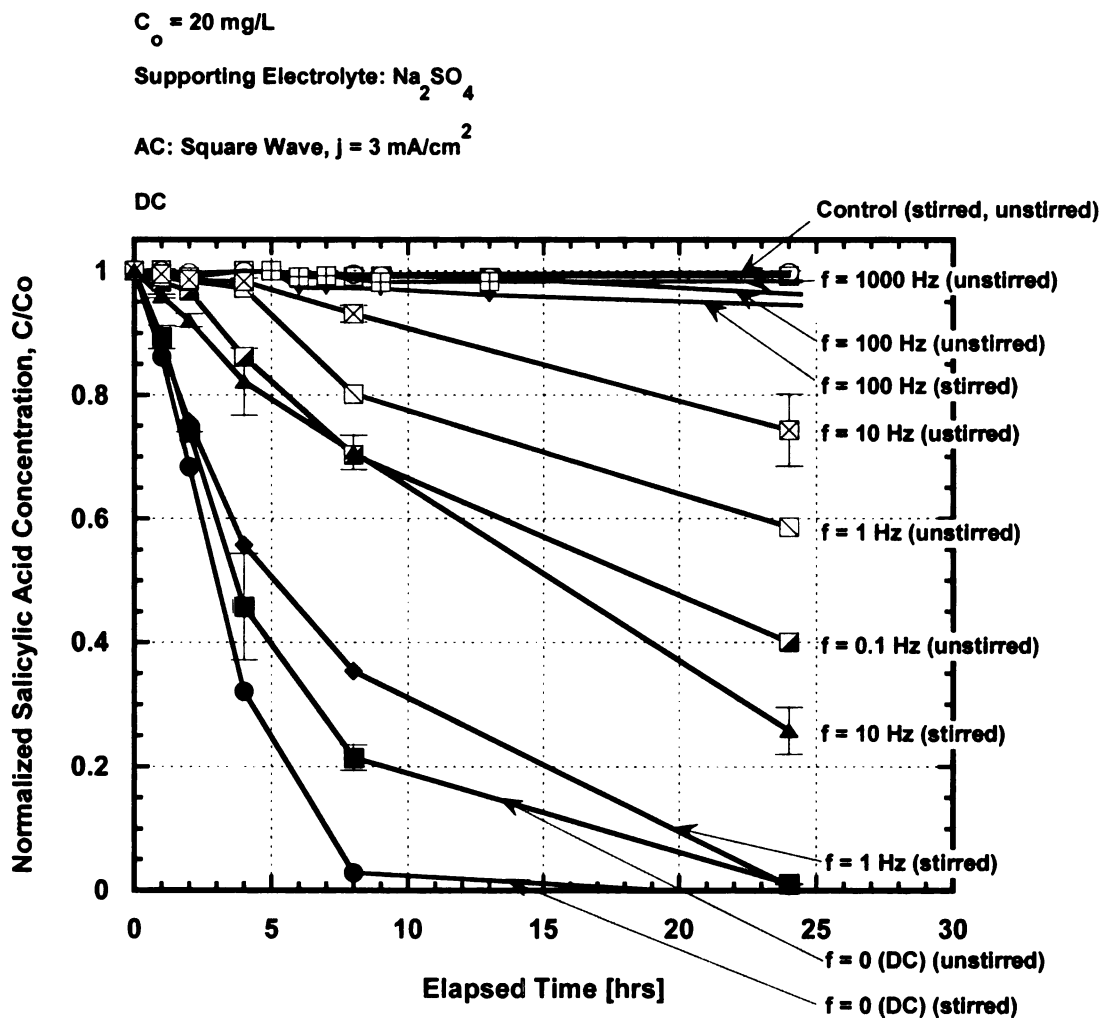


Figure 3-10: Effect of stirring on degradation rate of salicylic acid at different AC frequencies

In the AC tests conducted at 1 Hz and 10 Hz frequencies, stirring significantly increased degradation rate. At 100 Hz frequency, stirring did not result in any significant increase in degradation rate. For degradation to occur, the reacting species have to move to the electrodes, and at the electrodes, OH radicals have to be produced to degrade the reacting species in the vicinity or on the surface of both electrodes. Back-and-forth movement of the salicylic acid molecules in solution subjected to AC slowed down the net flux towards

the electrodes. Stirring the solution increased the mass flux towards the electrodes. At 1 Hz and 10 Hz AC frequencies, enough OH radicals were generated at the electrodes and hence degradation rates were enhanced. However, at 100 Hz frequency, although stirring increased the mass flux towards the electrodes, less OH radicals were produced such that the rate of production of OH radicals was the rate limiting step. Stirring the DC test solution did not significantly increase the degradation rate as compared to the test cell in which the solution was not stirred. In the DC tests, OH radicals were produced at only one of the electrodes (the anode) while the cathode acted as a “passive” electrode in the oxidation of salicylic acid. Because only one electrode participated in the degradation, the degradation rate in the DC test was not as high as in the AC tests at 1 Hz and 10 Hz frequencies.

### **Intermediate Byproducts**

LC/MS analyses indicated molecular masses that suggest the formation of degradation products such as naphthol, dihydroxynaphthalene, trihydroxynaphthalene, dihydrotrihydroxynaphthalene, naphthoquinone, hydroxynaphthoquinone, and benzenedicarboxylic acid. The exact isomers formed were not determined. These degradation byproducts formed are relatively more soluble than the parent compound (naphthalene), hence it is expected that they would be more bio-available in solution for subsequent degradation by microorganisms. The change in color of the test solutions to light yellow as the tests progressed may have been due to the formation of naphthoquinone in the solutions. Formation of quinones is a common observation of the hydroxylation process in oxidizing media (Oturán 2000). The formation of naphthoquinone is consistent with those found by other researchers who also observed

aromatic quinones during electrolytic oxidation of aromatic hydrocarbons (Brillas *et al.* 2000; Panizza *et al.* 2000; Saracco *et al.* 2000). GC/MS analysis by Goel *et al.* (2003) indicated the presence of at least one reaction product, 1,4-naphthoquinone, when naphthalene solutions were electrolyzed and concluded that naphthalene degradation could be due to direct anodic oxidation, oxidation by an intermediate (e.g. hydroxyl radicals), or a combination of both.

### **Reaction Mechanism and Pathway**

$\text{OH}^\cdot$  react with organic pollutants in two different ways:

1. by electrophilic addition to a double bond or an aromatic system; and
2. by abstraction of a hydrogen atom from a carbon atom (Schwarzenbach *et al.* 2003).

Based on the identified degradation products, a simplified degradation pathway for the electrochemical degradation of naphthalene in aqueous solution is proposed as illustrated in Figure 3-11.



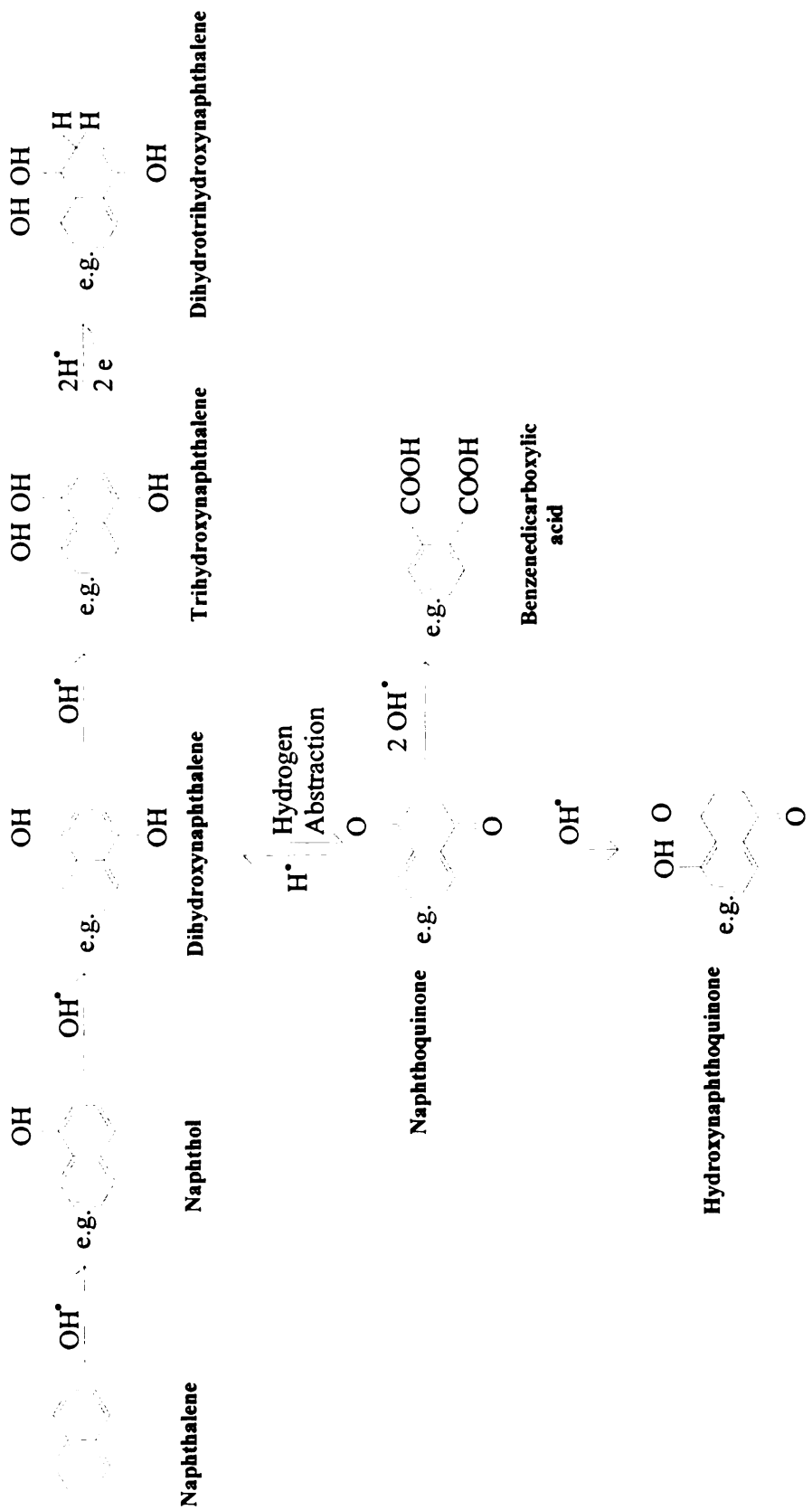
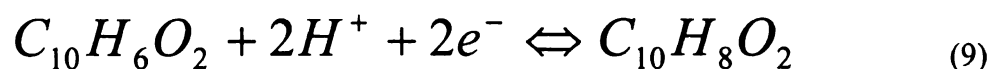


Figure 3-11: Simplified electrochemical degradation pathway of naphthalene in aqueous solution

The exact isomers formed were not determined. Hence the structures shown are just one example of the possible isomers of each byproduct. Initial hydroxylation of naphthalene by an OH<sup>•</sup> radical resulted in the formation of naphthol. Further hydroxylation resulted in the formation of dihydroxynaphthalene (naphthalenediol), which was further oxidized by hydroxylation to trihydroxynaphthalene or by hydrogen abstraction to naphthoquinone. It is possible that addition of hydrogen atoms to naphthoquinone may have reduced it back to dihydroxynaphthalene, which is similar to a reaction step reported in a previous study (Chin and Cheng 1985). Chin and Cheng (1985) reported that in an undivided cell, benzoquinone produced at the anode was subsequently reduced to hydroquinone at the cathode. Therefore, it is possible that in our setup, the naphthoquinone, produced by the oxidation of naphthalene on an instantaneous anode, was subsequently reduced to dihydroxynaphthalene on an instantaneous cathode as shown in Equation 9.



Addition of hydrogen atoms to the trihydroxynaphthalene resulted in the formation of dihydrotrihydroxynaphthalene. Further hydroxylation of the naphthoquinone formed resulted in the formation of hydroxynaphthoquinone. With sufficient OH<sup>•</sup> radicals in the reaction medium, ring cleavage in naphthoquinone may have occurred leading to the formation of benzenedicarboxylic acid. Li *et al.* (2005) reported that benzoquinone formed from the oxidation of phenol could be degraded with ring breakage to various carboxylic acids. One of the proposed mechanisms involves the adsorption of benzoquinone onto the anode surface, which gives up an electron, and the carbon that is

double-bonded with oxygen is attacked by a neighboring hydroxyl radical. When this process is repeated at the *para* position, the ring could be opened and benzoquinone would be broken down into small organic molecules such as carboxylic acids (Houk *et al.* 1998; Lund and Baizer 1991). The present experimental finding is consistent with the proposed mechanism because both naphthoquinone and benzenedicarboxylic acid (from probable ring cleavage of naphthoquinone) were identified as intermediate byproducts. The possible mineralization of naphthalene was not investigated in this study.

### **Divided Cell Setup**

In order to prove that anodic oxidation occurred on both electrodes in AC electrolysis, unlike DC electrolysis in which anodic oxidation occurred on only one electrode (the anode), further tests were conducted in a divided cell setup. The anode compartment was separated from the cathode compartment by means of a Nafion membrane (N-117) at the interface of two 30 mm diameter glass tubes connecting one-liter glass beakers. In studies (Alshawabkeh and Sarahney 2005; Marselli *et al.* 2003) Nafion membrane has been used as a proton-permeable membrane at a cell junction that physically separates the electrolytes in the two compartments.

Figure 3-12 shows the change in concentration of naphthalene with time for both AC ( $3 \text{ mA/cm}^2$ , 0.1 Hz) and DC ( $3 \text{ mA/cm}^2$ ) divided cell setup as well as a control divided cell setup.

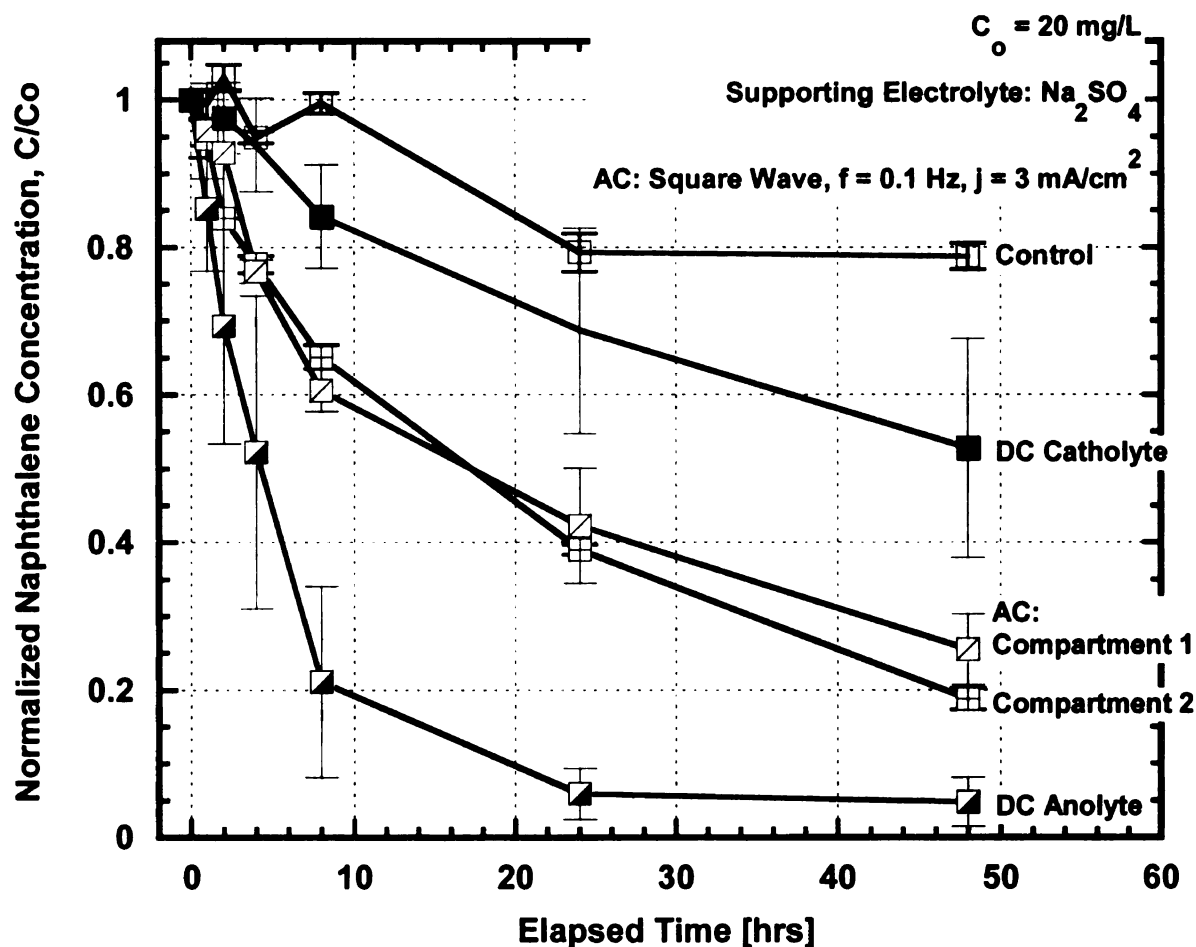


Figure 3-12: Change in concentration of naphthalene with time in a divided cell setup using AC and DC.

Both compartments in the AC test exhibited approximately the same reduction in concentration over time but the anolyte in the DC divided cell setup depicted much faster rate of decrease in the concentration than the catholyte. LC/MS analysis of samples electrolyzed with  $3 \text{ mA/cm}^2$  square wave AC at 0.1 Hz frequency indicated the presence of hydroxylated byproducts including dihydroxynaphthalene, naphthoquinone, in both compartments. However, no hydroxylated byproducts were detected in the cathode compartment (catholyte) of the divided cell DC setup. Hydroxylated byproducts were detected in the anode compartment (anolyte). The reduction in concentration of

naphthalene in the catholyte may have been due to potential sorption on the reactor components and sparging due to continuous bubbling of hydrogen gas from the reduction of water molecules. Goel *et al.* (2003) showed some loss of naphthalene in a control cell experiment over a 9 hr period when nitrogen gas was bubbled through a naphthalene solution at a rate of 1.6 L/day corresponding to a passed current of 100 mA. Also, using salicylic acid as the test solution resulted in the formation of 2,3-dihydroxybenzoic acid and 2,5-dihydroxybenzoic acid in both compartments of the AC divided cell setup, accompanied by reduction in concentration in both compartments. However, these byproducts were only detected in the anolyte in the DC divided cell setup but not in the catholyte, in which approximately 10% loss in concentration was attributed to sparging by H<sub>2</sub> formed from the reduction of water molecules in the catholyte. Since salicylic acid is relatively more soluble in water as compared to naphthalene and hence a lower Henry's constant, loss of mass in the catholyte of the salicylic acid test solution was significantly less than that of the naphthalene test solution. Hence it is likely that a greater proportion of the reduction in concentration of naphthalene in the catholyte was mainly due to sparging. Possible reduction of naphthalene in the catholyte could have also contributed to the reduction in concentration.

Figure 3-13 shows the concentration change of salicylic acid in solution that depicted the same trend as the naphthalene test solutions.

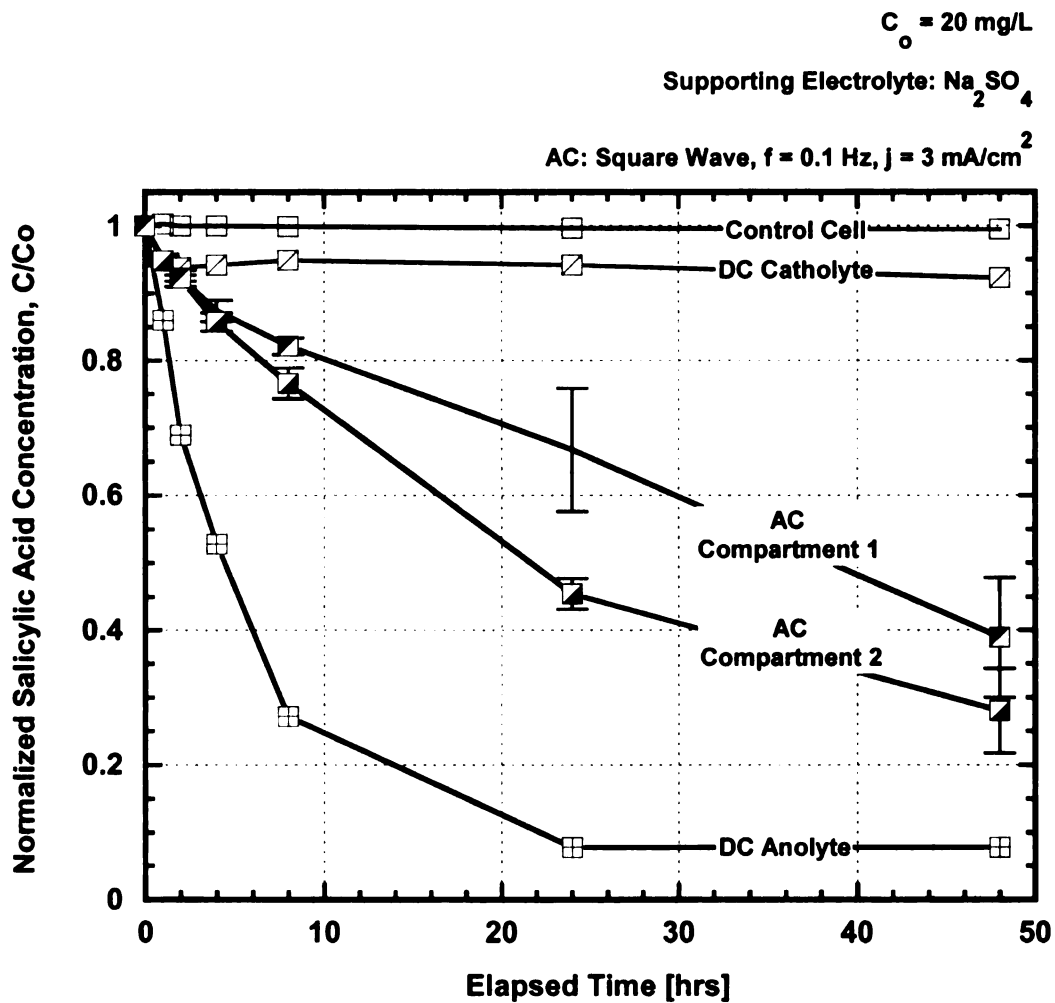


Figure 3-13: Change in concentration of salicylic acid with time in a divided cell setup using AC and DC.

Thus, it was concluded that anodic oxidation, mediated by  $\text{OH}^\cdot$  attack occurred on both electrodes in AC electrolysis but on only the anode in DC electrolysis. The experimental results are summarized in Table 3-2.

#### Measured Initial and Final Key Test Parameters

Measured initial and final values of key experimental parameters are shown in Table 3-3.

Table 3-3: Summary of Measured Initial and Final Key Test Parameters

Compound	Cell	AC	Peak AC Density [mA/cm <sup>2</sup> ]	Temperature [°C]		pH		Standard Redox Potential [mV]		Dissolved Oxygen Concentration [mg/L]	
				Initial	Final	Initial	Final	Initial	Final	Initial	Final
Naphthalene	Undivided	60 Hz (Square)	3	18.5	18.0	6.6	4.6	410	557	3.4	7.0
Naphthalene	Undivided	60 Hz (Sine)	3	19.4	17.1	6.8	4.7	376	460	4.2	9.6
Naphthalene	Undivided	60 Hz (Triangular)	3	18.6	16.8	6.6	5.0	411	527	3.3	6.5
Naphthalene	Undivided	DC	3	19.2	22.7	6.5	11.5	447	177	3.7	3.1
Naphthalene	Undivided	0.1 Hz (Square)	3	19.2	18.0	6.5	4.5	394	415	4.6	6.5
Naphthalene	Undivided	1 Hz (Square)	3	19.2	18.3	6.6	4.4	393	460	4.2	5.5
Naphthalene	Undivided	10 Hz (Square)	3	19.2	18.4	6.6	4.4	393	470	3.7	4.3
Naphthalene	Undivided	100 Hz (Square)	3	19.1	17.1	6.7	4.9	416	461	3.8	6.9
Naphthalene	Undivided	1,000 Hz (Square)	3	19.3	17.9	6.7	4.8	416	467	3.9	6.6

Table 3-3 Cont'd

Naphthalene	Undivided (Anolyte)	-	0 (Control)	19.2	19.0	6.5	6.5	394	422	4.6	7.4
Naphthalene	Divided (Cell 1)	0.1 Hz (Square)	3	19.1	21.9	6.3	2.7	433	458	3.7	7.4
	Divided (Cell 2)	0.1 Hz (Square)	3	19.1	21.4	6.3	11.4	433	193	3.6	8.2
Naphthalene	Divided (Anolyte)	-	3 (DC)	21.2	39.7	6.0	1.7	435	792	3.7	3.8
	Divided (Catholyte)	-	3 (DC)	21.4	24.7	6.0	12.3	435	5	17.0	1.7
Naphthalene /tert-butanol (0.15 mM)	Undivided	0.1 Hz (Square)	3	20.6	19.2	6.5	4.31	459	474	3.9	5.0
Naphthalene /tert-butanol (1.5 mM)	Undivided	0.1 Hz (Square)	3	20.3	19.5	6.7	4.1	477	482	4.1	4.5
Salicylic acid	Undivided	0.1 Hz (Square)	3	20.3	18.1	4.4	4.3	449	472	6.8	7.5
Salicylic acid	Undivided	10 Hz (Square)	3	20.3	17.7	4.4	4.3	449	479	6.9	7.1
Salicylic acid	Undivided	1,000 Hz (Square)		21.0	18.3	4.0	3.9	479	487	8.4	8.7
Salicylic acid	Undivided	0	3 (DC)	21.2	25.7	4.0	11.0	467	351	8.0	9.0
Salicylic acid	Undivided	-	0 (Control)	20.9	19.6	4.0	4.0	558	537	8.6	8.7



Table 3-3 Cont'd

Salicylic acid	Divided (Cell 1)	0.1 Hz (Square)	3	21.7	22.8	4.4	2.3	473	529	8.0	7.3
	Divided (Cell 2)	0.1 Hz (Square)	3	21.7	23.0	4.4	10.9	473	236	8.0	5.6
Salicylic acid	Divided (Anolyte)	0	3 (DC)	20.9	28.6	4.0	1.5	450	889	8.5	13.7
	Divided (Catholyte)	0	3 (DC)	20.9	25.5	4.0	12.3	450	-21	8.5	2.3
Salicylic acid	Divided (Cell 1)	-	0 (Control)	21.7	22.8	4.4	4.4	473	461	8.0	7.8
	Divided (Cell 2)	-	0 (Control)	21.7	23.0	4.4	4.4	473	461	8.0	7.8

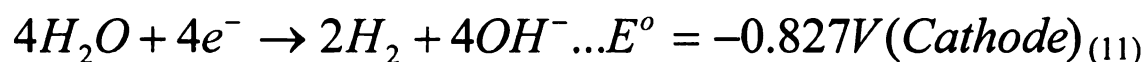
## Notes:

1. All tests were performed by passing 165 mA current (peak or DC).
2. Current density  $[\text{mA}/\text{cm}^2] = \text{current} [\text{mA}] / \text{cross sectional area of electrodes} [\text{cm}^2]$ .

The temperature of the test solutions ranged between approximately 17 °C and 22 °C.

The heat that might have been generated in the test solutions as a result of Joule heating was absorbed by the water bath so no drastic increase in temperature was observed.

The measured initial pH of the naphthalene AC test solutions generally ranged between 6.5 and 6.8 while the final pH values were between 4.1 and 5.0, indicating that the AC test solutions became acidic at the end of the 48-hr testing period. In a divided cell set-up where electrolytes are separated to prevent mixing, but the flow of charge is permitted, pH and redox conditions may develop (Alshawabkeh and Sarahney 2005). At the anode, protons and oxygen gas are produced (oxidizing, acidic conditions develop), and at the cathode, hydroxyl anions and hydrogen gas are produced (reducing, alkaline conditions develop) as presented in Equations 12 and 13.



Other electrolysis products may result depending on the availability of ions and their electrochemical redox potential. Although some secondary reactions might be favored at the cathode because of their lower electrochemical potential, water reduction is dominant (Alshawabkeh and Sarahney 2005). Therefore, it is likely that the oxidation of water molecules was dominant at the time of measurement, resulting in the generation of more H<sup>+</sup> ions in the solutions and hence the test solutions became more acidic at the end of the testing period. The type of supporting electrolyte, degradation byproducts formed, among other factors may also influence the complex acid/base chemistry of the

reaction media. The formation of byproducts such as benzenedicarboxylic acid, with acidic properties could have also made the final pH of the test solution acidic. The initial and final pH values of the salicylic acid AC test solutions however, remained approximately unchanged, between 4.2 and 4.5. The DC test cells used in electrolyzing the naphthalene solutions recorded initial pH of 6.5 and final pH of 11.5 and that of the salicylic acid solution were respectively 4.4 and 11.4; indicating that the DC test solutions became alkaline at the end of the 48-hr testing period.

The measured final standard redox potential of the test solutions was generally higher than the corresponding initial values. The measured dissolved oxygen concentration was also depicted a similar trend, indicating that the AC test solutions became more oxidizing at the end of the test period. However the DC test cell solutions became more reducing at the end of the test period. Continuous bubbling of gases was observed on both electrodes in test cells throughout the testing period when solutions were electrolyzed at  $3 \text{ mA/cm}^2$  current density (at 0.1 Hz and 1 Hz AC frequencies). The rate of evolution of gases at the electrodes was observed to decrease with increasing AC frequency. At higher frequency (over 100 Hz) no gas bubbles were observed with unaided eye. The observed gas bubbles could have been due to the evolution of  $\text{O}_{2(g)}$  and/or  $\text{H}_{2(g)}$ . During the AC half cycle, when one electrode is at a positive electrical potential (instantaneous anode), oxygen gas is produced at that electrode (Equation 12) and hydrogen gas is produced at the other electrode (instantaneous cathode) according to Equation 13. Therefore it is likely that the generation of  $\text{O}_{2(g)}$  in the test solutions was more dominant at the end of the test period.

The measured final electrical conductivity of the test solutions remained approximately the same as the initial values, ranging between 810  $\mu\text{S}$  and 860  $\mu\text{S}$ .

## SUMMARY AND CONCLUSIONS

The key objectives of this study were to: (1) use alternating current (AC) to investigate the effect of AC waveform and frequency on the rate of degradation of naphthalene in aqueous solution; (2) explore the mechanism of degradation of naphthalene when subjected to AC and DC; and (3) prove that anodic oxidation of naphthalene occurred on both electrodes (instantaneous anodes) when AC electrolysis was used, unlike direct current (DC) electrolysis in which anodic oxidation of naphthalene occurred on only one electrode (the anode).

Three AC wave forms (square, sine and triangular) supplied at a frequency of 60 Hz were used to investigate the efficiency of the AC wave forms in degrading naphthalene in aqueous solution. Square wave AC having with peak current density of 3  $\text{mA}/\text{cm}^2$  and frequency varying between 0.1 Hz and 1,000 Hz was used to investigate the effect of AC frequency on degradation rates of naphthalene. A divided cell setup was used to isolate the degradation byproducts formed at both electrodes to identify the key degradation mechanisms and differences in AC and DC electrolyses. The *Nernst-Planck* equation was used to model the rate of mass transfer to the electrodes, where reactions were expected to occur, and the simulated concentration-time profiles were compared with test results. The key conclusions of this study are as follows:

1. For a fixed peak current density and frequency of applied AC, the square wave AC was most efficient for the degradation of naphthalene in solution. The next

most efficient wave form was sine wave followed by the triangular wave form. The key reason for this, for a given peak current, the total electrical power (product of rms current to rms voltage) applied by a square wave AC is greater than sinusoidal wave form followed by a triangular wave form.

2. For a fixed peak current density, increase in AC frequency resulted in a decrease in the rate of degradation of naphthalene. The key reason for this decrease is the rate of migration of naphthalene to the electrodes was reduced due to the rate of change in the direction of the current which is a function of the frequency of the wave form. In addition, increase in the AC frequency may have suppressed the rate of production of hydroxyl radicals.
3. The hydroxylation of the  $\text{OH}^\bullet$  probe (salicylic acid) to form 2,3-dihydroxybenzoic acid and 2,5-dihydroxybenzoic acid, and the suppression of the degradation of naphthalene in the test cells in the presence of an  $\text{OH}^\bullet$  scavenger, t-butanol, is consistent with numerous studies that  $\text{OH}^\bullet$  radicals were the primary oxidizing agent in the electrochemical cells for AC as well as DC tests.
4. The reduction in concentration of naphthalene and salicylic acid in both compartments of a divided cell setup as well as the formation of hydroxylated by-products in both compartments is an indication that anodic oxidation occurred on both electrodes in AC electrolysis. In DC electrolysis, hydroxylated by-products were detected in only the anolyte. In DC application, there was rapid reduction in concentration in the anolyte (over 90% degradation in 24 hrs of testing) where naphthalene and salicylic acid were used as the reactants. The rate of reduction in

concentration in the catholyte of the salicylic acid and naphthalene tests, during the 48 hr testing period was relatively small.

5. The rate of anodic oxidation of naphthalene and salicylic depends on the rate of production of OH radicals at the anode (or instantaneous anode) as oxidizing agents as well as the rate of migration of reacting molecules to the reaction site (the anode or instantaneous anode). At higher current densities, not only more OH radicals are produced at the anode but also the rate of migration of the reacting molecules to the anode (or instantaneous anode) increases during a DC application. However, when AC is used, the change in the direction of the current decreases the rate of migration of the reactant to the instantaneous anode. Hence, as the frequency of the applied AC increases, the rate of degradation decreases.
6. Both diffusion and migration processes were responsible for the rate of mass transfer of naphthalene to the reaction sites (surface of electrodes or in the vicinity of the electrodes) where naphthalene was degraded or converted by the hydroxyl radicals. However, migration was the dominant mass transfer phenomenon responsible for the degradation of naphthalene in the AC and DC electrochemical cells.

## **PAPER NO. 4: A COMPARATIVE STUDY OF SONOCHEMICAL AND ELECTROCHEMICAL DEGRADATION OF NAPHTHALENE IN AQUEOUS SOLUTION**

### **ABSTRACT**

The objective of this study was to compare the rate of degradation of naphthalene, a model polycyclic aromatic hydrocarbon (PAH) in aqueous solution was subjected to ultrasound energy and electrical energy (AC and DC) delivered at the same output powers (30 W and 60 W). Under the experimental conditions, DC and ultrasound exhibited approximately equal degradation rates at 60 W output power. However, at 30 W, rate of degradation for DC was slightly higher. AC was least efficient at both output powers. As the output power was increased from 30 W to 60 W for AC, DC as well as ultrasound, it resulted in faster degradation of naphthalene. The energy applied in each test exhibited *pseudo*-first-order degradation kinetics for the decrease in the concentration of naphthalene in solution. The degradation byproducts identified in both electrical (AC and DC) and sonochemical degradation were identical, which suggested that it is highly likely that the primary oxidizing agent was the same. Formation of 2,3-dihydroxybenzoic acid and 2,5-dihydroxybenzoic acid from both sonochemical and electrical degradation of salicylic acid (a hydroxyl radical probe) was consistent with the findings in literature which indicated that hydroxyl radicals were the primary oxidizing agent. The *Nernst-Planck* equation was used to model the rate of mass transfer to the electrodes in the AC and DC tests, where reactions were expected to occur, and the simulated concentration-time profiles were compared with test results. Both diffusion and migration processes were responsible for the rate of mass transfer of naphthalene to the reaction sites (surface

of electrodes or in the vicinity of the electrodes) where naphthalene was degraded or converted by the hydroxyl radicals. However, migration was the dominant mass transfer phenomenon responsible for the degradation of naphthalene in the AC and DC electrochemical cell.

## **INTRODUCTION**

PAHs constitute an extraordinarily large and diverse class of organic molecules. The major sources of PAHs are crude oil, coal and oil shale. Coal tar and petroleum residues produced in the refining process contain high percentages of PAHs, representing a wide range of molecular sizes and structural types (Harvey 1997). According to Lee *et al.* (1981), PAHs are the largest class of chemical carcinogens, and both Clar (1964) and Harvey (1991) also have presented reported in detail about the evidence of PAH carcinogenicity in animals. When ingested, PAHs are rapidly absorbed into the gastrointestinal tract due to their high lipid solubility (Cerniglia 1984). The United States Environmental Protection Agency (USEPA) estimates that 3,000 to 5,000 former manufactured gas plant (MGP) sites are located across the United States and many of these contaminated sites contain substantial quantities of PAHs (USEPA 2000).

Adewuyi (2001) reported in a review that sonolysis is capable of degrading several target compounds including, amongst others, phenol, chlorophenols, nitrophenols, polychlorinated biphenyls, chloroaromatics, pesticides, dyes, CFCs, PAHs, surfactants, present in relatively dilute solutions typically in micro- to milli-molar range. Frequencies above 16 kHz, above the threshold of human hearing, are classed as ultrasound. In ultrasound applications, the utilized frequencies usually begin at 20 kHz and extend to



500 MHz (Thompson and Doraiswamy 1999). The lower frequency range is utilized for many studies into sonoluminescence, synthesis, and degradation. This range is also utilized in many ultrasound baths which tend to operate between 30 and 40 kHz (Little *et al.* 2002). Ultrasonic waves pass through any substance having elastic properties. Molecules oscillate in the direction of the wave in a compression cycle followed by a rarefaction cycle. In fluids, ultrasound causes high-energy acoustic cavitation, that is, the formation of microscopic vapor bubbles in the low pressure (rarefied) part of the ultrasonic wave when the low pressure overcome the surface tension of the fluid. The bubbles collapse or implode in the compression part of the wave creating very minute high-energy movements of the solvent that result in localized high shear forces (Meegoda and Veerawat 2002). The implosive collapse of the bubbles in the liquid can cause localized pressures of the order of 1,000 atm and temperature as high as 5,000 K generated over a few microseconds time interval. Their lifespan of these bubbles is of approximately 2  $\mu$ s and size is approximately 200  $\mu$ m make direct measurements difficult (Suslick and Flint 1987). Sonolysis of environmental pollutants constitute a remediation method of increasing promise (Goskonda *et al.* 2002). Chemical changes attributable to the effect of ultrasound are largely theorized as being a result of reactions within the resultant cavitation bubbles, observed within the sound wave (Suslick and Flint 1987). Much of degradation chemistry is accepted as depending on the formation of free radicals within these bubbles (Little *et al.* 2002).

On the other hand, the electrochemical degradation of organics such as PAHs, phenol, benzene etc. has been investigated by various researchers using DC electrolysis. However, relatively few studies have been conducted where AC electrolysis was

explored for the degradation of organics in solutions. Comninellis (1994), Brillas *et al.* (2000), and Panizza *et al.* (2000) have reported that electrochemical systems generate hydroxyl radicals ( $\text{OH}^\bullet$ ) at the anode due to the oxidation of water molecules. Among oxygen radicals such as  $\text{O}_2^{\bullet-}$ ,  $\text{OH}^\bullet$ ,  $\text{HO}_2^\bullet$ , and  $\text{ROO}^\bullet$  that may be generated electrochemically in solution, the  $\text{OH}^\bullet$  is the most reactive (Oturán and Pinson 1995). Nakamura *et al.* (2005) proposed a mechanism based on selective redox reactions with various radicals generated by AC electrolysis that allows both oxidation and reduction at the same reaction site between adjacent electrodes. Based on the analysis of intermediate products of the degradation process, Nakamura *et al.* (2005) reported that the mechanism involved selective redox reactions with short-lived and highly reactive radicals: hydrogen atoms ( $\text{H}^\bullet$ ) and hydroxyl radicals ( $\text{OH}^\bullet$ ) that are electrochemically generated on the electrodes. Therefore both sonochemical and electrochemical degradation of organics in solution involve the generation of free radicals; the  $\text{OH}^\bullet$  being the most reactive of the radicals. However, these two methods have not been compared to find out which method is more efficient for degrading the target contaminant.

Therefore, the objective of this study is to compare the rate of degradation of a model PAH – naphthalene, in aqueous solution using ultrasound energy and electrical energy (AC and DC) delivered at the same output power. The ultrasound equipment used for this study was capable of delivering a maximum ultrasound power at 60 W to our test solutions. Hence tests were conducted at 60 W and half of the maximum output power, i.e. 30 W, respectively. Naphthalene, which contains two fused benzene rings, was selected as a model PAH compound because in published studies Alshawabkeh and

Sarahney (2005) and Goel *et al.* (2003) have also used naphthalene in electrochemical and sonochemical studies. Also, naphthalene has chemical and physical properties similar to other PAHs, except that it is more soluble in water, a property that makes naphthalene more available in aqueous solution and more exposed to reactivity than other PAHs (Alshwabkeh and Sarahney 2005).

## **MATERIALS AND EXPERIMENTAL METHODOLOGY**

The experimental setup for the sonochemical tests is presented in Figure 4-1 whereas the electrochemical setup is presented in Figure 4-2.

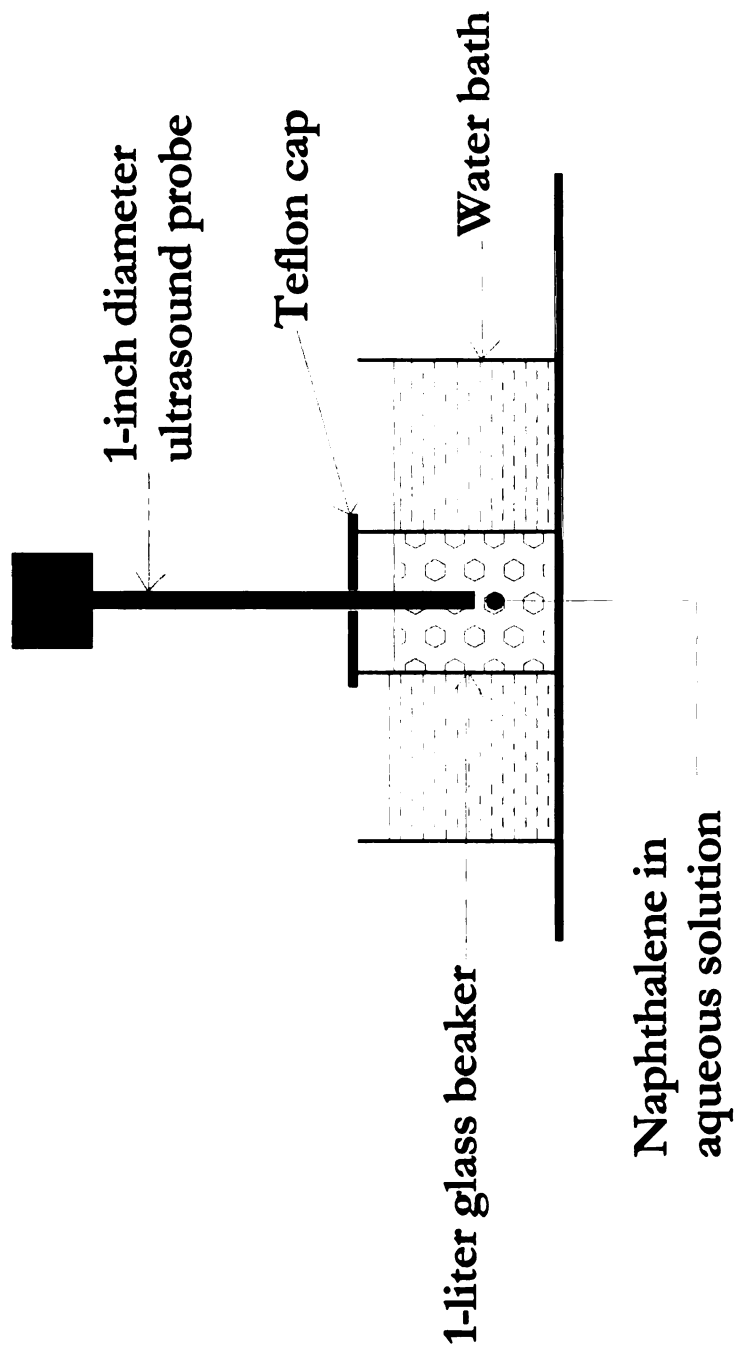


Figure 4-1: Schematic of experimental setup for sonochemical degradation of naphthalene in solution

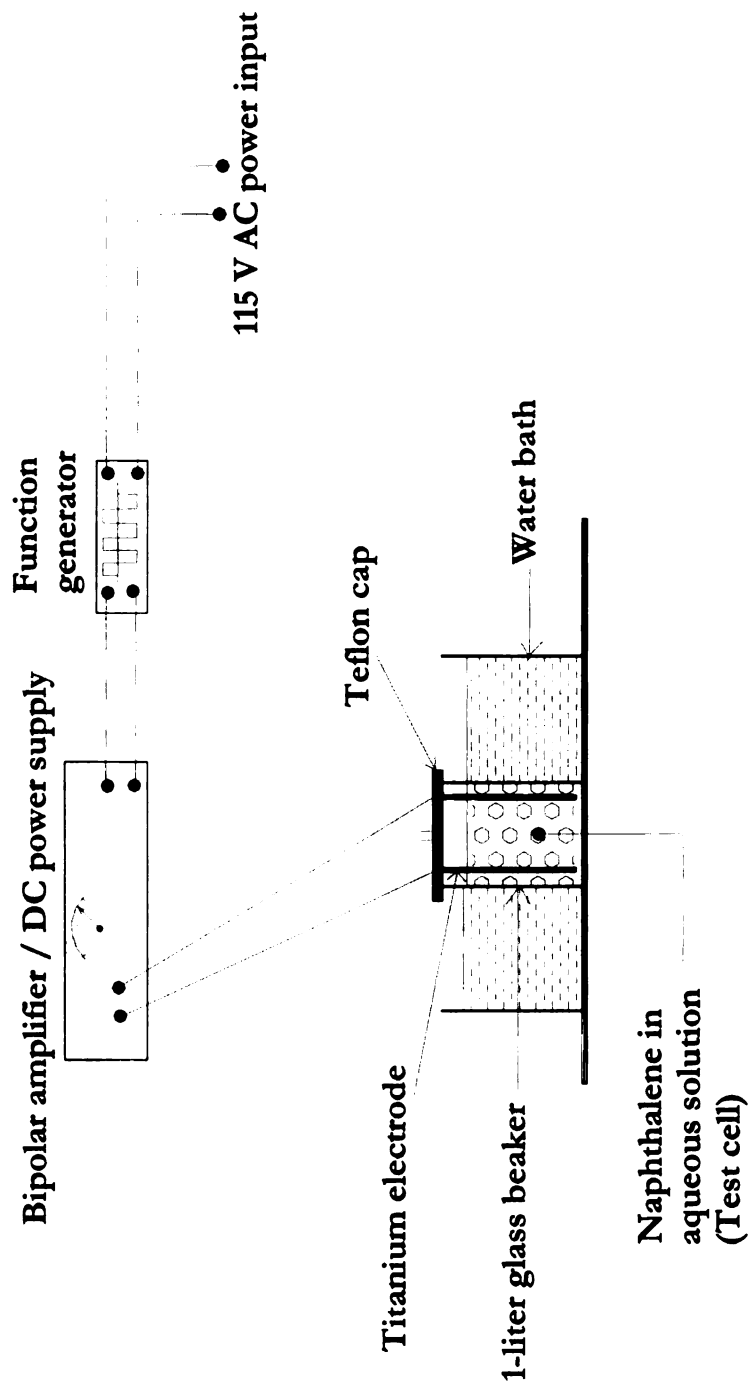


Figure 4-2: Schematic of experimental setup for electrochemical degradation of naphthalene in solution

## **Reaction Chambers**

The reaction chamber consisted of a 1 liter Pyrex glass beaker with a Teflon cap for sonochemical as well as electrochemical tests. These materials of the cell were selected to eliminate or reduce sorption of the contaminants onto the walls of the reaction vessel and the cap. Titanium plates were used as electrodes in electrochemical tests for this study. Alshawabkeh and Sarahney (2005), Li *et al.* (2005) and Goel *et al.* (2003) have used titanium as a base metal and coated it with mixed metal oxides such as RuO<sub>2</sub>, IrO<sub>2</sub>, and SnO<sub>2</sub>. The titanium plates used in this study were not coated. Uncoated titanium being cheaper than commonly used electrodes such as platinum, or titanium coated electrodes, was selected for this project. Also, titanium offers resistance to corrosion in a wide range of aggressive conditions and hence, could be used for potential field scale application. The titanium sheets used as electrodes in this study were 12.0-cm-long by 5.0-cm-wide by 1.72-mm-thick and the distance between them was maintained at about 8.0 cm. The contact area of the solution with the electrode ranged from 53 cm<sup>2</sup> and 55 cm<sup>2</sup> as samples were collected for analyses. The reaction vessel for the sonochemical tests was a 1-liter glass beaker with a Teflon cap.

## **Electrical Equipment**

A 0.1 Hz to 2 MHz Sweep Function Generator was used to generate the AC signals. The power supply consisted of a bipolar operational power supply/amplifier capable of producing 200 V AC/DC and 1 A AC/DC output or a maximum electrical power of 200 W. Voltage and current measurements were obtained with the aid an oscilloscope.

### **Ultrasound Equipment**

The ultrasound equipment used was a Sonics VCX 750 that was operated in a continuous mode at a fixed frequency of 20 kHz. The ultrasound was delivered through a one inch diameter titanium alloy probe and the ultrasound output amplitude ranged from 1% to 100%. Although the maximum output of this model was 750 W, the power it delivered depended on the viscosity of the liquid being processed. The higher the viscosity, the greater the power delivered by the ultrasound equipment. By setting the amplitude to 100%, the maximum power delivered to our test solutions was 60 W. Hence all tests were conducted at 30 W and 60 W ultrasound power output.

### **Spiked Solution Preparation**

Aqueous solutions, spiked with naphthalene were prepared by adding naphthalene (98%, purity) crystals to one liter of deionized (DI) water in a capped Pyrex bottles and allowing the suspensions to stand for about three days. This was followed by the addition of 0.5 g of anhydrous sodium sulfate to each suspension, to increase its electrical conductivity. Sodium sulfate was selected as a supporting electrolyte because Goel *et al.* (2003) and Pepprah and Khire (2008) have used sodium sulfate in electrochemical degradation of naphthalene in aqueous solution. The resultant concentration of  $\text{Na}_2\text{SO}_4$  was approximately 500 mg/L (~3.5 mM). This concentration was selected in order to maintain it at USEPA's maximum contaminant level (MCL) for sulfate, which is equal to 500 mg/L (~3.5 mM). Saracco *et al.* (2000) performed tests where electrolyte salt (e.g. NaCl,  $\text{Na}_2\text{SO}_4$ ) concentrations ranged from 0.2 – 2 M and concluded that higher salt concentrations reduce the electrical resistance between the electrodes and hence will reduce the operating costs. However, greater salt concentration would result in greater

post-treatment costs and hence would be less favorable. The only exception might be represented by discharging the treated effluent into the sea (Saracco *et al.* 2000). The excess suspended naphthalene crystals were then filtered off and the collected filtrate was for the tests. Although no supporting electrolyte was required for the sonochemical test solutions, in order to simulate similar reaction media in all tests, the test solutions used for the sonochemical tests also contained 500 mg/L sodium sulfate.

### **Testing Procedure**

Electrochemical tests were conducted in a batch mode in 1-liter undivided cells. Prior to the commencement of the passage of AC through the cells, initial samples were collected for high performance liquid chromatography (HPLC) analyses. Replicate tests were conducted for some of the tests. The effect of AC on the degradation rate of naphthalene in solution was explored using a sine wave at a frequency of 60 Hz. This frequency was selected because AC is supplied at 60 Hz frequency in the United States. The AC power was obtained by the product of the root-mean-square (*rms*) current and the *rms* voltage. During the tests, samples were collected for HPLC analyses at elapsed time intervals equal to 0, 1, 2, 4, 6, and 8 hours. Sonochemical tests were also conducted in a batch mode in 1-liter glass beakers and sampled at the same frequency as the electrochemical tests. The samples were analyzed directly without extracting the naphthalene from the aqueous solution. HPLC analyses were performed using a diode array detector (detection at 255 nm), a Waters C-18 PAH, 250 mm x 4.6 mm x 5  $\mu$ m column, an automated gradient controller, and deionized water (DI)/acetonitrile mobile phase. The flow rate of the mobile phase was 1.2 mL/min and the column was flushed with 10:90 (v/v) acetonitrile/DI water for 5 minutes followed by 60:40 (v/v) acetonitrile/ DI water for 10



minutes, and by 100:0 (v/v) acetonitrile/ DI water for 5 minutes. This gradient was used for the analysis in order to obtain appropriate separation of the degradation product peaks on the chromatograms during the tests. Standard solutions were prepared to bracket the expected concentration level of the analytes. Calibration curves with an average obtained  $R^2$  value of 0.998 were used to determine the concentration of naphthalene in the solutions as the tests progressed. Samples were also collected for Liquid Chromatography / Mass Spectrometry (LC/MS) analyses to determine the degradation products formed. Control cells, similar to the test cells except without any current or ultrasound passed through them, were set up, sampled, and analyzed at the same time intervals as the test cells. The test cells were placed in a relatively large volume water bath to reduce the rate of temperature rise of the test solutions.

### **Experimental Parameters Monitored**

Apart from monitoring the concentration of naphthalene in aqueous solution over time, other experimental parameters monitored included the initial and final values of pH, temperature, redox potential, electrical conductivity, and dissolved oxygen concentration of the solutions. A portable dissolved oxygen/pH meter, equipped with a pH electrode, an oxidation-reduction probe and dissolved oxygen probe, was used to measure pH, redox potential and dissolved oxygen, respectively, of the test solutions. An electrical conductivity meter was used to measure the electrical conductivity and a thermometer was used to measure the temperature of the spiked solution in the control and test cells throughout the testing period.

## RESULTS AND DISCUSSION

Table 4-1 outlines the list of parameters explored and varied in the experimental program.

Table 4-1: Experimental Variables

<b>Compound</b>	<b>Energy</b>	<b>Power Output [W]</b>	<b>Frequency</b>	<b>No. of tests</b>
Naphthalene	Electrical (AC)	60	60 Hz	1
Naphthalene	Electrical (AC)	30	60 Hz	1
Salicylic Acid	Electrical (AC)	60	60 Hz	1
Salicylic Acid	Electrical (AC)	30	60 Hz	1
Naphthalene	Electrical (DC)	60	0	1
Naphthalene	Electrical (DC)	30	0	1
Salicylic Acid	Electrical (DC)	60	0	1
Salicylic Acid	Electrical (DC)	30	0	1
Naphthalene	Ultrasound	60	20 kHz	2
Naphthalene	Ultrasound	30	20 kHz	2
Salicylic Acid	Ultrasound	60	20 kHz	1
Salicylic Acid	Ultrasound	30	20 kHz	1
Naphthalene	-	Control	-	1
Naphthalene	-	Control	-	1
Salicylic Acid	-	Control	-	1
			<b>Total No. of tests</b>	<b>17</b>

Figure 4-3 shows the change in concentration (~ 20 mg/L, initial concentration) of naphthalene in the test cells run at 30 W and 60 W ultrasound, DC and AC power, as well as the control cell.

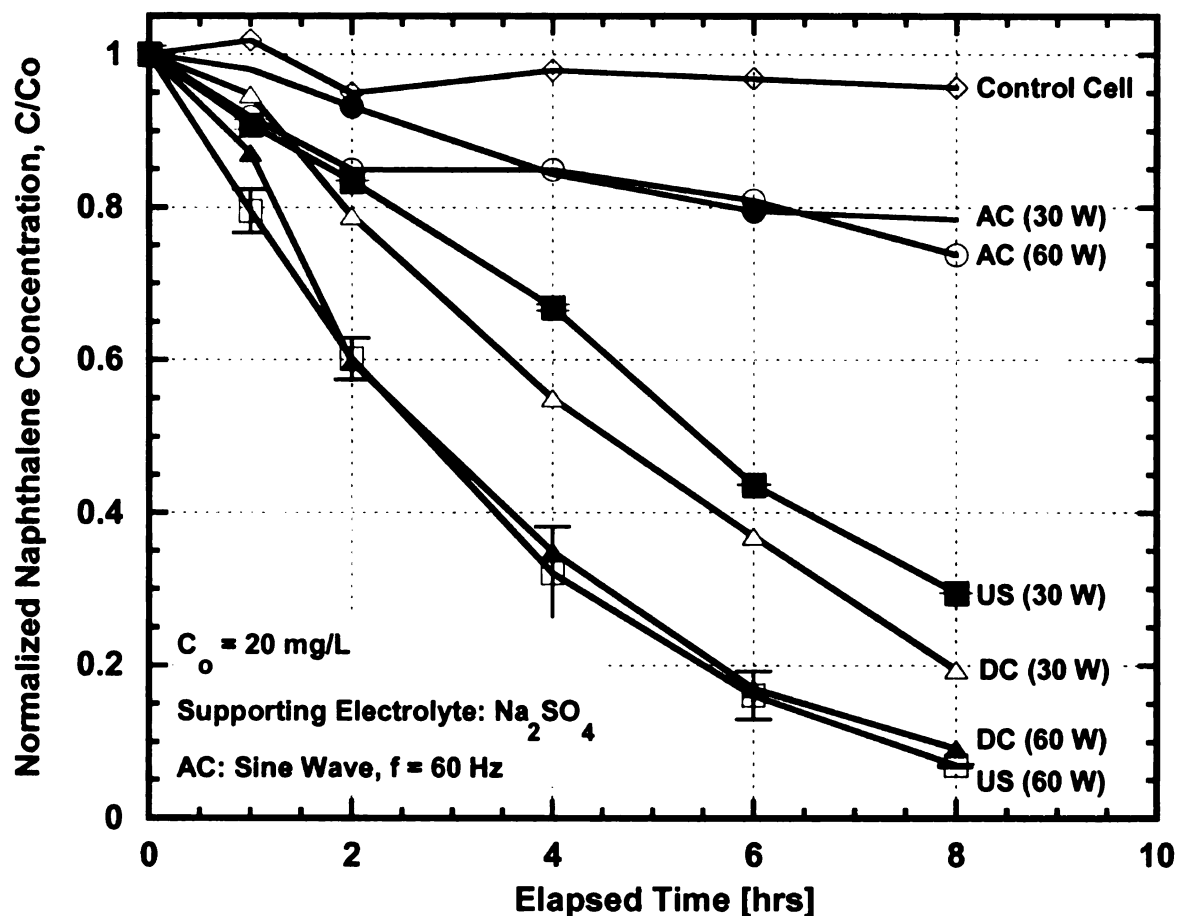


Figure 4-3: Concentration-time profile for both sonochemical and electrical degradation of naphthalene in solution at 30 W and 60 W output power

#### Effect of Power (AC, DC and Ultrasound)

The error bars in Figure 4-3 represent the maximum and minimum values of the normalized concentration ( $C/C_0$ ). The DC test and the ultrasound test cells exhibited similar degradation rates at 60 W and 30 W power output. However, the AC test cell

showed significantly lower rate of degradation at 60 Hz frequency. At 30 W output power, DC showed slightly higher rate of degradation. Therefore, for a given current density, DC was more efficient in degrading naphthalene in solution compared to an equivalent AC at 60 Hz. At lower frequency, the rate of degradation of AC increases (Paper No. 3). It is due to factors such as competing anodic and cathodic reactions at the same reaction site (the electrodes) in AC electrolysis unlike DC electrolysis where anodic oxidation occurs only on the anode. The key reason for DC showing greater degradation rate than AC is the constant reversal in the direction of the current when AC is applied decreases the rate of migration of the PAH to the reaction sites which are both electrodes (instantaneous anodes) in an AC cell. Because the degradation of the PAH only occurs at the electrodes, the decrease in the rate of migration of the PAH to electrode decreases the rate of degradation. As the frequency of the applied AC increases, the rate of migration further decreases because the rate of change of direction of the current flow increases and hence taking longer time for the PAH to reach one of the electrodes.

Another possibility for the higher degradation rate for DC compared to AC is that DC produces hydroxyl radicals at a greater rate at an equivalent current. However, it was not possible to quantify the rate of production of hydroxyl radicals.

Figure 4-3 also illustrates that the higher the output power of DC, AC or ultrasound, the greater the degradation rate of naphthalene in solution. This is consistent with other studies (Psillakis *et al.* 2004; Park *et al.* 2000) that reported increased rate of conversion of PAHs with increased ultrasound output power. As ultrasound power increases, the number of collapsing cavitation bubbles increases, resulting in enhanced degradation rates. Increasing electrical power output results in increased electrical current

density and hence increased rate of degradation of target organics in solution. This is consistent with findings by Alshawabkeh and Sarahney (2005) who reported increased rate of degradation of naphthalene in aqueous solution with increased applied current density.

### **Similarities between Sonochemical and Electrochemical Degradation**

#### *Oxidizing Agents*

Sonolysis has been shown to produce reactive species including  $\text{H}_2\text{O}_2$ ,  $\text{HO}_2$ ,  $\text{H}^\bullet$ , and  $\text{OH}^\bullet$ , which potentially can start radical chain reactions throughout the sonolyzed media (Lorimer and Mason 1987). Riesz *et al.* (1990 and Sehgal *et al.* (1982) have verified the presence of hydroxyl radicals by techniques such as electron spin resonance and 2,2-Diphenyl-1-picrylhydrazyl. Brillas *et al.* (2000) reported that the primary oxidizing agent in an electrochemical degradation study was the hydroxyl radical ( $\text{OH}^\bullet$ ), although secondary oxidizing agents such as  $\text{H}_2\text{O}_2$  and  $\text{HO}_2^\bullet$  radicals could have been formed. Hydroxyl radicals attack the benzene rings of aromatic compounds to produce hydroxylated compounds. Various OH radical probes and techniques have been used in many studies to detect the generation of  $\text{OH}^\bullet$  in the reaction media. These include salicylic acid (Li *et al.* 2003; Marselli *et al.* 2003; Jen *et al.* 1998; Scheck and Frimmel 1995), 4-hydroxybenzoic acid (Anderson *et al.* 1987), benzoic acid (Oturán and Pinson 1995), *para*-chlorobenzoic acid (*p*CBA) (Elovitz and von Guten 1999; Haag and Yao 1992), 2,2-diphenyl-1-picrylhydrazyl (DPPH) (Sehgal *et al.* 1982), 5,5-dimethyl-1-pyrroline-N-oxide (DMPO) and electron spin resonance (ESR) (Marselli *et al.* 2003), *p*-

nitrosodimethylaniline (RNO) and spectrophotometer measurements (Tanaka *et al.* 2004), and RNO / ESR (Comninellis 1994). Since ESR methods require expensive and sophisticated equipments; they were not used in this study due to budget constraints. Trapping of OH<sup>•</sup> using salicylic acid, and HPLC measurements were selected as hydroxyl radical probe technique for this study.

Jen *et al.* (1998) reported that the oxidation efficiency of OH<sup>•</sup> is usually limited by the rates of OH<sup>•</sup> generation and hence, increasing the OH<sup>•</sup> generation and keeping it at a high level are the main factors that control the degradation efficiency of aqueous organic substances. Haag and Yao (1992) also reported that in contrast to most other oxidants, reactions of OH<sup>•</sup> with organics containing C-H or C-C multiple bonds generally proceed with rate constants approaching diffusion-controlled limit ( $10^{10} \text{ M}^{-1} \text{ s}^{-1}$ ) and therefore oxidation rates are usually limited by the rate of OH<sup>•</sup> generation and competition by other OH<sup>•</sup> scavengers in solution rather than by inherent reactivity with the oxidant. This implies that, the higher the rate of generation of OH<sup>•</sup> in solution, the faster the hydroxylation rate of the OH radical probe and hence the faster the rate of decrease of the concentration of the probe (salicylic acid) in solution. However, in an electrochemical setup, the rate of diffusion and migration of the PAH also is an important factor controlling the rate of degradation. Figure 4-4 shows a plot of the rate of degradation of the hydroxyl radical probe, salicylic acid ( $C_0 \sim 20 \text{ mg/L}$ ) using both ultrasound and

electrical energy (AC and DC) at 30 W and 60 W power output. Degradation rates increased with increased power as observed in the naphthalene test cells.

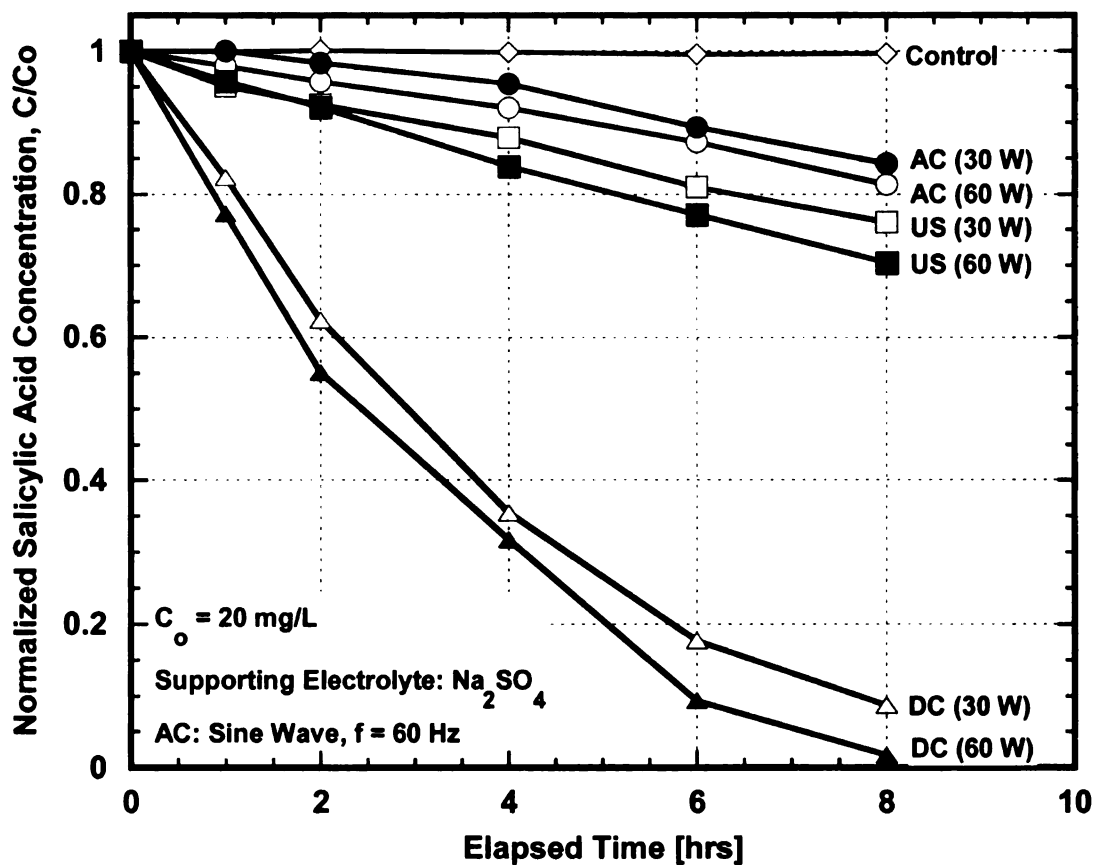


Figure 4-4: Concentration-time profile for both sonochemical and electrical degradation of salicylic acid (OH radical probe) in solution at 30 W and 60 W output power

Figure 4-5 shows the *pseudo*-first-order degradation rate constants for both sonochemical and electrical degradation for applied power of 30 W and 60 W.

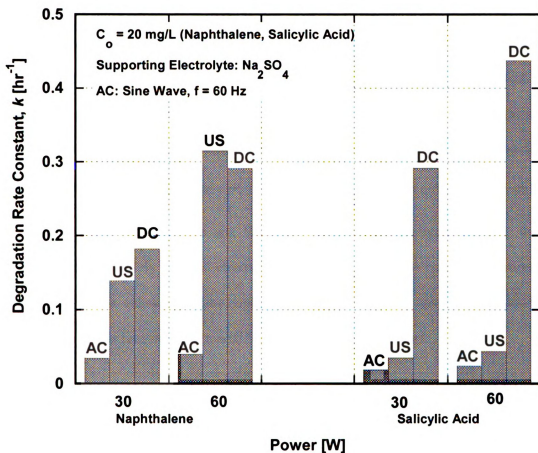


Figure 4-5: Pseudo-first-order degradation rate constants for naphthalene and salicylic acid

The reduced rate of sonochemical degradation of salicylic acid compared with naphthalene may be due to the fact that degradation occurred mainly in the bulk solution by OH radical attack because salicylic acid, being partially polar preferred to stay in solution unlike non-polar naphthalene that migrated into cavitation bubbles and hence was degraded by pyrolysis as well. Also, in general, reaction rates involving OH radicals increase with increasing molecular size based upon a rule of additivity (Westerhoff *et al.* 1999). Therefore naphthalene having eight hydrogen atoms as potential sites that can be substituted by OH radicals tend to exhibit higher degradation rate than salicylic acid with



four potential sites. This suggests that the main degradation mechanism in sonochemical degradation was mediated by OH radicals. However, electrochemical degradation rates of salicylic acid were generally higher compared with naphthalene, suggesting that an alternative degradation mechanism may have contributed to the degradation. Also the rate of movement of the reacting molecules in the electrochemical test cell to the reaction sites (anodes) was enhanced by the partial dissociation of salicylic acid in solution to  $H^+$  and negatively charged salicylate ion. Salicylate ions, being negatively charged, were attracted by the positively charged electrode (anode) and hence, the rate of migration to the reaction site was enhanced unlike naphthalene molecules which have no net charge in solution. Due to this reason, DC showed the highest degradation rates.

#### *Degradation Kinetics*

Park *et al.* (2000) reported that the degradation of PAHs by ultrasonic irradiation in solution was first-order with respect to the PAHs. Zhaobing *et al.* (2005) reported that ultrasonic degradation of 2,4-dinitrophenol fitted a pseudo-first-order degradation kinetics. The degradation of naphthalene as well as salicylic acid in all the test solutions in this study also depicted *pseudo*-first-order degradation kinetics. A plot of  $\ln[C/C_0]$  versus time yielded the observed *pseudo* first-order degradation rate constants ( $k$ ) reported in Figure 4-5.

#### *Degradation Byproducts*

Because both sonochemical and electrical degradation of organics in solution involve the utilization of hydroxyl radicals as the primary oxidizing agent, similar degradation products were observed in all the tests. LC/MS analyses indicated molecular masses that

suggest the formation of degradation products such as naphthol, dihydroxynaphthalene, trihydroxynaphthalene, dihydrotrihydroxynaphthalene, naphthoquinone, hydroxynaphthoquinone, and benzenedicarboxylic acid. The exact isomers formed were not determined. These degradation byproducts formed are relatively more soluble than the parent compound (naphthalene), hence it is expected that they would be more bio-available in solution for subsequent degradation by microorganisms. The change in color of the test solutions to light yellow as the tests (sonochemical and electrochemical) progressed may have been due to the formation of naphthoquinone in the solutions. Formation of quinones is a common observation of the hydroxylation process in oxidizing media (Oturán 2000). The formation of naphthoquinone is consistent with those found by other researchers who also observed aromatic quinones during electrolytic oxidation of aromatic hydrocarbons (Brillas *et al.* 2000; Panizza *et al.* 2000; Saracco *et al.* 2000). GC/MS analysis by Goel *et al.* (2003) indicated the presence of at least one reaction product, 1,4-naphthoquinone when naphthalene solutions were electrolyzed and concluded that naphthalene degradation could be due to direct anodic oxidation, oxidation by an intermediate (e.g. hydroxyl radicals), or a combination of both.

Formation of 2,3-dihydroxybenzoic acid and 2,5-dihydroxybenzoic acid as electrochemical as well as sonochemical degradation products of salicylic acid is consistent with numerous studies indicating that hydroxyl radicals were the primary oxidizing agent.

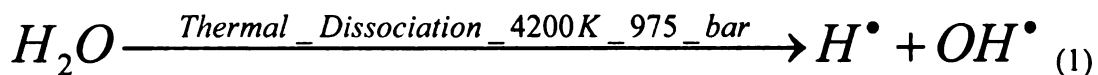
#### *Heat Generation*

Both sonochemical and electrical degradation tests resulted in heat generation. Hence all test solutions were placed in a water bath to maintain the temperature of the test solutions

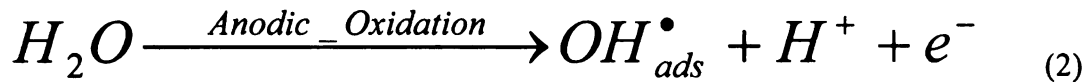
between 19 °C and 25 °C. One major drawback of using ultrasound or electrical energy for potential field scale application is the loss of part of the applied energy as heat. However, no additives are required for the oxidation process unlike chemical methods where additives such as hydrogen peroxide, ozone or ferrous ion are commonly used.

#### *Mechanism for OH Radical Generation*

Ultrasound causes high-energy acoustic cavitation, which consists of formation of microscopic vapor bubbles in the low pressure (rarefied) part of the ultrasonic wave when the low pressure overcome the surface tension of the fluid. The bubbles collapse or implode in the compression part of the wave creating very minute high-energy movements of the solvent that result in localized high shear forces (Meegoda and Veerawat 2002). The implosive collapse of the bubbles in water can cause localized pressures of the order of 975 bars and temperature as high as 4200 K generated over a few microseconds time interval (Lorimer and Mason 1987). Temperatures of over 5,000 K have been reported in the ultrasonic cavitation of organic and polymeric liquids (Flint and Suslick 1991). Under these conditions, water vapor undergoes a thermal dissociation to yield extremely reactive hydrogen and hydroxyl radicals (H• and OH•) (Hung *et al.* 2002).



On the other hand, Comninellis (1994), Brillas *et al.* (2000), and Panizza *et al.* (2000) have reported that DC electrochemical systems generate hydroxyl radicals at the anode due to the oxidation of water:



AC electrochemical systems also generate hydroxyl radicals (Paper No. 3) by anodic oxidation of water molecules at an instantaneous anode. During one half of a cycle when one of the electrodes has a positive electrical potential (instantaneous anode), it instantaneously acts as the anode while the other electrode, at a negative electrical potential (instantaneous cathode), instantaneously acts as the cathode. In the subsequent half cycle, polarities are reversed and the electrodes acquire electrical potentials opposite to what they had in the previous cycle and this continues throughout the period of application of the AC.

#### *Reaction Site*

It is generally believed that there are three potential sites for chemical reactions in ultrasonically irradiated aqueous solutions: (1) the bubble itself; (2) the interface between the bubble, and the surrounding liquid; and (3) the bulk solution. Compounds may degrade directly *via* pyrolytic reactions occurring inside the bubble and/or at the interfacial region or indirectly *via* radical reactions occurring at the interface and/or the solution bulk (Thompson and Doraiswamy 1999). For electrochemical systems, it is generally believed that the reaction site in electrochemical processes is the surface of the electrodes. Chen (2004), Feng and Li (2003), and Stucki *et al.* (1991) have reported that the effectiveness of electrochemical wastewater treatment depends on the nature of the anodes used in the process.

Therefore, in sonochemical degradation, hydroxyl radicals generated in the solution attack target organic contaminants in solution near as well as at a distance from the

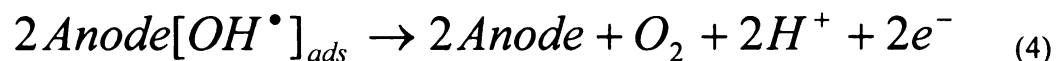
ultrasound probe. In electrical degradation, adsorbed hydroxyl radicals generated on the surface of the electrodes (anode) are responsible for the degradation of organics in solution. As a result, the type of electrode material used and the rate of migration of the chemical specie to the electrode affect the degradation rates and degradation mechanism. Gattrell and Kirk (1993 and Comninellis and Pulgrin (1991) have reported that using platinum as electrodes resulted in the formation of products such as maleic acid and oxalic acid from the anodic degradation of phenol. However, complete mineralization of phenol to CO<sub>2</sub> was achieved by using PbO<sub>2</sub> as an anode (Feng and Li 2003; Iniesta *et al.* 2001; Schumann and Grundler 1998).

### **Reaction Mechanism and Pathway**

Sonochemical degradation of organics in solution generally occurs through two distinct degradation pathways: oxidation by hydroxyl radicals and pyrolytic decomposition (Thompson and Doraiswamy 1999). In electrochemical oxidation, organic compounds in aqueous solutions can be oxidized on an anode (anodic oxidation) by indirect oxygen atom transfer and direct electron transfer (Rodgers *et al.* 1999; Kirk *et al.* 1985). During the indirect oxygen atom transfer, oxygen radicals, especially the hydroxyl radicals generated from water electrolysis, help in the oxidation of organic substances (Iniesta *et al.* 2001; Simond *et al.* 1997; Comninellis 1994; Lee *et al.* 1981). The hydroxyl radicals readily react with the organic molecules adsorbed on or in the vicinity of the anode to cause the reaction presented in Equation 3 (Simond *et al.* 1997).



Meanwhile, the hydroxyl radicals react with each other to form molecular oxygen to complete the electrolysis of water molecules (Li *et al.* 2005; Comninellis 1994) as shown in Equation 4.



Hydroxyl radicals react with organic pollutants in two possible ways presented as follows:

1. by electrophilic addition to a double bond or an aromatic system, and
2. by abstraction of a hydrogen atom from a carbon atom (Schwarzenbach *et al.* 2003).

Based on the identified degradation products, a simplified degradation pathway for the electrochemical degradation of naphthalene in aqueous solution is proposed as illustrated in Figure 4-6.

See Figure 7 for alternative degradation pathway

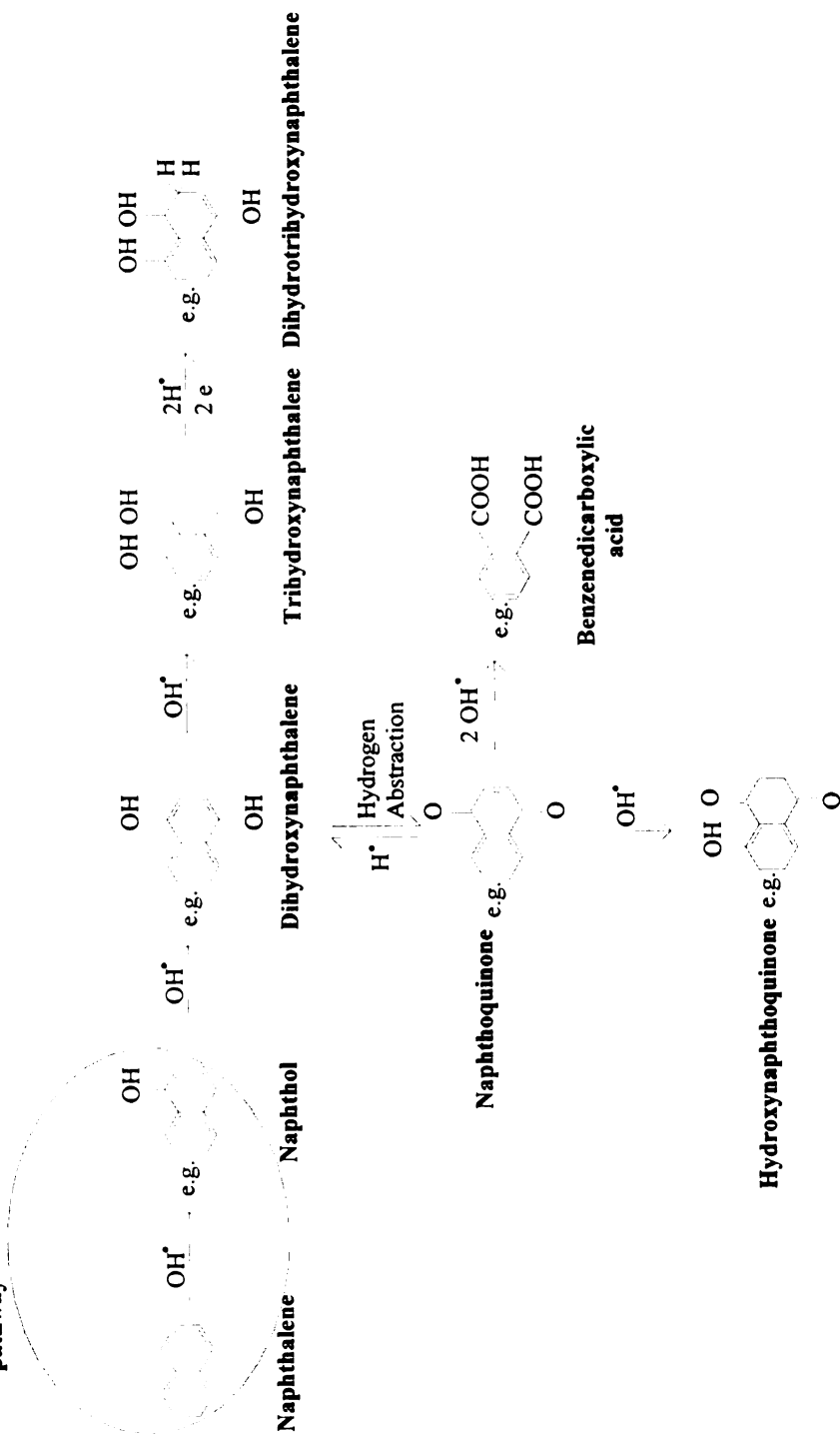
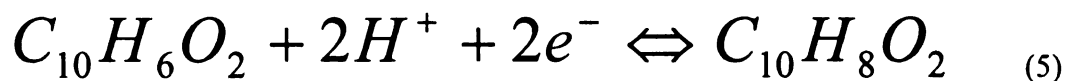


Figure 4-6: Simplified sonochemical and electrochemical degradation pathway of naphthalene in solution with OH radicals as the primary oxidizing agent

The exact isomers formed were not determined. Hence, the presented molecular structures are an example of the possible isomers of each byproduct. Initial hydroxylation of naphthalene by an OH radical resulted in the formation of naphthol. Further hydroxylation resulted in the formation of dihydroxynaphthalene (naphthalenediol), which was further oxidized by hydroxylation to trihydroxynaphthalene, or by hydrogen abstraction to naphthoquinone. It is possible that addition of hydrogen atoms to naphthoquinone may have reduced it back to dihydroxynaphthalene, which is similar to a reaction step reported by previous studies (Chin and Chen 1985). Chin and Cheng (1985) reported that in an undivided cell, benzoquinone produced at the anode was subsequently reduced to hydroquinone at the cathode. Therefore, it is possible that in our setup, the naphthoquinone, produced by the oxidation of naphthalene on an instantaneous anode, was subsequently reduced to dihydroxynaphthalene on a cathode (or instantaneous cathode) as shown in Equation 5.



Therefore naphthoquinone and dihydroxynaphthalene were probably in redox equilibrium. Addition of hydrogen atoms to the trihydroxynaphthalene resulted in the formation of dihydrotrihydroxynaphthalene. Further hydroxylation of the naphthoquinone formed, resulted in the formation of hydroxynaphthoquinone. With sufficient hydroxyl radicals in the reaction medium, ring cleavage in naphthoquinone may have occurred leading to the formation of benzenedicarboxylic acid. Li *et al.* (2005) reported that benzoquinone formed from the oxidation of phenol could be degraded with ring breakage to various carboxylic acids. One of the proposed mechanisms involves the adsorption of benzoquinone onto the anode surface, which gives up an electron, and the carbon that is



double-bonded with oxygen is attacked by a neighboring hydroxyl radical. When this process is repeated at the *para* position, the ring could be opened and benzoquinone would be broken down into small organic molecules such as carboxylic acids (Comninellis 1994; Lee *et al.* 1981). The present experimental finding is consistent with the proposed mechanism because both naphthoquinone and benzenedicarboxylic acid (from probable ring cleavage of naphthoquinone) were identified as intermediate byproducts. The possible mineralization of naphthalene was not investigated in this study.

In the direct electron transfer process, organics are adsorbed on the anode surface and give up electrons to the anode as presented in Equation 6.



Naphthalene may undergo direct anodic oxidation to form a naphthalene radical cation that can act as a precursor for the formation of hydroxylated species such as naphthol as illustrated in Figure 4-7.

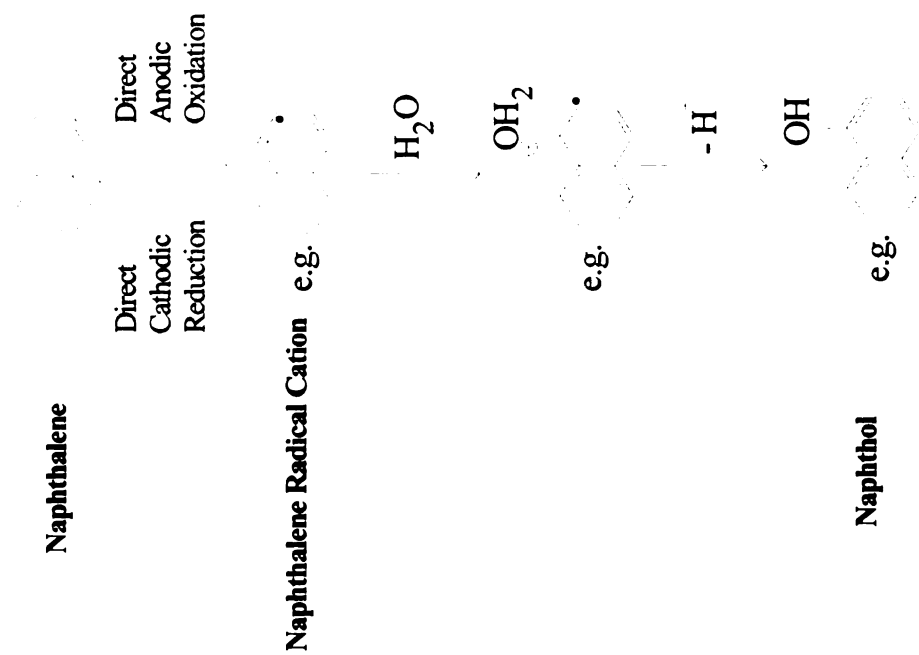


Figure 4-7: Simplified alternative electrochemical degradation pathway of naphthalene in solution to naphthol with radical cation precursor.

The naphthalene radical cation may also undergo cathodic reduction in AC electrolysis, when electrode polarities are reversed from positive to negative, and reform back to naphthalene. This probably accounted for the slow reaction kinetics encountered in the AC test cells (Figures 4-3 & 4-4). Also, continuous bubbling of gases was observed on the electrodes in the DC test cells but no continuous bubbling of gases was observed in the AC test cell except few bubbles that were stagnant on the electrode surface. Therefore according to Equation 4, if the formation of hydroxyl radicals are precursors for formation of molecular oxygen to complete the electrolysis of water molecules, then it is also possible that less hydroxyl radicals were produced at the electrodes as a result of polarity reversal in the AC test cells unlike the DC test cells in which continuous production of OH radicals at the anode efficiently produced more for faster rate of oxidation of naphthalene or salicylic acid.

#### **Modeled *versus* Measured Concentrations of Naphthalene**

It is generally believed that electrochemical reactions occur mainly on the surface or in the vicinity of the electrodes. Therefore, the rate of reaction of the organic reactants in the test cell depends on the rate of generation of OH radicals at the electrodes as the oxidizing agents, as well as the rate at which the reacting molecules move to the electrodes for subsequent oxidation by the OH radicals. Mass transfer in solution occurs by diffusion, migration and convection. Diffusion and migration result from a gradient in electrochemical potential and convection results from imbalance of forces on the solution when the solution is mixed or stirred (Bard and Faulkner 2001). Assuming a linear mass transfer, and linear electric field, the mass flux to the electrode can be expressed by the *Nernst-Planck Equation* (Equation 7):

$$J(x) = -D \frac{\partial C(x)}{\partial x} - \frac{zF}{RT} DC \frac{\Delta E}{l} + Cv(x) \quad (7)$$

where  $J$  is the mass flux,  $D$  is the diffusion coefficient of the reacting specie in solution,  $C$  is the instantaneous concentration of the reactants in solution at time  $t$ ,  $x$  is the distance in the  $x$  direction or along the direction of the electrical current,  $z$  is the net charge on the reacting species,  $F$  is Faraday's constant,  $R$  is molar gas constant,  $T$  is temperature (K),  $\Delta E/l$  is the gradient arising from the change in potential  $\Delta E$  over a distance  $l$ , and  $v$  is the linear velocity of the solution. Because the test cell solutions were not stirred, the third term in Equation 7 can be neglected and hence Equation 7 becomes:

$$J(x) = -D \frac{\partial C(x)}{\partial x} - \frac{zF}{RT} DC \frac{\Delta E}{l} \quad (8)$$

For uncharged reactant, the second term in Equation 8 can be neglected to yield *Fick's* first law as follows:

$$J(x) = -D \frac{\partial C(x)}{\partial x} \quad (9)$$

Equation 9 was applied to model the rate of mass transfer of naphthalene to the electrodes in the DC setup. The following assumptions were made when applying Equation 7 (or Equation 8) to simulate the naphthalene concentrations:

1. Reactants (naphthalene) are instantaneously converted to products when they come into contact with the electrode. Hence,  $C(t)$  at the surface of electrode is equal to zero for  $t \geq 0$ . This establishes a concentration gradient that drives reactants by diffusion to the surface of the electrodes and this condition is

considered as the maximum concentration gradient that may be established in a given time step;

2. Steady-state diffusion conditions exist in a given time step which was assumed equal to 1 hr;
3. Linear mass transfer exists in the given time step of 1 hr; and
4. Linear electric field exists in the given time step of 1 hr.

Equation 9 was applied with  $C$  of naphthalene equal to  $C_0$  ( $\sim 20$  mg/L) for  $t = 0$  at the cathode and  $C = 0$  for  $t \geq 0$  at the anode. Assuming a time step equal to 0.1 hr, the  $C$  of naphthalene at cathode was estimated by subtracting the mass of naphthalene that moved to the anode for degradation during the previous time step. This computation was carried out for the test duration of 8 hours and the modeled normalized concentrations were compared (Figure 4-8) to the test results for DC tests carried out at constant power output of 30 W and 60 W respectively.

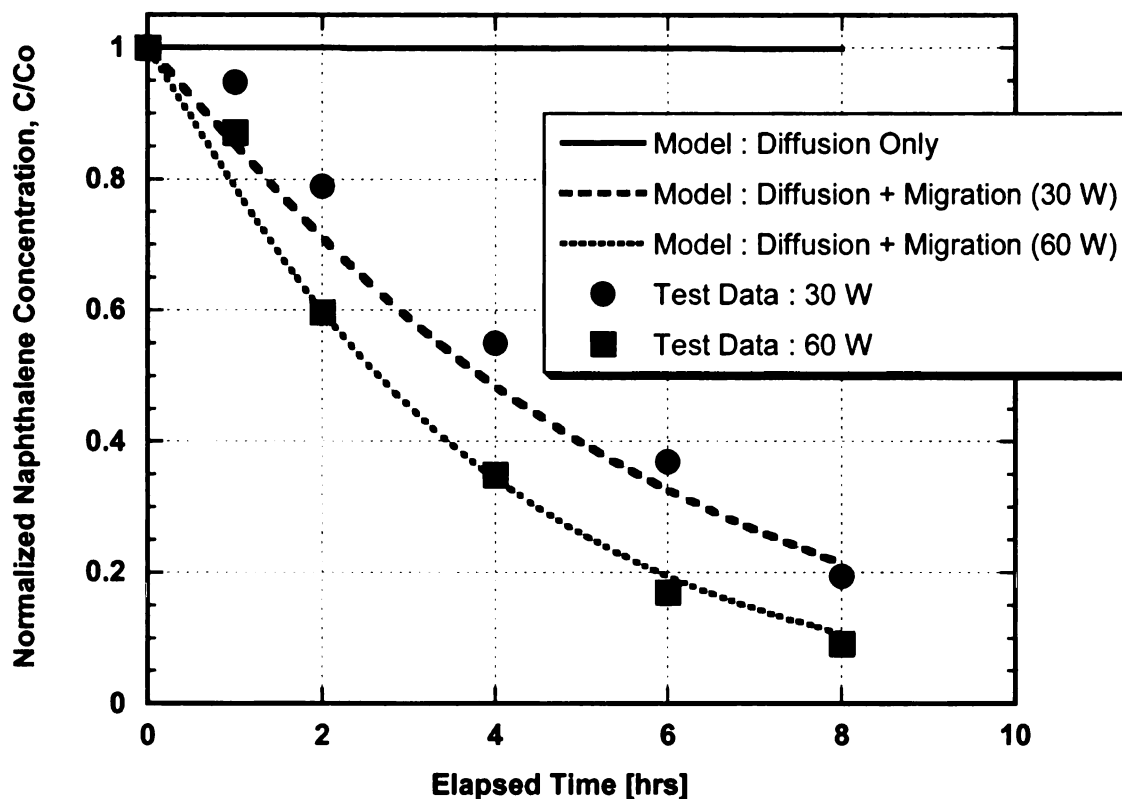


Figure 4-8: Simulated concentrations *versus* test data for naphthalene tests using DC

Schwarzenbach *et al.* (2003) reported diffusion coefficients of organic solutes equal to about  $3.0 \times 10^{-5} \text{ cm}^2 \text{ s}^{-1}$  for small molecules to  $5.0 \times 10^{-6} \text{ cm}^2 \text{ s}^{-1}$  for those of molar mass near 300 g/mol. Based on this data, the diffusion coefficient of naphthalene was estimated as  $9.0 \times 10^{-6} \text{ cm}^2 \text{ s}^{-1}$  from the diffusion coefficients *vs.* molar mass chart presented by Schwarzenbach *et al.* (2003). Equation 9 was applied to simulate only diffusion driven mass flux of naphthalene to the anode for oxidation. The simulated normalized concentration is presented in Figure 4-8. The simulated degradation rate as a result of naphthalene migration to anode only due to diffusion is orders of magnitude less than that observed during the experiments run at constant DC power output of 30 W and

60 W with  $\text{Na}_2\text{SO}_4$  as the supporting electrolyte. When both diffusion and migration are used for simulating the mass flux of naphthalene to the anode by using Equation 8, the simulated normalized concentrations are presented in Figure 4-8 when the net charge,  $z$ , was assumed equal to -0.2 for naphthalene.

For neutral molecules such as naphthalene,  $z$  should be equal to zero. However, it is hypothesized that the presence of anions in the test solution (from the supporting electrolyte) impart an effective negative charge on the naphthalene molecules. These anions dragged the naphthalene molecules along as they migrated to the positively charged electrode (anode), where anodic oxidation resulted in the degradation of the naphthalene molecules. Therefore, the naphthalene molecules moved in the solution as a result of migration simulated by the second term in Equation 7. The rate of migration of naphthalene molecules towards the anode is enhanced by assigning a negative value to  $z$  for naphthalene. By assigning the naphthalene molecule an effective partial negative charge of -0.2, the simulated normalized concentrations versus time data fits well with that for the experimental data when  $\text{Na}_2\text{SO}_4$  was used as the supporting electrolyte for DC power output of 30 W and 60 W.

The simulated degradation rate as a result of salicylic acid migration to anode only due to diffusion is orders of magnitude less than that observed during the experiments run at constant DC power output of 30 W and 60 W with  $\text{Na}_2\text{SO}_4$  as the supporting electrolyte. When both diffusion and migration are used for simulating the mass flux of naphthalene to the anode by using Equation 8, the simulated normalized concentrations

are presented in Figure 4-9 when the net charge,  $z$ , was assumed equal to  $-0.35$  for salicylic.

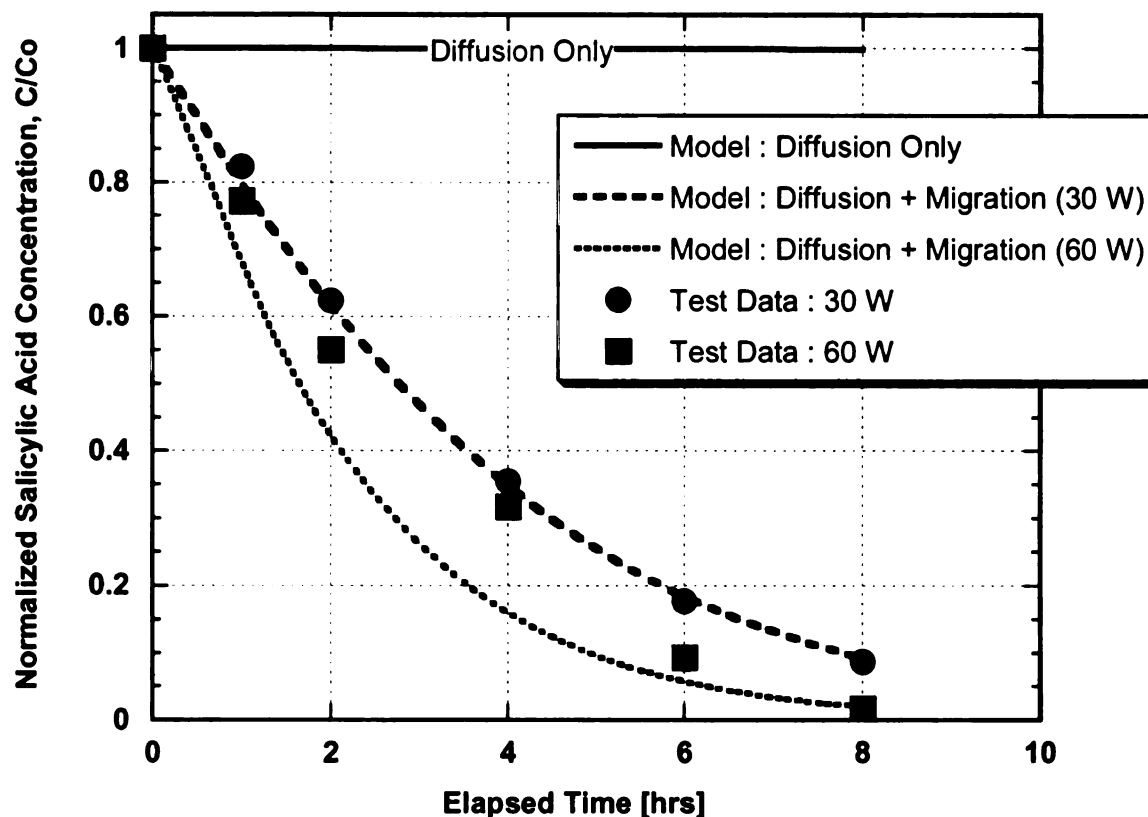


Figure 4-9: Simulated concentrations *versus* test data for salicylic acid tests using DC

Salicylic acid dissociates partially in solution for form the salicylate anion and  $H^+$ , hence it was expected that its apparent effective charge in the test solution would be greater than naphthalene which is a neutral molecule as depicted by the model.

The rate of anodic oxidation of naphthalene (or salicylic acid) depends not only on the rate of migration of reacting molecules to the reaction site (the anode or instantaneous anode) but also on the rate of production of OH radicals at the anode (or instantaneous anode). Hence, as the current density is decreased, it may decrease the rate of production



of OH radicals at the anode and may become the rate limiting step. When Equation 8 is applied, the rate limiting step assumed is the rate of mass transfer to the anode (by diffusion and migration). Hence, Equation 8 would overestimate the decrease in the concentration at a given time,  $t$  of the reactant when current density is low enough not to degrade all naphthalene mass diffusing and migrating to the anode (or instantaneous anode). At higher current densities, the predictions from Equation 8 would be more accurate. It is beyond the scope of this study to estimate the rate of hydroxyl radical production as a function of current density and other variables. Hence, it is not possible to calculate analytically at what current densities the assumptions are valid when Equation 8 is applied.

While Equation 8 is for DC and cannot be applied for an AC, it can be used to explain the reduced rate of degradation when AC was applied. Proposed reasons for the decrease in degradation rates using AC are as follows:

1. By assuming that the naphthalene molecules had an effective partial negative charge of say  $z = -0.2$  under our experimental conditions based on the acceptable fit for DC data, increasing the frequency of the AC resulted in back-and-forth movement of the reacting molecules, and hence the net mass flux of the molecules toward the electrodes was reduced. If the net distance traveled by the naphthalene molecules to get to an instantaneous anode,  $L$ , in Equation 8, is varied, until the modeled values of concentrations fit with the experimental data the values of  $L$  obtained is 40 cm compared to the electrode spacing of 8 cm. Assuming degradation rate at the electrodes are the same for each frequency, it can be hypothesized that AC frequency results in taking longer duration for a

naphthalene molecule(s) to reach the instantaneous anode. This may be due to the back and forth movement of the molecule due to the reversal in the direction of the current.

2. Continuous bubbling of gases at both electrodes (probably O<sub>2</sub> and H<sub>2</sub>) in the test solution was observed as the tests progressed. However, no gas bubbles were visible at an AC frequency of 60 Hz. Simond *et al.* (1997) and Comninellis (1994) reported that the hydroxyl radicals, formed on an anode react with each other to form oxygen gas at the anode to complete the electrolysis of water molecules. Stock and Bunce (2002) reported that hydrogen radicals formed on a cathode react with each other to produce hydrogen gas at the cathode. If the formation of OH radicals and hydrogen radicals are precursors for the generation of oxygen gas and hydrogen gas at the anode and cathode, respectively, then it is likely that the rate of gas bubbling at the electrode gives an indication of the rate of formation of these radicals at the electrodes. The higher the rate of the observed bubbling of the gas(es), the greater the rate of hydroxyl or hydrogen radical formation at the electrodes. Hence, based on the visual observation of gas bubbles, it is likely that the AC frequency resulted in decrease in the rate of formation of hydroxyl radicals at the electrodes. This impacted the rate of oxidization of naphthalene at the instantaneous anodes.
3. Competing anodic reactions (oxidation) and cathodic reactions (reduction) at the same reaction sites (on the surface of the electrodes) may have been responsible for the decrease in the oxidation rate of both naphthalene (Figure 4-5) and salicylic acid (Figure 4-7) as the AC frequency was increased. However, in DC

electrolysis, oxidation reactions occurred at the anode only and reduction reactions occurred at the cathode only and hence there was no competing anodic oxidation and cathodic reduction at the same reaction site. Therefore DC was more effective in degrading naphthalene or salicylic acid in the test cells.

Table 4-2 summarizes the measured initial and final values of the experimental parameters.

Table 4-2: Summary of Measured Parameters

Compound	Energy	Power [W]	Temperature (°C)		pH		Standard redox potential (mV)		Dissolved oxygen concentration (mg/L)		Electrical conductivity ( $\mu\text{S}/\text{cm}$ )	
			Initial	Final	Initial	Final	Initial	Final	Initial	Final	Initial	Final
Naphthalene	Electrical (AC)	60	19.6	24.8	6.7	3.6	443	393	3.8	9.6	806	820
Naphthalene	Electrical (AC)	30	19.6	24.8	6.7	4.2	443	419	3.8	6.0	806	812
Salicylic Acid	Electrical (AC)	60	20.6	23.0	3.9	3.8	448	391	8.5	12.3	887	862
Salicylic Acid	Electrical (AC)	30	20.6	24.9	3.9	3.8	478	451	8.5	9.7	880	848
Naphthalene	Electrical (DC)	60	20.0	24.9	6.8	10.2	458	234	3.8	13.8	816	857
Naphthalene	Electrical (DC)	30	19.7	21.8	6.7	10.4	450	272	3.8	7.6	777	795
Salicylic Acid	Electrical (DC)	60	18.6	24.9	3.8	10.8	462	237	7.9	13.3	860	940
Salicylic Acid	Electrical (DC)	30	19.7	23.1	3.9	10.2	476	389	8.4	7.9	856	820
Naphthalene	Ultrasound	60	20.0	24.0	6.8	4.3	421	472	3.9	4.9	808	820
Naphthalene	Ultrasound	30	20.0	23.0	6.8	4.5	431	423	3.8	4.4	811	827

Table 4-2 Cont'd

Salicylic Acid	Ultrasound	60	20.0	25.0	4.0	3.9	475	478	8.4	7.2	860	869
Salicylic Acid	Ultrasound	30	20.0	23.0	4.0	3.9	469	464	8.4	7.6	856	882
Naphthalene	-	Control	19.9	19.6	6.7	6.7	458	469	3.8	6.3	811	815
Salicylic Acid	-	Control	20.9	19.6	4.0	4.0	558	537	8.6	8.7	860	857

## SUMMARY AND CONCLUSIONS

The key objective of this study was to compare the rate of degradation of PAHs in aqueous solution using ultrasound energy and electrical energy (AC and DC) delivered at the same output power. Tests were conducted at 60 W and 30 W output powers. Naphthalene, which contains two fused benzene rings, was selected as a model PAH compound. Salicylic acid was used as a hydroxyl radical probe. The key conclusions of this study are as follows.

- Both ultrasound and electrical (AC and DC) energies are capable of oxidizing naphthalene as well as salicylic acid in solution.
- DC, at a given power output, degraded naphthalene at a rate faster than a sine wave AC having a frequency equal to 60 Hz, at an equivalent output power. However, both DC and ultrasound exhibited comparable degradation rates for naphthalene but DC exhibited a faster degradation rate than ultrasound when salicylic acid was used. This was attributed to the formation of negatively charged salicylate ion in solution which was attracted by the positively charged electrode (anode) and hence the rate of migration of the reacting molecules to the reaction site (surface of anode) was enhanced. AC showed the least degradation rate possibly due to decrease in the migration of the PAH to the electrode due to the constant reversal of the direction of the current. It is also possible that the rate of hydroxyl radical formation for AC was less than an equivalent DC.
- The higher the output power, the greater the degradation rate of naphthalene or salicylic acid in solution which is due to a greater rate of formation of hydroxyl radicals

- DC, AC and ultrasound, all depicted *pseudo*-first-order degradation kinetics with respect to naphthalene or salicylic acid in solution.
- Formation of 2,3-dihydroxybenzoic acid and 2,5-dihydroxybenzoic from the oxidation of salicylic acid is consistent with reported findings that hydroxyl radicals were the primary oxidizing agents in both sonochemical and electrochemical degradation.
- The rate of anodic oxidation of naphthalene depends on the rate of production of OH radicals at the anode (or instantaneous anode) as oxidizing agents as well as the rate of migration of reacting molecules to the reaction site (the anode or instantaneous anode). At higher power output, not only more OH radicals are produced at the anode but also the rate of migration of the reacting molecules to the anode (or instantaneous anode) increases during a DC application. However, when AC is used, the change in the direction of the current decreases the rate of migration of the reactant to the instantaneous anode.
- Naphthalene molecules in solution exhibited an “effective” partial negative charge due to the presence of the supporting electrolyte subjected to electrical gradients.

## **PAPER NO. 5: DEGRADATION OF NAPHTHALENE IN THE AQUEOUS PHASE OF SPIKED SATURATED OTTAWA SAND**

### **ABSTRACT**

The objectives of this study were to assess degradation of naphthalene in the aqueous phase of spiked Ottawa sand and to explore the effect of AC frequency and current density on degradation rates. AC having sine wave shape and frequencies equal to 0.1 Hz and 60 Hz as well as square wave AC at 0.1 Hz were used for the tests. The peak AC current densities were 3 mA/cm<sup>2</sup>, 6 mA/cm<sup>2</sup>, and 10 mA/cm<sup>2</sup>. Direct current (DC) was applied in a separate test at current density equal to 3 mA/cm<sup>2</sup>. The key conclusions of this study are: (1) both DC and sine and square AC can degrade naphthalene or PAHs in the aqueous phase of spiked sand; (2) the rates of degradation of naphthalene in the aqueous phase when sand was also present was less than the degradation rate at an equivalent current density when only the aqueous solution (without the sand) was subjected to electrochemical degradation; (3) increase in the peak density of AC resulted in an increase in the degradation rates due to greater rate of formation of the hydroxyl radicals which are primarily responsible for the PAH degradation; and (4) an increase in the AC frequency resulted in a decrease in the degradation rate due to slower rates of migration of the PAH to the electrodes due to periodic reversal in the direction of the current.



## INTRODUCTION

Much of the practical work on electroremediation on soils has been undertaken in the laboratory on spiked synthetic soils (Page and Page 2002). Direct current (DC) is mostly used in studies involving electroremediation of soils. Current densities applied have been in the range 0.025 to 5 A/m<sup>2</sup> (Acar *et al.* 1991; Hamed *et al.* 1991). Initially, electroremediation was applied to remove salts or alkalis from soils (Puri and Anand 1936; Gibbs 1966; Vadyinina 1968). Its application to the removal of heavy metals was first attempted in the early 1980s (Hamnett 1980; Segall *et al.* 1980; Agard 1981). Successful transport of a large number of heavy metals through soils by electric fields with subsequent removal onto an electrode or into the solution surrounding the electrode (catholyte or anolyte) has since then been demonstrated in several laboratory studies (Page and Page 2002). The metals are usually present as cations and are therefore transported mainly by electromigration toward the cathode. However, certain elements, e.g. Cr and As, may be present as oxy-anions and are therefore transported to the anode (Banerjee 1987; Lindgren *et al.* 1994; Pamakcu, and Wittle 1994). Reddy and Saichek (2004) conducted laboratory investigation to determine contaminant mass removal from low permeability clay, by using periodic DC voltage application and surfactants. The results showed that considerable contaminant removal can be achieved by employing a voltage gradient of 2.0 V (DC)/cm, along with a periodic mode of voltage application.

PAHs have been found in at least 600 of the 1,430 National Priorities List (NPL) sites identified by the United States Environmental Protection Agency (USEPA) (ASTDR 1995) and are classified as potential carcinogens. For molecular substances, electro-osmosis is the predominant form of transport under an electric field, although

partial dissociation into ions of some organic molecules will result in electromigration as well (Page and Page 2002). Lageman *et al.* (1990) has demonstrated that the removal of a range of aromatic organic compounds from soils was feasible.

Most studies on the electroremediation of organic compounds have focused on using DC to transport them by electromigration and/or electroosmosis with subsequent removal onto electrodes or into solutions surrounding the electrodes (catholyte or anolyte). The objective of this study, was to use alternating current (AC) to assess the degradation of a PAH (naphthalene) in a clean poorly graded sand spiked with spiked naphthalene solution Naphthalene was used as the model PAH compound because it has relatively high solubility in water ( ~ 30 mg/L) as compared to other higher order PAHs. Clean Ottawa sand was selected as the porous media because it would not significantly sorb naphthalene from the spiked solution used for saturating the sand.

## **MATERIALS AND EXPERIMENTAL METHODOLOGY**

The experimental setup is illustrated in Figure 5-1 and the setup components are described below.

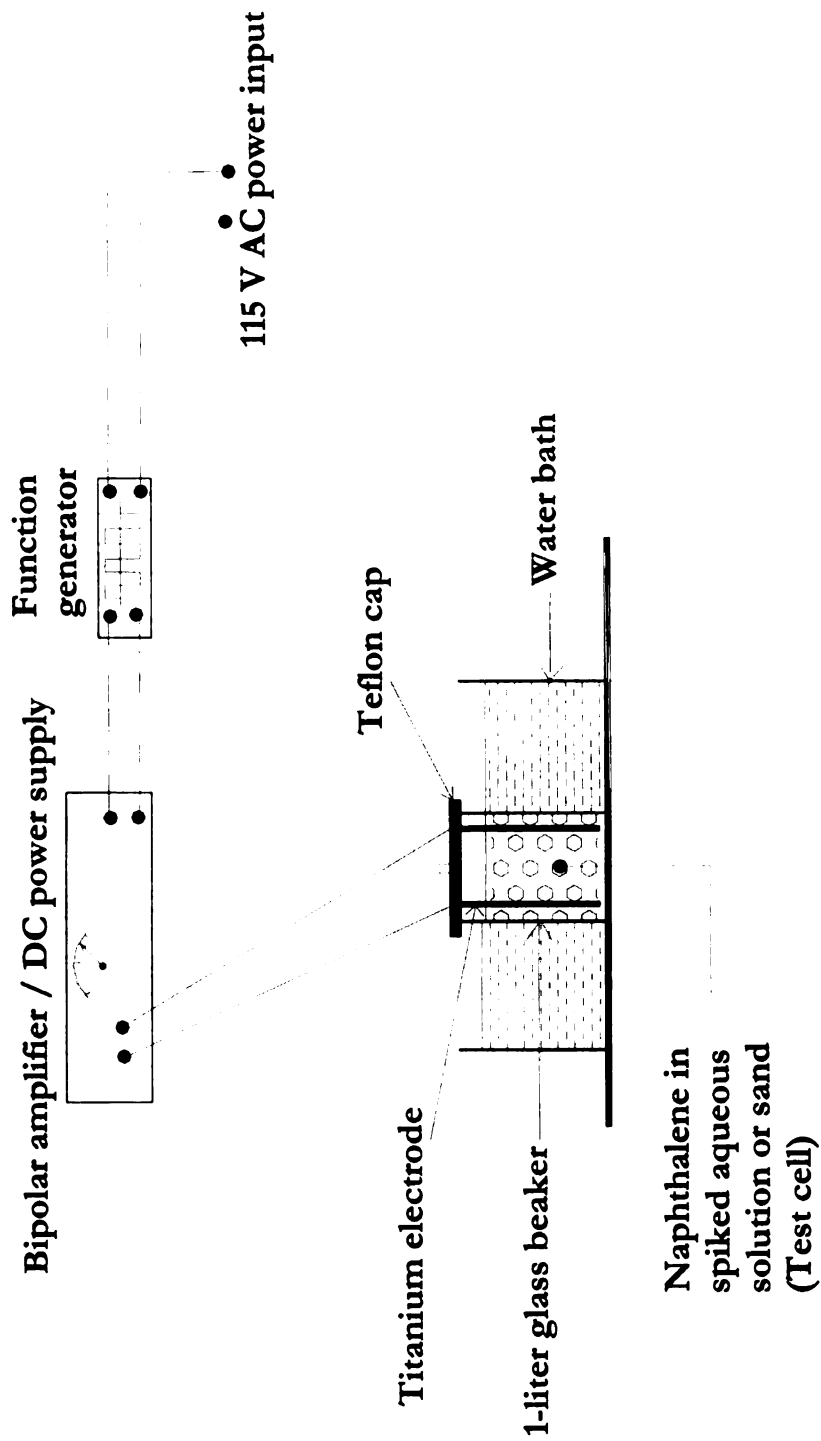


Figure 5-1: Schematic of the experimental setup.

### **Reaction Chamber**

The test cell setup consisted of a 1 liter Pyrex glass beaker with a Teflon cap. These materials of the cell were selected to eliminate or reduce sorption of the contaminants onto the walls of the reaction vessel and the cap. Titanium plates were used as electrodes in electrochemical tests of this study. Alshawabkeh and Sarahney (2005), Li *et al.* (2005), and Goel *et al.* (2003) have used titanium as a base metal and coated it with mixed metal oxides such as RuO<sub>2</sub>, IrO<sub>2</sub>, and SnO<sub>2</sub>. The titanium plates used in this study were not coated. Uncoated titanium being cheaper than commonly used electrodes such as platinum, or titanium coated electrodes, was selected for this project. Also, titanium offers resistance to corrosion in a wide range of aggressive conditions. The titanium sheets used as electrodes in this study were 12.0-cm-long by 5.0-cm-wide by 1.72-mm-thick and the distance between them was maintained equal to 8.0 cm. The purity of the titanium was about 99%.

### **Electrical Equipment**

A 0.1 Hz to 2 MHz Sweep Function Generator was used to generate the AC signals. The power supply consisted of a bipolar operational power supply/amplifier capable of producing up to 200 V AC/DC and 1 A AC/DC output or a maximum electrical power of 200 W. Voltage and current measurements were obtained with the aid of an oscilloscope with accessories.

### **Spiked Sand**

Aqueous solutions, spiked with naphthalene were prepared by adding naphthalene (98%, purity) crystals to one-liter of deionized (DI) water in a capped Pyrex bottle and allowing

the suspension to stand for up to three days. This was followed by the addition of 0.5 g of anhydrous sodium sulfate ( $\text{Na}_2\text{SO}_4$ ) to each suspension, to increase its electrical conductivity. Sodium sulfate was selected as the supporting electrolyte because all aqueous solution tests without sand were carried out using  $\text{Na}_2\text{SO}_4$  as the supporting electrolyte. The target concentration of  $\text{Na}_2\text{SO}_4$  was approximately 500 mg/L (~3.5 mM). This concentration was selected to meet the USEPA's maximum contaminant level goal for sulfate equal to 500 mg/L (~3.5 mM). The resulting spiked aqueous solution was added to 1,000  $\text{cm}^3$  of dry Ottawa sand placed in a 1-liter glass beaker until the sand was fully saturated. It was assumed that saturation was attained when a thin film of the spiked solution formed on the surface of the sand in the glass beaker.

### **Testing Procedure**

Tests were conducted in batch mode in 1-liter undivided cells. Prior to applying AC to the cells, initial samples were collected for high performance liquid chromatography (HPLC) analyses. For each sampling event, three aqueous samples were collected, one from the middle of the test cell and one each close to the surface of the electrodes, with the aid of a glass syringe and needle. During the tests, samples were collected for HPLC analyses at elapsed time intervals of 0, 1, 2, 4, 8, 24, and 48 hours. The samples were analyzed directly without extracting the naphthalene from the aqueous solution. HPLC analyses were performed using a diode array detector (detection at 255 nm), a Waters C-18 PAH, 250 mm x 4.6 mm x 5  $\mu\text{m}$  column, an automated gradient controller, and deionized water (DI)/acetonitrile mobile phase. The flow rate of the mobile phase was 1.2 mL/min and the column was flushed with 10:90 (v/v) acetonitrile/DI water for 5 minutes

followed by 60:40 (v/v) acetonitrile / DI water for 10 minutes and by 100:0 (v/v) acetonitrile / DI water for 5 minutes. This gradient was used for the analysis in order to obtain appropriate separation of the degradation product peaks on the chromatograms during the tests. Standard solutions were prepared to bracket the expected concentration level of the analytes. Calibration curves with an average obtained  $R^2$  value of 0.998 were used to determine the concentration of naphthalene in the solutions as the tests progressed.

## RESULTS AND DISCUSSION

### Comparison of Degradation Rates

Table 5-1 shows the experimental variables.

Table 5-1: Experimental Variables

Medium	AC Wave Form	AC Peak Current Density [mA/cm <sup>2</sup> ]	AC Frequency [Hz]	No. of Tests
Solution	Square	3	0.1	2
Sand	Square	3	0.1	1
Sand	Sine	6	0.1	1
Sand	Sine	6	60	1
Sand	Sine	10	60	1
Sand	DC	3	0	1
Sand	Control	0	0	1
Solution	Control	0	0	2
			<b>Total No. of Test</b>	<b>11</b>

Figure 5-2 shows a comparison of the degradation of naphthalene in spiked aqueous solution and with and without Ottawa sand using square wave AC. The peak current density and frequency were equal to  $3 \text{ mA/cm}^2$  and  $0.1 \text{ Hz}$ , respectively.

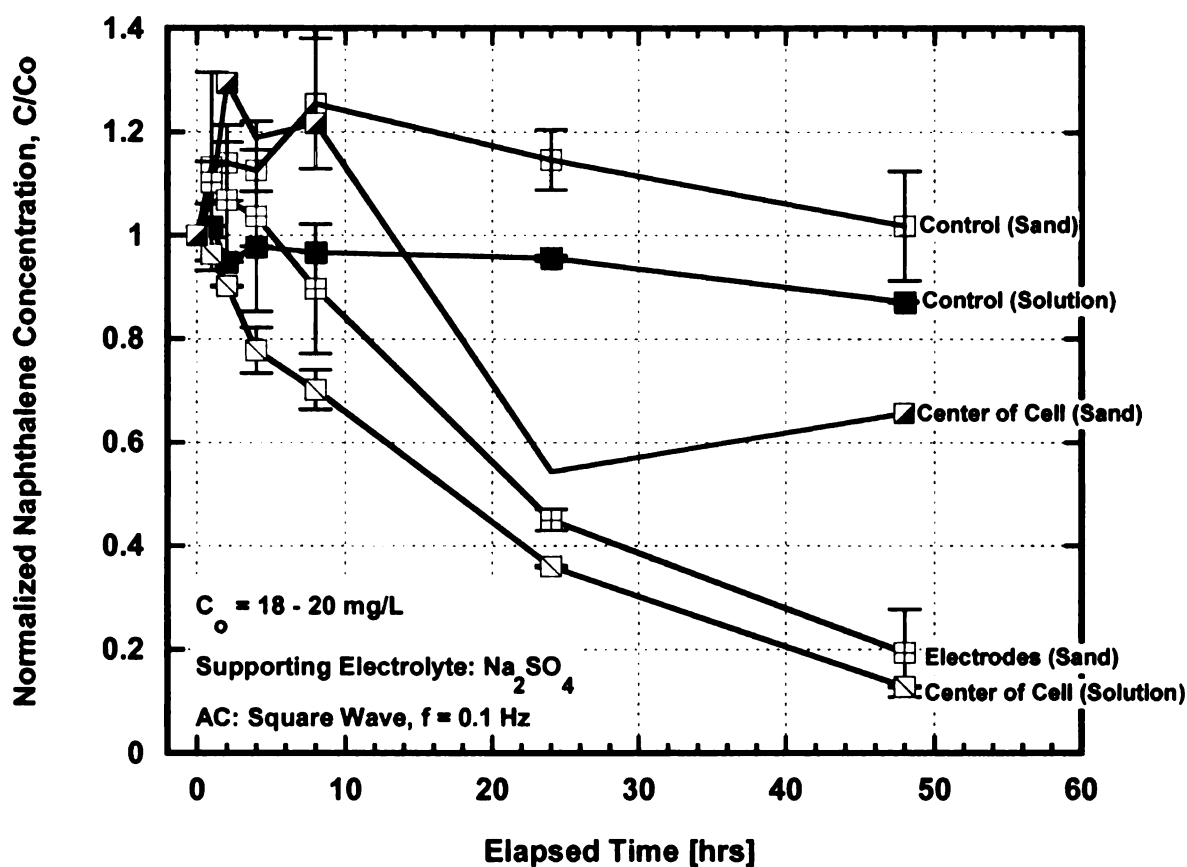


Figure 5-2: Comparison of electrochemical degradation of naphthalene in spiked solution with and without sand using AC.

The control tests were carried out without the passage of AC or DC while the rest of the experimental setup was similar to other tests where AC or DC was passed. In addition, the control cell for sand was placed in a static temperature chamber at  $44 \text{ }^\circ\text{C}$  to simulate a conservative scenario of heating. When AC or DC was applied, while the

water bath kept the temperature rise to a minimum, it reached 32.9 °C when DC was applied for the cell containing sand. For other tests, the temperature was less than 21 °C. DC test produced higher temperature because the DC resistance of the system was greater than the impedance when AC was applied. Hence, greater electrical power was utilized in the DC cell for a fixed current.

Aqueous phase samples collected close to the surface of the electrodes generally exhibited faster degradation rate than samples collected from the center of the cell when sand was present. This result is consistent with the general belief that electrochemical reactions occur on the surface or in the vicinity of the electrodes. Samples collected in the vicinity of both electrodes showed significant degradation. Pepprah and Khire (2008) reported that in AC electrolysis, constant polarity reversal of the electrodes ensures that both electrodes participate in the anodic oxidation process. By applying an AC, which resulted in constant polarity reversal of the electrodes at a rate dependent upon the AC frequency, anodic oxidation of naphthalene in solution occurred on both electrodes. Previous studies on electrochemical degradation have focused on the use of DC where the cathode acts as a “passive” electrode in the oxidation process. However, when an AC is used, the constant polarity reversal creates anodic oxidation reactions on both electrodes alternately, depending on their polarity in a given AC cycle. During half cycle when one of the electrodes has a positive electrical potential, it instantaneously acts as the anode (instantaneous anode) while the other electrode, at a negative electrical potential acts instantaneously acts as the cathode (instantaneous cathode). In the subsequent half cycle, polarities are reversed and the electrodes acquire electrical potentials opposite to



what they had in the previous cycle and this continues throughout the period of application of the AC.

As shown in Figure 5-2, the control cell samples did not indicate significant reduction in concentration during the 48-hr testing period.

Figure 5-3 shows a comparison of the normalized naphthalene concentration samples with and without sand subjected to DC having current density equal to  $3 \text{ mA/cm}^2$ .

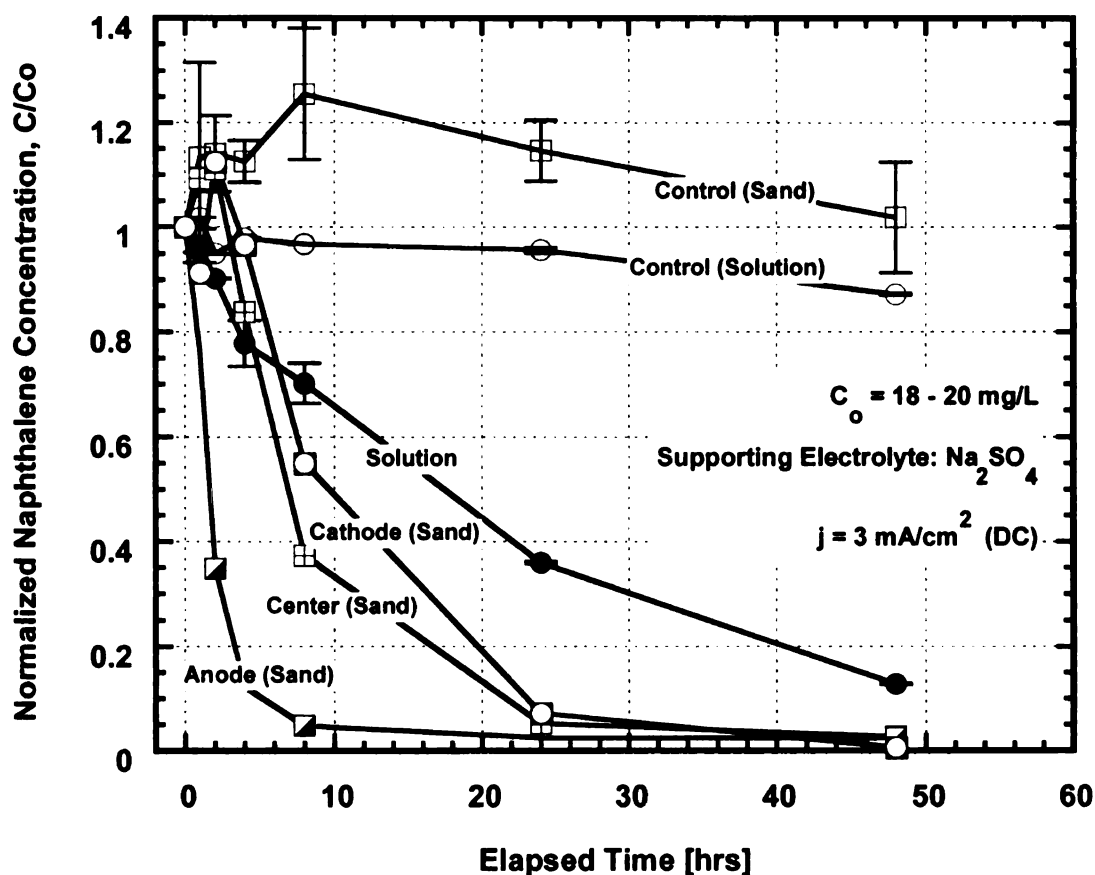


Figure 5-3: Comparison of electrochemical degradation of naphthalene in spiked solution and sand using DC

Aqueous phase samples collected in the vicinity of the anode of the cell with sand exhibited faster degradation of naphthalene, comparable to samples collected from the

middle of the test cell in the aqueous solution tests. Samples collected in the vicinity of the cathode did not showed less degradation because in DC electrolysis, anodic oxidation occurs only on one electrode (the anode). Hence, unlike in an AC test, the cathode in DC test does not participate in the oxidation of the organics in the aqueous phase.

### Comparison of Degradation Rates in Spiked Sand Using AC and DC

Figure 5-4 shows the normalized concentration of naphthalene for cells containing the sand where AC and DC having current densities equal to  $3 \text{ mA/cm}^2$  were passed.

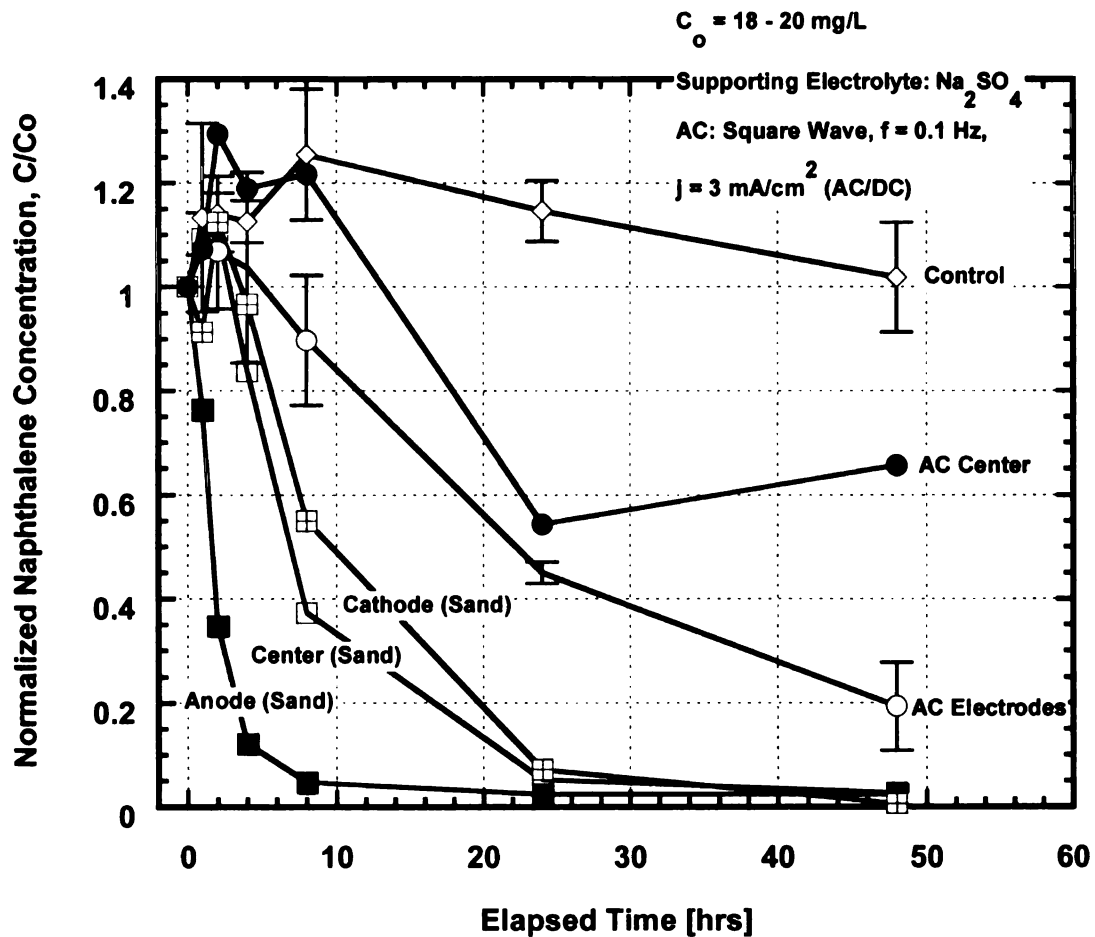


Figure 5-4: Comparison of electrochemical degradation of naphthalene in spiked sand using AC and DC

Samples collected from the vicinity of both the electrodes in the AC tests exhibited degradation. However, samples collected from the vicinity of the anode showed much faster degradation than those collected in the vicinity of the cathode in the DC test. Based on the observed concentration profile, it is likely that anodic oxidation occurred only at the anode, and as naphthalene was being oxidized, more molecules moved from the center of the cell as well as in the vicinity of the cathode, towards the anode where they were subsequently oxidized. Table 5-2 shows that samples collected at the end of the test indicated acidic/oxidizing conditions at the anode and alkaline/reducing conditions at the cathode.

Table 5-2: Measured initial and final values of temperature, pH, standard redox potential, and electrical conductivity of test cells

Medium	AC Wave Form	AC Peak Current Density [mA/cm <sup>2</sup> ]	AC Frequency [Hz]	Temperature (°C)		pH		Standard redox potential (mV)		Electrical conductivity (μS/cm)	
				Initial	Final	Initial	Final	Initial	Final	Initial	Final
Solution	Square	3	0.1	19.2 (C)	18.0 (C)	6.5 (C)	4.5 (C)	394 (C)	415 (C)	811 (C)	818 (C)
Sand	Square	3	0.1	20.1 (C)	20.8 (C)	6.8 (C)	11.5 (C) 6.4 (E1) 6.3 (E2)	339 (C)	184 (C)	835 (C)	1297 (C)
Sand	Sine	6	0.1	20.1 (C)	24.2 (C)	6.9 (C)	12.1 (C) 1.6 (E1) 1.9 (E2)	416 (C)	310 (C) 661 (E1) 637 (E2)	838 (C)	2420 (C) 7890 (E1) 4240 (E2)
Sand	Sine	6	60	22.6 (C)	26.0 (C)	6.5 (C)	9.3 (C) 9.8 (E1) 5.7 (E2)	397 (C)	386 (C) 367 (E1) 421 (E2)	800 (C)	910 (C) 942 (E1) 956 (E2)
Sand	Sine	10	60	19.6 (C)	31.6 (C)	8.8 (C)	2.5 (C) 12.1 (E1) 2.3 (E2)	442 (C)	630 (C) 349 (E1) 659 (E2)	850 (C)	2170 (C) 3280 (E1) 2560 (E2)
Sand	DC	3	0	21.5 (C)	31.9 (C)	6.7 (C)	3.1 (C) 2.9 (A) 12.2 (CT)	359 (C)	771 (C) 804 (A) 235 (CT)	874 (C)	1044 (C) 1555 (A) 355 (CT)

Table 5-2 Cont'd

Sand	Control	0	0	20.0 (C)	44.1 (C)	7.2 (C)	8.0 (C)	420 (C)	394 (C)	867 (C)	1052 (C)
Solution	Control	0	0	19.9 (C)	19.6 (C)	6.7 (C)	6.7 (C)	458 (C)	469 (C)	811 (C)	815 (C)

Notes:

- A = Sample collected in the vicinity of anode (DC);
- C = Sample collected from the center of the test cell;
- CT = Sample collected in the vicinity of the cathode (DC);
- E 1 = Sample collected in the vicinity of electrode 1 (AC);
- E 2 = Sample collected in the vicinity of electrode 2 (AC);

This observation is consistent with a review presented by (Page and Page (2002)). Page and Page (2002) reported that in DC electrolysis of moist soils, the predominant process is the electrolysis of water molecules, which results in the formation of  $H^+$  and oxygen at the anode and  $OH^-$  and hydrogen at the cathode. Therefore under the condition of hindered migration in soils, the immediate result is a local change in pH of the pore solution so that acidity increases with time at the anode and alkalinity increases at the cathodes.

### **Effect of Current Density**

Because AC from the power grid is supplied as a sine wave at 60 Hz frequency in the United States, tests were conducted using sine wave at 60 Hz frequency to explore the potential for pilot-scale application. If AC available from the power grid can be used for this application, it would be cheaper for capital cost compared to DC. DC requires power supplies which are relatively expensive for power demand required to run pilot-scale or field-scale electrochemical tests. Figure 5-5 illustrates normalized concentration versus time profile for tests conducted using 60 Hz AC sine wave at  $6 \text{ mA/cm}^2$  and  $10 \text{ mA/cm}^2$  peak current densities.

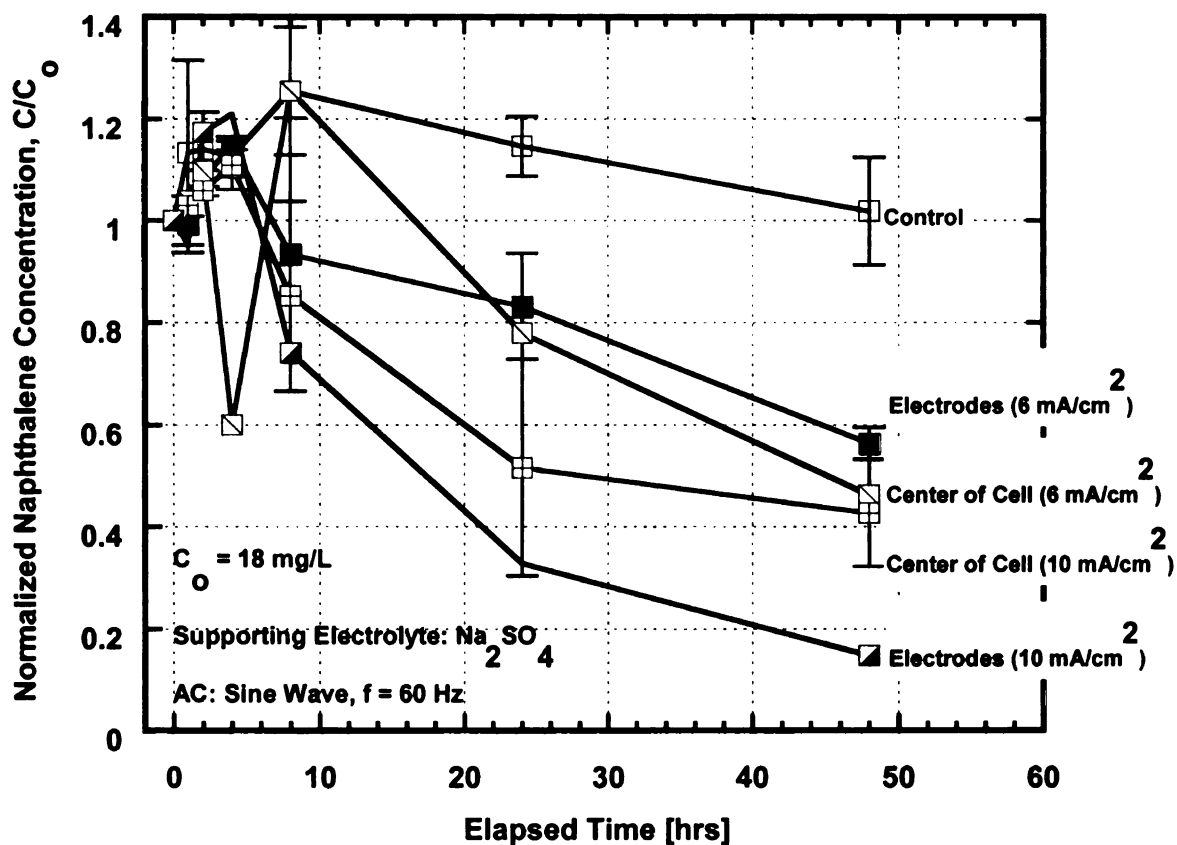


Figure 5-5: Effect of current density on electrochemical degradation of naphthalene in spiked sand using AC

The concentration of naphthalene decreased near the electrodes and away from the electrodes as the tests progressed. Increasing the current density from  $6 \text{ mA/cm}^2$  to  $10 \text{ mA/cm}^2$  resulted in an increase in the degradation rate. This is similar to the trend reported by Pepprah and Khire (2008) that the rate of degradation of naphthalene in spiked aqueous solution increased with increased current density for both AC and DC.

### Effect of AC Frequency

Figure 5-6 illustrates normalized concentration versus time profile of tests conducted using  $6 \text{ mA/cm}^2$  peak AC density at 0.1 Hz and 60 Hz frequency.

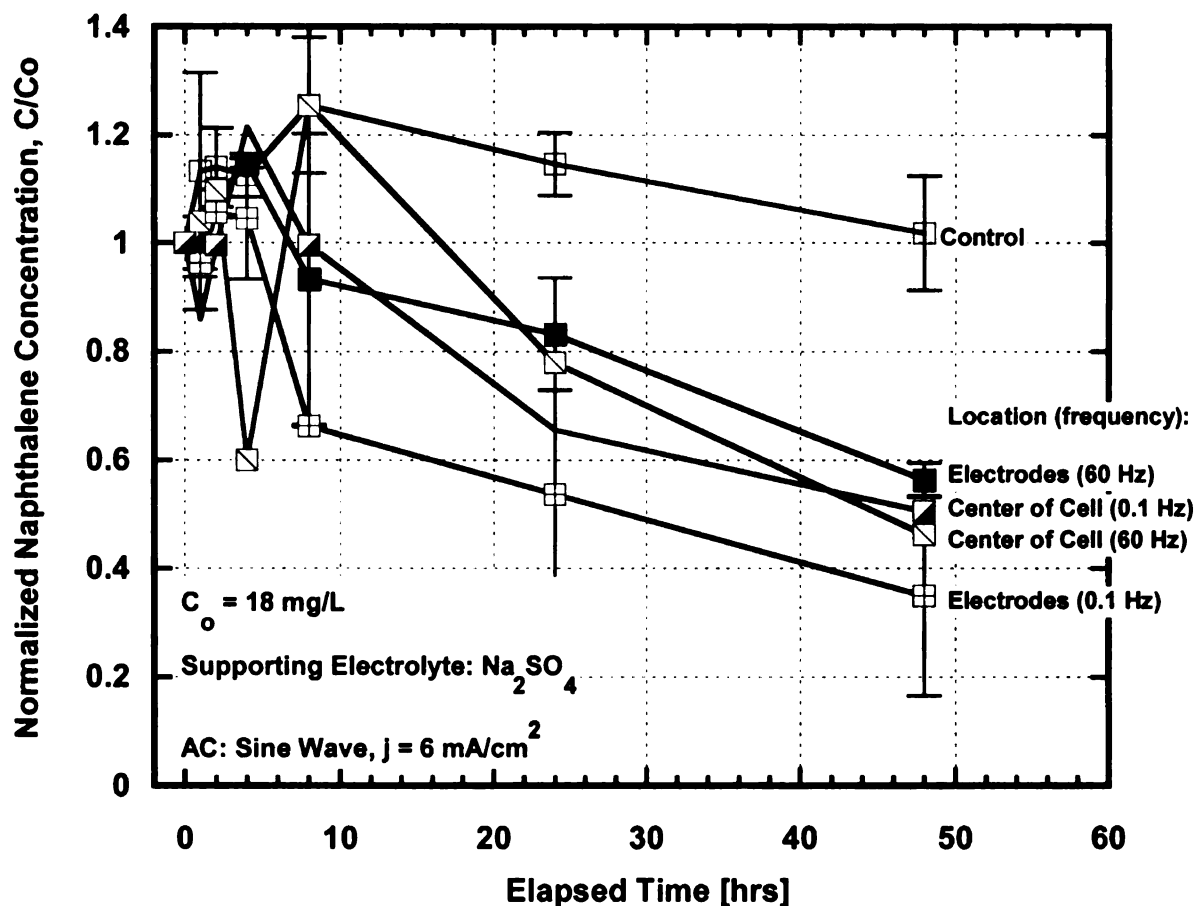


Figure 5-6: Effect of AC frequency on electrochemical degradation of naphthalene in spiked sand using AC

Degradation rate of naphthalene for the 0.1 Hz frequency test was greater than that at 60 Hz frequency. This is consistent with the findings by Chen and Chin (1985) who reported that degradation rate of phenol in solution decreased with increased AC frequency superimposed on a DC.

#### Experimental Parameters Monitored

Apart from monitoring the aqueous phase concentration of naphthalene in the spiked sand over time, other experimental parameters monitored included the initial and final values



of pH, temperature, redox potential, and electrical conductivity. A portable dissolved oxygen/pH meter, equipped with a pH electrode, and oxidation-reduction probe, was used to measure pH and redox potential respectively, of the test solutions. An electrical conductivity meter was used to measure the electrical conductivity and a thermometer was used to measure the temperature of the spiked solution in the control and test cells throughout the testing period. Table 5-2 shows the various measurements.

## **SUMMARY AND CONCLUSIONS**

AC and DC were separately applied to spiked naphthalene solutions with and without Ottawa sand to assess degradation. Potential application of this technology would be for cleanup of PAH contaminated ground water in sandy or rocky aquifers. Square wave AC having frequency equal to 0.1 Hz was used. The current density for both AC and DC was 3 mA/cm<sup>2</sup>. The key findings of this study are: (1) both DC and square wave AC degraded naphthalene in the aqueous phase of the sand; (2) at an equivalent current density, the rate of degradation of naphthalene in the aqueous phase when sand was present was less than when only the aqueous solution were subjected to AC or DC; and (3) rate of degradation for AC was less than that for DC at an equivalent current density.

## SUMMARY AND CONCLUSIONS

The key objectives of this research dissertation were to: (1) demonstrate that alternating current (AC) can be used for electrochemical degradation of PAHs (naphthalene, phenanthrene and pyrene) in spiked aqueous solutions; (2) investigate the effect of AC characteristics such as shape of the waveform, current density, and frequency on the degradation rates when only the aqueous solution of the PAH versus the spiked solution added to a clean coarse sand were subjected to AC electrolysis; (3) compare the rate of degradation for naphthalene (a model PAH), in aqueous solution using ultrasound energy and electrical energy (AC and DC) delivered at the same output power, and (4) identify degradation mechanisms and pathways. Laboratory-scale tests were conducted in order to achieve the objectives listed above.

The key findings of this study are as follows.

1. Similar to DC, AC also can degrade PAHs in free standing solutions or when these solutions are mixed in sandy media;
2. DC at a given current density, was more efficient in degrading PAHs than an equivalent AC. However, it is expected that pilot-scale or field-scale application using AC would be potentially cheaper than DC for capital cost when AC from the power grid is used because no rectification is required;
3. Rate of degradation increases when the current density is increased;
4. Rate of degradation decreases when the frequency of the AC is increased. DC has the lowest frequency ( $f = 0$ ) and achieves the highest rate of degradation for an equivalent input power;

5. For square, sine, and triangular AC waveforms explored, square wave AC signal produced the fastest degradation rate for a given current density of the AC. Thus, the rate of degradation is a function of the *rms* input power;
6. Degradation kinetics observed in the tests could be fitted using *pseudo*-first-order decay model all PAHs tested;
7. Mass loss of electrodes during AC electrolysis was significantly less than during DC electrolysis for an equivalent power input;
8. Oxidation of PAHs occurred on both electrodes in AC electrolysis whereas, it occurred on only one electrode (the anode) in DC electrolysis. This indicates that in AC electrolysis, each of the electrodes acted as instantaneous anodes alternately during the half cycle of the AC where the oxidation took place;
9. Both DC and ultrasound, at an equivalent power output, exhibited comparable degradation rates of naphthalene in solution unlike AC at 60 Hz frequency, which produced significantly less degradation rate at the same power output. This indicates that, compared to DC, while there will be saving in the capital cost when AC from the power grid is used, the treatment time would be longer when AC is used.
10. Formation of 2,3-dihydroxybenzoic acid and 2,5-dihydroxybenzoic from the oxidation of salicylic acid (a hydroxyl radical probe) is consistent with reported findings that OH radicals were the primary oxidizing agents in both sonochemical and electrochemical degradation; and
11. Both diffusion and migration processes were responsible for the rate of mass transfer of PAHs to the reaction sites (surface of electrodes or in the vicinity

of the electrodes). However migration was the dominant mass transfer process.

## REFERENCES

- Acar, Y. B., Alshawabkeh, A. N. (1996). Electrokinetic remediation. 1. Pilot-scale tests with Pb-spiked kaolinite. *J. Geotech. Eng.* 122(3), 173-185.
- Acar, Y. B., Gale R. J., Putnam, G. A. (1991). Acid/base distributions in electrokinetic soil processing. *Transp. Res. Rec.* 1288, 23-34.
- Adewuyi, Y. G. (2001). *Sonochemistry: Environmental science and engineering applications*, *Ind. Eng. Chem. Res.*, 40, 4681-4715.
- Agard, J. B. R. (1981). A study of electro-reclamation and its application to the removal of toxic metals from contaminated soils. MSc. thesis, Manchester Univ., Manchester, England.
- Agency for Toxic Substances and Disease Registry (ATSDR) (1995). *Toxicological profile for polycyclic aromatic hydrocarbons*. Atlanta, GA: U.S. Department of Health and Human Services, Public Health Service.
- Alshawabkeh A. N., Sarahney (2005). Effect of current density on enhanced transformation of naphthalene. *Environ. Sci. Technol.* 39, 5837-5843.
- Anderson, R. F., Patel, K. B., Stratford, M. R. L. (1987). Radical spectra and product distribution following electrophilic attack by the OH radical on 4-hydroxy-benzoic acid and subsequent oxidation. *J. Chem. Soc. Faraday Trans.*, 83, 3177.
- Bamforth, S. M. and Singleton, I. (2005). Review: Bioremediation of polycyclic aromatic hydrocarbons: Current knowledge and future directions. *J. Chem. Technol. Biotechnol.*, 80(7), 723-736.
- Banerjee, S. (1987). Electro-decontamination of chrome-contaminated soils. *Proc.*, 13<sup>th</sup> Annual Research Symp.: Land Disposal, Remedial Action, Incineration & Treatment of Hazardous Waste, EPA, Cincinnati, 193-200; Rep. No. EPA/600/9-87/0115, U.S. Environmental Protection Agency, Cincinnati.
- Bard, A. J., Faulkner, L. R. (2001), *Electrochemical methods: fundamentals and applications*, John Wiley & Sons Inc., New York.
- Basu D. K., Saxena J. (1978a). Monitoring of polynuclear aromatic hydrocarbons in water: II. Extraction and recovery of six representative compounds with polyurethane foams. *Environ. Sci. Technol.* 12, 791-795.
- Basu D. K., Saxena J. (1978b). Polynuclear aromatic hydrocarbons in selected U.S. drinking waters and their raw water sources. *Environ. Sci. Technol.* 12, 795-798.

- Birke, V., Burmeier, H., Rosenau, D. (2003). Design, Construction, and Operation of Tailored Permeable Reactive Barriers. *Pract. Periodical of Haz., Toxic, and Radioactive Waste Mgmt.*, 7 (4), 264-280.
- Bjorseth, A., Ramdahl, T. (1985). *Handbook of Polycyclic Aromatic Hydrocarbons*. Vol. 2, eds. A. Bjorseth & T. Ramdahl, Marcel Dekker: New York, pp. 1-20.
- Brillas, E., Calpe, J. C., and Casado, J. (2000). Mineralization of 2,4-D by advanced electrochemical oxidation processes. *Water Research*, 34(8), 2253-2262.
- Buxton, G. V., Greenstock, C. L., Helman, W. P., Ross, A. (1988). Critical review of rate constants for reactions of hydrated electrons, hydrogen atoms and hydroxyl radicals (OH/O<sup>-</sup>) in aqueous solution. *J. Phys. Chem. Ref. Data*, 17, 513-886.
- Cerniglia, C. E. (1984). Microbial degradation of polycyclic aromatic hydrocarbons, *Adv Appl Microbiol.* 30, 351-368.
- Cerniglia, C. E. (1992). Biodegradation of polycyclic aromatic hydrocarbons. *Biodegradation*, 3(2-3), 351-368.
- Chen, G. H. (2004). Electrochemical technologies in wastewater treatment, *Sep. Purif. Technol.*, 38, 11-41.
- Chen, W. P., Wang, Y., Wang, X. X., Wang, J., and Chan, H. L. W. (2003). Water-induced DC and AC degradation in TiO<sub>2</sub>-based ceramic capacitors. *Materials Chemistry and Physics*, 82(3), 520-524.
- Chiang, L. C., Chang, J. E., and Wen, T. C. (1995). Indirect oxidation effect in electrochemical oxidation treatment of landfill leachate. *Water, Research* 29(2), 671-678.
- Chin, D-T, and Cheng, C. Y (1985). Oxidation of phenol with AC Electrolysis. *J. Electrochem. Soc.*, 132 (11), 2605-2611.
- Clar, E. (1964). *Polycyclic hydrocarbons*. Academic Press, New York.
- Cole R. H., Frederick R. E., Nealy R. P., et al. (1984). Preliminary findings of the priority pollutant monitoring project of the nationwide urban runoff program journal. *J. Water Pollut. Control Fed* 56, 898-908.
- Cominellis, C., De Battisti, A. (1996). Electrocatalysis in anodic oxidation of organics with simultaneous oxygen evolution. *J. Chim. Phys.* 93, 673-679.
- Cominellis, Ch. (1994). Electrocatalysis in electrochemical conversion/combustion of organic pollutants for waste water treatment. *Electrochim. Acta* 39, 1857-1862.

- Comninellis, Ch., Pulgrin, C. (1991). Anodic-oxidation of phenol for wastewater treatment, *J. Appl. Electrochem.* 21, 703-708.
- Elovitz, M. S., von Guten, U. (1999). Hydroxyl radical/ozone ratios during ozonation processes I, *Ozone Sci. Eng.*, 16, 113-120.
- Fedkiw, P. S., Chao, J. C. (1985). selectivity modification in electroorganic reactions by periodic current control: Electroreduction of nitrobenzene." *AIChE Journal*, 31(9), 1578-1580.
- Feng, Y. J., Li, X. Y. (2003). Electrocatalytic oxidation of phenol on several metal-oxide electrodes in aqueous solution, *Water Res.* 37, 2399-2407.
- Fernández, P., Vilanova, R. M., Martínez, C., Appleby, P., and Grimalt, J. O. (2000). The historical record of atmospheric pyrolytic pollution over Europe registered in the sedimentary PAH from remote mountain lakes. *Environ. Sci. Tech.* 34(10), 1906 – 1913.
- Flint, E. B., Suslick, K. S. (1991). The temperature of cavitation, *Science* 253, 1397-1399.
- Gattrell, M., D.W. Kirk, D. W. (1993). A study of the oxidation of phenol on platinum and preoxidized platinum surfaces, *J. Electrochem. Soc.* 140, 1534-1540.
- Gibb, H. J. (1966). Research on electroremediation of saline-alkali soils. *Trans. Am. Soc. Agricultural Eng.* 9(2), 164-169.
- Goel, R. K., Flora, J. R. V., Ferry, J. (2003). Mechanisms of naphthalene removal during electrolytic aeration. *Water Res.* 37, 891-901.
- Goskonda, S., Catallo, W. J. Junk, T. (2002). Sonochemical degradation of aromatic organic pollutants. *Waste Management* 22, 351-356.
- Grimm, J., Bessarabov, D., Sanderson, R. (1998). Review of electro-assisted methods for water purification. *Desalination* 115, 285-294.
- Grimmer, G. (1983). *Environmental Carcinogens: Polycyclic Aromatic Hydrocarbons. CRC Press: Boca Raton, Fla.*
- Guo, Z., Zheng, Z., Zheng, S., Hu, W., Feng, R. (2005). Effect of various sono-oxidation parameters on the removal of aqueous 2,4-dinitrophenol. *Ultrasonics Sonochemistry* 12, 461-465.
- Gupta, N., Sass, B. M., Gavaskar, A.R.; Sminchak, J.R.; Fox, T.C.; Snyder, F.A.; O'Dwyer, D.; Reeter, C. (1998). Hydraulic Evaluation of a Permeable Barrier Using Tracer Tests, Velocity Measurements, and Modeling. *Designing and*

- Applying Treatment Technologies: Remediation of Chlorinated and Recalcitrant Compounds. Battelle Press, Columbus, OH. 157-162, 1998.
- Haag, W. R., Yao, C. C. D. (1992). Rate constants for reaction of hydroxyl radicals with several drinking water contaminants, *Environ. Sci. Technol.*, 26(5), 1005-1013.
- Hamed, J., Acar, Y. B., Gale, R. J. (1991). Pb(II) removal from kaolinite by electrokinetics. *J. Geotech. Eng.* 117(2), 241-271.
- Hamnett, R. (1980). A study of the process involved in electroreclamation of contaminated soils. MSc. thesis, Manchester Univ., Manchester, England.
- Harvey, R. G. (1997). Polycyclic Aromatic Hydrocarbons, Wiley-VCH, Inc., New York.
- Harvey, R.G. (1991). Polycyclic aromatic hydrocarbons; Chemistry and carcinogenicity. Cambridge University Press, New York.
- Ho, S. V., Athmer, C. J., Sheridan, P. W., Shapiro, A. P. (1997). Scale-up aspects of Lasagna (TM) process for *in situ* soil decontamination. *J. Haz. Mat.* 55, 39-60.
- Houk, L. L., Johnson, S. K., Feng, J. R., Houk, R. S., Johnson, D. C. (1998). Electrochemical incineration of benzoquinone in aqueous media using quaternary metal oxide electrode in the absence of a soluble supporting electrolyte. *J. Appl. Electrochem.* 28(11), 1167-1177.
- Hung, H.-M., Kang, J.-W., Hoffmann, M. R. (2002). The sonolytic destruction of methyl *tert*-butyl ether present in contaminated groundwater. *Water Environ. Res.* 74, 545-556.
- Iniesta, J., Gonzalez-Garcia, J., Expósito, E., Montiel, V., Aldaz, A. (2001). Influence of chloride ion on the electrochemical degradation of phenol in alkaline medium using bismuth doped and pure PbO<sub>2</sub> anodes, *Water Res.* 35, 3291-3300.
- Iniesta, J., Michaud, P. A., Panizza, M., Cerisola, G., Aldaz, A., Comninellis, Ch. (2001). Application of synthetic boron-doped diamond electrode in electro-oxidation and in electro-analysis, *Electrochim. Acta* 46 (2001) 3573-3578.
- Jen, J.-F., Leu, M.-F., T.C. Yang, T. C. (1998). Determination of hydroxyl radicals in an advanced oxidation process with salicylic acid trapping and liquid chromatography, *J. Chromatogr. A*, 796(2), 283-288.
- Johnson, A. R., Wick, L. Y., Harms, H. (2005). Principles of microbial PAH-degradation in soil. *Environmental Pollution* 133: 71-84.
- Kappana, A. N. and Joshi, K. M. (1952). Part I. Oxidation of glucose to gluconic acid. Survey of techniques. *J. Ind, Chem, Soc.*, 50, 331-338.



- Kim, D. K., O'Shea, K. E., Cooper, W. J. (2002). Degradation of MTBE and related gasoline oxygenates in aqueous media by ultrasonic irradiation. *J. Environ. Engr.* 128, 806-812.
- Kirk, D. W., Sharifian H., Foulkes, F. R. (1985). Anodic oxidation of aniline for waste water treatment, *J. Appl. Electrochem.* 15, 285-292.
- Ko, S., Schlautman, M. A., Carraway, E. R. (1998), Effects of solution chemistry on the partitioning of phenanthrene to sorbed surfactants. *Environmental Science Technology*, 32(22), 3542-3548.
- Kreysa, G., Heitz, E. (1986). *Principles of Electrochemical Engineering*. VCH, Weinheim, New York.
- Lageman, R. (1993). Electro-reclamation (applications in the Netherlands). *Environ. Sci. Technol.* 27(13), 2648-2650.
- Lageman, R., Pool, W., Seffinga, G. A. (1990). Electro-reclamation: State-of-the-art and future developments. *Contaminated Soil '90*, F. Arendt, M. Hinsenveld and W. J. van den Brink, eds., Kluwer Academic, Dordrecht, The Netherlands, 1071-1078.
- Lageman, R., Pool, W., Seffinga, G. (1989). Electro-reclamation: Theory and practice. *Chem. Ind.* 18, 585-590.
- Laor, Y., Farmer, W. J., Aochi, Y., Strom, P.F. (1998), Phenanthrene binding and sorption to dissolved and mineral-associated humic acid. *Water Research*, 32(6) 1923-1931.
- Lee, M. L., Novotny, M. V., and Bartle, K. D (1981). *Analytical chemistry of polycyclic aromatic compounds*. Academic Press, New York.
- Li X-Y., Cui, Y-H., Feng, Y-J., Xie, Z-M., Gu, J-D. (2005). Reaction pathways and mechanisms of electrochemical degradation of phenol on different electrodes. *Water Res.* 39, 1972-1981.
- Li, Y., Wang, F., Zhou, G., Ni, Y. (2003). Aniline degradation by electrolytic oxidation, *Chemosphere* 53(10), 1229-1234.
- Lindgren, E. R., Mattson, E. D., Kozak, M. W. (1994). Electrokinetic remediation of unsaturated soils. *ACS Symp. Ser.* 554, 33-50.
- Little, C., Hephher, M. J., El-Sharif, M. (2002). The sono-degradation of phenanthrene in an aqueous environment. *Ultrasonics* 40, 667-674.

- Lorimer, J. P., Mason, T. J. (1987). Sonochemistry part I – the physical aspects, *Chem. Soc. Rev.* 16, 239.
- Lund, H., Baizer, M. M. (1991). *Organic Chemistry*. Marcel Dekker, New York, p. 616.
- Marcelli, B., Garcia-Gomez, J., Michaud, P.-A., Rodrigo, M. A., Comninellis, Ch. (2003). Electrogeneration of hydroxyl radicals on boron-doped diamond electrodes. *J. Electrochem. Soc.* 150, D79-D83.
- Meegoda, J. N., Veerawat, K. (2002). Ultrasound to decontaminate organics in dredged sediments, *Soil and Sediment Contamination* 11(1), 91-116.
- Morselli L, Zappoli S. (1988). PAH determination in samples of environmental interest. *Sci. Total Environ.* 73, 257-266.
- Mueller, J. G., Cerniglia, C. E., Pritchard, P. H. (1996). Bioremediation of environments contaminated by polycyclic aromatic hydrocarbons, in *Bioremediation: Principles and Applications*, ed by Crawford R. L. and Crawford, D. L. *Cambridge University Press*, Idaho, 125-194.
- Nakamura, A., Hirano, K., and Iji, M. (2005). Decomposition of trichlorobenzene with different radicals generated by alternating current electrolysis in aqueous solution. *Chemistry Letters*, 34 (6), 802-803.
- Naumczyk, J., Szpyrkowicz, L., and Zilio-Grandi, F. (1996). Electrochemical treatment of textile wastewater. *Wat. Sci. Tech.*, 34 (11), 17-24.
- Ottinger, S. E., Mayura, K, Lemke, S. L., McKenzie, K. S., Wang, N. Kubena, L. F., Phillips, T. D. (1999). Utilization of electrochemically generated ozone in the degradation and detoxification of benzo[a]pyrene. *Journal of Toxicology and Environmental Health Part A*, 57(8), 565-583.
- Oturan, M. A. (2000). An ecologically effective water treatment technique using electrochemically generated hydroxyl radicals for in situ destruction of organic pollutants: Application to herbicide 2,4-D. *J. Appl. Electrochem.* 30(4), 475-482.
- Oturan, M. A. and Pinson, J. (1995). Hydroxylation by electrochemically generated OH<sup>•</sup> radicals. Mono- and polyhydroxylation of benzoic acid: Products and isomers' distribution. *J. Phys. Chem.*, 99, 13948-13954.
- Page, M. M., Page, C. L. (2002). Electroremediation of contaminated soils. *J. Environ. Engr.* 128(3), 208-219.
- Pamakcu, S., Wittle, J. K. (1994). Electrokinetically enhanced *in situ* soil decontamination. *Remediation of Hazardous Waste Contaminated Soils*, D. L. Wise, and D. J. Trantolo, eds., Marcel Dekker, New York, 245-298.

- Panizza, M., Cerisola, G. (2003). A comparative study of direct and indirect electrochemical oxidation of polyaromatic compounds. *Annali di Chimica* 93, 977-984.
- Panizza, M., Bocca, C., Cerisola, G. (2000). Electrochemical treatment of wastewater containing polyaromatic organic pollutants. *Water Res.* 34, 2601-2605.
- Park, J. K., Hong, S. W., Chang, W. S. (2000). Degradation of polycyclic aromatic hydrocarbons by ultrasonic irradiation, *Environ. Technol.* 21, 1317-1323.
- Pepprah, E., Khire, M. V. (2008). Electroremediation of naphthalene in aqueous solution using alternating and direct currents. *J. Environ. Engr., ASCE*, 134-1 (in press).
- Polcaro, A. M., Palmas, S., Renoldi F., Mascia, M. (1999). On the performance of Ti/SnO<sub>2</sub> and Ti/PbO<sub>2</sub> anodes in electrochemical degradation of 2-chlorophenol for wastewater treatment, *J. Appl. Electrochem.* 29, 147-151.
- Psillakis, E., Telekom, A., Maintains, D., Nikolopoulos, E., Kalogerakis, N. (2003). *J. Environ. Mont.* 5, 135-140.
- Puri, A. N., Anand, B. (1936). Reclamation of alkali soils by electro dialysis. *Soil Sci.* 42, 23-27.
- Rajeshwar, K., Ibanez, J. G., Swain, G. M. (1994). *J. Appl. Electrochem* 24, 1007.
- Reddy, K. R., Saichek, R. E. (2004). Enhanced electrokinetic removal of phenanthrene from clay soil by periodic electric potential application. *J. Environ. Sci. & Health A39(5)*, 1189-1212.
- Riesz, P., Kondo, T., Khrishna, M. C. (1990). Sonochemistry of volatile and non-volatile solutes in aqueous solutions: e.p.r. and spin trapping studies, *Ultrasonics* 28, 295-303.
- Rodgers, J. D., Jedral, W. J., N.J. Bunce, N. J. (1999). Electrochemical oxidation of chlorinated phenols, *Environ. Sci. Technol.* 33, 1453-1457.
- Saracco G., Solarino, L., Aigotti, R., Specchia, V., Maja, M. (2000). Electrochemical oxidation of organic pollutants at low electrolyte concentrations. *Electrochim. Acta* 46, 373-380.
- Schwarzenbach, R. P., Gschwend, P. M., and Imboden, D. M. (2003). *Environmental Organic Chemistry*. John Wiley & Sons, Inc., New Jersey.
- Scheck, C. K., Frimmel, F. H. (1995). Degradation of phenol and salicylic acid by ultraviolet radiation/hydrogen peroxide/oxygen, *Water Res.*, 29 (10), 2346-2352.

- Schumann, U., Grundler, P. (1998). Electrochemical degradation of organic substrate at PbO<sub>2</sub> anodes: monitoring by continuous CO<sub>2</sub> measurements, *Water Res.* 32, 2835-2842.
- Segall, B. A., O'Bannon, C. E., Matthias, J. A. (1980). Electroosmosis chemistry and water quality. *J. Geotech. Eng.* 106(10), 1148-1152.
- Sehgal, C., Yu, T. J., Sutherland, R. G., Verrall, R. E. (1982). Use of 2,2-Diphenyl-1-picrylhydrazyl to investigate the chemical behavior of free radicals induced by ultrasonic cavitation, *J. Phys. Chem.* 86, 2982-2986.
- Shiraishi H, Pilkington N. H., Otsuki A., et al. (1985). Occurrence of chlorinated polynuclear aromatic hydrocarbons in tap water. *Environ. Sci. Technol.* 19, 585-590.
- Simond, O., Schaller V., Comninellis, C. (1997). Theoretical model for the anodic oxidation of organics on metal electrodes, *Electrochim. Acta* 42, 2009-2012.
- Sorrel R. K., Brass H. J., Reding R. (1980). A review of occurrences and treatment of polynuclear aromatic hydrocarbons. EPA-600/D-81-066.
- Staples C. A., Werner A. F., Hoogheem T. J., et al. (1985). Assessment of priority pollutant concentrations in the United States using STORET database. *Environ. Toxicol. Chem.* 4, 131-142.
- Stock N. L., Bunce, N. J. (2002). Electrocatalytic dechlorination of atrazine. *Can. J. Chem.* 80, 200-2006.
- Stucki, S., Kötzt, R., Carcer, B., W. Suter, W. (1991). Electrochemical wastewater treatment using high overvoltage anodes II: anode performance and application, *J. Appl. Electrochem.* 21, 99-104.
- Suslick, K. S., Flint, E. B. (1987). Sonoluminescence from non-aqueous liquids, *Nature* 330, 553-555.
- Tanaka, F., Feng, C., Sugiura, N., Maekawa, T. (2004). p-nitrosodimethylaniline (RNO)-based evaluation of enhanced oxidative potential during electrochemical treatment of high-salinity wastewater, *J. Environ. Sci. & Health*, A39 (3), 773-786.
- Thompson, L.H., Doraiswamy, L. K. (1999). Sonochemistry: science and engineering, *Ind. Eng. Chem. Rev.* 38, 1215-1249.
- Titanium and the Environment (Issue 1 April 2002). Data Sheet No. 19. Titanium Information Group.
- USEPA <<http://www.epa.gov/safewater/mcl.html>> (05/16/2006)

- USEPA (2000). A Resource for MGP Site Characterization and Remediation. EPA/542-R-00-005.
- Vadyunina, A. F. (1968). Meliorative effect on direct electric current on leaching of solonchakous solonetz. Proc. Trans. of the 9th Int. Congress of Soil Science, Adelaide, 455-463.
- Wang, S., Huang, B., Lu, X., Liao, L. (2005). Sonochemical decomposition of organic pollutants in landfill leachate. Fresenius Environmental Bulletin 14(5), 727-731.
- Wang, S. L. (1995). The study and application of electronic pulse irradiation facility. Doctoral dissertation, University of Science and Technology of China, Hefei.
- Westerhoff, P., Aiken, G., Amy, G., Debroux, J. (1999). Relationships between the structure of natural organic matter and its reactivity towards ozone and hydroxyl radicals, Wat. Res. 33(10), 2265-2276.
- Will, F. (1995). Removing toxic substances from the soil using electro-chemistry. Chem. Ind., 15<sup>th</sup> May, 376-379.
- Yasman, Y., Bulatov, V., Gridin, V. V., Agur, Sabina., Galil, N., Armon, R., Schechter (2004). A new sono-electrochemical method for enhanced detoxification of hydrophilic chloroorganic pollutants in water. Ultrasonics Sonochemistry 11, 365-372.
- Yusem, G. J., Pintauro, P. N. (1992). The Electrocatalytic Hydrogenation of Soybean Oil, J. Am. Oil Chem. Soc. 69, 399-404.
- Zhaobing, G., Zheng, Z., Shourong, Z., Wenyong, H., Feng, R. (2005). Effect of various sono-oxidation parameters on the removal of aqueous 2,4-dinitrophenol. Ultrasonics Sonochemistry, 12, 461-465.